IDENTIFICATION AND CHARACTERIZATION OF *BURKHOLDERIA MALLEI* CROSS-PROTECTIVE AND *IN-VIVO*-EXPRESSED HIGH VALUE TARGET ANTIGENS FOR THE DEVELOPMENT OF COUNTERMEASURES AGAINST GLANDERS AND MELIOIDOSIS

By

JEREMY SHANE DYKE

(Under the Direction of Eric R. Lafontaine and Robert J. Hogan)

ABSTRACT

Burkholderia mallei (Bm) and *Burkholderia pseudomallei (Bp)* are two closely-related Gram-negative bacteria that cause the severe respiratory illnesses glanders and melioidosis, respectively. Both diseases occur as an acute or chronic bacterial pneumonia. They cause high mortality, are resistant to most antibiotics, and have no vaccine available. Additionally, there are concerns that they could be misused as biological warfare agents, leading to their classification as Tier 1 Select Agents. Being highly related, the feasibility of devising a single vaccine protecting against both organisms seems high. Additionally, we have shown that protective antibodies generated during infection with *Bm* are capable of conferring protection against both organisms.

Many candidates have been identified, but there remains a need to discover novel immunoprotective antigens as current lead targets fail to prevent chronic infection. One major class of targets is autotransporter proteins. Autotransporters form one of the largest

families of virulence factors in Gram-negative bacteria and cause a wide range of pathogenic phenotypes. They are expressed at the bacterial surface which puts them at the host-pathogen interface. While characterizing several autotransporters we found several were not produced *in vitro*, but were expressed *in vivo* evidenced by the production of antibodies against the proteins during *Bm* infection in mice.

Here, we discuss the use of protective antibodies from survivor mice infected with *Bm* to probe the NEB PhD-12 phage display library to find mimetopes reactive with antibodies which were used to discover novel *in vivo* expressed *Bm* antigens. After determining the amino acid sequence of the mimetope, we probed the proteome of *Bm* and found proteins containing the same sequence within their structure. Additionally, this dissertation discusses the characterization of an *in vivo* expressed peptidoglycan associated lipoprotein (pal) found in both *Bm* and *Bp*. Pal was shown to be a component of the *B. mallei* cell wall and disrupting its function removed the ability of *B. mallei* to survive and persist. Finally, we discuss the involvement of BorP in the *in vivo* expression of the high value target antigen BpaB. BorP is an OmpR-like DNA-binding response regulator that modulates the *in vivo* expression of BpaB.

INDEX WORDS: *Burkholderia mallei*, *Burkholderia pseudomallei*, autotransporters, Type V Secretion Systems, *in vivo*, *in vitro*, BpaB, Omp7, Peptidoglycan associated lipoprotein, Pal, OmpR, BorP, intracellular survival, virulence, pathogenesis, vaccine, medical countermeasures, phage display, epitope library, mimetope, mimetic epitope, subunit vaccine, live attenuated strain vaccine, Two-Component Regulatory Systems, selective gene regulation.

IDENTIFICATION AND CHARACTERIZATION OF *BURKHOLDERIA MALLEI* CROSS-PROTECTIVE AND *IN-VIVO*-EXPRESSED HIGH VALUE TARGET ANTIGENS FOR THE DEVELOPMENT OF COUNTERMEASURES AGAINST GLANDERS AND MELIOIDOSIS

By

JEREMY SHANE DYKE

BS, University of New Mexico, Albuquerque, New Mexico, 2013.

A Dissertation Submitted to the Graduate Faculty of The University of Georgia in Partial Fulfillment of the Requirements for the Degree

DOCTOR OF PHILOSOPHY

ATHENS, GEORGIA

2020

IDENTIFICATION AND CHARACTERIZATION OF *BURKHOLDERIA MALLEI* CROSS-PROTECTIVE AND *IN-VIVO*-EXPRESSED HIGH VALUE TARGET ANTIGENS FOR THE DEVELOPMENT OF COUNTERMEASURES AGAINST GLANDERS AND MELIOIDOSIS

By

JEREMY SHANE DYKE

Major Professor:	Eric R. Lafontaine
	Robert J. Hogan
Committee:	M. Stephen Trent
	Biao He
	Danny G. Mead

Electronic Version Approved:

Ron Walcott
Interim Dean of the Graduate School
The University of Georgia
August 2020

DEDICATION

This dissertation if dedicated to my wife, Shawn Zimmerman. Without her love and support I would never have completed this degree. This dissertation is also dedicated to my parents and sister: Jimmy, Angie, and Ashley Dyke. Without them I would never have made it to The University of Georgia to begin with. Lastly, Jack Daniel, Nathan Green, and Jeff Arnett. Their mastery of their craft has been a blessing to me in some of my most stressful times.

ACKNOWLEDGEMENTS

I would like to thank those who have made an impact on me, both professionally and personally during my time at UGA:

- Dr. Eric Lafontaine – He has been a tremendous mentor to me. I may not be the smartest or most successful graduate student but the opportunities given to me by Eric have made me the luckiest. I would not be where I am today without all of his guidance and support. Because of my time in his lab I will never forget how to maintain a laboratory notebook.
- My dissertation committee members – Drs. Jeff Hogan, Daniel Mead, Stephen Trent, and Biao He. They have all furthered my scientific development in one way or another. I have truly appreciated all of the constructive criticism and advice that I received from them during my time at UGA.
- Post-Docs and Lab personnel – that have helped me along the way including, Dr. Tomislav Jelesijevic, Frank Michel, and Nathan Holladay for helping me along the way. Working and socializing with them made the day-to-day grind of completing a PhD fun and enjoyable.
- Friends and fellow PhD students – We stormed the metaphorical beach together, and most of us are still around to tell our tales.

Table of Contents

CHAPTER 1

INTRODUCTION

PURPOSE OF THIS STUDY

We hypothesize that there are antigenic proteins expressed by *B. mallei* and *B. pseudomallei* selectively *in vivo* that are of high value for their ability to produce a protective immune response, and that the selective expression of these antigens is orchestrated through the regulatory actions of two-component regulatory systems including the BorP two-component DNA binding response regulator. The purpose of this study is to understand the selective *in vivo* expression of high value target antigens in *Burkholderia mallei* and *Burkholderia pseudomallei*, as well as the discovery of novel high value antigens selectively expressed *in vivo*. *Burkholderia mallei* is a host adapted Gram-negative bacterium that causes the disease Glanders, while *Burkholderia pseudomallei* is a Gram-negative environmental saprophyte that causes the disease Melioidosis. Both diseases present as severe bacterial pneumonia with accompanying bacteremia, and can occur as both an acute or chronic infection. During the course of infection, both organisms modulate their proteome in order to accomplish certain tasks vital for their persistence within a host. This highly orchestrated expression dynamic has led to the selective *in vivo* only expression of high value antigens. The existence of high value target antigens that are selectively expressed *in vivo* is evidenced by the fact that serum taken from mice that survived infection with *Bm* had antibodies reactive with constitutively expressed *in vitro* antigens removed from their composition and were still capable of conferring a high level

of protection against acute lethal infection with both *Bm* and *Bp*. Understanding what these high value antigens are, as well as their underlying expression dynamics, is important as while there have been some promising vaccine candidates found, the field as a whole is still in the antigen discovery phase due to a lack of demonstrated consistent ability to prevent chronic infection. By discovering novel high value target antigens, the field as a whole is advanced allowing for a broader library of immunoprotective epitopes that can be used as vaccines.

HOW THIS STUDY IS ORIGINAL

This studies contained herein represent the first described use of phage display library technology in order to discover endogenous *Burkholderia mallei* antigens that are selectively expressed *in vivo.* Antibodies were generated within our lab by infecting mice with *Burkholderia mallei* and collecting the serum of mice who survived. This serum was then adsorbed with whole cell live bacteria as well as bacterial lysates in order to remove antibodies present in the serum that were reactive with constitutively expressed *in vitro* antigens. Once these irrelevant antibodies were removed, the remaining antibodies were used to probe a commercially available phage display library of randomly generated, linear, 12 amino acid epitopes. This process of generated serum that is solely reactive with *in vivo* antigens, probing the library, and using the obtained sequences to find endogenous proteins within the *B. mallei* and *B. pseudomallei* proteome has never been previously described.

Additionally, this study discusses the functional characterization of the *in vivo* expressed *Burkholderia mallei* peptidoglycan associated lipoprotein (pal). While pal is a well-studied structure in other Gram-negative bacteria, this work represents the first examination of the pal lipoprotein of the *B. mallei* cell wall, as well as its functional

characterization. Our manuscript is the first to discuss the generation of a pal knockout mutant in *B. mallei* and the first to discuss the effects that a lack of *pal* expression has on the pathogenesis of *B. mallei*. Additionally, this work is the first to demonstrate that *B. mallei* pal can be used as an effective subunit vaccine against aerosol challenge with the organism.

Lastly, this study describes the novel OmpR-like regulator BorP in *Burkholderia mallei*. Our manuscript is the first to discuss the *borP* gene, a gene upstream of a high value target autotransporter antigen BpaB previously described by our lab. The manuscript is the first to discuss the generation of a *borP* KO mutant and its effect on the *in vivo* expression of the BpaB protein. It is also the first manuscript to discuss the forced *in vitro* expression of the exclusively *in vivo* expressed BpaB protein as a result of an overexpression mutant. With this manuscript, we demonstrate that the BorP protein is functionally controlling the expression of *bpaB* by directly binding to the promoter region of the BpaB gene.

EXPECTED RESULTS

We expect that using antibodies from serum shown to confer protection against lethal challenge with *B. mallei* in passive serum transfer experiments to probe the NEB PhD-12 library for randomly generated epitopes will allow us to identify *in vivo* expressed antigens. The NEB PhD-12 kit contains M13 bacteriophage virions that are expressing 5 identical copies of the same randomly generated dodecapeptide epitopes fused to their minor coat protein (pIII). By sequencing the individual virions, the nucleotide sequence of the expressed 12 amino acid peptides can be determined. By converting the nucleotide sequences to the corresponding amino acid sequences, these reactive epitopes can be compared to the endogenous proteins expressed by all sequenced strains of *B. mallei* and

B. pseudomallei. We believe that by doing this, we will find overlap between these short peptide sequences and the *B. mallei* and *B. pseudomallei* proteome. Once these target endogenous proteins are found, we believe that they can be purified and used in subunit vaccines to confer protection. Additionally, it has been demonstrated in the literature that M13 phages expressing short epitopes can be used as vaccines themselves through a process known as mimetope vaccination (29, 33, 66, 70, 87, 90, 108, 119, 141, 163, 165, 220, 247). We believe that by finding phages that are reactive with immune serum antibodies, we will be able to use the obtained phages to use as mimetope vaccines producing antibodies capable of conferring protection.

We further believe that we will demonstrate that *pal* is an essential part of the *B. mallei* cell wall, and is necessary for intracellular survival and the associated pathogenic phenotypes as has been demonstrated in the literature when disrupted in other Gram-negative bacterial pathogens. By disrupting the expression of the *pal* gene in *B. mallei*, we expect to show a drastically reduced ability of the mutant to survive and persist within professional phagocytic cells. We also expect to see a resulting inability to survive the same levels of osmotic and antibiotic stress, a phenomena that has been demonstrated in the literature with other *pal* mutants (105, 205). Additionally, we believe that delivering the Pal protein via a viral vaccine system will elicit a high level of protection against *B. mallei*, and will be a strong vaccine candidate.

Lastly, we expect to demonstrate that the *borP* gene product is an OmpR-like DNA binding response regulator that is directly affecting the expression of BpaB as a transcriptional regulator. Additionally, we expect to show that overexpression of BorP will result in a corresponding overexpression of BpaB, and as a result a BorP overexpression

mutant will exhibit the associated biofilm phenotype seen in a BpaB mutant. We further expect to demonstrate that knocking out the expression of *borP* results in a reduction in virulence in the mutant.

CHAPTER 2

LITERATURE REVIEW

BURKHOLDERIA MALLEI AND GLANDERS

Microbiology

Burkholderia mallei is a Gram-negative, rod shaped bacillus that is aerobic and non-motile. Until 1992 it was a member of the *Pseudomonas* genus, but in 1992 it was phylogenetically reclassified as a member of the genus *Burkholderia*. The majority of the *Burkholderia* species are non-pathogenic, and *B. mallei* is only one of two *Burkholderia* species believed to be capable of purely pathogenic behavior as opposed to the opportunistic pathogen behavior of *B. cenocepacia, B. cepacia, B. gladioli,* and *B. fungorium.* It is a facultative intracellular pathogen that is host-adapted to equine species and incapable of prolonged environmental persistence longer than 1-2 months and the causative agent of the fatal, zoonotic illness glanders (97). *Burkholderia mallei* was once worldwide in distribution, but due to aggressive eradication efforts it has been cleared from the U.S., Canada, and Western Europe and is now endemic to Asia, Africa, the Middle East, and South America as shown in figure 2.1, specifically among the Equatorial and Torrid zones of these regions. Occasional diagnoses of animals with glanders have been reported in Eastern Europe and Mexico.

In equine species, glanders has three presentations; nasal, pulmonary, and cutaneous, and can manifest as either an acute or chronic infection. More than one

presentation may be found at a time meaning nasal, pulmonary, and cutaneous glanders are not mutually exclusive, and in fact the disease will often progress from one presentation to multiple. Cutaneous glanders, also known as farcy, is characterized by the presence of ulcers, erosions, and abscesses that appear on the skin along the course of the lymphatic vessels. These abscesses often rupture, releasing a yellow discharge that is highly infectious and contains pus and viable *B. mallei*. Internal signs of infection such as abscesses in the spleen or liver may be present, but are not unique characteristics of cutaneous glanders. The rupturing of these external nodules can lead to the contamination of harness components and blankets which can then lead to fomite transmission of the agent from animal to human or animal to animal. Nasal glanders is characterized by erosions, nodules, and abscesses present within the nasal passages in the mucosa, particularly along the nasal septum. These abscesses will often rupture resulting in a thick purulent unilateral or bilateral discharge from the nasal passages. As with cutaneous glanders, this discharge is highly contagious and is loaded with viable *B. mallei*. The nasal discharge of *B. mallei* can result in the contamination of shared drinking water and thus animal to animal spread, or can be aerosolized by a snorting horse resulting in animal to human transmission. The most common form of glanders, the pulmonary form is found in the lungs where erosions, ulcers, and abscesses develop in the upper respiratory tract while widespread pneumonia affects the lower respiratory tract (85). The abscesses in the upper respiratory tract often rupture releasing the characteristic highly infectious discharge directly into the lower respiratory tract which serves to prolong the infection as shown in figure 2.2.

While glanders is primarily an animal illness, humans are highly sensitive to infection. Exposure typically occurs via percutaneous inoculation and inhalation of

contaminated aerosols. In humans, untreated glanders causes 100% mortality while the treated mortality rate remains greater than 50%. The mortality rate remains high despite years of research in the field due to the fact that glanders is difficult to diagnose and treat, and is resistant to many antibiotics including penicillin, first and second-generation cephalosporins, rifamycins, macrolides, and colistin. Fortunately, *B. mallei* remains susceptible to aminoglycosides, amoxicillin-clavulanate, chloramphenicol, doxycycline, trimethoprim-sulphamethoxazole, ureido-penicillins, ceftazidime, and carbapenem (97).

History

Glanders is an ancient disease, and is one of the oldest known diseases of horses. Around 425 B.C. Hippocrates described a disease in a horse that closely resembled the symptoms of what we know as glanders today (81). Around 350 B.C. Aristotle further described glanders in a donkey stating, “The ass suffers chiefly from one particular disease which they call melis. It arrives first in the head, and a clammy humour runs down the nostrils, thick and red; if it stays in the head the animal may recover, but if it descends into the lungs, the animal will die”. Around 310 A.D. a horse doctor in the army of Constantine the Great, A.D. Apsyrtus, and a Roman historian named Vegetius, recognized that horses with glanders symptoms should be kept separate from others as well as the careful burning and disposal of the corpses of affected animals, otherwise other horses would get sick. Glanders-like illness continued to be described through the European Dark Age and was blamed on everything from Jewish poisons to the ever present Miasma. Many descriptions of glanders and unknown glanders-like illnesses exist with proposed causes ranging from spontaneous generation and fungus to syphilis and Tuberculosis (85). In 1761 Claude

Bourgelat, a French lawyer, is credited with founding the first true veterinary college to study glanders and rinderpest when he saw the devastation that the two illnesses wreaked on French herds (81, 231). Some of the best records of glanders exist in the documents and journals produced during the U.S. Civil War. In one such account, it is described by Confederate surgeons John R. Page and John J. Terrell that a federal horse captured by the confederate army was suffering from glanders and in time "spread the disease far and wide among the horses of the confederate army" (231). Remount stations used to house horses during travel such as the one shown in figure 2.3 were often contaminated with *B. mallei* which allowed the rapid transmission of the bacterium between horses through contaminated water troughs.

It wasn't until 1882, however, that Löffler and Schütz identified the bacterium now known as *Burkholderia mallei* as the root cause of the disease glanders (81). In 1916 Anton Dilger, an American born physician with German ties, cultured *B. mallei* which was then used to inoculate horses in Baltimore, Newport, and Norfolk which were to be sent to the allied front lines during World War 1 (274). *Burkholderia mallei* was also used as a biological warfare agent during World War 2 as the infamous Japanese Unit 731 engaged in unrestricted biological warfare in the Zhejiang, Hunan, Jiangsu, Jilin, Kwangtung, Yunnan, and Heilongjiang provinces of China using *B. mallei* (274). In 1972, the signing of the Convention on the Prohibition of the Development, Production, and Stockpiling of Bacteriological and Toxin Weapons and on Their Destruction treaty by 109 signatories including Russia, The United Kingdom, The United States, and Canada should have stopped the development and use of *B. mallei* as a biological warfare agent but there is evidence that it was used by the Soviet Union as recently as 1982 in Afghanistan (274).

Equine glanders was eradicated from the U.K in 1928, the U.S. in 1934, and Canada in 1938 (148). *Burkholderia mallei* is easy to acquire, culture, and spread, and has a history of use as a biological warfare agent. To make matters worse there is currently no commercially available vaccine (11). For those reasons, as well as the ability of the agent to cause a high degree of incapacitation among those infected, it has been classified as a Tier 1 Select Agent by the Federal Select Agent Program. This means that there are enhanced regulations and strict monitoring of when and how the agent is used and stored in general laboratory procedures.

BURKHOLDERIA PSEUDOMALLEI AND MELIOIDOSIS

Microbiology

Burkholderia pseudomallei is a gram-negative, rod shaped bacillus, and an aerobe. Like *B. mallei* it is a facultative intracellular pathogen, but unlike *B. mallei* it is not host adapted. *Burkholderia pseudomallei* is an environmental saprophyte that is readily isolated from wet soils and stagnant waters in Southeast Asia, northern Australia, Africa, the Middle East, China, India, and parts of Central and South America as shown in figure 2.4 (37). As is true of *B. mallei*, *B. pseudomallei* is one of only two *Burkholderia* species capable of what is traditionally thought of as pathogenic behavior rather than opportunistic infection. Prior to 1992 it was also classified as a *Pseudomonas* species but was genotypically reclassified as a *Burkholderia* species member. *Burkholderia pseudomallei* is the causative agent of the disease Melioidosis, and is most often spread through the inhalation or ingestion of contaminated water or soil, or through percutaneous inoculation (6, 97, 176, 279). *Burkholderia pseudomallei* has been referred to as a great imitator due

the ability of the pathogen to cause a wide range of symptoms. While *B. pseudomallei* infection can present in a diverse way, the hallmark symptom of Melioidosis is pneumonia with accompanying septicemia. It is also important to note that Melioidosis is an important emerging tropical disease, and that *B. pseudomallei* accounts for greater than 20% of all bacterial pneumonia in endemic regions (97, 176, 279). *Burkholderia pseudomallei* is not host adapted and persists in the environment. It also has a broad host range (6, 290). In addition to humans and livestock, *B. pseudomallei* has been shown to infect wild and domesticated dogs, domesticated cats, fish, primates, dolphins, and avian species.

History

Melioidosis was identified by Captain Alfred Whitmore, an English pathologist, and his assistant C.S. Krishnaswami in 1912 in Rangoon, Burma when they observed an illness that closely resembled glanders in morphine addicts (128). While initially believed to be glanders, the colony morphology of the bacterium isolated from tissue specimens was different from that of *B. mallei* and the patients had no history of interacting with horses or other equine species. Further, the bacterium grew faster than *B. pseudomallei* on peptone agar and was motile (128). From this, Captain Whitmore concluded that this illness was separate from glanders and thus a new disease was described (125, 128 176, 254). During autopsy, the bacterium was noted to cluster in abscesses in the lungs, liver, spleen and kidneys, similar to *B. mallei*. Melioidosis is also known as Whitmore Disease in his honor. The following year in 1913, an outbreak of what was believed to be distemper was studied in Maylasia (254). The bacterium was isolated and in 1917 Ambrose Thomas Stanton and

William Fletcher, a bacteriologist and pathologist, respectively, characterized it and officially named the disease Melioidosis, meaning glanders-like (254).

Between 1948 and 1954 at least 100 cases of confirmed melioidosis were reported in Indochina within the French military during the Vietnamese uprising. At least 300 U.S. Infantrymen and service dogs were diagnosed with Melioidosis during the course of the Vietnam conflict. Most of these diagnoses were believed to have been caused by direct contact of contaminated soil and water with open wounds, but a high number of cases within helicopter pilots and air cavalrymen may be due to inhalation of aerosolized water and soil contaminated with *B. pseudomallei* (97). It has been estimated that at many as 225,000 Americans may have been exposed to *B. pseudomallei* during the Vietnam conflict and the potentially decades long latent period of infection has earned melioidosis the nickname of Vietnamese time bomb. *Burkholderia pseudomallei* continues to be routinely detected in endemic regions (97). Like *B. mallei*, *B. pseudomallei* has been classified as a Tier 1 Select Agent by the Federal Select Agent Program meaning that it is in the highest risk group of organisms capable of misuse as biological terrorism agents. Further, there is no vaccine commercially available. The ability to be misused as a bioweapon as well as the high levels of endemicity leading to natural infection illustrate the importance of developing vaccines and medical countermeasures against *B. pseudomallei* (11).

BURKHOLDERIA MALLEI AND *BURHOLDERIA PSEUDOMALLEI* AS CLOSELY RELATED ORGANISMS

Genetics

Burkholderia mallei and *B. pseudomallei* are two very closely related organisms (250). *Burkholderia mallei* ATCC 23344 and *B. pseudomallei* K96243, two prototypical strains often used in the lab and the first to have their genomes sequenced, both have two circular chromosomes. While *B. pseudomallei* K96243 has the larger genome at 7.2 Mb compared to the *B. mallei* ATCC 23344 5.8 Mb genome, the two are > 99% identical where the two overlap (97, 171, 226, 233). Within each species, there are two opposite levels of diversity. Among seven *B. mallei* strains sequenced, all but one strain were almost identical to each other (171, 182). Among eight sequenced *B. pseudomallei* strains sequenced, however, there was a large degree of genetic diversity which is believed to be due to large genomic islands found in the *B. pseudomallei* genome but not in the *B. mallei* genome (182, 200).

There is evidence that *B. mallei* evolved from a single strain of *B. pseudomallei*. In fact, Multilocus Sequence Typing results suggest that *B. mallei* may have originated from a *B. pseudomallei* strain that infected a host and through a large deletion mutation lost many of the genes required for motility and environmental persistence but retained the genes required for survival in the host resulting in the obligate pathogen that we see today (92, 182, 200). This hypothesis has gained much traction due to the fact that nearly all of the genes found among the various strains of *B. mallei* have orthologs in *B. pseudomallei*, but an additional ~1,200 genes, including many of those used by *B. pseudomallei* to persist in the environment, are absent from the sequenced *B. mallei* strains. It is believed that *B.*

pseudomallei has undergone genomic erosion during which an ancestral strain that was not host-specific lost genes due to intense selective pressure from having to survive within a host resulting in a separate species that is host adapted and that *B. mallei* is not yet collectively in its "final form" (92). Rather, *B. mallei* is in an intermediate from much like *Shigella flexneri* or *Salmonella typhi* meaning *B. mallei* is expected to continue undergoing genomic erosion as multiple *B. mallei* strains were still found to contain some of the genes typically associated with persistence within the environment despite its inability to persist outside of the host long term (69, 178).

From the sequenced *B. mallei* and *B. pseudomallei* strains, a core genome was established. In this sense, a core genome is defined as the group of genes that is found in all of the sequenced strains. Among seven fully sequenced *B. mallei* strains, a core genome of 3,456 genes was established (171). By contrast, a core genome of 4,619 genes was established among eight fully sequenced *B. pseudomallei* strains (92). In both species, many genes associated with virulence were found to be conserved within their core genomes. By comparing the core genomes of *B. pseudomallei* and *B. mallei*, a core virulome of 650 genes has been proposed (224, 226). Among the gene functions found in this core virulome are the genes for the production of lipopolysaccharide (LPS) (193, 202), Type 3 and Type 6 secretion systems (14, 44, 59, 106, 118, 146, 167, 211, 257, 261, 263, 270, 297), and the production of a capsule (87, 193, 230). In addition to this core virulome, the presence of potential global virulence regulators was observed (24). While characterizing one such global virulence regulator in *B. mallei*, the two-component regulatory system VirAG, it was observed that overexpression of the regulator resulted in the upregulation of over 60 virulence genes. Further, the removal of the ability to express

VirAG rendered mutant strains avirulent to mice and hamsters (227). Another regulator, BPSL1887, or YelR, is a sigma-54 dependent transcriptional regulator that has been characterized in *B. pseudomallei* and has an ortholog in *B. mallei* strain ATCC 23344. While being characterized it was discovered that a mutant lacking its expression was reduced in virulence, and that when overexpressed a biofilm-type phenotype was observed (17). Our laboratory has also identified a gene predicted to encode a DNA binding regulatory protein, BMA0838, upstream of the *bpaB* gene in the genome of *B. mallei* and *B. pseudomallei* (296).

As expected, a high degree of genetic similarity between the two organisms makes them clinically difficult to distinguish from one another. In addition to being difficult to diagnose and detect, both *B. mallei* and *B. pseudomallei* are difficult to treat. For animals, a positive diagnosis of infection with *B. mallei* or *B. pseudomallei* is treated with summary euthanasia as treating animals is costly, ineffective, and dangerous. For both organisms an aggressive antimicrobial regimen mixed with surgical intervention are required. While both strains are resistant to many antimicrobials, *B. mallei* is susceptible to tetracycline, doxycycline, sulfonamides, trimethoprim, aminoglycosides, ceftazidime, and piperacillin (72). Depending on the nature of the glanders infection, two routes of treatment are available. For a widely dispersed systemic infection, intravenous doses of ceftazidime are most often used. For focal infections characterized by the presence of abscesses, surgical removal of the abscesses is recommended in conjunction with a prolonged (>90 day) regimen of oral antibiotics such as doxycycline or trimethoprim-sulfamethoxazole (72). *Burkholderia pseudomallei* is much more resistant to antimicrobials than *B. mallei* due in large part to the presence of multiple antibiotic efflux pumps and β-lactam production in

addition to a dense capsule (97). As with *B. mallei*, surgical removal of abscesses is required for focal infections, but aggressive treatment with doxycycline, amoxicillin-clavulanate, ceftazidime, and trimethoprim-sulfamethoxazole remain the most efficacious treatments due to the inherent antibiotic resistance (72, 87).

Common Virulence Traits

As would be expected given the genetic similarities between *B. mallei* and *B. pseudomallei* as well as the overlapping similarities between glanders and melioidosis, the two organisms share several common virulence traits including a facultative intracellular pathogenic lifestyle (11, 67, 279), adhesins (22, 155), biofilm formation (14, 296), and serum complement resistance (8, 11). Similar or identical type 3 and 6 secretion systems can be found in both organisms (14, 44, 59, 106, 113, 118, 132, 146, 167, 211, 227, 253, 257, 259, 270, 297) as well as eight different autotransporter genes (4, 5, 48, 155, 295, 296). Both organisms have a capsule of group III capsular polysaccharides that are made up of a homopolymer of -3)-2-*O*-acetyl-6-deoxy-β-*D*-manno-heptopyranose (193, 230). This capsule allows for the intracellular replication of both organisms within professional phagocytic cells in addition to contributing to complement resistance (230). In serum, the capsule reduces opsonization and phagocytosis by reducing C3b activity (193). It has been shown to be an important virulence factor due to the fact that knocking out the genes required for capsule production attenuated *B. pseudomallei* in hamsters and mice, and made *B. mallei* avirulent in mice and horses. It has further been shown that mice given passive transfers of serum containing anti-capsule antibodies were protected against acute lethal infection (15). The LPS O-antigen of both organisms is an unbranched heteropolymer of

repeating *D*-glucose and *L*-talose subunits. *Burkholderia pseudomallei* OPS has the structure-3)-β-*D*-glucopyranose-(1-3)-6-deoxy-α-*L*-talopyranose-(1- while *B. mallei* has a similar structure that is only lacking an *O-acetyl* group at 4' position of the talose subunits (193). For both organisms, the O-antigen confers protection against killing via the alternative complement pathway. O-antigen knockout mutants of both species are highly attenuated in hamsters and mice and show no complement resistance. Immunization with the purified OPS region of lipopolysaccharide has also been shown to provide protection against acute lethal infection of *B. pseudomallei* in mice when challenged intraperitoneally, but not the aerosol route of infection (186).

A key virulence determinant of *B. mallei* and *B. pseudomallei* is the ability to invade, replicate, and traffic within host cells, including professional phagocytic cells (41). Once within a host, a bacterium will begin to encounter host cells. Upon infection, the bacterium adheres to the host cell through the use of adhesins. Two adhesins studied by the Lafontaine laboratory are ***B****urkholderia* ***O***ca-like **A**dhesin (*boa*) *A* (155) and ***B****urkholderia* ***p****seudomallei* **a**utotransporter (*bpa*) C (22). Additionally, *B. mallei* and *B. pseudomallei* both have the Type IV pilus subunit encoding gene *pilA*, and *B. pseudomallei* expresses BoaB which further promotes adhesion to epithelial cells (155). Once attached to a cell, bacteria will begin to invade the cell or be phagocytosed if the cell is a phagocytic cell (6, 279). A common way to invade a cell is through the use of flagellar motion to punch through the wall. This mechanism is possible for *B. pseudomallei,* but not for *B. mallei* as it lacks flagella due to frameshift mutations in its flagellar biogenesis genes (29). A second common way for bacteria to invade a cell is through the use of Type 3 Secretion Systems, which are a syringe-like structure of around 20 distinct proteins that spans from the

bacterial inner membrane, through the thin peptidoglycan layer, and through the outer membrane. Both *B. mallei* and *B. pseudomallei* are able to express a type 3 secretion system (T3SS) that has homology with the *inv/spa/*prg and *ipa/mxi/spa* T3SS of *Salmonella typhimurium* and *Shigella flexneri*, respectively, referred to as the *Burkholderia* secretion apparatus (bsa) T3SS (187, 210, 211, 261, 263). Three proteins, BopE, BipD, and BsaQ, have been directly implicated in the invasion of epithelial cells. BopE, a homolog of the *Salmonella* SopE and SopE2 effector proteins, is hypothesized to be a guanine nucleotide exchange factor that activates the endogenous ρGTPases Cdc42 and Rac1 that regulate the eukaryotic actin network within a cell (245, 246). Its involvement in invasion was confirmed when a *bopE* mutant was generated using a *B. pseudomallei* strain 1026b showed a significantly stunted ability to invade HeLa cells compared to wild-type *B. pseudomallei* and failed to induce membrane ruffling. Like BopE, BipD, a structural component of the T3SS needle, was shown to be involved in invasion as a separate *B. pseudomallei* mutant was generated that lacked BipD expression had an even greater reduction in the ability to invade HeLa cells (146, 253). BsaQ is largely identical to the *Salmonella typhimurium* effector protein InvA and is believed to be a conserved inner-membrane channel protein found at the base of the T3SS scaffold (187) It was confirmed to be involved in invasion when a knockout mutant was generated using a *B. pseudomallei* K96243 backbone had a 30% reduction in its ability to invade A549 cells. Further, mutation of the *bsaQ* gene resulted in an inability to secrete BopE and BipD (187).

Whether phagocytosed by a professional phagocytic cell or endocytosed by an epithelial cell, once inside, bacteria will need to escape from the phagocytic/endocytic vesicle and replicate intracellularly. Both *B. mallei* and *B. pseudomallei* do this rapidly,

generally within 15 minutes of internalization (67, 279). The major virulence factor involved in this process is BopA (106). A *bopA* mutant in both *B. mallei* and *B. pseudomallei* had a drastically reduced ability to escape the phagocytic vacuole in J774A.1 and RAW 264.7 macrophages respectively. Further, the *B. mallei bopA* mutant was unable to escape the phagocytic vacuole of MH-S murine alveolar macrophage cells (106). Once a bacterium has successfully escaped the vesicle, the expression of biosynthetic pathway genes are vital for intracellular replication and survival. Four such genes, *purM* and *purN*, *hisF*, and *pabB,* for purine, histidine, and *para*-aminobenzoate, respectively, have all been shown to be key genes in this process. Knockout mutants of these genes were produced in both *B. mallei* and *B. pseudomallei* and both mutants had wild-type levels of cell invasion and vesicle escape, but a drastically impaired ability to replicate and grow within the intracytoplasmic environment 198, (208).

In order to persist in the cell after escaping the phagosome, *B. mallei* and *B. pseudomallei* will eventually have to spread both intercellularly and intracellularly to survive as well as evade autophagy. To accomplish this, both species utilize the **B**urkholderia **i**ntracellular **m**otility (Bim) A and Type 6 Secretion System (T6SS) cluster 1 proteins to utilize actin-based motility (237, 257). BimA is an autotransporter with a carboxyl terminus similar in structure to the YadA and Hia autotransporters of *Yersinia enterocolitica* and *Haemophilus influenzae*, respectively (237, 246). BimA has been shown to induce cellular actin rearrangement in both phagocytic and non-phagocytic cells (29). Most bacterial pathogens that are capable of actin-based motility exploit the Arp2/3 complex, a complex of seven highly-conserved polypeptides that is chiefly responsible for actin filament nucleation and arrangement. The Arp2/3 complex is activated by nucleation

promoting factors (NPFs) such as the Wiskott-Aldrich syndrome protein (WASP) family of proteins. The complex can be activated by protein mimics as is the case with the ActA and RickA proteins of *Listeria monocytogenes* and *Rickettisia prowazekii* respectively, or by the production of surface antigens that attract the NPFs such as the IcsA protein of *Shigella flexneri* (237). Actin polymerization has been shown to be achieved in an Arp2/3 complex protein mimic manner in both *B. mallei* and *B. pseudomallei* as evidenced by the *in vitro* production of actin tails by *B. pseudomallei* was observed in both WASP deficient cells as well as cells supplied with an Arp2/3 binding and sequestering effector protein (29, 237). A second gene likely involved in the production of actin tails is *tssE*. A *B. mallei* strain lacking the *tssE* gene was shown to adhere, invade, and escape the vacuole of RAW 264.7 murine macrophages as effectively as wild type *B. mallei*, but had a reduced level of actin polymerization (259). As the T6SS has been suggested to be involved, another key protein is the **H**emolysin-**c**oregulated **p**rotein (Hcp) 1 protein, a hexameric ring structure protein vital to the formation of the T6SS secretion tube (62, 167). By utilizing actin polymerization and T6SS/T3SS effector proteins, *B. mallei* and *B. pseudomallei* are able to escape from/spread to neighboring cells, form **m**ulti-**n**ucleated **g**iant **c**ells (MNGCs) (136, 253), and persist within the cellular environment to be trafficked throughout the host in professional phagocytic cells or enter the extracellular environment and cause bacteremia spreading to target tissues such as the spleen and liver (145).

ANTIGENS OF INTEREST FOR DEVELOPING VACCINES AND MEDICAL COUNTERMEASURES

While there have been some promising vaccine candidates, the field as a whole is still in the antigen discovery phase. With no commercially available vaccine, the push to discover novel protective antigens is a key focus of the field. Some of the best protective antigens discovered so far are BopA, Hcp1, LolC, Capsular polysaccharide (CPS), and purified LPS (80). Monovalent subunit vaccines of BopA (275), Hcp1 (275), LolC (202, 275), CPS and LPS (193, 275), have been generated and tested. Each of these subunit vaccines was able to protect mice against severe acute infection, but failed to achieve compelling levels of sterile immunity (100, 130). This means that the mice were still chronically infected and would eventually, if allowed to progress long enough, die from their infection. Additionally, outer membrane vesicles (OMVs) of *B. pseudomallei* have been used to achieve high levels of protection against acute infection but have also failed to achieve sterile immunity (195-197). Live attenuated strains of *B. mallei* and *B. pseudomallei* lacking the expression of *bimA* (202), *purN* and *purM* (198, 208, 232), *bipD* (253), quorum sensing components (173), and *ilvI* (182), to name a few, have been used with mixed success, but all have been incapable of achieving high levels of sterilizing immunity. While these vaccines have been shown to either provide protection directly or be able to produce passive transfer antibodies capable of conferring protection (15, 124,199), there is still no licensed commercial vaccine (112). With this in mind, other antigens need to be studied.

Our lab is interested in autotransporter antigens. Autotransporters are a large group of virulence factors expressed by Gram-negative bacteria in their outer membranes.

Autotransporters can be characterized by four common structures: The signal sequence or leader peptide that is necessary for the production and secreting of the autotransporter, a transporter domain, a surface exposed passenger domain, and an α-helical linker region that joins the passenger and transporter domains (113). Autotransporters are one of the largest classes of virulence factors in Gram-negative bacteria and have been shown to be involved in flocculation (132), biofilm formation (296), complement resistance (5), intracellular motility and replication (236, 252), and lipolytic activity (295). Additionally, the use of autotransporter proteins has been shown to be a highly effective method of protecting against infection with Gram-negative organisms (4). For example, the DTaP vaccine which is given to prevent whooping cough contains Pertactin, a *Bordetella pertussis* autotransporter protein (131).

Autotransporters can be organized into two mutually exclusive groups based on the structure of their C-terminal transporter domain, the region of the autotransporter that anchors it into the outer membrane of the bacterium. Conventional autotransporters have a large C-terminus with 10 to 12 ß-strands and are expressed as monomers. Oligomeric autotransporters, by contrast, have much shorter C-terminus structures that typically form four anti-parallel ß-strands and are expressed as trimers. Sequenced genomes of *B. mallei* and *B. pseudomallei* have been shown to have eight autotransporter genes in common (4, 226, 233). Six of these genes are believed to encode oligomeric autotransporters while the remaining two are predicted to specify conventional autotransporters. Previous work by the Lafontaine laboratory has functionally characterized four of these, namely BoaA (155) and BpaC (22) (in *B. pseudomallei* and *B. mallei*), and BpaB (296) and BatA (295) (in *B. mallei).* The aforementioned intracellular motility protein BimA, which is classified as an

oligomeric autotransporter, has been characterized functionally in *B. mallei* and *B. pseudomallei* by other groups (29, 237, 246).

BoaA is an oligomeric autotransporter with a high degree of sequence and structural similarity to other known bacterial adhesins, namely the oligomeric coiled-coil adhesion family such as YadA and Hia from *Yersinia enterocolitica* and *Haemophilus influenzae*, respectively (155). The *boaA* gene can be found in all *B. mallei* and *B. pseudomallei* isolates sequenced to date for which genomic data are available and the genes share a high degree of similairity (>90%) between the two species with most of the differences being accounted for by the differing number of SLST repeats as shown in figure 2.5 (45). BoaA was shown to be an adhesin when the *B. mallei* ATCC 23344 sequence of the *boaA* gene was cloned into an expression vector which was then introduced into *E. coli* EPI300. When inserted into *E. coli*, the non-adherent bacterium was able to adhere to HEp2 and A549 cells at levels that were significantly higher than those of the wild-type. This was further shown when a *boaA* gene mutant of *B. mallei* ATCC 23344 displayed a significantly reduced ability to bind to HEp2 and A459 cells (45). Taken together, this illustrates the potential importance of BoaA as a target for countermeasures as adherence is a crucial step in the pathogenesis of both *B. mallei* and *B. pseudomallei*. Interfering with, or removing, adherence to host cells represents a key step in the infection process that could be targeted.

BpaC is also an oligomeric autotransporter that was shown to be expressed *in vivo* during the acute phase of infection with both *B. mallei* strain ATCC 23344 and *B. pseudomallei* strain DD503 evidenced by the production of anti-BpaC antibodies in mice infected with both organisms (22). The *bpaC* gene product has sequence and structural

similarities to known bacterial adhesins and produces a 94.7 kDa protein in *B. mallei* ATCC 23344 and a 107.4 kDa protein in *B. pseudomallei* DD503 as shown in figure 2.6 (22). *Burkholderia mallei* and *B. pseudomallei* mutants lacking expression of the *bpaC* gene did not have significantly reduced LD_{50} values when used to infect mice, however, indicating that BpaC is not necessary for virulence. When the *bpaC* gene of *B. pseudomallei* strain DD503 was cloned and constitutively expressed in *E. coli* EPI300, however, the previously non-adherent *E. coli* cells bound to HEp-2 laryngeal/NHBE human bronchial epithelial and A549 human lung epithelial cells at levels 7- and 5- fold greater than *E. coli* that were carrying a control plasmid lacking the *bpaC* gene, respectively (22). This demonstrates that while not necessary for virulence, the *bpaC* gene is still involved in the adherence of *B. mallei* and *B. pseudomallei* to cells which is a key step in the pathogenesis of both organisms (22). *Burkholderia mallei* and *B. pseudomallei* contain numerous adhesins including the Type IV pilus making the targeting of a single adhesin potentially ineffective, however, its involvement in this key pathogenesis step makes it a potential target for developing countermeasures.

BpaB is an oligomeric autotransporter that was initially characterized in *B. pseudomallei* (locus tag BP106B_I2046) whose expression coincides with the ability to adhere to human lung epithelial cells (296). BpaB has also been shown to be a virulence factor that is expressed *in vivo* during infection evidenced by the presence of antibodies targeting BpaB found in the sera of mice infected with wild-type *B. mallei* and an 8-14 fold reduction in virulence of a mutant strain of *B. mallei* ATCC 23344 lacking expression of the *bpaB* gene (296). To determine its role in *B. mallei* adherence, the *bpaB* gene of *B. mallei* ATCC 23344 (locus tag BMA0840) was inserted into an expression vector and

introduced into *E. coli* EPI300. It was determined that overexpression of the *bpaB* gene in *E. coli* EPI300 resulted in the adherence of *E. coli* to A549 lung epithelial cells at a 5-fold greater level than *E. coli* carrying a vector control (296). In addition to increased attachment to A549 cells, expression of the *bpaB* gene in *E. coli* EPI300 coincided with the formation of a biofilm. Further, when the *bpaB* gene was overexpressed in a *B. mallei* mutant lacking the expression of *bpaB*, a biofilm was again present. The gene product of the *bpaB* gene is a trimeric autotransporter that is 1,090 amino acids long with a predicted molecular weight of 105-kDA in *B. mallei* ATCC 23344 as shown in figure 2.7 (296). BLAST searches indicate that the *bpaB* gene is highly conserved among all fully sequenced *B. mallei* and *B. pseudomallei* isolates for which there is genomic data available with >99% sequence identity among the sequences that were compared (296). While antibodies produced against BpaB were detected in the serum of mice infected with *B. mallei* ATCC 23344, production of the protein by *B. mallei* or *B. pseudomallei* was not detected under routine *in vitro* growth conditions in the laboratory suggesting that it is exclusively produced *in vivo* (296). The reduction in virulence when expression is neutralized, its exclusive *in vivo* expression, and being the first suspected biofilm formation factor for *B. mallei* makes it a potentially valuable target antigen for the development of countermeasures.

BimA is an oligomeric autotransporter that has a high degree of similarity with the YadA protein of *Yersinia enterocolitica* (237). It is the only autotransporter mentioned here that was not functionally characterized by the Lafontaine lab in *B. mallei*. The protein has proline-rich motifs that are common to actin formation factors in other bacterial pathogens such as the PRM1 region of *Listeria* ActA, and was thus hypothesized to be involved in the observed actin-based motility of *B. pseudomallei* and *B. mallei* (237). This function

was confirmed in *B. pseudomallei* when a *bimA* gene mutant lacking its expression was generated using a *B. pseudomallei* 1026b backbone was able to adhere to, invade, and escape the phagocytic vacuole of J774.2 murine macrophages but failed to polymerize actin once in the cytoplasm (237). *Burkholderia mallei* also contains a *bimA* gene that has been shown to be vital to the polymerization of monomeric actin tails, but there is a significant degree of sequence variation between the gene of *B. mallei* and the gene of *B. pseudomallei* as shown in figure 2.8. Despite the sequence variation, the *bimA* gene has been shown to have the same function in *B. mallei* (237). Further, it has been shown that a *bimA* gene taken from both *B. mallei* (BMAA0749) and the more distantly related *B. thailandensis* (BTH_II0875) can restore the actin-based motility phenotype of the BimA deficient *B. pseudomallei* mutant (237). The importance of this protein as a virulence factor has been demonstrated as antibodies against the *B. pseudomallei* BimA protein can be found in abundance in mice and hamsters infected with *B. pseudomallei* as well as its ability to confer some protection against challenge with *B. pseudomallei* (237). Also, its requirement for intracellular motility, a key step in pathogenesis, makes it an attractive target in the development of countermeasures.

Unlike the previously mentioned autotransporters, BatA is a conventional autotransporter rather than an oligomeric. The Lafontaine lab identified an ortholog of the *B. pseudomallei* K96243 *batA* gene (BPSL2237) on chromosome I of the *B. mallei* ATCC 23344 genome (BMA1647). Further, the *batA* genes were found to be highly-conserved between 30 distinct *B. mallei* and 325 *B. pseudomallei* isolates with >99% identity shared between all of them. It has been shown to encode an outer membrane protein of 64 kDa and sequence analysis showed that it possessed the key features of a conventional

autotransporter such as a 12 β-strand transporter domain as shown in figure 2.9. Through analysis with the NCBI Conserved Domain Database service it was determined that the gene product belongs to the SGNH_hydrolase superfamily much like the EstA and McaP proteins of *Pseudomonas aeruginosa* and *Moraxella catarrhalis*, respectively (295). Proteins of this family are typically lipases or esterases (295). The *batA* gene product contains a highly conserved GDSL motif, which is a common bacterial lipase/esterase motif (295). Based on sequence and structural similarity to the EstA and McaP proteins the *batA* gene product was predicted to have lypolytic activity, which was later confirmed through the use of pNitrophenyl cleavage assays. The BatA protein has been shown to be a virulence factor that is expressed *in vivo* due to the presence of anti-BatA antibodies in the serum of mice infected with *B. mallei* and a greatly reduced virulence of a *B. mallei batA* mutant. It is also important to note that the *batA* mutant was cleared by the mice by 25 days post-infection, meaning the bacteria fail to establish a chronic infection within the mice. Taken together, the expression of the protein *in vivo*, the high degree of conservation of the protein among *B. mallei* and *B. pseudomallei* isolates, and the greatly reduced virulence of the *batA* mutant all suggest that it is an important antigen that can be studied for use in the development of countermeasures.

NON-SUBUNIT VACCINE STRATEGIES

Live-Attenuated Vaccine Strains

The guiding principle behind the use of live-attenuated vaccines is that a sufficiently weakened pathogen can trigger a host immune response, and even multiply and persist to an extent, but is not capable of establishing a long term infection in a host. Two

common ways of creating live-attenuated strains is the successive passaging of viruses through a non-human host cell line, most commonly chicken embryos or a canine kidney cell line (MDCK cells) until the virus is no longer capable of replicating well in a human cell line, and the deletion of bacterial virulence genes.

Several live attenuated strains of *B. mallei* and *B. pseudomallei* have been generated and examined as potential vaccines including the *aroC* (242), *purM* (198, 208), *relA* (9, 188), and *spoT* (9. 188) gene knockouts of *B. pseudomallei* and the *bimA* (236, 237, 244), *hcp1* (167), *tonB/hcp1* (124, 149-150, 185), and *batA* (295) genes of *B. mallei* to name a few. While many attempts at generating a live-attenuated vaccine have been made, so far none has been able to be licensed, though the *tonB/hcp1* double knockout mutant has been proposed as a Tier 1 Select Agent excluded strain as of 2019 (149-150). While there are many who pursue this as a viable vaccine strategy, as shown by its effective use in other bacterial strains, there is a considerable amount of dissention in the field due to the risk of misuse of strains excluded from the strict regulation of *B. mallei* and *B. pseudomallei* as well as the risk of natural reversion of attenuation from horizontal gene transfer of genes potentially capable of restoring virulence.

Outer Membrane Vesicle Vaccination

One common feature of Gram-negative bacteria is the production of outer membrane vesicles. These are generated as portions of the outer membrane of Gram-negative bacteria which lack membrane-peptidoglycan layer bonding extend outward forming blebs which become secreted into the extra-cellular milieu. This process allows

bacteria to secrete portions of their outer membrane as well as their periplasm in an ATP-independent manner, though there remains the inherent cost of replacing the material lost in the process (195-197). Often, these OMVs contain insoluble proteins, though soluble proteins can also be found in OMVs as well (134-135). While the process of generating OMVs readily occurs, bacteria can be stimulated to produce them in orders of magnitude higher concentration compared to their basal production rate in a process known as hypervesiculation (266).

The use of OMVs as vaccines is dependent on either an adjuvanted or non-adjuvanted delivery system, and can be harvested from wild-type bacteria or from mutants over-expressing an antigen of interest. OMVs are inherently immunogenic, containing LPS and other outer membrane proteins, carbohydrates, and lipids (195-197). Their use as potential vaccines was examined in both mice (195, 197), and non-human primates (21), using OMVs produced by a *B. pseudomallei purM* knockout mutant strain (195-197). A major benefit of OMVs over live-attenuated strains is that they maintain a comparable or greater level of immunogenicity while lacking the inherent danger of using a live whole organism in vaccination. However, much like with the use of live-attenuated strains, there was no demonstrated ability of OMVs to prevent the establishment of a chronic infection of *B. mallei* (21, 195-197).

Phage Display Library Technology

Phage display technology allows for a modern approach for the rapid and high throughput screening of epitopes that are immunoreactive with antibodies. When

antibodies play a large role in the clearance of an infection, as is the case with *B. mallei* and *B. pseudomallei*, those same antibodies can be used to screen a library of small peptide sequences to find a mimic of antigenic epitopes recognized by these antibodies (i.e. mimotopes) which can then be used for vaccination. With that in mind, New England Biolabs has developed a series of phage display libraries known as the Ph.D. Phage Display library available in three separate formats with varying lengths of antigens present in five copies on the minor coat protein pIII of an M13 bacteriophage virion. The phages display a pre-made library of randomly generated epitopes consisting of either a linear seven (PhD-7) or twelve (PhD-12) amino acid chain or a constrained conformational seven (PhD-C7C) amino acid loop. In a process known as biopanning, these pentavalent peptide bearing phages are incubated with immune sera conjugated to a solid surface to allow for the capture of phages. Phages that are not bound to the immune sera antibodies are washed away and the phages that did bind are then eluted. These eluted phages are amplified in *E. coli* and can then be panned again for successive rounds of enrichment. At the end of a series of enrichments, individual colonies of phages can be amplified and used directly in vaccination, or the peptide sequences of interest can be synthesized together with spacers and attached to a carrier such as keyhole limpet hemocyanin (KLH) and used to vaccinate. This process is known as mimotope vaccination and has already been demonstrated to work against other pathogens in a murine model such as *Leishmania infantum* (66), Respiratory Syncytial Virus (247), *Avibacterium paragallinarum* (268), and *Cryptococcus neoformans* (87, 291), among others (58, 63, 82, 99, 117, 172, 201, 204, 239, 267, 269, 280, 282, 288, 292). Additionally it has been used in an attempt to develop medical counter measures against multiple types of cancers (90, 119), toxins (289) and auto-immune disorders (165).

Alternatively, the sequence of the synthetic epitope can be determined using pre-made primers designed to sequence the region of the bacteriophage genome in which the synthetic peptide gene is located. Once the sequences are known, they can be used to search a database of endogenous proteins in a desired species. Once identified, these genes can be used in deletion and overexpression mutants, or the entire protein can be studied for use as a vaccine.

INFECTION MODELS USED TO STUDY *BURKHOLDERIA MALLEI* AND *BURKHOLDERIA PSEUDOMALLEI*

Rodents have been widely used as infection models of both melioidosis and glanders (272). Of the rodent models, Balb/C and C57BL/6 mice are the most widely used (271-272). Additionally, guinea pigs, hamsters, and certain types of immunocompromised mice/rats are also used (271). In addition to rodents, horses, donkeys, mules, dogs, cats, sheep, and goats have also been used (151, 271). Horse, donkey, and mule models are particularly valuable due to their being solipeds, the natural host of *B. mallei*. Non-human primate models have been established in rhesus macaques, African green monkeys, and the common marmoset (192). Finally, the Madagascar hissing cockroach and the wax moth larvae have been used to model individual virulence factors of the organisms rather than the full host-pathogen interaction (226). The Lafontaine and Hogan laboratories have established two animal models for use in *B. mallei* and *B. pseudomallei* infection studies, the mouse aerosol infection model (156) and the common marmoset (142).

In order to perform our infection studies, our group developed a safe, reproducible, and rapid aerosol delivery method to study glanders and melioidosis in BALB/c and

C57BL/6 mice. In addition to being safe and highly reproducible, the resulting infection caused pulmonary infection rather than nasal infection, a common problem with traditional nasal inhalation models (161). In our model, mice are first sedated with approximately 250 ul of Tribromoethanol (TBE). Mice are suspended by their front teeth on a work stand and a fiber optic arm equipped with a light source is placed over the front of the throat of the suspended mice as shown in figure 2.10. The mouth is opened and the tongue is displaced using forceps. A modified pediatric otoscope is used to guide the nebulizing portion of a Penn-Century Model IA-1C Microsprayer into the tracheal opening between the vocal cords. Once in position agent in aerosolized directly into the lower respiratory tract. The microsprayer device consists of 2 parts. The first part is a high pressure stainless steel syringe in which bacterial suspensions are loaded. The second part, which is attached to the syringe, is the aforementioned nebulizing portion. It consists of a 23 gauge flexible tube fitted with a diamond at the tip which functions as a nebulizer as fluids are pushed through it (156). This published method has allowed for the reproducible infection of mice in our laboratory.

The common marmoset infection model, also developed by the Lafontaine and Hogan labs, serves as a higher order large animal infection model for the characterization of intranasal infection with *B. mallei* (142). In this model, male and female adult *Callithrix jacchus* marmosets (>36 months old) were obtained from Worldwide Primates Inc. Marmosets were anesthetized in their nest boxes using an inhaled isoflurane gas method. Once appropriately anesthetized, the marmosets were restrained on their backs with their faces up and 50ul of agent was dispensed directly into the right nostril in 5-10 ul increments using a pipetman with sterile filtered tips. Once infected, marmosets were allowed to

recover on heating pads at a temperature of 37 °C. This model allows for the study of *B. mallei* infection in a dose-sensitive manner that accurately and reproducibly models the disease course of glanders in a manner similar to other infection models (156).

FIGURE 2.1

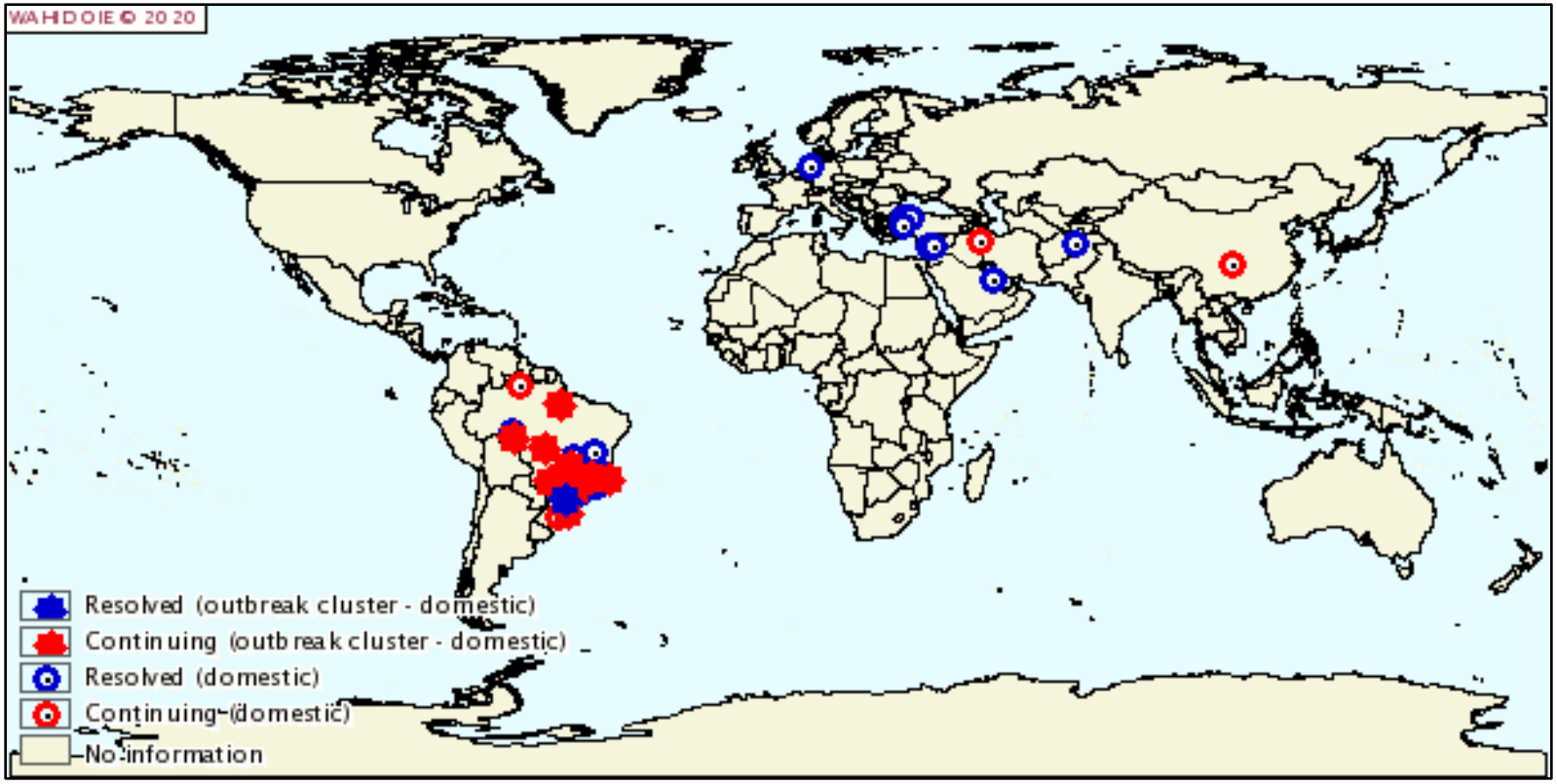

OIE World Animal Health Glanders Distribution Map from 1-1-2005 to 12-31-2019. As shown, there are sporadic outbreaks in the Middle East, Eastern Europe, Asia, and South America. Brazil, China, and Iran are currently undergoing active cases of Glanders as of January 2020. This map does not include data from Africa or Southeast Asia, both of which have sporadic and active cases for Glanders as of January 2020 (37).

FIGURE 2.2

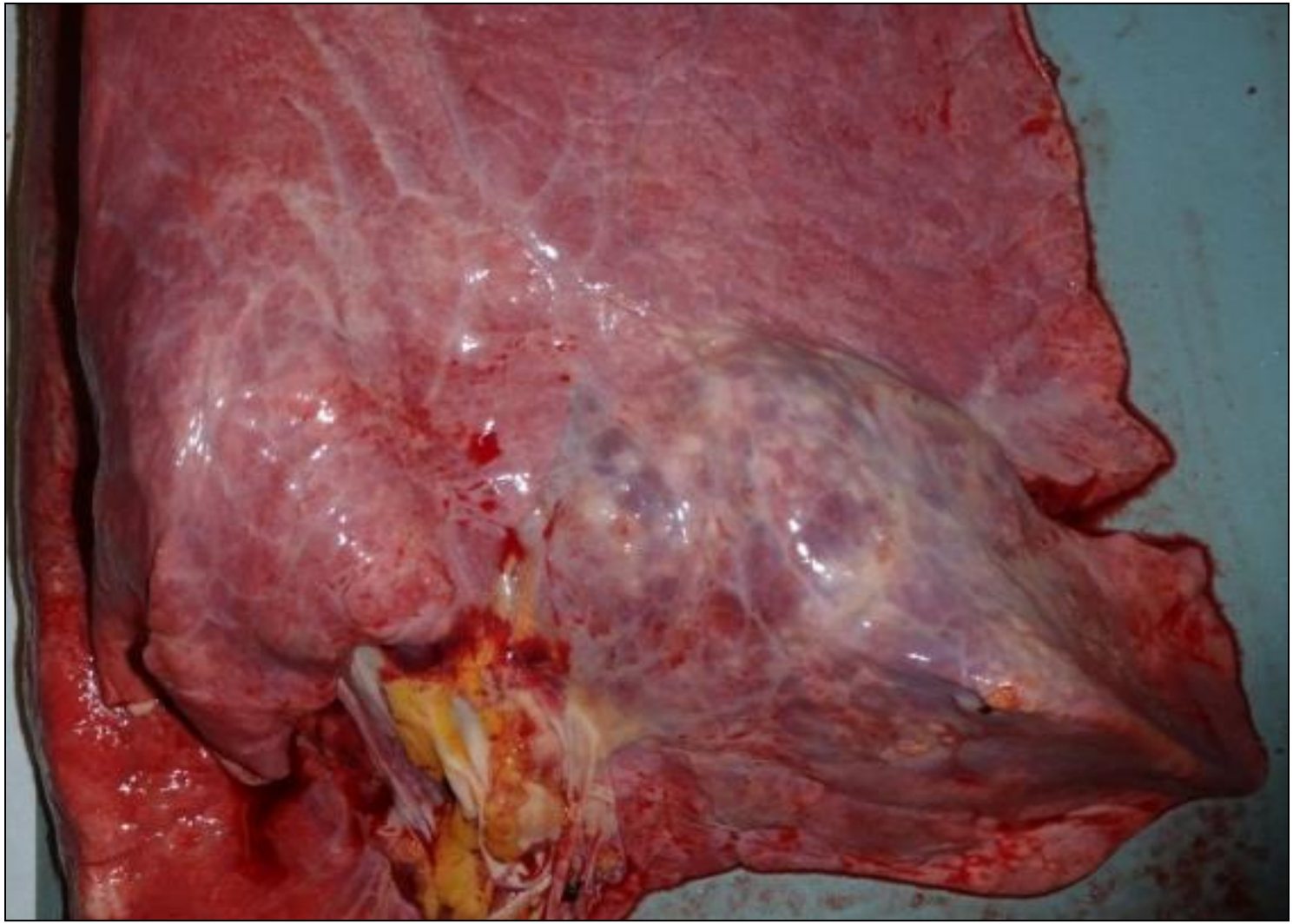

Shown is a lung from a horse suffering from pulmonary glanders. Note the large abscess with black necrotic regions as well as the purulent discharge.

FIGURE 2.3

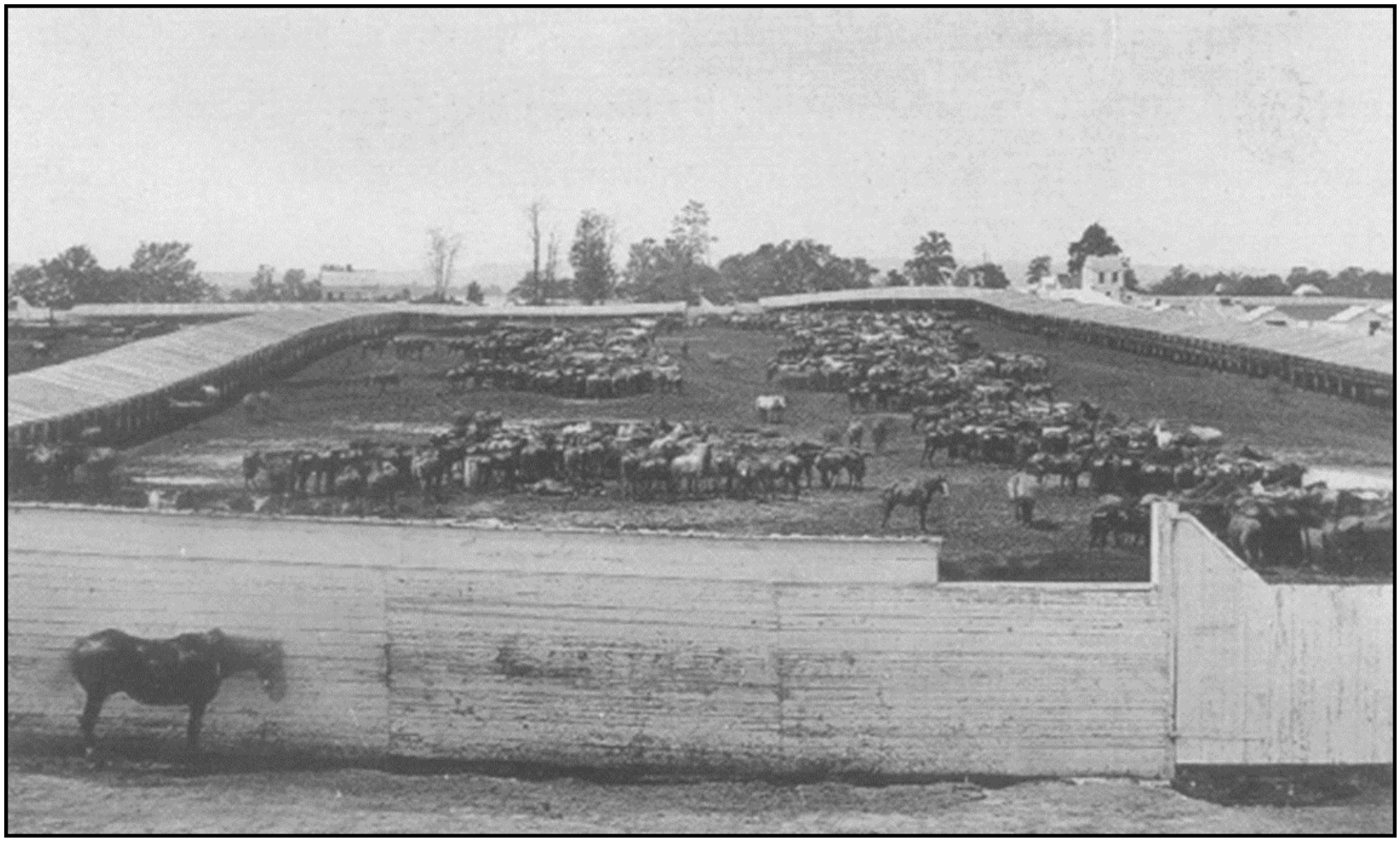

Shown here is the Giesboro Point Remount Station near Washington D.C. circa 1865. Remount Stations were horse storage depots used by the U.S. Army as part of the Quartermaster Corps that allowed for the remounting of cavalry units until 1918 when the service was turned over to the Department of Agriculture.

FIGURE 2.4

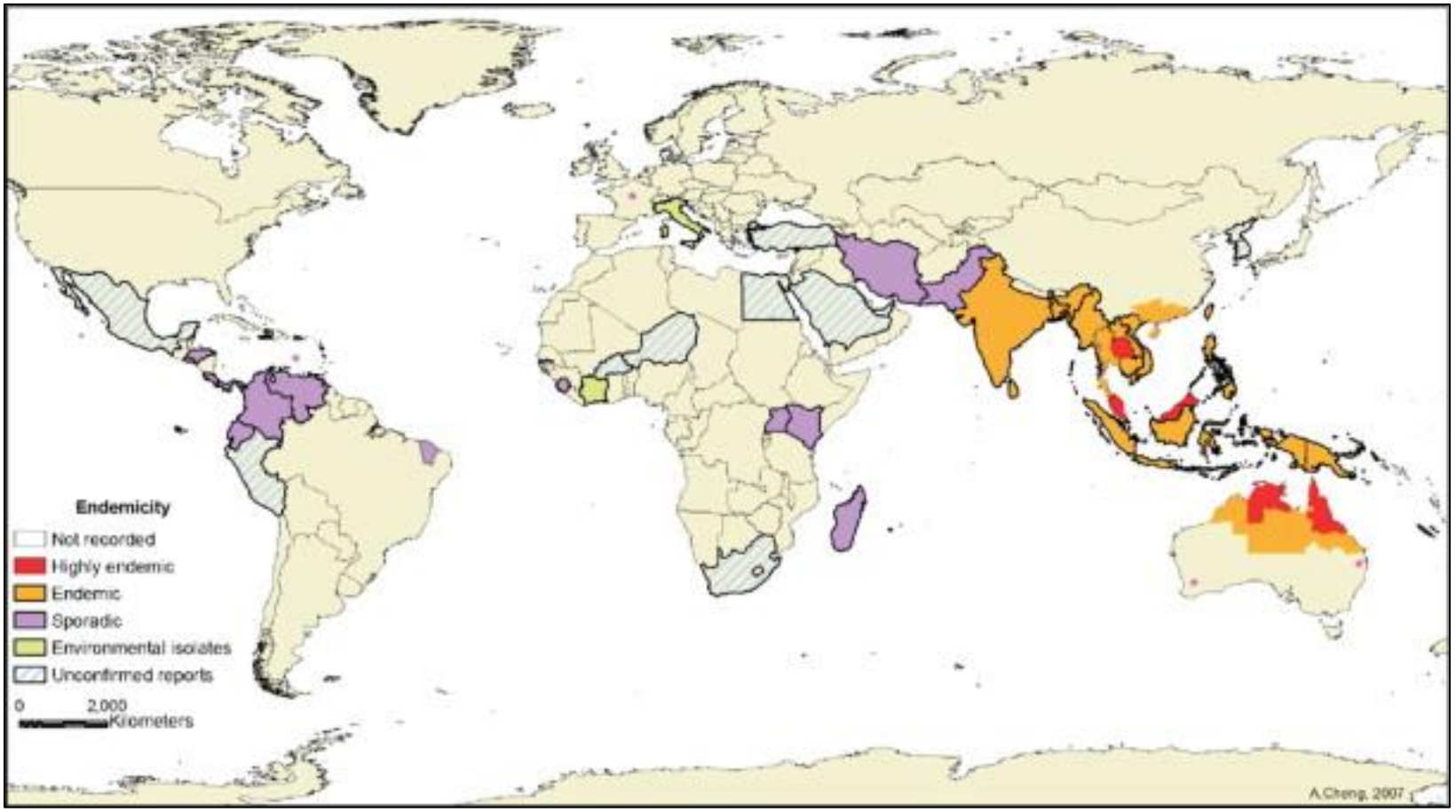

Shown here is the environmental range of *Burkholderia pseudomallei*. As shown, it is endemic to regions along the equator, with edemicity especially high in Northern Australia and Southeast Asia. (254)

FIGURE 2.5

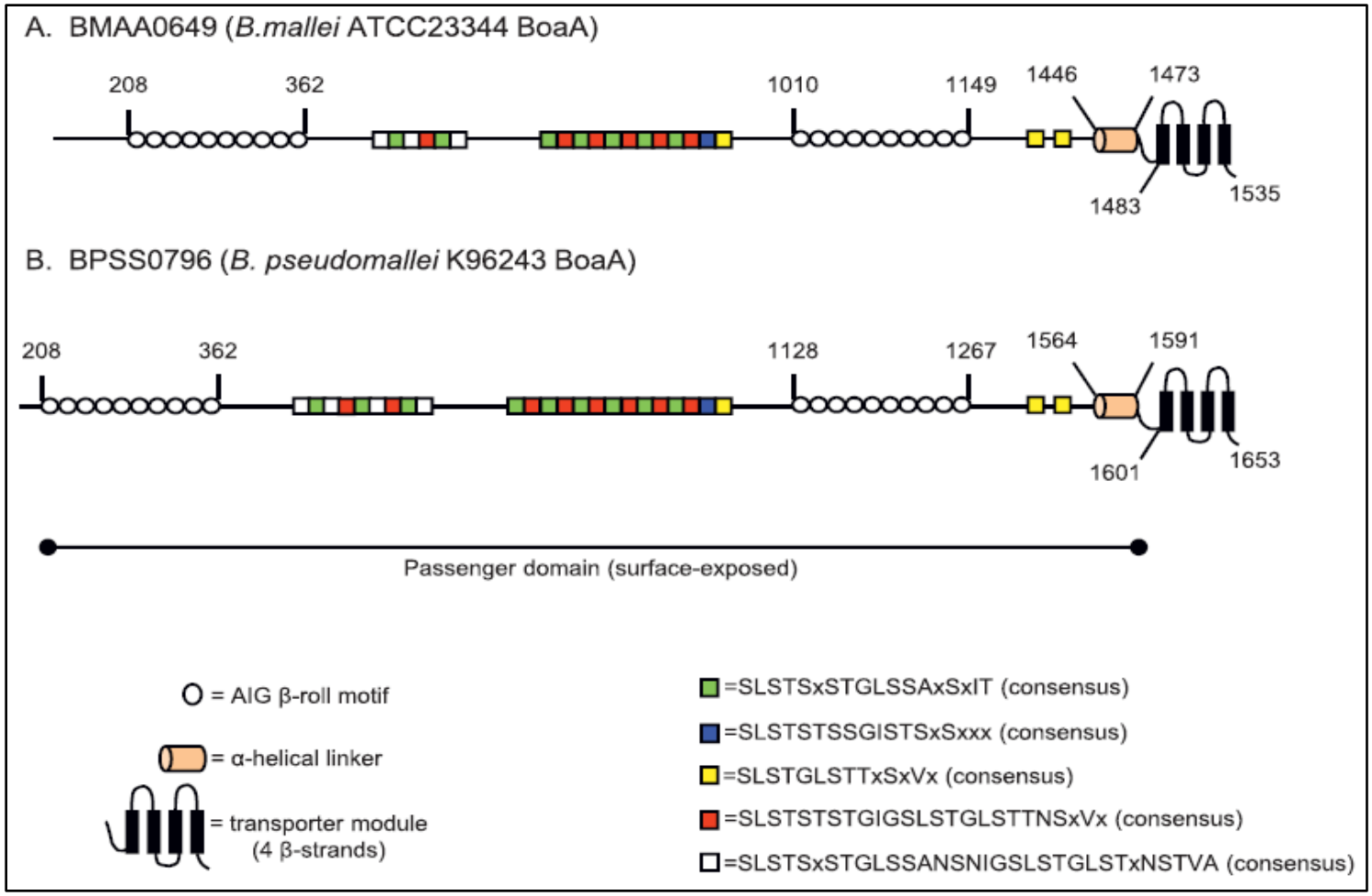

Schematic of the gene products of the B. mallei ATCC 23344 (A) and B. pseudomallei K96243 (B) boaA genes showing the structural features of each product including the transporter domain, the α helical linker, and the passenger domain. Colored squares indicate consensus SLSTS 5-mer residues. (155)

FIGURE 2.6

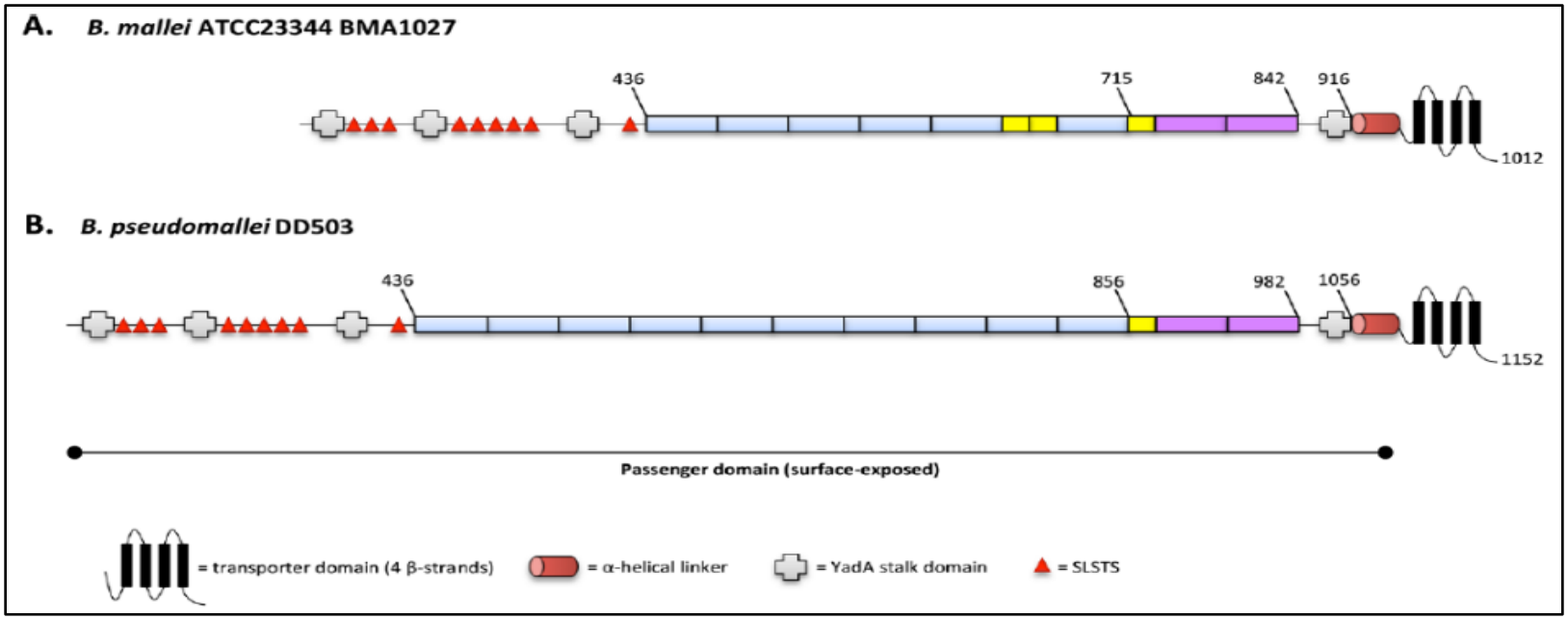

Schematic of the gene products of the *B. mallei* ATCC 23344 (A) and *B. pseudomallei* DD503 (B) bpaC genes showing the transporter domain, α helical linker, and passenger domain indicated for each. (22)

FIGURE 2.7

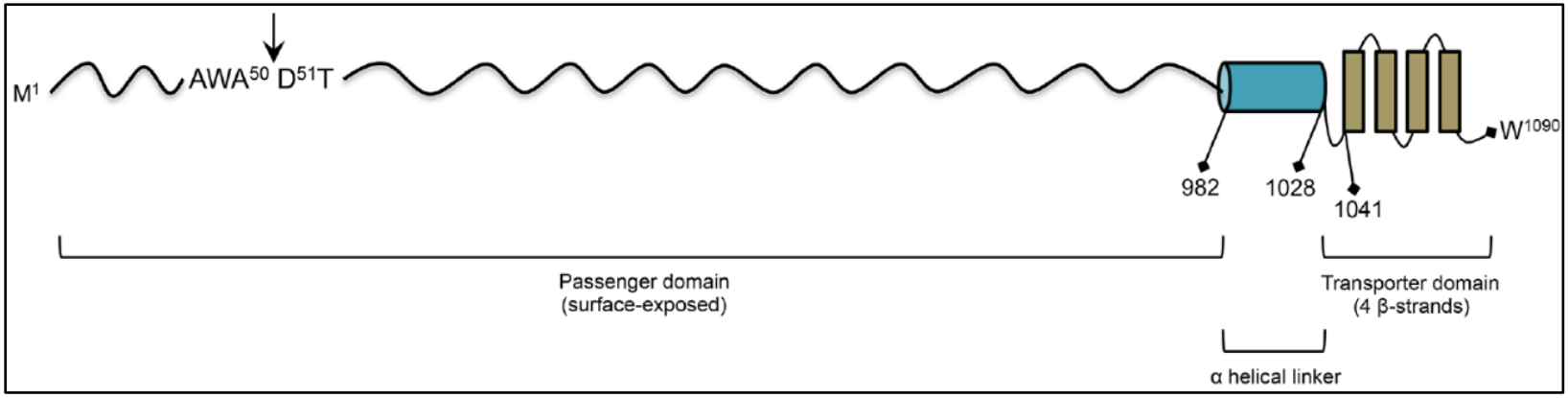

Schematic of the *B. mallei* ATCC 23344 bpaB gene product showing the predicted regions of the BpaB protein including the transporter domain, the α helical linker, the passenger domain, and the signal sequence/signal. (296)

FIGURE 2.8

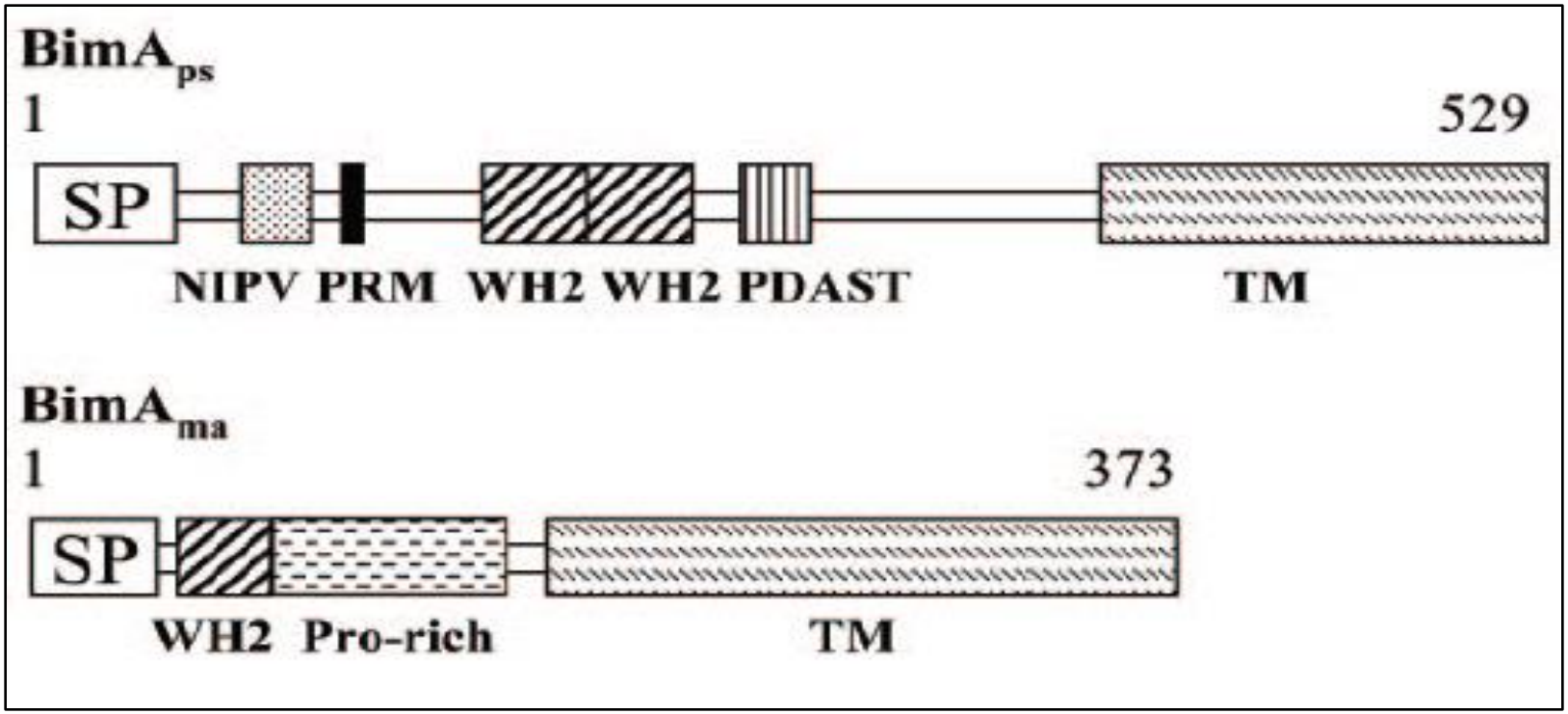

Schematic of the gene products of the *B. pseudomallei* (top) and *B. mallei* (bottom) *bimA* gene with the transporter domain (TM), signal sequence (SP), and passenger domain shown. As shown, both contain a proline-rich domain (PRM and Pro-Rich) as well as at least one WH2 domain which has been shown to be essential for actin binding. (237)

FIGURE 2.9

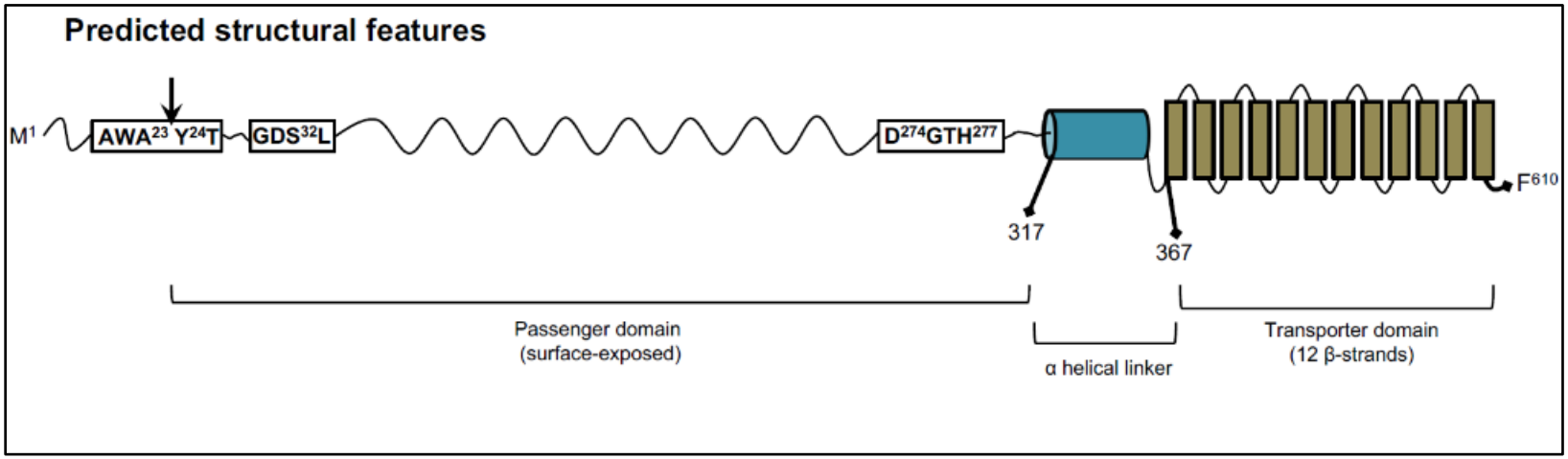

Schematic of the *B. mallei* ATCC 23344 *batA* gene product illustrating the large conventional transporter domain, the alpha-helical linker, the passenger domain, and the signal sequence/sequence cleavage site (295).

FIGURE 2.10

Mice are sedated and suspended on a work stand by their front teeth with a fiver optic light over their throats (left). Once in position, a modified pediatric otoscope guides the nebulizing portion of a microsprayer into the tracheal opening where a bacterial suspension can be aerosolized directly into the lower respiratory tract (right) (156).

CHAPTER 3

THE USE OF MIMOTOPE ANTIGENS FOR VACCINATION AND NOVEL *IN VIVO* ANTIGEN DISCOVERY IN *BURKHOLDERIA MALLEI* AND *BURKHOLDERIA PSEUDOMALLEI*

INTRODUCTION

Burkholderia mallei and *Burkholderia pseudomallei* are two closely related Gram-negative bacterial organisms that cause the severe respiratory illnesses Glanders and Melioidosis, respectively (37, 97). *B. mallei* is endemic to the Middle East, Africa, Asia, and South America. It is host adapted to solipeds, and cannot persist in the environment for long periods of time (97). Humans are susceptible to infection by *B. mallei*, but as dead end hosts, and human to human transmission of *B. mallei* is exceedingly rare (97). *B. pseudomallei*, by contrast, is an environmental saprophyte that is endemic to equatorial countries, but is most common in Northern Australia and Southeast Asia (37). Both organisms are highly infectious, difficult to diagnose and treat, and are resistant to most antibiotics. They both cause a high degree of morbidity and mortality, and there is currently no licensed vaccine available to reduce the risk of infection (37, 97). In addition, there is concern that *B. mallei* and *B. pseudomallei* could be misused as biological terrorism or warfare agents. For these reasons, both organisms are classified as Tier 1 Select Agents, and the development of effective vaccines and medical countermeasures is a high priority.

Being closely related organisms, *B. mallei* and *B. pseudomallei* share a large degree of genetic similarity. While *B. mallei* has a smaller genome than *B. pseudomallei,* 5.8 Mb vs 7.2 Mb respectively, the two genomes have >99% sequence similarity where they overlap (97, 171, 226, 233). Comparative analyses indicated that *B. mallei* evolved from *B. pseudomallei* through a large gene deletion event (171, 182, 200). As a result of this genetic similarity, the diseases they cause are also similar. Both illnesses present as either an acute or chronic pneumonia with accompanying bacteremia (85, 97). A major hallmark of *B. mallei* and *B. pseudomallei* infection is the capability of each organism to persist for long periods of time in a host, surviving and replicating within professional and non-professional phagocytic cells, and evading clearance by the immune system through modulation of the expression of major virulence determinants (11, 67, 97, 279).

Currently, there is no commercially available vaccine for either organism due largely to an absence of effective antigens. Experimentally, lead candidates in the field are capable of conferring protection against acute infection with *B. mallei* and *B. pseudomallei*, but there remains the issue of chronic persistent infection which will inevitably lead to death. A major hurdle in the discovery of novel protective antigens is a lack of *in vitro* expression of major classical virulence factors. While the two genomes contain numerous virulence hallmarks, they are often not produced at detectable levels by the organisms under routine growth conditions. Due to this disparity of *in vivo* vs *in vitro* expression of these potentially valuable antigens, the field has largely focused on constitutively expressed classical factors such as Lipopolysaccharide (LPS) (80, 193, 275) and capsular polysaccharide (CPS) (193, 275) as well as on live attenuated strains such as the *ilvB* (182) and *tonB* (149-150) knockout mutants. While live attenuated strains are capable of

conferring a high degree of protection, they are unlikely to be licensed and used widely due to past eradication efforts and the potential for restoration of virulence. Despite their likelihood of licensure, their study remains a valuable endeavor as it allows for the *in vivo* characterization of a known antigen's importance in virulence, once a novel antigen is discovered.

In previously published work, while characterizing a live attenuated strain of our own, a *batA* knockout mutant of *B. mallei*, we discovered that the mutant lacking expression of *batA* was highly attenuated in virulence, and was completely cleared by BALB/c mice that had been infected with doses equivalent to 80 median lethal doses of wild-type organisms (295). Further, we found that when mice were inoculated with the *batA* knockout mutant then subsequently back-challenged with wild-type bacteria, the mutant conferred a high degree of protection against both *B. mallei* and *B. pseudomallei* (295). When serum was collected from mice vaccinated with the *batA* knockout mutant and used in serum transfer experiments, we found that serum alone was capable of conferring protection against *B. mallei* and *B. pseudomallei*, even when that serum had been depleted of antibodies reactive with plate grown bacteria (295). In order for this to be possible, the immune system of the BALB/c mice must be responding to antigens that are expressed by *B. mallei* during the course of infection *in vivo* but not *in vitro*. The ability of these antigens to spur the production of cross-protective antibodies renders them as high value immunoprotective targets for developing vaccines and countermeasures. Their identification and validation as vaccine candidates could lead to the discovery of novel protective antigens and advance the field through the expansion of available targets.

One method of discovering novel antigens is the use of peptide display libraries. In this method, a set of peptides is displayed on a living or synthetic surface, and probed for reactivity with antibodies. The peptide library can be a small or large collection of known or unknown short or long peptides. There are several different published methods, but generally either antibodies are immobilized to a surface and tagged epitopes are exposed to the antibodies. Peptides that are recognized by the immobilized antibodies are bound and retained while those that are not are washed away. In some systems the library of peptide epitopes is generated by the user, while in others a library of known or randomly generated peptides conjugated to an abiotic surface or expressed by a living cell is purchased from a commercial vendor. Once probed, the obtained peptides can be used to screen the proteome of an organism to discover orthologous proteins, or can be used directly in vaccination through a process known as mimotope vaccination. Here, we describe the use of a commercially available M13 Bacteriophage based peptide library as a vehicle for the discovery of novel antigens expressed exclusively *in vivo* by *B. mallei* through the use of a process we termed biopanning, a simplified flowchart of which can be found below (Fig 3.1).

RESULTS

Reactivity Between Immune Serum and Constitutively Expressed *in vitro* Antigens is Lost with Adsorption and Panning

Our lab has previously shown that passive transfer of serum from mice vaccinated with the *batA* knockout mutant is sufficient to protect mice against acute lethal infection of *B. mallei* (295). Additionally, we have shown that serum depleted of antibodies reactive

with constitutively expressed *in vitro* antigens from plate grown *B. mallei* is also capable of conferring protection (295). We believed that this adsorption process removed all antibodies reactive with *in vitro* expressed antigens. However, we observed that despite being adsorbed using live, plate grown *B. mallei* ATCC 23344, adsorbed immune serum still maintained reactivity with whole cell lysates of *B. mallei* ATCC 23344 grown on agar plates (Fig 3.2 A). We reasoned that this reactivity must be to antigens found within the bacterial cell rather than on its surface that the immune system is only exposed to during the immune response as these antigens would not be available to the serum during the adsorption process using intact cells. In order to remove these antibodies from our serum samples, we did a second round of adsorption using whole cell lysates of plate grown *B. mallei* ATCC 23344 rather than intact live cells. After the second round of adsorption, which we termed panning, all reactivity between the adsorbed immune serum and the *in vitro* grown whole cell lysates was removed. However, there remains reactivity between lysates of tissues containing *in vivo* expressed *B. mallei* ATCC 23344 antigens (Fig 3.2 B). In order to confirm that the reduced reactivity was from a true removal of antibodies specific to *in vitro* expressed antigens rather than a dilution effect, the amount of IgG in the samples was quantified so that equivalent amounts of IgG could be used in the screening and subsequent experiments (Fig 3.2 C). While the concentration of IgG had been reduced due to dilutions, there still remained a significant enough amount that equivalent amounts of antibody could be used.

Protein G Beads can be Saturated with IgG Antibodies from Naïve and Panned Adsorbed Immune Mouse Serum

For downstream applications, there was a need for IgG antibodies affixed to a solid and captive surface that could be used to selectively recover reactive phages of interest. To accomplish this, Protein G beads from Miltenyi Biotec were chosen. Protein G beads were saturated with IgG from both naïve mouse serum and panned adsorbed immune serum. After saturation with the preferred IgG, the beads were exposed to a FITC tagged mouse IgG2a monoclonal antibody. We used a Mouse IgG2a monoclonal antibody as the Protein G beads were indicated in the manufacturer instruction kit as having the highest affinity for the mouse IgG2a isotype. This high affinity would allow any free unsaturated spots to bind the FITC-labeled monoclonal antibody. There is a high degree of variability between the numbers of beads retrieved from the column during repeated wash and elution cycles (Fig 3.3 A-D). However, despite the number of beads retrieved there is an obvious shift in fluorescence when the beads do (Fig 3.3 B) and do not (Fig 3.3 A) bind the FITC tagged monoclonal antibody. This shift in fluorescence allows us to rapidly establish our beads as either saturated or not saturated. We concluded that our beads are saturated with naïve (Fig 3.3 C) and 20x panned adsorbed immune serum (Fig 3.3 D), and that the slight shift of the beads post-exposure to the FITC-tagged monoclonal antibody is due to the high affinity monoclonal antibody outcompeting the non-IgG2a IgG antibodies found in the polyclonal serum that will bind to the protein G beads but with a lower affinity than an IgG2a antibody.

Naïve IgG Saturated Protein G Beads can Pre-Clear Irrelevant Mimotopes from the Stock PhD-12 Library

We reasoned that exposure of the PhD-12 phage library to naïve serum coated beads would pre-clear irrelevant mimotopes from the stock PhD-12 library as any epitope reacting with the IgGs would be irrelevant to our needs and would be bound and removed. Using a series of three pre-clearing incubations (Fig 3.4 A), we were able to reduce the overall number of phages in our sample by $>1.0x10^{12}$ (Fig 3.4 B). From this result we concluded that by pre-clearing the stock PhD-12 phage display library at least three times with naïve control serum saturated protein G beads we can remove irrelevant epitope bearing phages from our pool. This is highly advantageous as it allows us to minimize the risk of amplifying an irrelevant phage due to non-specific binding of the phage to the 20x panned adsorbed immune IgG antibodies by simply removing them from the pool of available phages exposed to the immune serum saturated beads.

20x Panned Adsorbed Immune Serum Saturated Protein G Beads can Capture Immunoreactive Phages

Once the library had been pre-cleared three times, a biopanning process was performed using protein G beads saturated with IgG antibodies from 20x panned adsorbed immune serum (Fig 3.4 A). There was a significant reduction in the number of phages eluted from the beads coated with 20x panned adsorbed immune serum (Fig 3.4 B). From this we concluded that biopanning our 3x pre-cleared PhD-12 phage display library with protein G beads saturated with 20x panned adsorbed immune serum IgG antibodies

allowed us to capture and elute phages that were immunoreactive with the 20x panned adsorbed immune serum.

Phages Eluted from 20x Panned Asorbed Immune Serum are Reactive with Immune Serum but Not Naïve Serum

Phages that had been eluted from the 20x panned adsorbed immune serum were screened to ensure that they were reactive with immune serum rather than just non-specifically taken in by the serum coated beads. Phages were used to infect aliquots of *E. coli* which were spread onto agar plates supplemented with Xgal and IPTG and allowed to form visible blue plaques in the *E. coli* lawn. Once visible blue plaques were obtained, phages were transferred to PVDF membranes (Fig 3.5 A) which were then screened in a method similar to a western blot. This method allowed for exact replicas of plates to be formed and screened. Phages were screened using both naïve and immune serum at a dilution of approximately 1:200 and secondary at a dilution of 1:2000. When screened, many phages were reactive with immune serum, while few were reactive with naïve serum. Based on these results, we were able to select a total of 25 phage plaques that were reactive with immune serum but not naïve serum (Fig 3.5 B-D. These phages were amplified and frozen stocks were generated. Once amplified stocks were made of each selected phage, they were used to make duplicate amplifications for use as working stocks to prevent excessive temperature changes to the frozen stock over the course of work. Once working stocks were generated, they were used to generate plaque lifts as done before. Phage immunoreactivity with both anti-M13 MAb and pooled immune IgG was determined as

described previously. 11 phages were chosen as a result of their consistent reactivity over numerous rounds of screening.

Selected Phages are Cross-Reactive with *B. pseudomallei* Immune Sera

The 11 chosen phages were screened for cross-reactivity with serum from mice that survived challenge with *B. pseudomallei*. We hypothesized that highly reactive mimotopes would have some cross-reactivity with antibodies produced against *B. pseudomallei* based on its genetic similarity to *B. mallei*. In order to screen for reactivity, 2 ul of amplified phage working stock or 1:10 dilute lysate control was spotted directly onto activated PVDF circles which had been labeled with a grid to allow for similar layouts between the various screens (Fig 3.6 A). The phages were screened at 1:400 dilutions of the following sera: purified pooled immune IgG from mice vaccinated with the *B. mallei batAKO* mutant, purified Naïve IgG from unvaccinated and uninfected mice, whole mouse serum from mice that were unvaccinated but survived challenge with wild-type *B. mallei*, whole mouse serum from mice that were unvaccinated but survived challenge with wild-type *B. pseudomallei*, mouse serum from mice that were vaccinated with the B. mallei ilvBKO live attenuated strain, a live attenuated strain conferring a lesser level of protection against challenge with wild-type B. mallei ATCC 23344 (Fig 3.6 C-G). Additionally, one set was screened with a 1:10,000 anti-M13 MAb control (Fig 3.6 B). The phages obtained through the biopanning process were cross-reactive with sera from mice who were exposed to *B. pseudomallei*, but were at no point exposed to *B. mallei*, including through vaccination with the *B. mallei batAKO* live attenuated strain. This lack of exposure to *B.*

mallei meant that phages were reactive with serum generated independently of *B. mallei* and were thus capable of cross-reactivity.

Obtained Phage Sequences Share Homology with Endogenous *B. mallei* Proteins

We hypothesized that since the phages were immunoreactive against immune sera from mice exposed to both *B. mallei* and *B. pseudomallei*, and presumably are linear epitopes (12-mer), they represent high value antigens and likely have sequence homology with endogenous antigens and can thus be used to identify potentially immunoreactive proteins. DNA was obtained from amplified stocks of the 11 select phages, and was sequenced by Macrogen Corp. using a sequencing primer that was included in the initial PhD-12 Library Kit. Once sequences were obtained, the epitope encoding region of the phage genomes were obtained and translated into amino acids (Fig 3.7A). The amino acid sequence was analyzed using the Immune Epitope Database (IEDB) from the National Institute of Allergy and Infectious Diseases (NIAID) using the linear epitope prediction algorithm. Using this database, a predicted B cell epitope was obtained for 10 of the 11 chosen mimotopes as one mimotope failed to be sequenced (Fig 3.7B). The obtained amino acid sequences were also analyzed using the protein Basic Local Alignment Search Tool (pBLAST) database from the National Institutes of Health (NIH) National Center for Biotechnology Information (NCBI). Using this tool we were able search a *B. mallei* ATCC 23344 specific database of proteins for structural similarities between the amino acid sequences of the mimotopes present on the bacteriophages and the full proteome of *B. mallei*. We were able to find several regions of overlap between the endogenous proteins and the mimotopes. Further, many of the low e-value hits overlapped with endogenous

proteins with the same sequence as was predicted by the B cell epitope prediction analysis. The epitopes were ranked subjectively based on the results of the screening, the pBLAST results, and the B-cell epitope analysis (Table 3.1).

Vaccination Using Phage Mimotopes and Phage Derived Proteins Fail to Provide a Sufficient Level of Protection Against Wild-Type *B. mallei* or *B. pseudomallei*

Based on the aforementioned results of the phage sequence analyses, full length mature proteins were ordered from Seattle Structure Genomics Center for Infectious Disease (Table 3.2). Additionally, the amino acid sequences of the 10 selected phages were synthesized conjugated to both Keyhole Limpet Hemocyanin (KLH) and Ovalbumine. Mice were vaccinated with amplified phages, conjugated epitopes, and full length mature proteins over the course of 3 separate injections. Initial vaccination was performed using Freund's complete adjuvant, while successive boosts were performed using Freund's incomplete adjuvant. These adjuvants were used as they produce a high level of antibodies which we have shown is important for a successful immune response to *B. mallei* and *B. pseudomallei*. Between each vaccination/boost mice were tail bled to collect serum, and the immune response was measured via ELISA. After 3 rounds of vaccinations, mice were challenged with wild-type *B. mallei* or *B. pseudomallei*. None of the various treatments was able to produce a statistically significant level of protection when compared to the unvaccinated controls (Fig 3.8).

DISCUSSION

Due to a lack of licensed vaccines for *Burkholderia mallei* and *Burkholderia pseudomallei*, as well as a lack of known protective antigens, there remains a high level of interest in the discovery of novel antigens in the field. A major confounding issue in that search is the differential expression of classical virulence factors *in vivo* but not *in vitro*. Because of this disparate expression dynamic, it is difficult to examine antigens of interest. Due to this difficulty, a large amount of research has gone into the study of constitutively expressed *in vitro* antigens (i.e. Capsular polysaccharide or CPS, Lipopolysacharide or LPS, etc.).

While these pursuits have been fruitful, and extensive progress has been made in developing protection against acute lethal infection with wild-type *B. mallei* and *B. pseudomallei*, there remains a need for vaccines or medical countermeasures capable of conferring protection against the development of chronic infection which will itself inevitably lead to death. The dogma of the field has long been that protection against *B. mallei* and *B. pseudomallei* is largely due to cell mediated immunity. While that is likely a large part of the field, previous work by the Lafontaine Lab has shown that antibodies alone are capable of conferring protection against acute lethal infection, as well as survival through the chronic phase, though it was incapable of conferring sterile immunity (295). This was shown through the use of serum transfer experiments in which immune and naïve serum from mice was given to naïve mice who were subsequently challenged with wild-type agents. One interesting finding was that serum from mice that had been adsorbed with live plate grown wild type bacteria was still capable of conferring a high level of protection.

We found through the course of this work that serum adsorbed of reactivity with plate grown *B. mallei* was still reactive with whole cell lysates of *B. mallei*. We reasoned that this reactivity was from antibodies produced against antigens that reside within the cell but are exposed on the surface of antigen presenting cells during the course of the immune reaction. To address this, serum was again adsorbed but with whole cell lysates generated using wild-type *B. mallei*, after which the serum was no longer reactive with whole cell lysates. However, the serum retained reactivity with spleen and lung lysates from mice infected with *B. mallei* while not reacting to control uninfected tissue lysates. This led us to conclude that there are antibodies present in the serum that was depleted of antibodies reactive with *in vitro* expressed antigens. This means that there must be antigens that are expressed exclusively *in vivo* that are causing an immune response. While the truly depleted serum was not used in passive serum transfer experiments, it is likely that it too confers some level of protection, though at a lower level than whole immune serum or adsorbed immune serum. Thus, understanding what these antigens are would be beneficial to not only our lab but to the field as a whole.

In order for the host to produce antibodies in response to the bacteria, they must first be presented with an antigen that is then targeted. When presented with a specific antigen, the body will then produce a specific antibody. In this sense, the natural flow is production of antigen by invading bacteria, interfacing of antigen with immune system through either antigen presenting cell to B-cell or B-cell directly interacting with antigen, and finally production of an immune response. We set out to use antibodies as our starting material which could be used to probe for a matching antigen. One benefit to using antibodies as a starting point was that they can be readily attached to a recoverable working

surface which can be used with an antigen presentation system to probe for a matching pair. In our case, we used Protein G beads as they bind the Fc region of the antibodies leaving the Fab region projected outward and able to bind to antigens. The use of beads also allowed us to easily verify that they were saturated with antibodies through use of a flow cytometer. Beads that were thought to be saturated with immune serum derived IgG antibodies were given a dose of FITC tagged IgG2a antibodies. If any binding region on the bead had remained unbound, it would have readily taken up the FITC tagged antibody and would thus have a visible shift with the flow cytometer. As our antibodies did not have the tell-tale shift in fluorescence we concluded that they were saturated and thus any binding of the antigen library would not be incidental to the protein G binding surface of the beads.

Our library of choice was the New England Biolabs PhD-12 Phage Display Library. This system was chosen as it was commercially available with a high level of quality control and was either used directly in other studies performed by other labs or was similar to other libraries used. Additionally, it could be purchased in a kit that included empty vectors that could be used as a control and pre-generated sequencing primers that bound to sequencing tags that had been inserted into the genome of the M13 bacteriophages. The New England Biolabs PhD-12 system is a library of randomly generated 12 amino acid linear epitopes that are expressed in 5 identical copies (i.e. 5 copies of the same randomly generated epitope) on the N-terminus of the minor coat protein of the M13 bacteriophage virion. The benefit of using this system is that the M13 virions are easily worked with in small volume suspensions, and can be readily amplified to obtain large quantities of individual epitopes. However, prolonged amplification of phages (>12 hours of

amplification) can result in mutations. Because of this, short amplifications and the use of frozen stocks to continually draw from are vital for the preservation of the initial reactive epitope. Due to the fact that the epitopes were randomly generated, and were present in large numbers (approximately 100 copies of each epitope in 10 uL of volume, $1.0x10^9$ total randomly generated epitopes) there is a large amount of irrelevant epitopes. To address this, we initially pre-cleared the library using beads that had IgG from naïve serum conjugated to their surface. We did this because we reasoned that any epitope that was reactive with naïve serum was either a broadly reactive epitope, a sticky epitope that will likely non-specifically bind to immune serum IgGs, or an irrelevant epitope that would simply be noise in our system. Once these epitopes were removed, we concluded that the remaining epitopes, while potentially still irrelevant, were less likely to be false positives. By winnowing down the number of initial epitopes, we also enriched for potentially valuable epitopes in the starting material used with immune serum beads.

Once the library was probed and the desired phages were obtained, we needed a method to confirm that they were in fact reactive with immune serum and not with naïve serum. We devised a method of using activated PVDF membranes which were kept moist to prevent them from drying out and losing their ability to bind proteins. Phage plaques were generated in round100mm petri dishes, so circular PVDF membranes were required, however, none were commercially available. Hand cutting the circles proved to be both time prohibitive and lacking in the level of reproducibility we desired. To solve this issue, a Fiskars brand circle cutter was used in conjunction with a rubber cutting mat which allowed us to rapidly cut identical circles which fit perfectly and completely onto the growth surface of the petri dish. When used in conjunction with orienteering marks drawn

onto the sides of the dish, identical colony lifts were able to be generated. Additionally, as the system was essentially proteins bound to PVDF membranes, we were able to screen them rapidly using a traditional western blot style of screening by blocking the unbound regions of the membrane, probing with desired primary antibody, then following up with a secondary labeled antibody to verify reactivity. This process allowed us to readily process high numbers of phages, and do so with multiple different types of primary serum. With this ability, we were able to screen identical phages to determine reactivity with immune serum, confirm a lack of reactivity with naïve serum, and ensure reactivity with the control anti-M13 monoclonal antibody. Due to the phage plaques being constrained within agar in a petri dish, and the phage surface being exactingly reproduced and screened, specific phages were able to be backtracked and harvested to amplify and stock individually, then screened a second time to confirm the results of the initial screens.

Through our method of screening individual phages, and due to the intrinsic benefits of the system used, chosen phages which seemed ideal based on the results of the screening were able to have their amino acid sequences determined using supplied nucleotide sequencing primers and converting the nucleotide sequence into the corresponding amino acid sequence. Obtained amino acid sequences were analyzed using a B-cell epitope identification algorithm. The B-cell epitope was focused on due to our interest in antibody involvement in immunity. Additionally, due to the 12mer linear nature of the epitopes, the full amino acid sequence could be used to probe the full proteome of *B. mallei* and *B. pseudomallei*. By doing this, we were able to fully go from antibody to antigen rather than antigen to antibody. While it is impossible to conclusively link one specific antibody to one specific antigen, we can at least find endogenous proteins that

remain reactive with serum depleted of all other reactivity which makes them intrinsically valuable. Once proteins were identified containing the complete 12mers or large portions of their 12 amino acid sequences, these proteins were flagged for further examination. Matching proteins that were available to be fully synthesized by an NIH collaborative protein synthesis core were obtained and further examined.

While the process of going from antibody to antigen is interesting in and of itself, ultimately there is an end goal of producing a meaningful level of protection through vaccination, or through the development of a medical countermeasure. To that end, groups of mice were vaccinated with amplified phages, select 12mer sequences conjugated to immunoreactive epitopes, or full mature synthesized proteins derived from the results of the phage sequencing. Mice were vaccinated using Freund's complete/incomplete adjuvant due to its ability to lead to vigorous production of antibodies through stimulated maturation of DCs by the complete adjuvant, as well as the Th2 biased response aiding in B-cell isotype switching and clonal expansion from CD4+ T-cell activity. Ultimately, it was found that vaccination with any of the aforementioned vaccines did not provide a conclusive level of protection.

While this initially seemed to be a setback, in reality it is not uncommon. Work previously done by the Lafontaine lab, as well as other labs, has shown that just because a protein itself does not confer protection, generation of a mutant lacking expression of that protein may. One example of this is the BatA knockout mutant referenced earlier in this writing and described elsewhere (295) as well as the BpaB knockout mutant also described by the Lafontaine lab elsewhere (296). Vaccination of mice with purified BatA or BpaB proteins also failed to provide a meaningful level of protection. However, generation of a

mutant lacking production of BatA produced a mutant that not only fails to colonize mice, and is also capable of producing a protective immune response that can keep mice alive through both the acute and chronic stages of infection though without the production of sterile immunity. Further, removal of BpaB production from wild-type *B. mallei* led to a greatly reduced virulence of that organism. It's possible through the production of mutants lacking the expression of genes identified through this process that antigens critical for the *in vivo* persistence of *B. mallei* and/or *B. pseudomallei* can be identified through *in vivo* infection of mice. This could allow for the identification of key players in the pathogenesis process that could be exploited through the use of drugs or other therapeutics. With this potential, taken together with the numerous publications in the literature in other pathogens showing the efficacy of using mimotope vaccination directly, the use of phage display library technology seems to be a fruitful endeavor and a useful tool for future basic research and pathogenesis studies.

MATERIALS AND METHODS

Determining the IgG concentration of serum samples

The IgG concentrations of sera of interest were quantified using the Affymetrix Ready! Set! Go! IgG Quantification ELISA kit according to the manufacturer directions. Briefly, Immulon 2HB ELISA plates were coated with 1:250 dilute capture antibody in 1X

PBS overnight at 4°C. The following morning, the plates were washed three times with an automatic plate washer, then blocked with 300 ul of a 1:10 dilution of the included 20x BSA based Buffer A for one hour. During the hour, the included lyophilized IgG standards were rehydrated in 720 ul of sterile water per the manufacturer instructions. In addition to rehydrating the standards, the sera being tested were dilute 1:100000 by diluting the sera 1:100, then 1:100 again, then 1:10. After the one hour blocking incubation, the plates were washed three times with the automatic plate washer and then loaded with 200 ul per well of standards, PBS (blank wells), or the 1:100000 dilute sera in duplicate wells. Wells were then serially diluted 2-fold by moving 100 ul from well to well, changing tips between dilutions. After the final dilution, 50 ul of 1:250 dilute detection antibody was added to each well. Each plate was parafilmed shut and incubated at room temperature for three hours on a 400 RPM shaker. After three hours, the plates was removed from the shaker and washed four times with the automatic plate washer. 100 ul of the included developer substrate was added to all wells and incubated at room temperature for 15 minutes after the four washes. After 15 minutes, 100 ul of 1M phosphoric acid was added to each well to stop the reaction. Once developed, the optical densities of the serial dilutions of the serum samples were plotted against the included known standards used to make a standard curve.

Depletion of Antibodies Reactive with Constitutively Expressed *in vitro* Antigens and Confirmation of Depletion

Serum Samples were depleted of antibodies reactive with *in vitro* antigens in a two phase process of incubation with whole live cell *B. mallei* and then whole cell lysates of *B. mallei* as previously described (295). Briefly, plate grown *B. mallei* ATCC 23344 was

grown on agar plates for 40 hours, then suspended to a concentration of $1x10^9$ CFU/mL in 45 mL of PBS. Bacterial cells were pelleted, then suspended in ≤ 10 mL of serum. This mix was incubated at room temp with inversion mixing for 30 minutes, then the cells were pelleted. This process of mixing with pelleted bacterial cells then incubating for 30 minutes was repeated two additional times for a total of 3 adsorption steps. After the final adsorption, the serum was collected, filter sterilized, and stored at -80. The second phase, exposure to whole cell lysates, took place over several days. 2 mL of 1 mg/mL B. mallei ATCC 23344 whole cell lysate was mixed with 45 mL DMEM media. This vortexed to mix and then evenly distributed over nine petri dishes in 5 mL volumes. Once the volumes of lysate in DMEM were distributed evenly to each petri dish, they were swirled to fully coat the dish, parafilmed to seal, and stored statically at room temperature overnight. The following morning, the supernatants were removed from the plates, and they were washed once with 1x PBS. To perform the panning process, 200 uL of adsorbed immune serum was mixed with 15 mL DMEM media. The lysate coated plates were divided into three sets of three plates and labeled to keep them separate. One washed plate from each set was given 5 mL of the serum DMEM mixture. Plates were swirled to coat, parafilmed to seal, and incubated statically at room temperature for two hours. After two hours of incubation, the supernatants were collected and transferred to a second set of plates where they were again swirled, parafilmed, and incubated statically for two hours at room temperature. After the second incubation, plate contents were again collected and transferred to a third set of plates. This third set of plates was swirled to evenly coat the plate, parafilmed to seal, and then transferred to 4 °C to incubate statically overnight. This process of coating plates one day and using them to pan the dilute immune serum the following day was repeated for

seven days for a total of twenty pans. After the twentieth pan, equivalent amounts of whole cell B. mallei ATCC 23344, control uninfected mouse lung, and B. mallei ATCC 23344 infected mouse lung lysates were resolved using 10% SDS-PAGE gel electrophoresis. The proteins were transferred to PVDF membranes where they were probed using a western blot protocol with naïve, unpanned adsorbed, whole live cell adsorbed, and whole live cell + whole cell lysate adsorbed serum. Serum that lost reactivity with *in vitro* expressed antigens present in the whole cell lysates was retained in storage, while serum that exhibited trace reactivity with *in vitro* antigens was adsorbed against whole cell lysates for an additional step of 9 plates in a single day as described above, then tested again for reactivity through Western Blotting.

Saturating Protein G Beads with IgG Antibodies from Serum Depleted of *in vitro* Reactive Antibodies

Protein G microbeads were coated with IgG from the 20x panned adsorbed immune serum over a two day process. First, 250 ul of protein G beads were diluted into 1 mL of 1x TBS. A 20U Miltenyi Biotec Magnetic Separation Column was placed on a uMacs Magnetic Separator magnet and the combined tube and magnet were placed on a magnet stand. The column was equilibrated by passing 150 ul of 70% ethanol through the filter and discarding what flowed through. The column was then washed three times with 1 mL 1x TBS, and the flowthrough discarded. The 1 mL dilution of protein G beads was added to the column, and the flowthrough discarded as the beads were captured by the magnetic separation column. The beads were washed three times with 1 mL 1x TBS, and the flowthrough discarded. Once the final wash was performed the magnetic separation

column was separated from the magnet and the beads were retrieved by passing 1 mL 1x TBS through the column. This process was repeated a second time to produce two sets of washed beads.

Washed beads were incubated overnight at 4 °C with 15 ug of either 20x panned adsorbed immune serum or naïve control serum on an inversion mixer in a cold room at a rotational speed of approximately 10 RPM. The following day, the beads were passed through separate equilibrated magnetic separation columns and washed three times with 1 mL 1x TBS per wash. The initial flowthroughs as well as the washes were collected and stored. After the last wash, beads were retrieved by removing the columns from the separation magnet and passing 1 mL of 1x TBS through the columns, collecting the eluate. The eluted beads were then incubated with 7.5 ug of either 20x panned adsorbed immune serum or naïve control serum, matching whichever they were exposed to on the first day and incubated at 4 °C on approximately 10 RPM rotation mixing. The following morning the beads were again passed through equilibrated columns on a magnetic separation stand. The beads were washed three times with 1 mL 1x TBS per wash, and then retrieved using 1 mL 1x TBS. As done before, the initial eluate as well as the washes were collected. Using the Affymetrix Ready! Set! Go! IgG Quantification ELISA as previously described, the amount of IgG in vs IgG out was compared to determine the amount of ug of IgG taken up by the Protein G beads.

In order to verify that the beads were saturated with IgG we used a flow cytometer to detect FITC fluorescence from an antibody added to aliquots of the coated beads. We obtained a FITC tagged Mouse IgG2a monoclonal antibody from BD Pharmigen, FITC Mouse Anti-Mouse H-2D[k]. We used a Mouse IgG2a monoclonal antibody because it is

listed in the manufacturer literature as having one of the highest affinities for the protein G beads of all IgG isotypes from all of the species tested including rats, humans, horses, and goats. Aliquots of naïve control and 20x panned adsorbed immune serum IgG coated beads were set aside. Simultaneously, a third set of beads was diluted and washed but not coated with any type of serum. 100 ul of beads from both types of serum as well as the uncoated set of beads were mixed with 10 ug of the FITC tagged monoclonal antibody and 890 ul of 1x TBS. These mixtures were incubated for 1 hour at 4 °C on 10 RPM inversion. After the hour incubation, beads were collected using equilibrated magnetic separation columns. Beads were washed three times with 1 mL 1x TBS per wash and the flowthroughs were discarded. The beads were then recovered from the columns by removing the columns from the magnetic separation magnet and passing 1 mL of 1x TBS through the columns and collecting the flowthroughs. Once the beads had been retrieved, they were read using a BD Accuri C6 Flow Cytometer. 300 ul of uncoated beads were read and used as a negative control, while 300 ul of the uncoated beads that had been exposed to the FITC tagged monoclonal antibody were read and used as a positive control. Saturation was confirmed by process of elimination, as beads that were saturated would not bind the tagged IgG antibody and would thus not have a shift in fluorescence.

Titering of the NEB PhD-12 Library

An overnight culture of E. coli ER2738 was grown and used to inoculate a 20 mL flask of LB media supplemented with tetracycline with 200 uL of culture. The culture was grown on 200 RPM shake at 37 °C until it reached OD600 0.5. The stock PhD-12 library and the 3x pre-cleared library were serially diluted to 10-10. 10 ul of each serial dilution was added

to 200 ul of OD600 0.5 E. coli ER2738. Once the serially dilute phages were added to the E. coli aliquots, they were left to incubate statically at room temperature for 5 minutes, after which each aliquot was individually mixed with 3 mL of molten top agar and inverted 10 times to mix thoroughly. Mixed top agar suspensions were poured onto pre-labeled LB agar plates supplemented with Xgal and IPTG that had been pre-warmed at 37 °C for one hour. Once the top agar was poured onto the pre-warmed and labeled plate it was swirled to coat the plate evenly and incubated at room temperature for 5 minutes to allow the top agar to solidify. Once solidified, the plates were transferred to a 37 °C incubator to incubate statically overnight.

Pre-Clearing NEB PhD-12 Library with Naïve Serum Coated Protein G Beads

100 ul of 1xTBS with 0.5% tween (TBST) was dispensed into a 5 mL culture tube and mixed with 100 ul of naïve control serum saturated protein G beads. 10 ul of the NEB PhD-12 M13 Phage Display library, corresponding to approximately $1.0x10^{13}$ PFU of bacteriophages, was dispensed into the tube, and the combination with mixed via pipetting. The mixture was incubated statically at room temperature for 30 minutes, with 5 seconds of inversion agitation every 10 minutes. After 30 minutes, the contents of the 5 mL culture tube were passed through an equilibrated magnetic separation column and the flowthrough was collected. The column was washed twice with 150 ul TBST per wash and the washes were collected along with the first flowthrough in a 5 mL culture tube. The process of mixing 100 ul of naïve control serum saturated beads with the diluted library was repeated twice for a total of 3 times. After the 3rd mix and wash, the obtained library was mixed with an equal volume of sterile glycerol, labeled as “3x Pre-cleared Library”, and stored at -20.

After pre-clearing, both the pre-cleared library and the stock PhD-12 library were titered as described previously. The obtained titer of the 3x pre-cleared library was compared to the titer of the stock PhD-12 to ensure a reduction in the number of PFU of M13 bacteriophages.

Probing the NEB PhD-12 Library with Protein G Beads Saturated with IgG from Serum Lacking Reactivity with *in vitro* Antigens

250 ul of the 3x pre-cleared PhD-12 phage display library, equivalent to approximately $2.5x10^{10}$ PFU of M13 bacteriophage virions, was dispensed into a 5 mL falcon culture tube along with 100 ul of Protein G beads saturated with IgG from serum lacing reactivity with *in vitro* antigens. The tube contents were mixed well with a pipet and then left to incubate statically for 30 minutes with 5 seconds of agitation every 10 minutes. After 30 minutes, the contents of the tube were run through an equilibrated magnetic separation column and the flowthrough was discarded rather than collected. The beads were washed four times with 1 mL 1x TBS with 0.5% Tween (TBST). After the four washes, the separation column was removed from the magnet and 1 mL of phage elution buffer (pH 2.2 0.2M Glycine-HCl with 1 mg/mL BSA) was passed through the column to elute the beads into a collection tube. Once the full flowthrough was collected, it was allowed to incubate statically at room temperature for ten minutes in order to elute the bacteriophages from the antibodies affixed to the beads. After ten minutes, the collected flowthrough was passed through a separate equilibrated magnetic separation column and the flowthrough was collected. The suspension was neutralized with 150 ul of pH 9.1 1M Tris-HCl. Once neutralized, the stock of eluted phages was given an equal volume of sterile

glycerol, labeled “Reactive Eluted Library”, and stored at -20 °C. The phages were titered as done previously and the obtained numbers were compared to the stock PhD-12 and 3x Pre-Cleared library titers.

Screening Obtained Reactive Eluted Library Phages for Reactivity with Immune and Naïve Serum

To test for immunoreactivity, the 20x eluted phage plaques were transferred to PVDF membranes. In short, Reactive eluted phages were serially diluted to 10^{-2}, then mixed in 5 ul volumes with 200 uL of E. coli ER2738 grown to an OD600 value of 0.7. Infected E. coli aliquots were incubated statically at room temperature for 5 minutes then transferred to 3mL molten top agar aliquots. The top agar aliquots were mixed via inversion and then poured onto pre-warmed and pre-labeled plates which were swirled to coat and incubated at 37 °C overnight. Using a Fiskars® brand circle cutter, 3.3” diameter PVDF circles were cut and labeled with a series of lines matching lines which were also drawn on the agar plate used to orienteer the PVDF membranes onto the plate to allow for exact replicas between lifts. Once cut and labeled, the PVDF membranes were activated in 100% methanol. Activated PVDF membranes were dipped into PBST (0.05%) to remove the methanol, blotted between damp paper towels to remove excess liquid, and then placed label-side down directly onto the lawn of titered phages and incubated at 37 °C to allow for the lifting of phages directly into the PVDF membrane. The process of lifting plaques was repeated for a total of 3 times per plate, and consecutive lifts were labeled A, B, and C. The first lift was performed at 37 °C for 2 hours, the second lift was performed at 37 °C for 4 hours, and the final lift was performed at 37 °C overnight. Once lifts were completed

the PVDF circles were removed from the plate, washed with PBST (0.05%), and spotted with a positive control of 1:10 dilute whole cell B. mallei ATCC 23344 lysate. PVDF membranes spotted with the positive control were then placed between two Whatman blotting paper circles and wrapped in foil to store at -20 °C.

For each lift, membranes A, B,and C were used to screen for reactivity with an anti-M13 bacteriophage monoclonal antibody and IgGs purified from a pool of naïve or immune serum from multiple *B. mallei* infection studies, respectively. Pads were thawed at room temperature, and then placed into petri dishes with approximately 20 mL of SuperBlock™ T20 (PBS) Blocking Buffer. Once in the buffer the membranes were blocked for 1 hour on 100 RPM orbital shake at room temperature. After 1 hour the blocking agent was removed and a pre-mixed solution of primary antibody comprised of 10 mL SuperBlock™ T20 (PBS) Blocking Buffer + 1 ug anti-M13 MAb or 60 ug purified pooled unpanned immune or naïve polyclonal IgG was dispensed directly onto the circles. Once in primary antibody the pads were again incubated for 1 hour at room temperature on 100 RPM orbital shake. After 1 hour, primary antibody was removed from the pads which were then washed three times by dispensing approximately 20 mL of PBST (0.05%) into each petri dish and incubating on 100 RPM orbital shake for 15 minutes. Once washed, a pre-mixed secondary antibody solution of 10 mL SuperBlock™ T20 (PBS) Blocking Buffer + 1 ug of goat anti-mouse Ig H+L HRP was dispensed directly onto the PVDF circles which were then incubated at room temperature on 100 RPM orbital mix for one hour, then washed three times as done before. Pads were developed using Luminata Crescendo Western HRP substrate using 3 minute exposures.

Amplification of Single M13 Bacteriophage Virions

An overnight culture of E. coli ER2738 was grown as previously described and in the morning, 2 mL aliquots of LB + 20 ug/mL Tetracycline liquid media were inoculated with 20 uL of overnight culture. Using a sterile pipet tip, individual phage plaques were scraped directly from a titer plate and dispensed into the culture tube. Tubes were incubated on 250 RPM orbital shake at 37 °C for 5 hours. After 5 hours, the supernatants were collected and transferred to individual corresponding 2 mL tubes. The amplified phage supernatants were centrifuged at 17,000 RPM using a benchtop centrifuge for 30 seconds, after which the supernatants were carefully collected and transferred to duplicate tubes and centrifuged again at 17,000 RPM for 30 seconds. The top 1.6 mL of supernatant was collected from each amplified phage suspension and transferred to correspondingly labeled 2 mL screw top tubes. 400 ul of phage precipitation solution (2.5 M NaCl in 20% (w/v) PEG-8000) was added to each of the tubes which were incubated at 4 °C overnight. The following day phages were centrifuged at 17,000 RPM for 10 minutes and the supernatants were discarded. Phage pellets were suspended in 500 ul of sterile 1x TBS + 500 ul sterile glycerol and stored at -20 °C.

Obtaining M13 Bacteriophage Epitope DNA and Amino Acid Sequences from Amplified Phage Stocks

M13 Bacteriophage DNA was extracted from amplified phage suspensions using an Omega Biotek E.Z.N.A. M13 Spin Mini Kit according to the manufacturer instructions. DNA from the phages are precipitated and suspended at a concentration of 100 ng/ul. Using

the 96 gIII sequencing primer provided by the Ph.D.-12™ Phage Display Peptide Library Kit, sequencing reactions were set up in individual tubes by mixing 5 ul of 100 ng/ul phage DNA, 2.5 ul of 10 uM 96 gIII primer, and 2.5 ul of sterile H2O. Sequencing reactions were sent to Macrogen Corp. for sequencing. Once sequences were obtained, the epitope encoding region of the phage genomes were obtained and translated into amino acids. The amino acid sequence was analyzed using the Immune Epitope Database (IEDB) from the National Institute of Allergy and Infectious Diseases (NIAID) using the linear epitope prediction algorithm. The obtained amino acid sequences were also analyzed using the protein Basic Local Alignment Search Tool (pBLAST) database from the National Institutes of Health (NIH) National Center for Biotechnology Information (NCBI) to search search a B. mallei ATCC 23344 specific database of proteins for structural similarities between the amino acid sequences of the mimotopes present on the bacteriophages and the full proteome of B. mallei.

Phage Derived Vaccine Development

Peptides conjugated to either chicken Ovalbumin (Ova) or keyhole limpet haemocyanin (KLH) were designed and ordered from Genescript. Genescript synthesized the following amino acid sequences with the KLH or Ova antigens on the N or C-terminus respectively: YTFAARGANGPG, SPLRAVAFSGAQ, ANSPRQMSMALD, HFLTPTGNIDSS, and SLSAGLLQMGLS. Additionally, full mature peptides based on

endogenous proteins sharing sequence homology with the lead candidates were obtained from the Seattle Structure Genomics Center for Infectious Disease. The materials described herein were provided by the Seattle Structural Genomics Center for Infectious Disease (www.SSGCID.org) which is supported by Federal Contract No. HHSN272201700059C from the National Institute of Allergy and Infectious Diseases, National Institutes of Health, Department of Health and Human Services.

Animal Experiments

Groups of specific-pathogen-free (SPF) female BALB/c mice between the ages of 6-8 weeks old were vaccinated intraperitoneally with concentrations of KLH-conjugated peptides, Ova-conjugated peptides, M13 bacteriophage virions, or synthesized mature proteins ranging from 50-100 ug suspended in Freund's complete or incomplete adjuvant on three separate occasions between 10-14 days apart. Mice were non-terminally bled and serum was collected in order to confirm an immune response specific to the vaccine antigen by enzyme-linked immunosorbent assay (ELISA).

Mice were challenged with bacteria via the aerosol route using a Microsprayer as has been previously described (156). Upon infection, mice were monitored daily, and provided food and water *ad libitum*. Human endpoints were strictly enforced, and mice exhibiting signs of severe clinical distress were euthanized according to AVMA guidelines. At the terminal endpoints of the studies, survivors were euthanized also according to AVMA guidelines. During and after infections, animals were contained in a HEPA filtered ventilated system manufactured by Innovive, which was housed under BSL3 conditions. Survival data was analyzed using the Kaplan Meier method, and all graphs were generated using GraphPad Prism.

Compliance and Ethics

All experiments described in this body fell within the approval of the University of Georgia's Institutional Biosafety Committee guidelines. All BSL3 work was performed under appropriate BSL3 conditions in accordance with the U.S. Federal Select Agent Program guidelines. All animal experiments were performed according to the Guide for the Care and Use of Laboratory Animals of the National Institutes of Health.

TABLES AND FIGURES

Table 3.1

Name	Rank	Sequence	Reactivity with: Pooled|*Bm*|*Bp*	Top pBLAST Results	B-Cell Epitope Analysis
27 #6	1	YTFAARGANPG	+++ | +++ | +++	*acpA*, Acid Phosphatase	Strong B-Cell Epitope
27 #1	2	SPLRAVAFSGAQ	+++ | +++ | +++	ATPase, Sensor/Kinase	Moderate B-Cell Epitope
27 #7	3	ANSPRQMSMALD	+++ | +++ | +++	BMA0008 Toxin-Like Protein	Strong B-Cell Epitope
28 #5	4	SLSAGLLQMGLS	+++ | +++ | +++	*lmpC* T6SS Protein, *tssC*	No B-Cell Epitope Predicted
26 #1	5	HFLTPTGNIDSS	+ | + | +++	*impL* T6SS Protein, *icmF*, *tssM*	Strong B-Cell Epitope
26 #2	6	DLIVATLMNPRS	++ | ++ | +++	Ion channel protein RND efflux protein	Moderate B-Cell Epitope
27 #5	7	SYWHPHSENNST	++ | +++ | +++	Mannose phosphate transferase	Strong B-Cell Epitope
28 #7	8	AHAHQGVTNSPA	+ | + | +	BMAA0402, *lmpC* T6SS Protein	Strong B-Cell Epitope
28 #4	9	QRSHTFISPSDV	+ | + | +	BMA0008 Toxin-Like Protein	No B-Cell Epitope Predicted
26 #4	10	TISAVNLLHPWH	+ | + | +	Lipoprotein, Outer membrane protein	No B-Cell Epitope Predicted

The DNA sequences for 10 of the 11 chosen phages were obtained and translated into the corresponding amino acid sequences. The resulting amino acid sequences were analyzed using pBLAST and IEDB B-Cell epitope prediction software. After thse analyses, the phages were subjectively ranked as shown above based on the results of the pBLAST search, B-cell epitope prediction, and the reactivity screenings with purified pooled immune serum IgG, unvaccinated wilf-type *B. mallei* survivor serum, and unvaccinated wild-type *B. pseudomallei* survivor serum listed as Pooled|*Bm*|*Bp*| above. The predicted B-Cell epitope sequence found for each of the mimotope sequences was highlighted in green and a judgement of strong vs moderate was made based on the cut-off value for each amino acid sequence. Two of the mimotopes had sequence overlaps with the same protein, a toxin-like protein tentatively named BMA0008, highlighted in yellow above.

Table 3.2

Gene Locus	**Description**	**Organism**
BURPS1710b_2508	RisS Sensor Histidine Kinase	*Bp* 1710b
BMA0715	Orn/Lys/Arg Decarboxylase	*Bm* ATCC 23344
BPSS0734	OprM O.M. Efflux Protein	*Bp* K96243
BP1026B_II0374	ABC Transporter Binder	*Bp* 1026b
BMA1695	LolD ATP-Binding Protein	*Bm* ATCC 23344
BPSS2145	Putative experted protein	*Bp* K96243
BMAA0454	T6SS-2 membrane protein	*Bm* ATCC 23344
BMA2888	AcpA Acid phosphatase	*Bm* ATCC 23344
BMA0008	TcdB Insecticide protein	*Bm* ATCC 23344
BMAA0439	T6SS-2 Contractile Protein	*Bm* ATCC 23344
BMAA1439	MetN ATP-binding protein	*Bm* ATCC 23344
BMA2801	Putative endonuclease	*Bm* ATCC 23344

Based on the amino acid sequences obtained from the results of the phage sequencing and the subsequent qualitative ranking, the above full mature proteins were obtained from the Seattle Structure Genomics Center for Infectious Disease. When choosing proteins, those which were likely involved in the *in vivo* pathogenesis environment were focused on. Within that sum of proteins, those which were available for synthesis were selected and obtained.

Figure 3.1

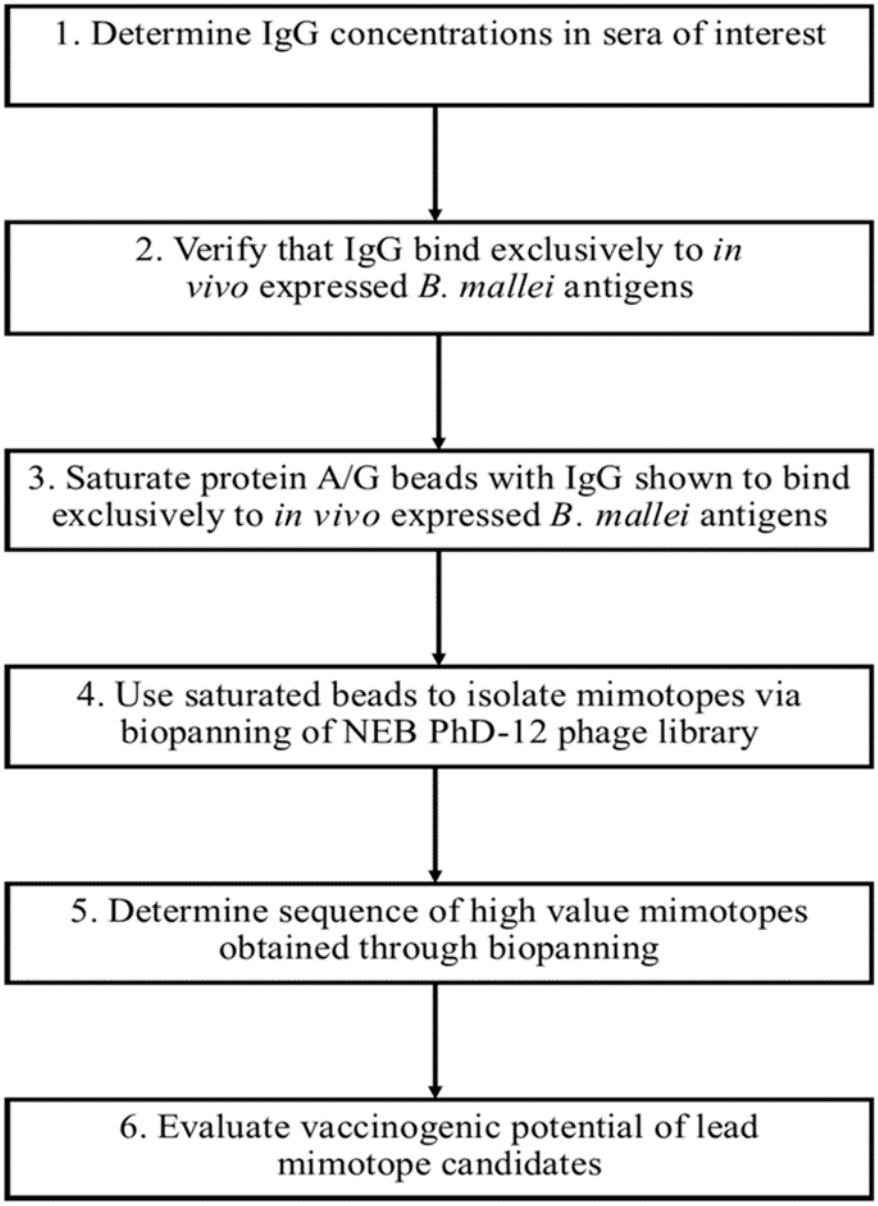

Experimental outline showing the general project workflow starting with calculating the IgG concentrations in sera of interest, using that number to saturate protein G beads, and then obtain epitopes for use in novel antigen discovery.

Figure 3.2

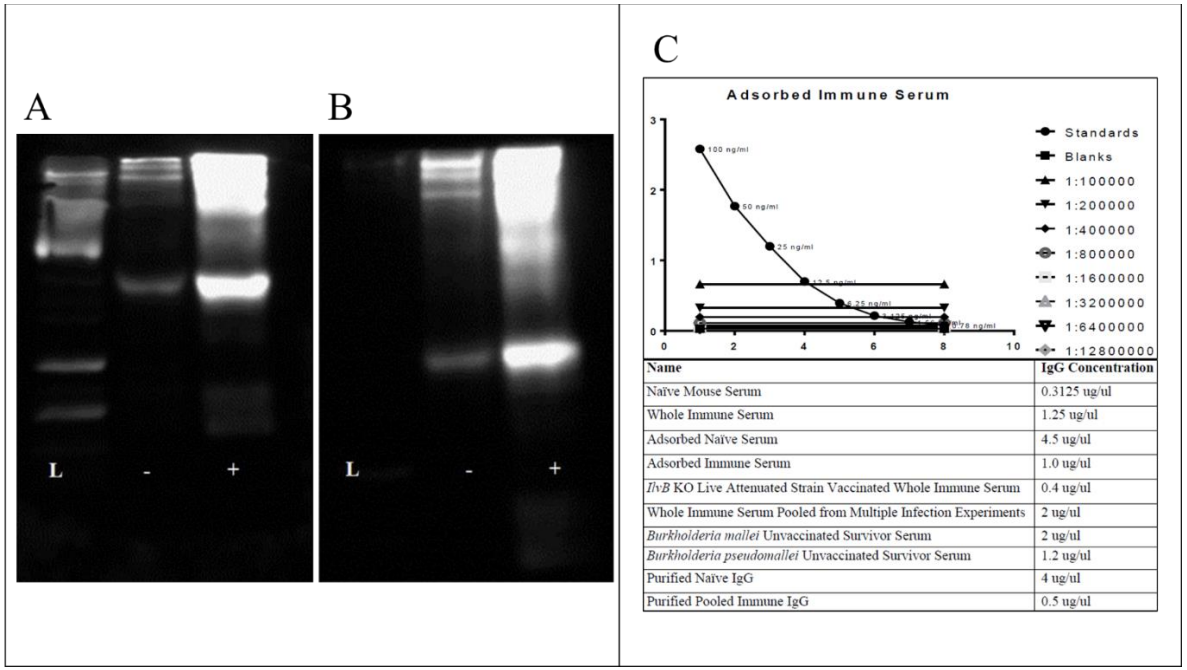

Name	IgG Concentration
Naïve Mouse Serum	0.3125 ug/ul
Whole Immune Serum	1.25 ug/ul
Adsorbed Naïve Serum	4.5 ug/ul
Adsorbed Immune Serum	1.0 ug/ul
IlvB KO Live Attenuated Strain Vaccinated Whole Immune Serum	0.4 ug/ul
Whole Immune Serum Pooled from Multiple Infection Experiments	2 ug/ul
Burkholderia mallei Unvaccinated Survivor Serum	2 ug/ul
Burkholderia pseudomallei Unvaccinated Survivor Serum	1.2 ug/ul
Purified Naïve IgG	4 ug/ul
Purified Pooled Immune IgG	0.5 ug/ul

As shown, adsorbed immune serum still reacts with *in vitro* antigens found in whole cell lysates of *B. mallei* ATCC 23344 (panel A lane L) 20x panned adsorbed immune serum does now (panel B lane L). Both serum samples lacked high levels of reactivity with control uninfected tissue lysates (panels A and B lane -), and reacted with the infected tissue controls (panels A and B lane +). The use of the Ready! Set! Go! Serum IgG ELISA Kit allows for the determination of serum IgG quantities compared to a known standard (panel C, graph). The results of the ELISA can be used to back calculate the IgG concentration in serum samples in ng/ul (panel C, table)

Figure 3.3

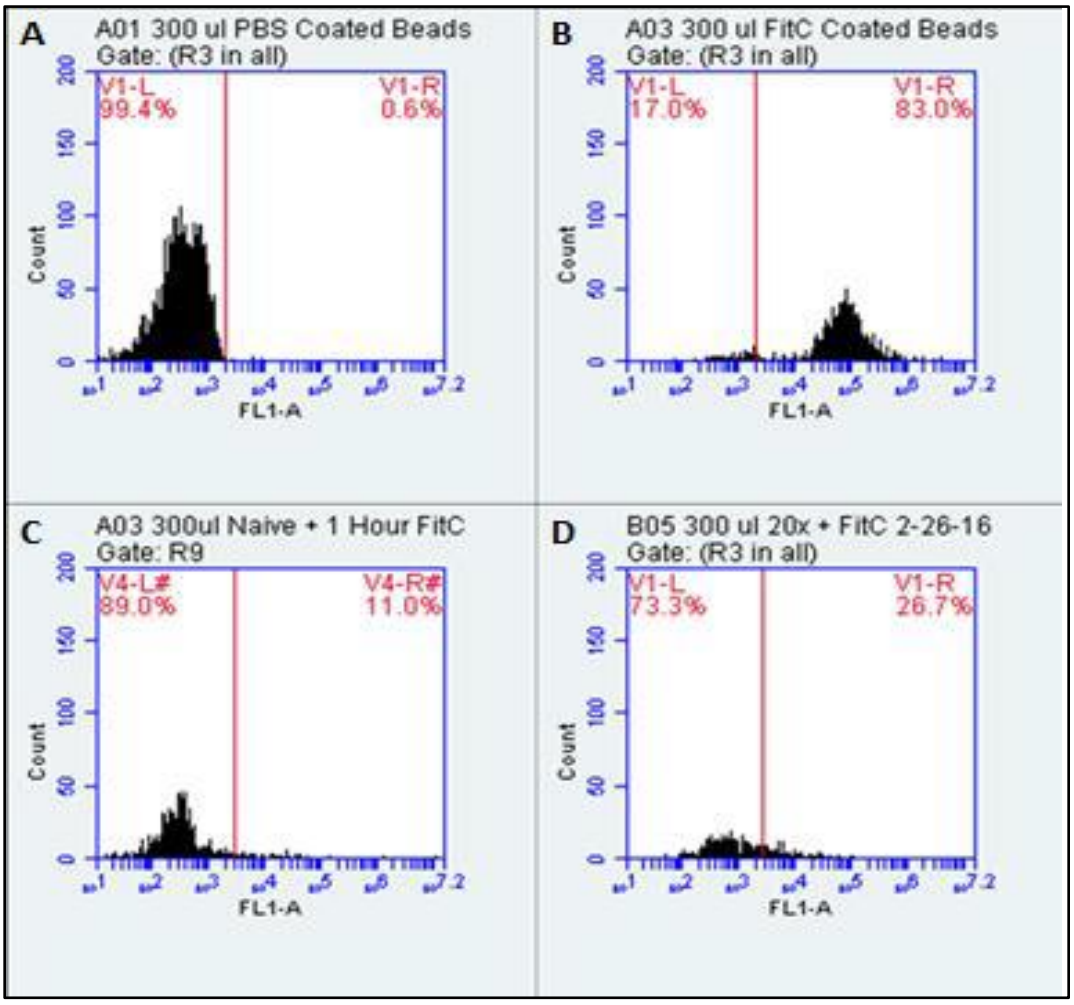

Shown here is flow cytometry data showing a lack of a fluorescent shift of beads saturated with naïve serum IgG antibodies (panel C) and 20x panned adsorbed immune serum (panel D). Saturated beads are unable to take up FITC tagged IgG2a monoclonal antibodies and when analyzed using a fly cytometer are visually indistinguishable from uncoated beads that were never exposed to FITC tagged IgG2a (panel A) when compared to beads saturated with the FITC tagged IgG2a antibody (panel B).

Figure 3.4

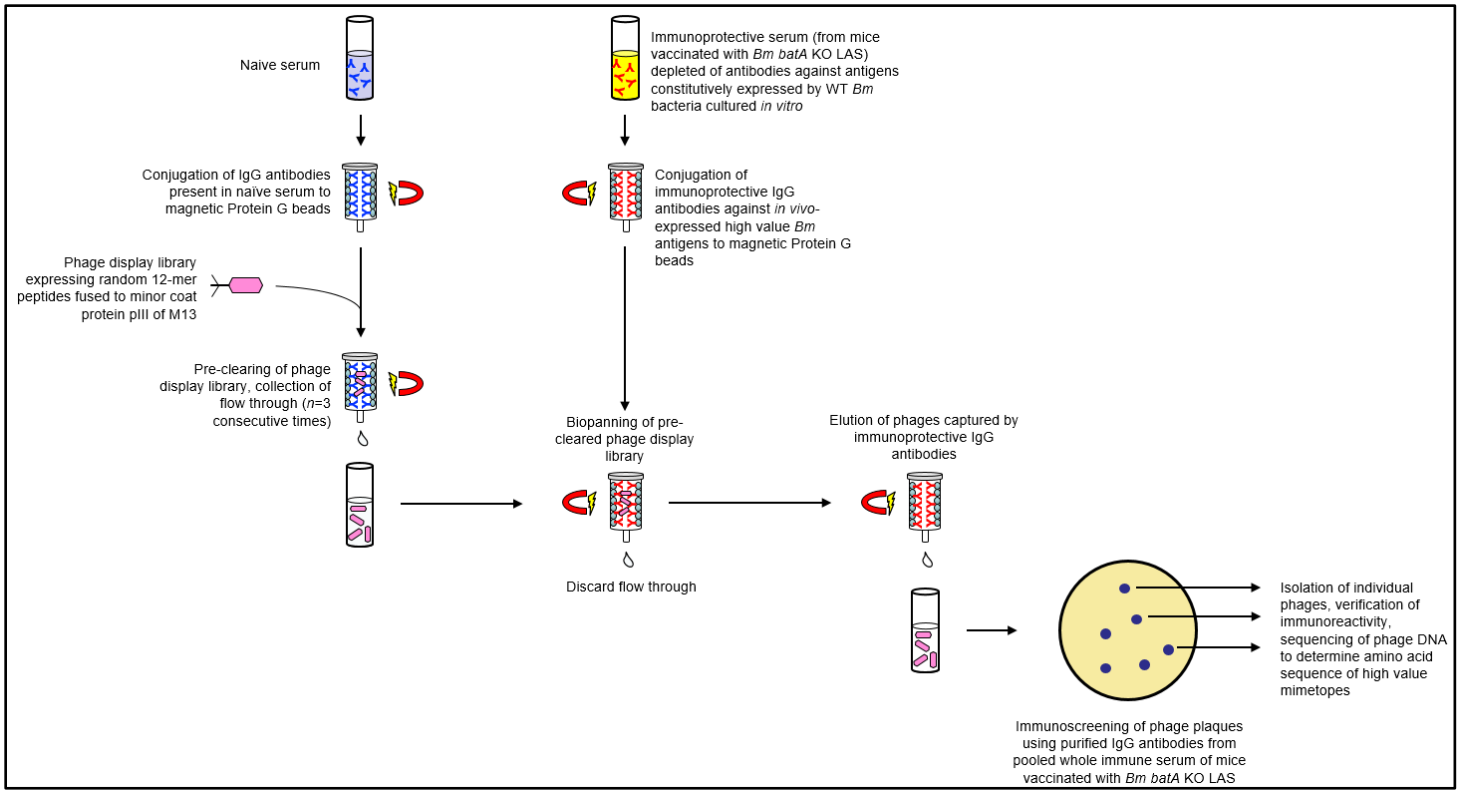

First the stock PhD-12 library, a library of randomly generated amino acid 12-mer affixed in 5 copies to the minor coat protein of an M13 bacteriophage virion, was pre-cleared three times by incubating the library with naïve serum coated protein G beads. After the pre-

clearing step, beads saturated with 20x adsorbed immune serum were incubated with the library, and phages that didn't bind were washed away. After panning the library, the bound phages were eluted resulting in a pool of phages that were reactive with immune serum antibodies specific to in vivo expressed antigens but not in vitro. Phages eluted from the 20x panned adsorbed immune IgG saturated beads were screened to ensure that they were truly reactive with immune serum by infecting aliquots of E. coli and plating them to form plaques which could be used for titering and further screening

Figure 3.5

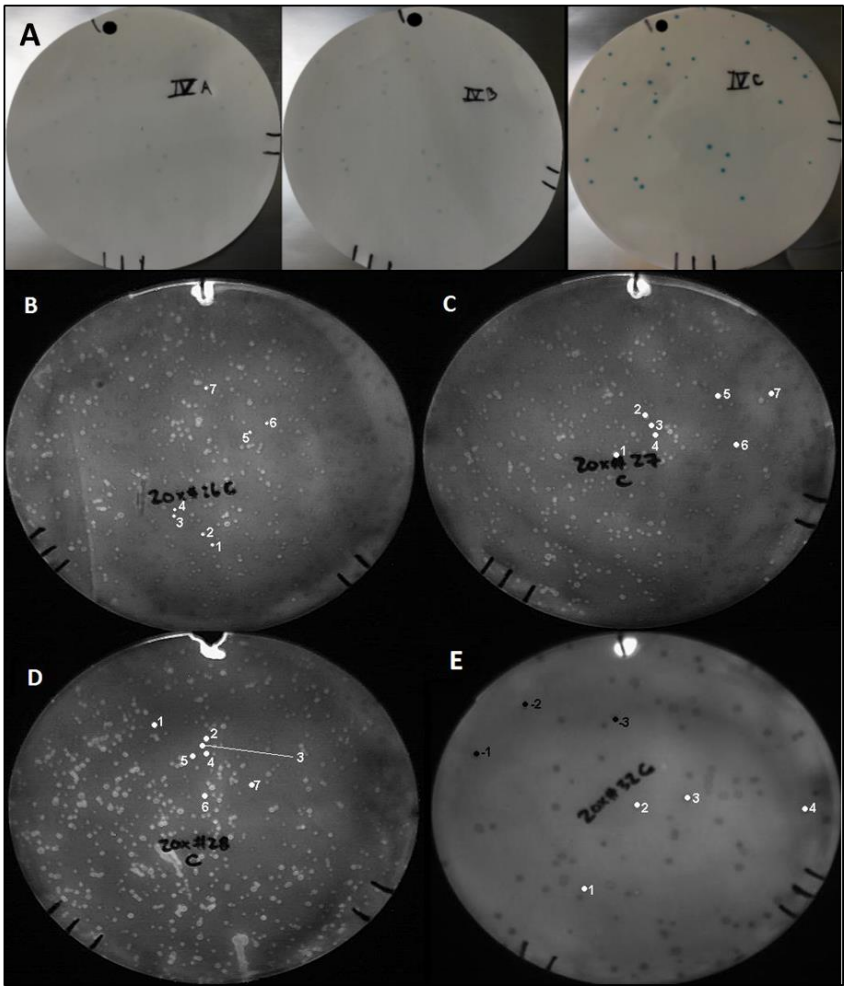

Panel A shows an example of an A, B, and C lift of phages from the titering plates onto the PVDF circle membranes. The black circle on each membrane is an artificially added effected showing where 2 uL of the 1:10 dilute *B. mallei* ATCC 23344 whole cell lysate positive control is spotted. Using these lifts a total of 25 immunoreactive phages were chosen from the 26th (B), 27th (C), 28th (D) and 32nd (E) screen lifts. These phages were selected based on serum reactivity with both the 1:10 dilute positive control (the white circle) and the phages found on the plates.

Figure 3.6

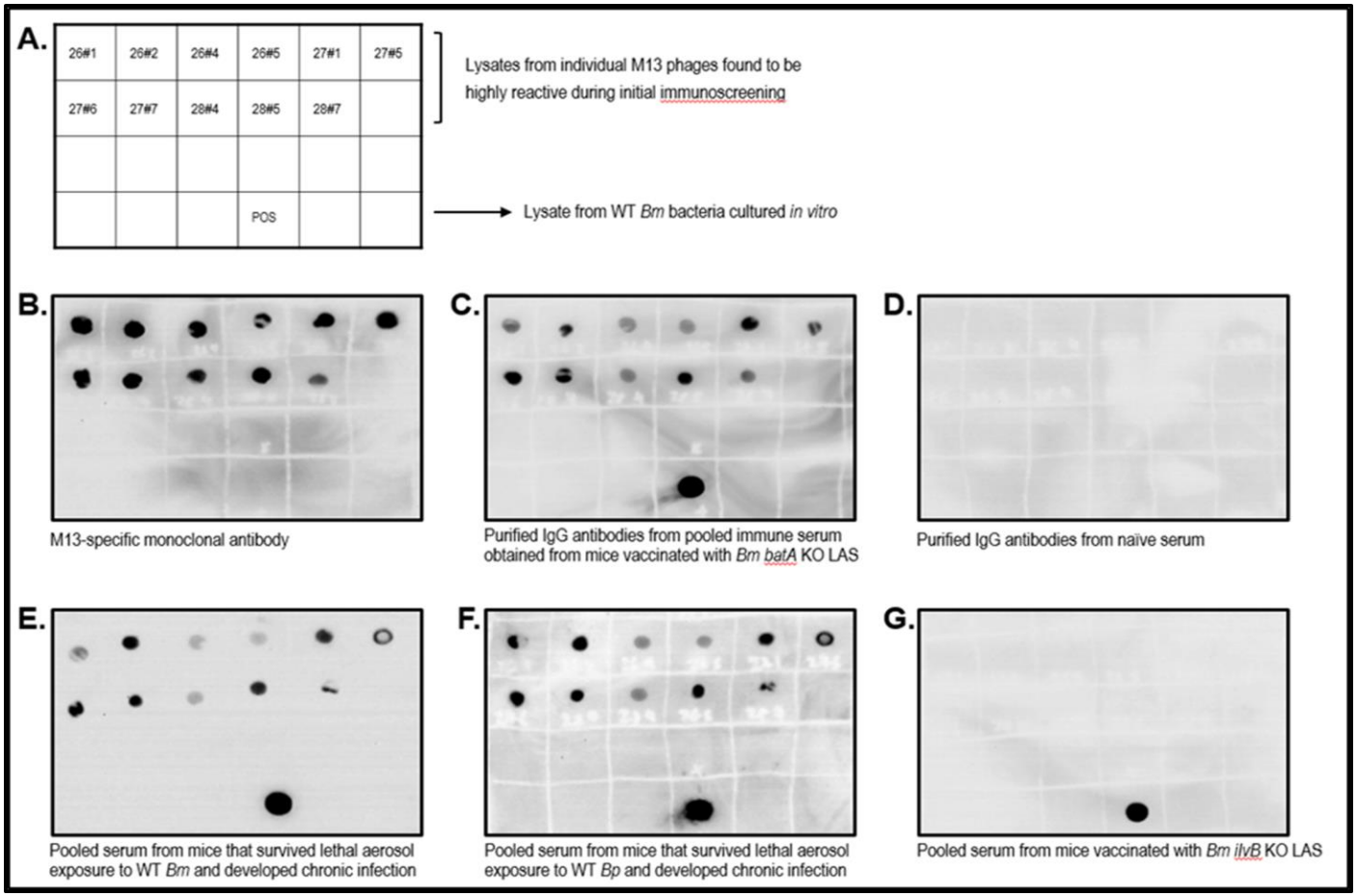

PVDF circles used to were cut using a Fiskars® brand circle cutter and were labeled with a grid with a labeled grid for each of the 11 chosen mimotopes as well as a positive control of 1:10 dilute *B. mallei* ATCC 23344 whole cell lysate (A). Each PVDF circle was

activated in methanol and then spotted with 2 ul of the corresponding phage/positive control in each of the labeled grids. Once the PVDF membranes absorbed the spotted liquids, they were screened for reactivity. 1 ug of M13-specific monoclonal antibody was used on n=1 pad for every round of screening to ensure that M13 titers remained at a detectible level (B). Using the IgG quantification data shown in table 1, PVDF circles with spotted bacteriophage and lysates were probed with 25 ug total of purified IgG antibodies from pooled immune serum (C), naïve unvaccinated and uninfected mice (D), whole serum from mice that survived infection with *B. mallei* (E), whole serum from mice that survived infection with B. pseudomallei (F), and mice that were vaccinated with the *B. mallei* ilvBKO live attenuated strain (G). As shown, the M13-specific monoclonal antibody and the purified naïve serum IgGs did not react with the *B. mallei* ATCC 23344 whole cell lysate controls as expected. The purified pooled immune IgG antibodies, wild-type *B. mallei* survivor, and ilvB live attenuated strain vaccinated mouse sera all reacted with the *B. mallei* ATCC 23344 lysate controls as expected. Importantly, pooled serum from mice that survived infection with wild-type *B. pseudomallei*, and were never exposed to *B. mallei* in any capacity, also reacted with the *B. mallei* ATCC 23344 lysate control as well as the mimotopes spotted onto the PVDF circle.

Figure 3.7

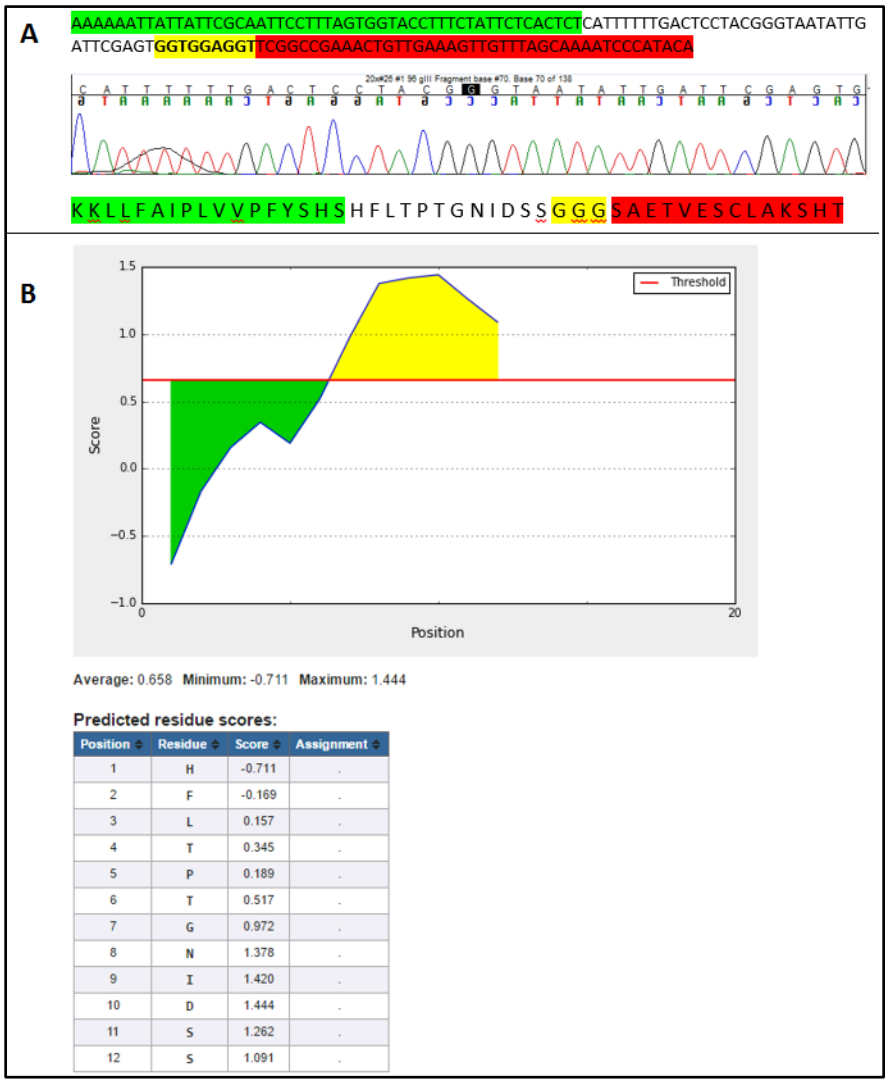

Position	Residue	Score	Assignment
1	H	-0.711	.
2	F	-0.169	.
3	L	0.157	.
4	T	0.345	.
5	P	0.189	.
6	T	0.517	.
7	G	0.972	.
8	N	1.378	.
9	I	1.420	.
10	D	1.444	.
11	S	1.262	.
12	S	1.091	.

Amino acid sequences were translated from the DNA sequences obtained from Macrogen (A). The upstream and downstream DNA and amino acid sequences flanking the mimotope sequences are shown highlighted in green and red respectively. Each mimotope is anchored into the minor coat protein via a triple glycine repeat protein, shown here highlighted in yellow. The unhighlighted region adjacent to the triple glycine represents the DNA/amino acid sequence of the mimotope expressed in 5 copies on the minor coat protein pIII of the M13 bacteriophage. The sequence was analyzed using IEDB B-cell epitope prediction

software (B). In this program, the amino acid sequences were compared to one another and a probability of involvement in an antibody recognition epitope was assigned to each one. Depending on the results of the sequence as a whole, an average probability was assigned and used as a cut-off value. Amino acids with a probability higher than the cut-off were assumed to be part of a B-cell epitope (yellow area under the graph) while amino acids with a probability lower than the cut-off were assumed not to be (green area under the graph). In this image, the amino acid sequence GNIDSS was predicted to be a B-cell epitope as they were all assigned probability values higher than the cut-off value of 0.658.

Figure 3.8

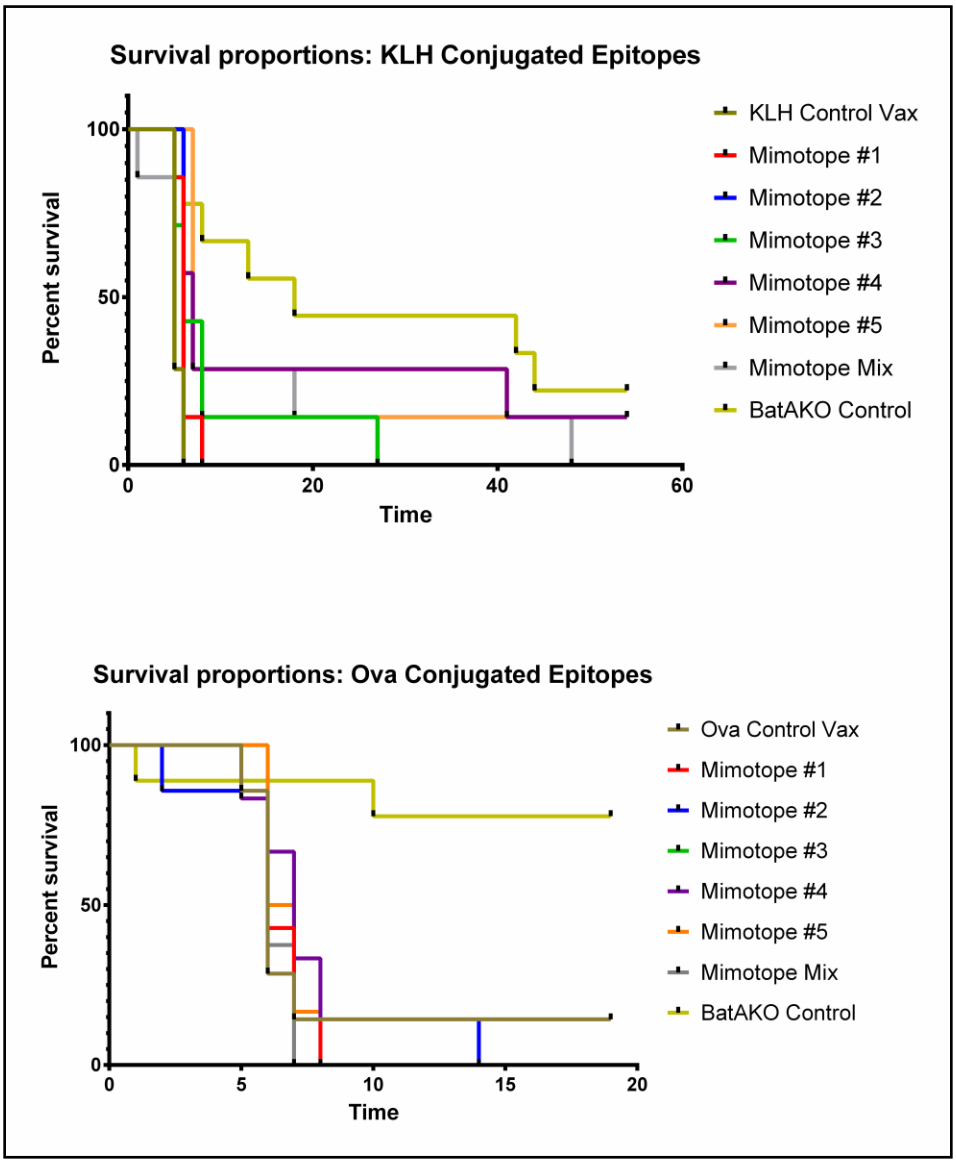

Survival data of mice vaccinated with the KLH and Ova conjugated epitopes. Mice were vaccinated subcutaneously with mixes of mimotopes in Freund's adjuvant over 3 separate injections. Mice were also vaccinated with mature proteins and purified live phages (data not shown). Each vaccination experiment was repeated for a total of at least n=2 experiments. During the various experiments, no statistically significant level of protection was found.

CHAPTER 4

THE PEPTIDOGLYCAN-ASSOCIATED LIPOPROTEIN PAL IS A MAJOR VIRULENCE FACTOR OF *BURKHOLDERIA MALLEI* AND A PROTECTIVE ANTIGEN AGAINST LETHAL AEROSOL CHALLENGE

Dyke J.S.*, Huertas-Diaz* M.C., Michel F., Holladay N.E., Hogan R.J., He B., and Lafontaine E.R.

* = Co-First Authors

Submitted to Virulence, 4/14/2020

ABSTRACT

Burkholderia mallei is a highly pathogenic bacterium that causes the fatal zoonosis glanders. The organism specifies multiple membrane proteins, which represent prime targets for the development of countermeasures given their location at the host-pathogen interface. We investigated one of these proteins, Pal, and discovered that it is involved in the ability of *B. mallei* to resist complement-mediated killing and replicate inside host cells *in vitro*, is expressed *in vivo* and induces antibodies during the course of infection, and contributes to virulence in a mouse model of aerosol infection. A mutant in the *pal* gene of the *B. mallei* wild-type strain ATCC 23344 was found to be especially attenuated, as BALB/c mice challenged with the equivalent of 5,350 LD_{50} completely cleared infection. Based on these findings, we tested the hypothesis that a vaccine containing the Pal protein elicits protective immunity against aerosol challenge. To achieve this, the *pal* gene was cloned in the vaccine vector Parainfluenza Virus 5 (PIV5) and mice immunized with the virus were infected with a lethal dose of *B. mallei*. These experiments revealed that a single dose of PIV5 expressing Pal provided 80% survival over a period of 40 days post-challenge. In contrast, only 10% of mice vaccinated with a PIV5 control virus construct survived infection. Taken together, our data establish that the Peptidoglycan-associated lipoprotein Pal is a critical virulence determinant of *B. mallei* and effective target for developing a glanders vaccine.

INTRODUCTION

Burkholderia mallei is a host-adapted Gram-negative bacterium and causes the incapacitating and highly fatal zoonotic disease glanders, which affects primarily horses, donkeys, and mules. The organism is extremely contagious through contact with diseased

equids and humans are susceptible to infection. Glanders is endemic in Asia, South America, Africa, and the Middle East and the disease is closely monitored by the World Organization of Animal Health as it is considered a biosecurity and biosafety threat (50, 148, 151).

Comparative analyses indicate that *B. mallei* evolved from the bacterium *Burkholderia pseudomallei* through genomic reduction. The latter is commonly found in water and wet soils of countries bordering the equator and causes the global emerging tropical disease melioidosis (168, 223, 277). The genes retained by *B. mallei* have a high level of sequence identity with their *B. pseudomallei* orthologs and the two species share many virulence determinants (133, 171, 194, 240). The clinical and pathological manifestations of disease caused by the organisms are also very similar. In humans, infection typically occurs through punctured skin and the respiratory route, and the most common manifestations are life-threatening pneumonia and bacteremia (50, 262, 276, 277). Pathogenesis is complex and entails the synchronized expression of genes supporting intracellular and extracellular replication of bacteria, colonization of deep tissues and organ systems, and development of hallmark chronic lesions that are difficult to treat and eliminate (68, 97, 125, 249).

Glanders and melioidosis lack reliable modern diagnostic tools and require extended therapy with low success rate due in part to the intrinsic resistance of *B. mallei* and *B. pseudomallei* to antibiotics (169, 216). No vaccine exists to protect animals or humans and there is concern that these highly pathogenic bacteria could be used as bioweapons, hence their classification as Tier 1 Select Agents by U.S federal agencies. Fortunately, the genetic, virulence, and disease similarities between *B. mallei* and *B.*

pseudomallei suggest the feasibility of devising medical countermeasures that protect against both organisms. This premise is supported by studies showing that antibodies against *in vivo* expressed *Burkholderia* antigens (295), vaccination with *Burkholderia* live attenuated strains (150, 295) and outer membrane vesicles (21, 197), and polysaccharide-based vaccines (112, 260) provide cross-species protection in animal models of melioidosis and glanders.

Immunoreactive proteins expressed by *B. mallei* and *B. pseudomallei* during human infections have been identified using immunoproteomic approaches and represent high value targets for developing countermeasures (84, 251, 255, 264). One particular *B. pseudomallei* antigen, designated BPSL2765 (locus tag in the genome of strain K96243), was found to induce immune responses linked to lower incidence of chronic and recurrent melioidosis (255). Immunization with subunit vaccines containing BPSL2765 was also shown to provide partial protection against intraperitoneal challenge in a mouse model of melioidosis (56, 121).

Comparative sequence analyses and determination of the crystal structure of BPSL2765 indicated that the protein is an ortholog of the well-characterized Peptidoglycan-associated lipoprotein (Pal) of Gram-negative bacteria (109). Pal is a component of the Tol-Pal system, which comprises the 5 core proteins TolQ, TolR, TolA, TolB, and Pal. The Tol-Pal proteins form a complex that spans the inner and outer membranes and is required for maintaining cell wall integrity (79, 105). The first amino acid of the mature Pal protein is a lipidated cysteine and the hydrophobic N-terminus anchors Pal in the outer membrane while the C-terminal region interacts with the meso-diaminopimelate residue of peptidoglycan in the periplasm. Pal also interacts with the

TolB and TolA proteins, which are located in the periplasm and the inner membrane, respectively. The other components of the Tol-Pal system, TolQ and TolR, are located in the inner membrane and interact with TolA. Together, the Tol-Pal proteins form a cross-bridge between the outer membrane, peptidoglycan cell wall, and inner membrane (79, 105).

Despite in-depth characterization in many organisms, the biological role of Pal in *B. mallei* and *B. pseudomallei* was not investigated previously and its value as a vaccine target against aerosol exposure has not been determined. The goals of this study were to engineer a *B. mallei pal* mutant strain, investigate the phenotypic traits of the mutant, and develop a delivery system to test the vaccinogenic potential of the antigen in a mouse model of infection.

MATERIALS AND METHODS

***In silico* analyses.** The ExPASy Bioinformatics Resource Portal (https://www.expasy.org) was used to analyze nucleotide and protein sequences. LipoP 1.0 (http://www.cbs.dtu.dk/services/LipoP/) and SignalP 5.0 (http://www.cbs.dtu.dk/services/SignalP/) were used to identify signal sequence cleavage sites within proteins. Conserved domains were identified with the NCBI Conserved Domain Database (CDD; https://www.ncbi.nlm.nih.gov/cdd/). NCBI BLAST (https://blast.ncbi.nlm.nih.gov/Blast.cgi) was used to search bacterial genomes and identify *pal* orthologs.

Plasmids, bacterial strains, and growth conditions. Table 1 lists the strains and plasmids used in this study. *B. mallei* strains were routinely propagated in brucella medium

(BD) containing glycerol (5% vol/vol) at a temperature of 37ºC. The medium was supplemented with zeocin (7.5 ug/mL), kanamycin (5 ug/mL), and/or Polymyxin B (5 ug/mL) when appropriate. For infection experiments (cell culture, mouse challenge), *B. mallei* was grown on agar plates for 2 days and bacteria were suspended to a concentration of 1 X 10^9 CFU per mL in phosphate-buffered saline (PBS). The suspensions were then serially diluted and used to infect cell cultures and mice. For all experiments, 100-uL portions of the bacterial suspensions (and dilutions) were spread onto agar plates to determine the number of CFU in the inoculum. *E. coli* strains were cultured in low-salt Luria-Bertani (LSLB) medium at 37ºC. The medium was supplemented with chloramphenicol (15 ug/mL), kanamycin (50 ug/mL), zeocin (50 ug/mL), and/or tetracycline (15 ug/mL) when appropriate.

Cells and culture conditions for work with PIV5 viruses. BHK21 cells (CCL-10, ATCC) were cultured in DMEM containing Tryptose Phosphate Broth (ThermoFisher Scientific, 10% vol/vol), fetal bovine serum (FBS, 5% vol/vol), penicillin (100 IU/mL), and streptomycin (100ug/mL). MDBK-A cells (USDA) were grown in DMEM supplemented with 10% FBS and the concentration of penicillin/streptomycin listed above. All cultures were maintained at 37°C with 5% CO_2.

Bacterial recombinant DNA methodologies. Standard molecular biology techniques were performed as described elsewhere (222). Genomic DNA was obtained from *Burkholderia* strains with the Easy-DNA gDNA purification kit (ThermoFisher Scientific). The QIAprep Spin Miniprep kit (Qiagen) was used to isolate plasmid DNA. PCR was carried out with the FailSafe PCR System (epicenter/Lucigen) according to the manufacturer's recommendations. DNA fragments were cloned into plasmids using T4

DNA ligase and restriction endonucleases purchased from New England Biolabs Inc. The *E. coli* strains EPI300 and EC100D *pir*$^{+}$ were used to propagate plasmids.

A DNA fragment of 812 nucleotides (nt) containing the *B. mallei* ATCC 23344 *pal* gene was synthesized with unique 5'-*Eco*RI and 3'-*Nco*I restriction sites for directional cloning (GenScript custom gene synthesis services). The DNA fragment was cloned into the corresponding sites of vector pBHR1 yielding plasmid $pPal_{Bm}$. A larger DNA fragment of 1,332 nt (with additional flanking sequences upstream and downstream of the *pal* gene) was also synthesized and cloned into pACYC184 in a similar manner, producing plasmid $pACYCPal_{Bm}$, and a 0.4 kb zeocin resistance marker from plasmid pEM7/ZEO was inserted into a *Pst*I site near the middle of the *pal* ORF. The resulting construct, $pACYPal_{Bm}ZEO$, was digested with *Dra*I and *Bsu*36I and a 2.2 kb DNA fragment containing the *pal* ORF disrupted with the zeocin cassette was purified using the High Pure PCR product purification kit (Roche Life Sciences), treated with the End-It DNA end repair kit (epicenter/Lucigen), and cloned into the *Eco*RV site of plasmid pKAS46, producing construct $pKASPal_{Bm}ZEO$.

A PCR product encoding amino acids 22 to 170 of the *pal* ORF was amplified from genomic DNA of *B. mallei* ATCC 23344 using the oligonucleotides primers P1 (5'-CTA GCT AGC AAG TCG GGC GTG AAG CT-3')[*Nhe*I site underlined] and P2 (5'-TTA ATT AAA GTT ACT GTT GAT AGA CGA-3')[*Pac*I site underlined]. The amplicon was purified, digested with *Nhe*I and *Pac*I, and cloned in the protein expression plasmid pETcoco-1. This approach created the construct $pHisPal_{Bm}$, which contains the *pal* gene product fused to an N-terminal histidine tag (His-tag). A similar strategy was used to clone a PCR product encoding amino acids 47 to 243 of the *B. mallei* ATCC 23344 *lolC* ORF

into pETcoco-1, yielding plasmid pHisLolC$_{Bm}$; the primers P3 (5'-CCC AAG CTT GTG CTG TCG GTG ATG AA-3')[*Hind*III site underlined] and P4(5-CCC TTA ATT AAA GCT CGC GCG CAA CC-3')[*Pac*I site underlined] were used to generate the amplicon containing the *lolC* gene fragment.

Electroporation was used to introduce plasmids into *E. coli* strains. The plasmids pBHR1ΔDra, pPal$_{Bm}$, and pKASPal$_{Bm}$ZEO were introduced into *B. mallei* via conjugative transfer using the *E. coli* strain S17, as previously outlined (68, 69). The plasmids pHisPal$_{Bm}$ and pHisLolC$_{Bm}$ were sequenced to verify that the cloned DNA did not contain mutations that would result in amino acid substitutions.

Construction of *B. mallei* ATCC 23344 *pal* mutant strain. After the transfer of plasmid pKASPal$_{Bm}$ZEO into *B. mallei* ATCC 23344, Polymyxin B resistant colonies were selected for resistance to zeocin and sensitivity to kanamycin. These colonies were then tested by PCR with primers P1 and P2, which produced amplicons of 0.5 kb in WT *B. mallei* ATCC 23344 and 0.9 kb in the *B. mallei pal* KO mutant (data not shown). This 0.4-kb difference in size was consistent with the aforementioned insertion of a zeocin resistance marker into a *Pst*I site near the middle of the *pal* gene, and confirmed allelic exchange in the genome of the mutant.

After the transfer of plasmids pBHR1ΔDra and pPal$_{Bm}$ into the *B. mallei pal* KO mutant strain, Polymyxin B resistant colonies were selected for resistance to zeocin and kanamycin. Plasmid DNA was purified from these colonies and tested with restriction endonucleases to authenticate the constructs (data not shown).

Construction of PIV5 producing the *B. mallei* Pal protein. A gene fragment encoding amino acids 22-170 of the *B. mallei* ATCC 23344 Pal protein was synthesized with codon usage optimized for human cells (GenScript custom gene synthesis services). The DNA fragment was cloned between the SH and HN genes of PIV5 in the plasmid ZL185, which contains the entire genome of the virus. The resulting construct, PIV5-Pal_{Bm}, was rescued and confirmed by RT-PCR sequencing as described previously (60, 126). PIV5 viruses expressing *Mycobacterium tuberculosis* protein Ag85B (PIV5-Tb) (61) and the *B. mallei* ATCC 23344 autotransporter BatA (PIV5-BatA) (157) were used as negative and protection benchmark controls in vaccination studies, respectively. WT PIV5, PIV5-Pal_{Bm}, PIV5-Tb, and PIV5-BatA viruses were propagated in MDBK cells as reported elsewhere (126).

Growth curves and plaque assay. Six-well plates seeded with MDBK cells were infected in triplicate with WT PIV5 or PIV5-Pal_{Bm} at a multiplicity of infection (MOI) of 0.01. One hundred μL samples of supernatant were then collected daily over 5 days. The virus titers in supernatant samples were determined by plaque assay as described previously using BHK21 cells (61).

Animal experiments. Female BALB/c mice (6-8 weeks of age) were obtained from Envigo. Challenge with bacteria was performed via the aerosol route as previously reported (156). The infected animals were monitored daily for clinical symptoms and humane endpoints were strictly observed. Mice showing signs of intermediate to severe distress were euthanized per AVMA guidelines. At study endpoints, tissues were harvested from euthanized survivors, homogenized, diluted, and spread onto agar plates to determine bacterial burden.

Vaccination with PIV5 viruses was performed intranasally (IN). Mice were first anesthetized intraperitoneally with 250 mg/kg tribromoethanol (Millipore Sigma). The animals were then held in supine position and 5-10 uL droplets of PIV5 virus stock were delivered to the nostrils; a dose of 10^7 PFU in a final volume of 40 uL was administered. Six weeks later, mice were challenged with 8,000 CFU of *B. mallei* ATCC 23344 (10 LD_{50} (156)). The controls in these experiments consisted of age- and weight-matched animals that were vaccinated IN with PBS.

Antigen preparation and analysis. Whole cell lysates were prepared from plate-grown bacteria suspended in 5 mL PBS to a concentration of 1 X 10^9 CFU per mL. Bacteria were pelleted by centrifugation, washed once with PBS, resuspended in 0.5 mL Bugbuster HT Protein Extraction Reagent (Millipore Sigma) supplemented with 1 uL/mL of rLysozyme Solution (Millipore Sigma), and incubated for 30 min at 65^{o}C. Western blot analyses were carried out as previously published (42, 295, 296). The *E. coli* strain TUNER containing plasmids pHisPal$_{Bm}$ and pHisLolC$_{Bm}$ was used to produce His-tagged Pal$_{Bm}$ and LolC$_{Bm}$ proteins, respectively. Protein expression was induced by the addition of 1 mM isopropyl-β-D-thiogalactopyranoside to broth cultures and incubating for 5 hours. Following this, bacteria were centrifuged and treated with Bugbuster HT Protein Extraction Reagent containing 1 uL/mL of rLysozyme Solution. Both His-tagged Pal$_{Bm}$ and LolC$_{Bm}$ proteins were soluble and purified with a His-Bind Purification kit (Millipore Sigma). Protein concentrations were determined with a BCA Protein assay kit (ThermoFisher Scientific). For ELISA, Immulon 2HB plates (ThermoFisher Scientific) were coated with antigen preparations or paraformaldehyde-inactivated *B. mallei* cells and antibody reactivity was measured as previously outlined (295, 296).

To investigate protein expression in cells infected with PIV5 viruses, monolayers of MDBK cells were first infected with PIV5-Pal_{Bm} and WT PIV5 (MOI of 10). After a 24 hr incubation period, cells were lysed with 1X Laemmli Sample Buffer (Bio-Rad) in PBS with 2-mercaptoethanol, and heated at 95 °C for 5 min. Samples were then resolved on a 4-20% gradient acrylamide gel by SDS-PAGE and transferred to an Amersham Hybond LFP PVDF membrane (GE Healthcare Life Sciences); purified His-tagged Pal_{Bm} protein was included as a control in these experiments. Upon protein transfer, the PVDF membrane was incubated with mouse anti-Pal_{Bm} polyclonal antibodies followed by incubation with Cy3-conjugated goat anti-mouse IgG (Jackson ImmunoResearch). A duplicate PVDF membrane was also probed with a mouse antibody against the PIV5 gene product P/V (Pk) antibody. The reactivity of antibodies with protein bands was visualized using a Typhoon FLA 7000 system (GE Healthcare Life Sciences).

Antibodies. Immune serum containing antibodies against Pal_{Bm} and $LolC_{Bm}$ was produced by immunizing mice with His-tagged Pal_{Bm} and His-tagged $LolC_{Bm}$ mixed with adjuvant, respectively. Mice were given 3 vaccine doses subcutaneously at 14 days interval. Each dose consisted of 25 ug purified protein mixed in a ratio of 1:1 with Freund's Adjuvant (Millipore Sigma; complete for prime, incomplete for boost). Immune serum was collected via the tail bleed procedure, pooled, and used in Western blot analyses. The monoclonal antibodies Pal_{Bm} MAb#1 and Pal_{Bm} MAb#2 were obtained by fusing spleen cells (from a vaccinated mouse) with Sp2/mIL6 cells (ATCC CRL 2016) as previously reported (295, 296). The supernatant from cultures of cells secreting the antibodies were used in Western blot analyses.

Macrophage killing assays. The mouse cell line JJ774A.1 (ATCC TIB-67) was cultured and infected with bacteria as previously outlined by our group (22, 155, 295, 296). The antibiotic streptomycin was used at a concentration of 50 ug/mL to kill extracellular bacteria.

Serum killing assays. Plate-grown organisms were used in all experiments. Bacterial suspensions were prepared in buffer supplemented with 5 mM $MgCl_2$ and 1.5 mM $CaCl_2$, mixed with normal human serum at a final concentration of 25% (vol/vol), and the mixtures were incubated at 37∘C. At time 0, 30, 60 and 120 minutes, duplicate 10 uL aliquots were removed and plated onto agar medium to determine the number of viable bacteria, as previously reported (62).

Data analysis. The Kaplan Meier method was used to plot survival data and the Log-rank Mantel-Cox and Gehan-Breslow-Wilcoxon tests were used to perform statistical analyses. The student's *t* and Mann-Whitney tests were used to analyze ELISA, bacterial burden data, and cell culture assay results. The two-stage linear step-up multiple *t* test procedure of Benjamini, Krieger and Yekutieli was used to analyze the data from macrophage and serum killing assays. These analyses were performed using the GraphPad Prism software and P values < 0.05 are reported as statistically significant. The method of Reed and Muench (215) was used to calculate LD_{50} values of *B. mallei* WT and recombinant strains.

Research compliance. All work with live *B. mallei* was performed in BSL3/ABSL3 laboratory space with approvals from the University of Georgia's Institutional Biosafety and Animal Care and Use Committees (IBC and IACUC,

respectively), and in compliance with the rules and regulations of the U.S. Federal Select Agent Program.

RESULTS

***In silico* characterization of the *B. mallei pal* gene.** Comparative sequence analyses identified the ortholog of the *B. pseudomallei* K96243 *pal* gene on chromosome I of the *B. mallei* ATCC 23344 genome (locus tag BMA2082). The open reading frame (ORF) encompasses 513 nucleotides (nt) and encodes a lipoprotein of 170 amino acids (aa) with a molecular mass of 18, 762. Analyses using the SignalP 5.0 and LipoP 1.0 servers detected a leader peptide at the N-terminus of the *B. mallei* Pal protein (Pal_{Bm}) with a signal peptidase II cleavage site between residues 20 and 21 (*i.e.* $GALAA^{20} \mid C^{21}KSGV$), which would provide a free cysteine residue for lipid modification of the mature protein.

Analysis with NCBI CDD indicated that Pal_{Bm} belongs to the OmpA_C-like Superfamily (domain ID cl28145; E value of 4.39e-64), which comprises peptidoglycan-associated lipoproteins of the Tol-Pal system. Consistent with this finding, orthologs of the *tolQ* (BMA2078), *tolR* (BMA2079), *tolA* (BMA2080) and *tolB* (BMA2081) genes were identified upstream of the *pal* ORF in the *B. mallei* ATCC 23344 genome. This particular arrangement of the genes encoding Tol-Pal system components (i.e. *tolQRABpal*) is conserved in most sequenced genomes of Gram-negative bacteria (105).

NCBI BLAST searches identified *pal* orthologs in the genomes of all *B. mallei* (n=51) and *B. pseudomallei* (n >1, 000) strains that are available through the service. The proteins encoded by these *pal* genes were all identical. An ortholog of *pal* was also identified in the genome of the closely related organism *Burkholderia thailandensis*, with

the gene product showing 99% identity. The Pal protein of other *Burkholderia* species, including *cenocepacia*, *cepacia*, and *multivorans*, exhibited 84% identity with Pal_{Bm}.

***In vitro* characterization of the *B. mallei pal* gene.** To study the function of the *pal* gene, we constructed a mutant strain of *B. mallei* ATCC 23344. Mutagenesis was achieved via genomic recombination of a DNA fragment containing the *pal* ORF disrupted with a zeocin resistance cassette. For complementation purposes, the plasmids pBHR1ΔDra (vector control) and $pPal_{Bm}$ (specifies constitutive expression of Pal_{Bm}) were introduced in the *pal* knockout (KO) mutant.

To examine expression of Pal_{Bm}, whole cell lysates from wild-type (WT) and recombinant bacteria were analyzed by Western blotting with the monoclonal antibody Pal_{Bm} MAb#2. As anticipated, no reactivity was observed with the mutant carrying the control plasmid pBHR1ΔDra (Fig 4.1A, lane 2). We found that the monoclonal antibody does not react with the lysate from WT *B. mallei* ATCC 23344 (Fig 4.1A, lane 1); Pal_{Bm}-specific polyclonal antisera and a second monoclonal antibody (Pal_{Bm} MAb#1) also failed to show reactivity (data not shown). Western blotting with polyclonal antibodies against the *B. mallei* LolC protein was used to demonstrate that equivalent amounts of lysates were analyzed for all strains (Fig 4.1B). Based on these results, we concluded that Pal_{Bm} is not produced at detectable levels by WT organisms cultured under standard laboratory conditions. As shown in lane 3 of Fig 4.1A, introduction of plasmid $pPal_{Bm}$ in the *pal* KO mutant strain results in the production of an 18 kDa protein reacting with antibody Pal_{Bm} MAb#2, which is consistent with the predicted molecular mass of the *B. mallei pal* gene product.

Mutations in the Tol-Pal system of Gram-negative bacteria typically result in disruption of cell envelope integrity and hypersensitivity to osmotic stress, antimicrobial peptides, detergents, and membrane-acting antibiotics (105). With this in mind, we assessed the susceptibility of the *B. mallei pal* KO mutant to high concentration of potassium chloride (osmotic stress) and Polymyxin B (antibiotic). The latter consists of a cationic polypeptide with an attached fatty acid tail and initially binds to negatively-charged LPS, allowing the hydrophobic tail to interact with bacterial membranes and destabilize them (205). Suspensions of *B. mallei* WT and recombinant organisms were serially diluted and spotted onto agar plates supplemented with 100 mM potassium chloride (Fig 4.2B) and 20 ug/mL Polymyxin B (Fig 4.2C). Each dilution was also spotted onto medium without additive to verify that the *pal* mutation does not cause a global growth defect (Fig 4.2A). We found that the *pal* KO mutant exhibits increased sensitivity to both osmotic stress and Polymyxin B compared to WT strain ATCC 23344, as evidenced by lack of visible growth when 10^2 and 10^3 CFU of bacteria carrying plasmid pBHR1ΔDra were spotted onto agar plates. Consistent with these results, the calculated minimum inhibitory concentration of Polymyxin B for the *pal* KO mutant harboring the control plasmid is approximately 10-fold lower than for WT organisms (Fig 4.3B and Fig 4.3A, respectively). Introduction of plasmid $pPal_{Bm}$ in the mutant, and concomitant production of the *pal* gene product, restored susceptibility of the *pal* KO strain to osmotic stress (Fig 4.2B) and Polymyxin B (Figs 2C and 3C) to WT levels.

The ability to thrive within host cells is an important pathogenicity trait of *B. mallei* (11, 97, 249, 276). Thus, we determined the intracellular fitness of the *pal* KO mutant using J774 murine macrophage cells. These experiments established that the *pal* mutation

substantially reduced fitness over a period of 7 hours (Fig 4.4A). By dividing the number of viable intracellular organisms at the experimental endpoint (CFU at 10 hours) by the number of phagocytized bacteria (CFU at 3 hours), fitness indexes of 1.38 and 0.08 were calculated for the WT strain and the *pal* KO mutant carrying control plasmid pBHR1ΔDra, respectively. To complement these assays, we compared the growth of the strains in broth medium and found that they replicated at similar rates (Fig 4.4B). These data indicate that the intracellular fitness phenotype of the *pal* KO mutant is not the result of a generalized growth defect. Introduction of plasmid $pPal_{Bm}$ in the mutant and constitutive production of the Pal_{Bm} protein restored intracellular fitness to WT levels (Fig 4.4A, calculated fitness index of 0.97). Taken together, these data demonstrate a role for Pal_{Bm} in the ability of *B. mallei* to survive and replicate inside host cells.

Serum resistance is another important pathogenicity trait of *B. mallei*, specifically resistance to complement membrane attack complex deposition and cell lysis (45, 159). Given the role of Tol-Pal system components in maintaining the integrity of the bacterial cell envelope and the increased sensitivity of the *B. mallei pal* KO mutant to osmotic stress and the membrane-acting antibiotic Polymyxin B (Fig 4.2), we compared the susceptibilities of WT and recombinant strains to normal human serum *in vitro*. As shown in Fig 4.4C, nearly 90% of WT organisms survived exposure to serum for 120 minutes. In contrast, only 20% of *pal* KO mutant bacteria carrying the vector control pBHR1ΔDra remained viable. The increased sensitivity of the mutant to complement-mediated lysis was detected as early as 30 minutes upon exposure to serum (72% survival compared to 106% for WT strain ATCC 23344). Complementation of the *pal* mutation with plasmid $pPal_{Bm}$ partially restored serum resistance. No statistically significant difference was

observed between survival of the mutant carrying plasmids pBHR1ΔDra and $pPal_{Bm}$ after 30 minutes incubation with serum (72-77% survival), but bacteria constitutively producing Pal_{Bm} show increased viability after 60 minutes (67% survival compared to 50% for the mutant carrying the control plasmid) and at the experimental endpoint (55% survival compared to 20% for control organisms). These data are consistent with the *pal* mutation causing a defect in the integrity of the *B. mallei* cell envelope, which in turn sensitizes the organism to complement-mediated lysis.

***In vivo* characterization of the *B. mallei pal* gene.** Based on the results of *in vitro* intracellular fitness and serum killing assays, we hypothesized that the *pal* gene contributes to pathogenesis *in vivo*. To test this, we calculated the median lethal dose (LD_{50}) of the *pal* KO mutant strain in a mouse aerosol infection model. At study endpoints, we collected tissues from survivors and determined bacterial loads as an indicator of *in vivo* fitness. Compared to WT organisms, the calculated LD_{50} value for *pal* KO bacteria carrying the control plasmid pBHR1ΔDra was > 5,000-fold higher (Figs 5A and 6A). No *B. mallei* organisms were cultured from the lungs, spleen or liver of any of the mice inoculated with the mutant, even those challenged with a high dose of 1.9×10^6 CFU (Panels B, C, and D in Figs 5 and 6). In contrast, the lungs and spleen of all mice inoculated with as few as 17 CFU of the parent strain ATCC 23344 were colonized with agent (Figs 5B and 5D). Introduction of the plasmid $pPal_{Bm}$ in the mutant and constitutive production of the Pal_{Bm} protein restored virulence and *in vivo* fitness, but not entirely. The LD_{50} of the complemented *pal* KO strain was found to be approximately 30-fold higher that WT *B. mallei*, and target tissues of many (but not all) survivors challenged with low doses of 15

and 150 CFU were colonized (Figs 5 and 6). Taken together, these data demonstrate that the *pal* gene product plays an important role in the virulence of *B. mallei*.

To gain insight into the immune response to WT and recombinant strains during infection, we also collected serum from survivors at study end points and measured immunoglobulin titers by ELISA using whole bacteria as well as purified His-tagged Pal_{Bm}. As shown in Fig 4.7A, challenge with the mutant carrying the vector control pBHR1ΔDra resulted in low titers against whole bacteria (< 3,200) compared to titers measured in the serum of mice that survived infection with WT *B. mallei* and *pal* KO organisms harboring plasmid $pPal_{Bm}$. These results are consistent with the considerably reduced virulence and *in vivo* fitness of the mutant, and suggest rapid clearance of bacteria lacking expression of Pal_{Bm}. In accordance with Western blot data showing different production levels of the *pal* gene product (Fig 4.1A), serum samples from mice challenged with the complemented mutant were found to contain higher antibody titers against the Pal_{Bm} protein than the serum of survivors infected with WT *B. mallei* (Fig 4.7B). As expected, the serum of mice inoculated with *pal* KO bacteria carrying plasmid pBHR1ΔDra did not show detectable titers of Pal_{Bm}-specific antibodies. Collectively, these data show that *B. mallei* produces Pal *in vivo* during infection, which in turn elicits production of Pal_{Bm}-specific antibodies. The data also suggest that the extent of the antibody response against Pal_{Bm} correlates with the amount of protein produced by bacteria.

To evaluate the usefulness of the mutant as a live attenuated vaccine, groups of mice were inoculated with the *pal* KO strain and, 4 weeks later, were infected with ~$10LD_{50}$ of *B. mallei* ATCC23344 organisms. The results of these experiments are

outlined in Table 2 and show that vaccinating mice with the *pal* KO mutant strain does not protect against lethal challenge with WT bacteria.

Vaccination with a virus vector expressing Pal_{Bm} protects against challenge with *B. mallei*. Based on the aforementioned *in vitro* and *in vivo* data, we hypothesized that delivering Pal_{Bm} with a virus vaccine vector system would elicit excellent protective immunity. This premise is supported by our studies showing that vaccination with Parainfluenza Virus 5 (PIV5) expressing the conserved *Burkholderia* autotransporter protein BatA protected 74% and 60% of mice against death upon infection with *B. mallei* and *B. pseudomallei*, respectively (157). Therefore, a gene fragment corresponding to amino acids 22-170 of Pal_{Bm} was cloned in PIV5 using a well-established reverse genetics approach developed by our group (Fig 4.8A) (60, 61, 157, 159). To verify that the recombinant construct drives expression of the Pal_{Bm} protein, lysates from MDBK cells infected with PIV5-Pal_{Bm} and WT PIV5 viruses were tested by Western blotting. As shown in Fig 4.8B, Pal_{Bm}-specific antibodies did not react with the control WT PIV5 lysate but reacted with a protein of 18-kDa in cells infected with PIV5-Pal_{Bm}. Purified His-tagged Pal_{Bm} protein was used as positive control. An antibody against the PIV5 P/V gene product was also used as loading control to show that comparable amounts of the lysates were analyzed. The replication rates of the viruses were compared in a multi-cycle growth curve experiment over a period of 5 days and found to be equivalent (Fig 4.8C), with PIV5-Pal_{Bm} reaching similar titers as WT PIV5. Hence, Pal_{Bm} expression does not reduce *in vitro* infectivity or fitness of PIV5. The genome of PIV5-Pal_{Bm} was also sequenced to verify that the *pal* gene fragment was properly cloned in its intended location (data not shown).

To investigate whether delivering Pal_{Bm} with a virus vector system elicits protection, mice were vaccinated intranasally (IN) with PIV5-Pal_{Bm} and, six weeks later, infected via the aerosol route with *B. mallei* ATCC 23344. Control groups consisted of age- and weight-matched mice treated with PBS, animals immunized with the aforementioned efficacy benchmark PIV5-BatA, and mice vaccinated with a PIV5-Tb construct expressing *Mycobacterium tuberculosis* protein Ag85b (PIV5 vector control) (61). As shown in Figs 9A and 9B, all PBS control mice reached humane endpoints within 5 days post-challenge. Likewise, animals vaccinated with the control virus PIV5-Tb rapidly succumbed to infection and showed negligible survival. In contrast, immunization with PIV5-Pal_{Bm} protected 90% and 80% of mice against death during acute and chronic infection, respectively, which was comparable to the survival rates observed in animals vaccinated with the efficacy benchmark control virus PIV5-BatA. At study endpoints, we determined bacterial loads in target organs of survivors and discovered that no agent was present in the liver of $n = 7$ out of 8 mice immunized with PIV5-Pal_{Bm} whereas all animals given the PIV5-Tb and PIV5-BatA vaccines were colonized with *B. mallei* (Fig 4.9C). Three mice from each cohort vaccinated with PIV5-BatA and PIV5-Pal_{Bm} had no bacteria in the lungs and the sole survivor immunized with the control PIV5-Tb vaccine had also cleared the agent (Fig 4.9C). All mice were colonized in the spleen (Fig 4.9E). Collectively, the data show that a single dose of PIV5-Pal_{Bm} provides excellent survival against *B. mallei* lethal aerosol challenge and promotes bacterial clearance from target organs, in particular the liver.

DISCUSSION

Published work by other groups and the data herein underscore the value of the Pal protein for developing countermeasures against highly pathogenic *Burkholderia* species. The *pal* gene is present in the genomes of all *B. mallei* and *B. pseudomallei* isolates sequenced to date and the encoded proteins are identical. We showed that Pal_{Bm} plays a role in *B. mallei* intracellular fitness and serum resistance (Fig 4.4), and is expressed *in vivo* as evidenced by the titer of Pal_{Bm}-specific antibodies in the serum of mice infected with the organism (Fig 4.7B). Moreover, we showed that a *B. mallei* mutant lacking the protein is greatly attenuated in virulence and completely cleared from host tissues even at high challenge doses (Figs 4.5 and 4.6). Immune response against the Pal protein of *B. pseudomallei* (Pal_{Bp}) has been linked to resolution of chronic and recurrent melioidosis in human patients (255). Experimental subunit vaccines containing purified Pal_{Bp} were also shown to provide partial protection against lethal intraperitoneal challenge with *B. pseudomallei* in mice (56, 121), and our data indicate that delivering Pal_{Bm} with a viral vaccine system elicits outstanding protection against aerosol exposure to *B. mallei* (Fig 4.9). Thus, Pal possesses many qualities of a strong candidate for devising medical intervention strategies and targeting the protein may interfere with the ability of *B. mallei* and *B. pseudomallei* to establish themselves in the host, persist, and cause infection.

We discovered that *B. mallei* ATCC 23344 does not produce detectable amounts of Pal when cultured under routine laboratory conditions. These results are consistent with published proteomics data for the organism. Specifically, Schell and colleagues analyzed outer membrane protein preparations from ATCC 23344 cells grown under multiple conditions and their data show that Pal (*i.e.* BMA2082) was present in very low abundance

and only in some of the conditions tested (228). A review of the literature indicated that Pal is produced at readily detectable levels by most organisms in which expression of the protein has been studied including *E. coli* (180), *Haemophilus influenzae* (190), *Erwinia chrysanthemi* (78), *Pseudomonas aeruginosa* (166), and *Haemophilus ducreyi* (89). Hence, the *pal* gene appears to be more stringently regulated in *B. mallei*.

Despite low expression levels, Pal_{Bm} significantly contributes to maintaining the integrity of the *B. mallei* cell envelope as illustrated by the hypersensitivity of the *pal* KO mutant to osmotic stress and the membrane-acting antibiotic Polymyxin B (Figs 2 and 3). The plasmid $pPal_{Bm}$, which specifies constitutive production of Pal_{Bm}, restored susceptibility of the *pal* KO strain to osmotic stress and Polymyxin B to WT levels. The *in vitro* phenotypic characterization of WT and recombinant bacteria also revealed a role for Pal_{Bm} in the ability of *B. mallei* to thrive intracellularly and withstand complement-mediated killing. While the $pPal_{Bm}$ construct restored intracellular fitness to parental levels, the serum resistance defect was partially complemented (Fig 4.4). Similar observations were previously made in a *Klebsiella pneumoniae* strain deleted for *pal* (138). The mutant exhibited reduced protection from serum and neutrophil killing; the serum resistance defect was partially rescued by complementation with an intact copy of the *K. pneumoniae pal* gene and intracellular fitness was fully restored to WT levels. Likewise, a mutation in the gene encoding the *Haemophilus influenzae* Pal ortholog P6 protein was shown to result in increased sensitivity to normal human serum and complementation partly restored resistance (190). Lack of full complementation of the serum resistance phenotype of the *pal* KO mutant is likely due to a gene dosage effect and overproduction of Pal_{Bm} by the complemented strain (Fig 4.1A). The disproportionate amounts of Pal_{Bm}

in the cell envelope may have the unintended effect of destabilizing bacterial membranes and sensitizing the organism to complement-mediated lysis.

Several studies have highlighted a significant role for Pal in the pathogenesis of bacterial infection. For instance, the virulence of a *pal* deletion mutant of *Burkholderia cenocepacia* was reduced by 88-fold in a *Galleria mellonella* larvae model (74). Deletion of the *pal* gene increased the LD_{50} of *K. pneumoniae* in a mouse model of intraperitoneal infection from less than 1×10^2 CFU for WT organisms to ~2×10^5 CFU (138). An isogenic *pal* mutant strain of *H. ducreyi* was also found to be considerably attenuated in a human challenge model (89). Our data demonstrate that a mutation in the *pal* gene of *B. mallei* ATCC 23344 is highly attenuating, as mice inoculated with 2, 500 LD_{50} all survived challenge and completely cleared the organism from target tissues (Figs 5 and 6). Introduction of the plasmid $pPal_{Bm}$ in the *pal* KO mutant restored virulence, but not back to parental levels; the LD_{50} of the complemented strain was still approximately 30-fold higher than WT *B. mallei*. In light of our results showing that serum samples from the mice infected with complemented *pal* KO bacteria contain higher antibody titers against Pal_{Bm} than the serum of survivors infected with WT *B. mallei* (Fig 4.7B), we propose that the ostensively incomplete rescuing of the virulence phenotype results from increased immune clearance via targeting of the Pal_{Bm} protein overexpressed by the complemented mutant. Alternatively, partial complementation may be due to gene dosage effect. Our laboratory as well as other groups have reported similar difficulties studying membrane proteins and complementing *in vivo* virulence defects with plasmid-based systems (49, 283, 295, 296). Collectively, our data indicate that Pal is a major virulence factor of *B. mallei*, although its specific role is not clearly defined yet. We can not exclude the possibility that

the intracellular fitness, serum resistance, and *in vivo* virulence phenotypes of the *pal* KO mutant are indirectly caused by a general defect in cell membrane integrity. Additional studies are ongoing to clarify the specific role of the *pal* gene product in these phenotypic traits.

The Pal proteins of several organisms have been shown to possess excellent vaccinogenic potential (105, 164, 181). One of the best studied examples is the aforementioned P6 protein, which is considered a lead vaccine candidate for prevention of non-typeable *H. influenzae* infections in humans (acute otitis media in children, sinusitis, exacerbations in COPD patients, pneumonia). Subunit vaccines containing P6 induce protective immune responses in several animal models including an infant rat model of invasive infection (110, 284), a rat pulmonary clearance model (154), and otitis media models in chinchillas and mice (73, 111, 219). An analysis of antibody titers to P6 in children has indicated that immune responses to the protein correlate with protection from *H. influenzae* otitis media (137, 152, 281). Moreover, T-cell responses to P6 in COPD patients are associated with protection from exacerbations caused by *H. influenzae* (1). Consistent with these studies, the antibody response to the Pal protein of *B. pseudomallei* was shown to be 10-fold higher in plasma from human patients who had only 1 episode of melioidosis than those with recurrent bouts of disease (255). Experimental subunit vaccines containing Pal_{Bp} were also shown to provide 50% survival in mice challenged intraperitoneally with *B. pseudomallei* (56, 121). Our data complement and expand upon these findings by demonstrating that one dose of the PIV5 viral vaccine vector expressing Pal_{Bm} affords excellent protection against *B. mallei* lethal aerosol challenge.

The exact mechanism of protection elicited by the PIV5-Pal_{Bm} vaccine is not clear at the moment. The analyses of serum and bronchoalveolar samples from immunized mice indicate little to no antibody titers against Pal_{Bm} (data not show). Based on these results and our published work using the PIV5 platform to develop bacterial vaccines for *Mycobacterium tuberculosis* (61) and highly pathogenic *Burkholderia* species (157), T-cell responses are likely the predominant effectors of protection in our model system. Future work should compare and contrast the kinetics, levels, and functionality of humoral as well as cellular responses stimulated by the PIV5-Pal_{Bm} vaccine prior to and during infection, test vaccine efficacy against lethal aerosol challenge with *B. pseudomallei*, and investigate prime-boost vaccination approaches to bolster protective immunity and bacterial clearance from target organs. These studies will identify critical immune components associated with protection and guide efforts for the rational design of PIV5-based vaccines targeting Pal_{Bm} and/or other established immunoprotective antigens such as BatA (see Fig 4.9) (157), with the goal of achieving sterilizing immunity and complete protection against acute and chronic infections by *B. mallei* and *B. pseudomallei*. Interestingly, the Pal protein of *Burkholderia* species *cepacia*, *cenocepacia*, and *multivorans* exhibit 84% sequence identity with Pal_{Bm}. These bacteria form the *Burkholderia cepacia* complex (Bcc) and are important opportunistic pathogens causing infections in people with cystic fibrosis and for which the availability of effective countermeasures is a critical unmet need (206). With this in mind, it may be possible to expand the use of the PIV5-Pal_{Bm} vaccine to these organisms.

TABLES AND FIGURES

Table 4.1

Strain or plasmid	Description	Source or reference
B. mallei		
ATCC 23344	Wild-type strain; polymyxin B resistant, kanamycin and zeocin sensitive	(194)
pal KO	Isogenic *pal* mutant strain of ATCC 23344; resistant to polymyxin B and zeocin, sensitive to kanamycin	This study
E. coli		
EPI300	Strain used for general recombinant DNA manipulations; sensitive to kanamycin, zeocin, tetracycline, and chloramphenicol	epicenter/Lucigen
EC100D *pir*$^{+}$	Strain used for recombinant DNA manipulations of plasmid pKAS46 and derivatives; sensitive to kanamycin and zeocin	epicenter/Lucigen
S17	Strain used for conjugational transfer of plasmids to *B. mallei*; sensitive to kanamycin, zeocin, and polymyxin B	(234)
TUNER	Protein expression strain used to purify His-tagged Pal_{Bm} and $LolC_{Bm}$ proteins; chloramphenicol sensitive	Millipore Sigma
Plasmids		
pBHR1	Cloning vector; confers resistance to chloramphenicol and kanamycin	MoBiTec
pBHR1Δ Dra	pBHR1 containing a 339 nt deletion in the chloramphenicol resistance marker; confers resistance only to kanamycin	(296)
$pPal_{Bm}$	pBHR1 in which a 812 nt DNA fragment containing the *pal* gene of *B. mallei* ATCC 23344 was inserted; confers resistance only to kanamycin	This study
pEM7/ZEO	Source of the zeocin resistance cassette; confers resistance to zeocin	ThermoFisher Scientific
pACYC184	Cloning vector; confers resistance to chloramphenicol and tetracycline	New England Biolabs Inc.

pACYCPal$_{Bm}$	pACYC184 in which a 1,332 nt DNA fragment containing the *pal* gene of *B. mallei* ATCC 23344 was inserted; confers resistance to tetracycline	This study
pACYCPal$_{Bm}$ZEO	pACYCPal$_{Bm}$ in which a zeocin resistance cassette was inserted near the middle of the *pal* gene; confers resistance to tetracycline and zeocin	This study
pKAS46	Gene replacement vector; confers resistance to kanamycin	(238)
pKASPal$_{Bm}$ZEO	pKAS46 containing the *pal* gene interrupted with a zeocin resistance cassette from pACYCPal$_{Bm}$ZEO; confers resistance to kanamycin and zeocin	This study
pETcoco-1	His-tagged protein expression vector; confers resistance to chloramphenicol	Millipore Sigma
pHisPal$_{Bm}$	pETcoco-1 in which a gene fragment encoding amino acids 22 to 170 of *B. mallei* ATCC 23344 Pal was inserted; confers resistance to chloramphenicol	This study
pHisLolC$_{Bm}$	pETcoco-1 in which a gene fragment encoding amino acids 47 to 243 of *B. mallei* ATCC 23344 LolC was inserted; confers resistance to chloramphenicol	This study
pMHD11	pZL185 (PIV5 genome) in which a gene fragment encoding amino acids 22 to 170 of *B. mallei* ATCC 23344 Pal was inserted; confers resistance to chloramphenicol	This study
Viruses		
PIV5-Pal$_{Bm}$ (MHD11)	PIV5 expressing amino acids 22 to 170 of *B. mallei* ATCC 23344 Pal protein	This study
PIV5-BatA	PIV5 expressing amino acids 30 to 307 of *B. mallei* ATCC 23344 BatA protein	(157)
PIV5-Tb	PIV5 expressing Ag85B protein of *M. tuberculosis*	(61)

Table 4.2

Treatment	**# mice challenged**	**Survival (10 days post challenge)**
pal KO vaccination (dose = 190 CFU)	4	0/4
pal KO vaccination (dose = 1,900 CFU)	5	0/5
pal KO vaccination (dose = 19,000 CFU)	5	0/5
pal KO vaccination (dose = 190,000 CFU)	5	0/5
pal KO vaccination (dose = 1,900,000 CFU)	5	0/5
PBS vaccination	5	0/5

BALB/c mice were inoculated with the indicated dose of the *pal* KO mutant strain using a Microsprayer device. Thirty days later the animals were challenged with 6,000 CFU of *B. mallei* ATCC 23344 using the Microsprayer. Age- and weight-matched mice vaccinated with PBS using a Microsprayer were used as controls.

Figure 4.1

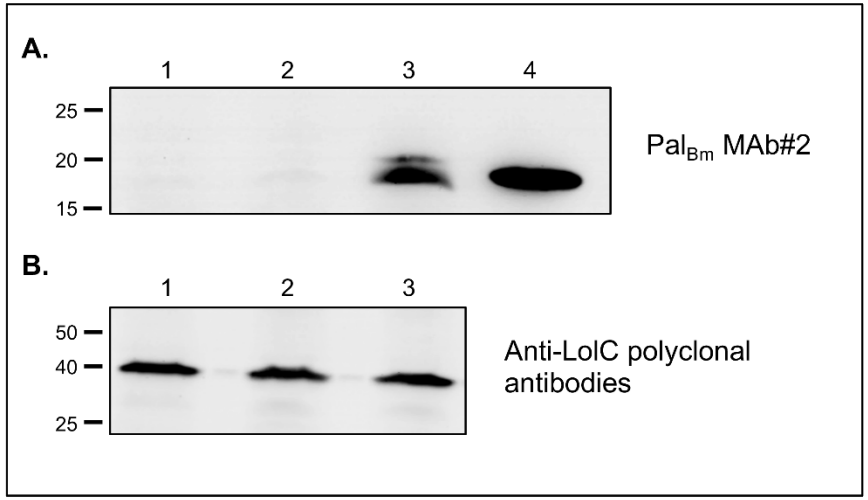

Western blot analysis of *B. mallei* WT and recombinant strains. Whole cell lysates were prepared from WT *B. mallei* (lane 1) and the *pal* KO mutant strain carrying the plasmids pBHR1ΔDra (lane 2) and pPal$_{bm}$ (lane 3) and analyzed by Western blotting with the monoclonal antibody Pal$_{bm}$ MAb#2 (panel A) and polyclonal antibodies against the LolC protein (panel B, used as loading control to demonstrate that equivalent amounts of proteins were analyzed). Molecular mass markers are shown to the left in kilodaltons. Lane 4 in panel A corresponds to 5 ug of purified His-tagged Pal$_{bm}$ protein (used as positive control to demonstrate reactivity and specificity of Pal$_{bm}$ MAb#2).

Figure 4.2

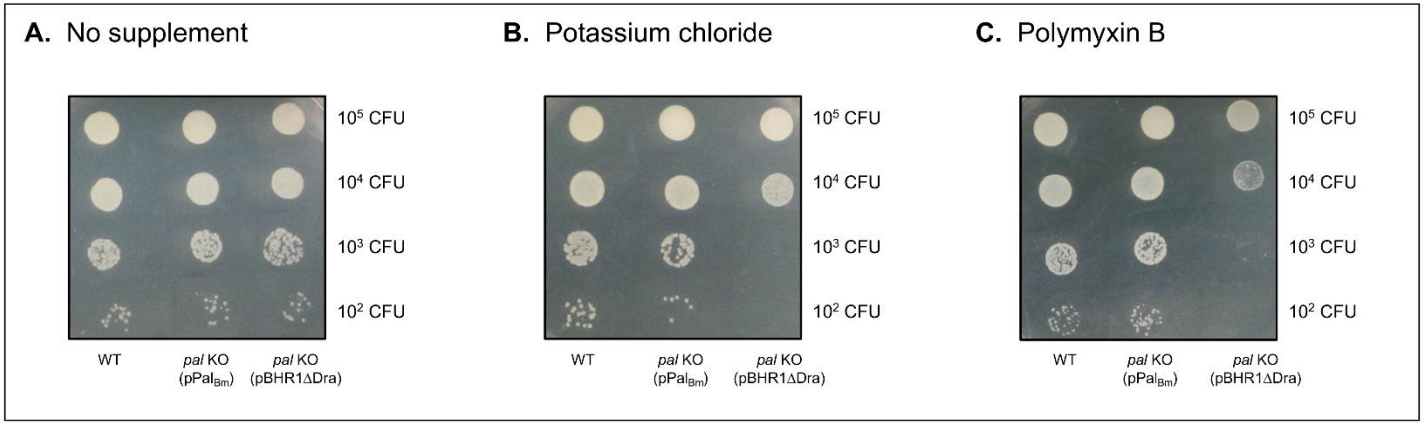

Effect of osmotic and antibiotic stresses on the growth of *B. mallei* WT and recombinant strains. Plate-grown organisms were suspended in PBS to a concentration of 1 x10^9 CFU/mL. Ten-fold serial dilutions of bacterial suspensions were then spotted onto agar plates and incubated at 37◦C for 40 hours. (A) Medium without supplement. (B) Medium supplemented with 100 mM potassium chloride for osmotic stress. (C) Medium supplemented with 20 ug/mL of the antibiotic Polymyxin B. The number of CFU spotted on the agar plates is shown to the right of each panel. Images are representative of 3 independent experiments.

Figure 4.3

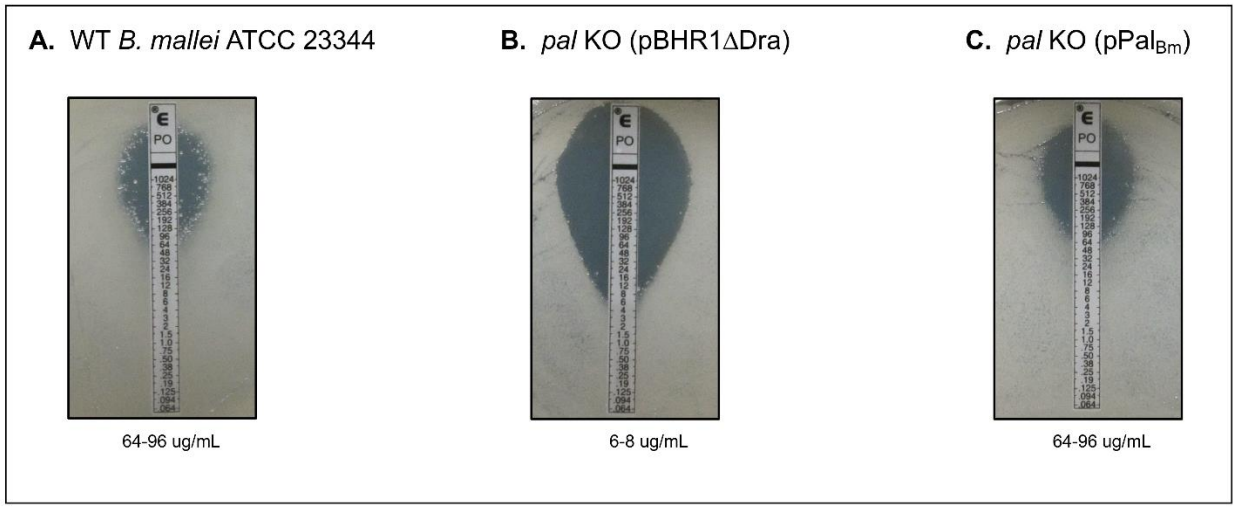

Polymyxin B sensitivities of *B. mallei* WT and recombinant strains. Plate-grown organisms were suspended in PBS to a concentration of 1 x10^9 CFU/mL. Portions of bacterial suspensions (10^8 CFU) were then spread onto agar plates and E strips containing a gradient of Polymyxin B concentrations (0.064 - 1024 ug/mL, Biomerieux) were applied onto the inoculated medium. After incubation at 37°C for 40 hours, minimal inhibitory concentration (MIC) values were determined by reading the intersection of the test strip with the lower part of the ellipse-shaped area of bacterial growth inhibition. (A) WT *B. mallei* ATCC 23344. (B) *pal* KO mutant carrying vector control pBHR1ΔDra. (C) *pal* KO mutant carrying plasmid $pPal_{Bm}$. Images are representative of 3 independent experiments. MIC values are shown at the bottom of each panel.

Figure 4.4

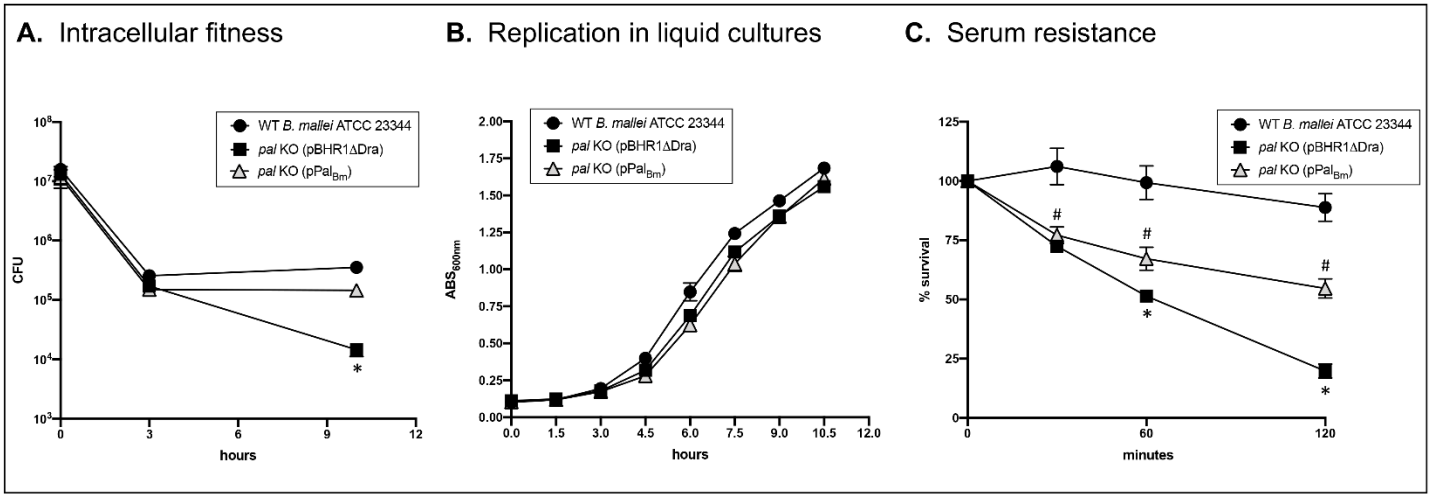

Serum resistance, intracellular fitness, and *in vitro* replication rate in liquid cultures of *B. mallei* WT and recombinant strains. (A) Plate-grown bacteria were suspended in PBS and used to infect 3 wells of duplicate tissue culture plates seeded with murine J774 macrophages (multiplicity of infection of 10:1). The infected cells were incubated for 1 hour at 37◦C to allow phagocytosis of the bacteria, washed, and treated with antibiotic for 2 hours to kill extracellular bacteria. Cells from one tissue culture plate were lysed, diluted, and plated onto agar medium to determine the number of bacteria phagocytized. The other tissue culture plate was incubated for an additional 7 hours, after which the cells were washed, lysed, diluted, and spread onto agar plates to calculate the number of intracellular organisms. The results are expressed as the mean CFU per well. The assays were performed on 3 separate occasions. The graph shows cumulative

results. The error bars correspond to standard errors of the mean. The asterisk indicates that the reduction in the number of intracellular *pal* KO bacteria carrying the vector pBHR1ΔDra at 10 hours post-infection, compared to WT *B. mallei* and the *pal* KO mutant carrying plasmid $pPal_{Bm}$, is statistically significant. The reduction in the number of intracellular *pal* KO bacteria carrying plasmid $pPal_{Bm}$ at 10 hours post-infection, compared to WT *B. mallei*, was not statistically significant. (B) Plate-grown bacteria were suspended in broth to an optical density at wavelength 600 nm (ABS_{600nm}) of 0.1. Following this, suspended bacteria were incubated at 37°C with shaking (200-rpm) and the optical density of cultures was measured at the indicated time intervals. Strains were tested on at least 2 separate occasions. The graph shows cumulative results. The error bars correspond to standard errors of the mean. (C) Plate-grown bacteria were suspended in PBS supplemented with Mg^{+2} and Ca^{+2} and aliquots containing 10^3 CFU were placed in duplicate tubes. Following this, normal human serum was added to the bacteria at a final concentration of 25% and the mixtures were incubated at 37°C. Portions were removed at the indicated time points and plated onto agar medium to determine the number of viable organisms. The results are expressed as the mean percentage of the original inoculum (time 0 minutes) remaining at each time point. The assays were performed on 4 separate occasions. The graph shows cumulative results. The error bars correspond to standard errors of the mean. The asterisk indicates that the reduction in the number of *pal* KO bacteria carrying the vector pBHR1ΔDra and surviving exposure to serum, compared to WT *B. mallei* and the *pal* KO mutant carrying plasmid $pPal_{Bm}$, is statistically significant. The hashtag indicates that the reduction in the number of *pal* KO bacteria carrying plasmid $pPal_{Bm}$ and surviving exposure to serum, compared to WT *B. mallei*, is statistically significant.

Figure 4.5

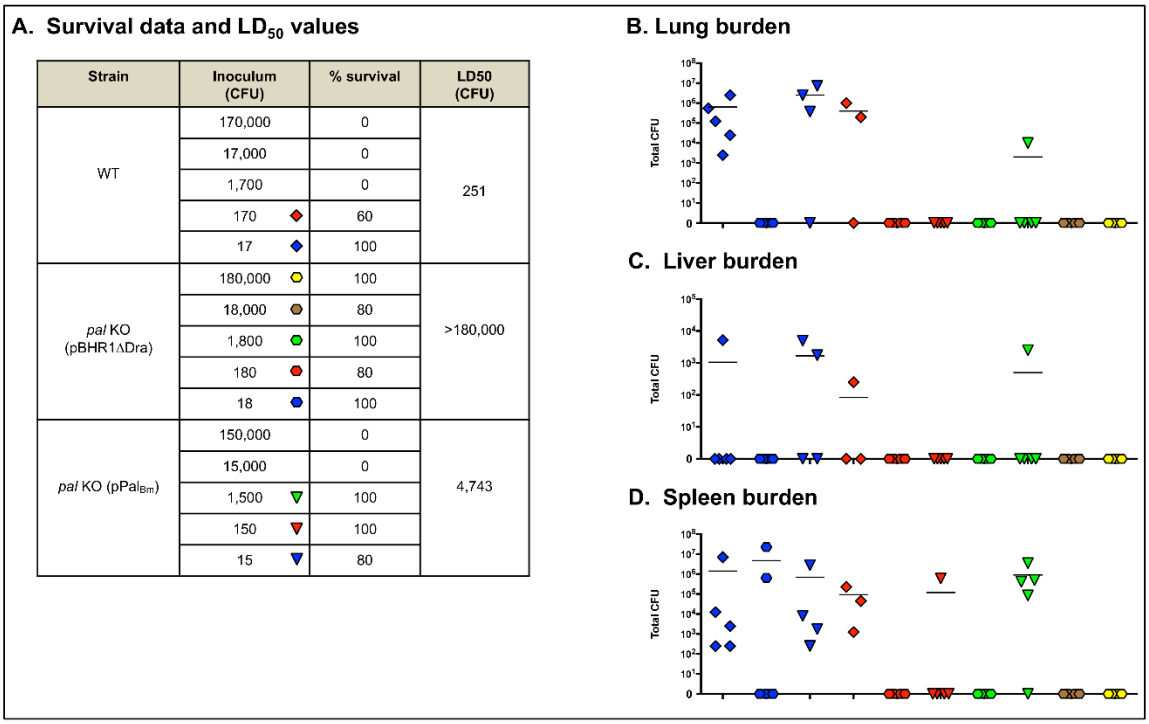

Median lethal dose comparison for *B. mallei* WT and recombinant strains. BALB/c mice were inoculated with a Microsprayer device to aerosolize the indicated numbers of bacterial CFU directly into the lungs (*n*=5 mice/dose). The animals were then monitored daily for clinical signs of illness and morbidity. (A) Survival data and calculated LD_{50} values. (B, C, and D) Tissues were collected from mice that survived challenge (day 22), homogenized, diluted, and spread on agar plates to determine bacterial loads. The symbols represent data from individual animals; horizontal lines represent the mean total number of CFU for each group.

Figure 4.6

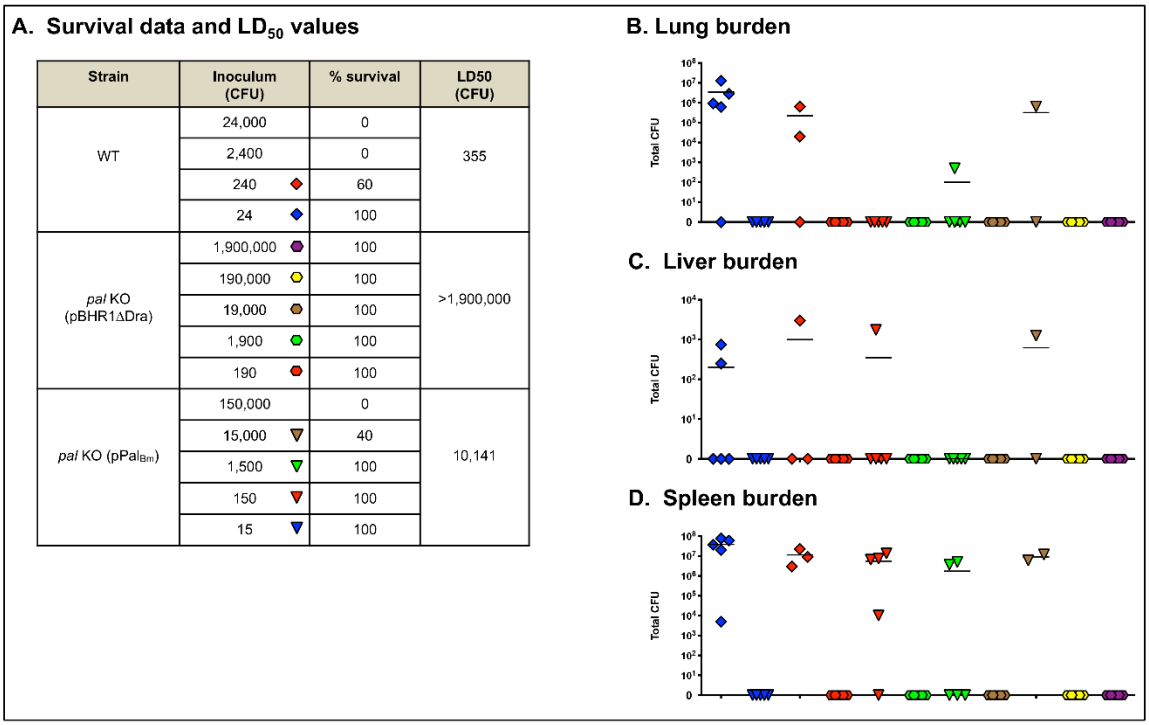

Median lethal dose comparison for *B. mallei* WT and recombinant strains. BALB/c mice were inoculated with a Microsprayer device to aerosolize the indicated numbers of bacterial CFU directly into the lungs (*n*=5 mice/dose). The animals were then monitored daily for clinical signs of illness and morbidity. (A) Survival data and calculated LD_{50} values. (B, C, and D) Tissues were collected from mice that survived challenge (day 27), homogenized, diluted, and spread on agar plates to determine bacterial loads. The symbols represent data from individual animals; horizontal lines represent the mean total number of CFU for each group.

Figure 4.7

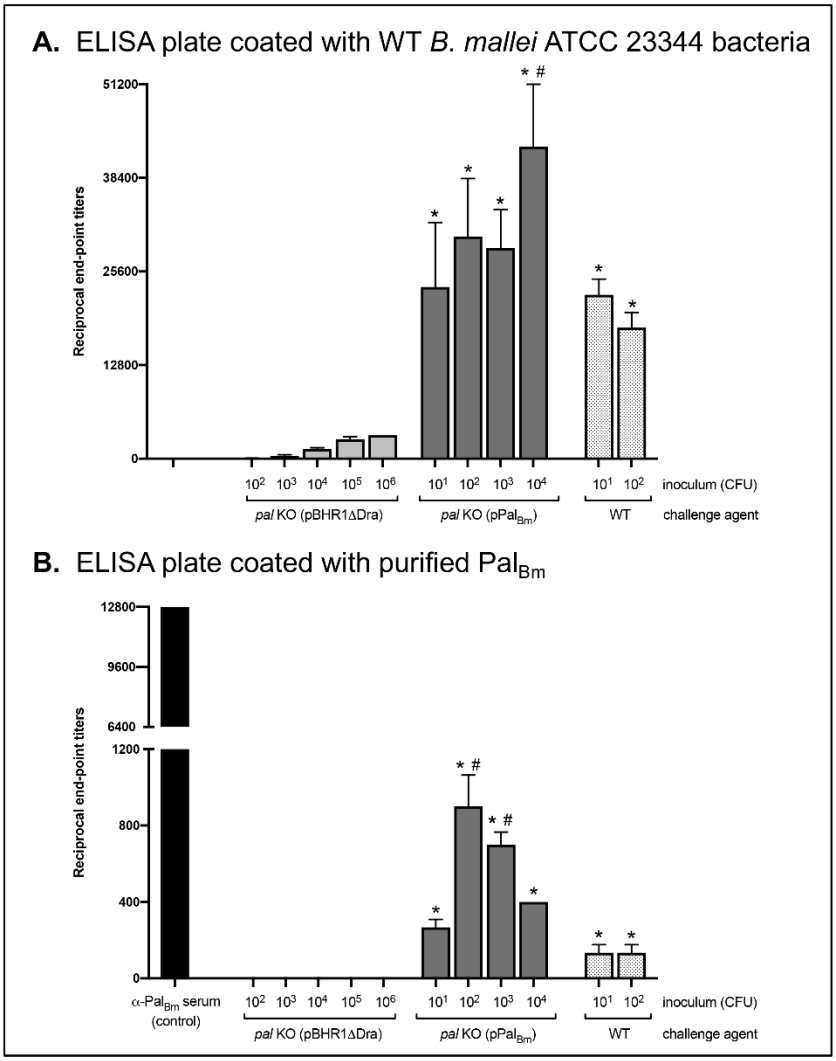

ELISA using serum from mice challenged with *B. mallei* WT and recombinant strains. Serum samples were serially diluted and placed in duplicate wells of plates coated with whole paraformaldehyde-fixed *B. mallei* ATCC 23344 bacteria (panel A) and with purified His-tagged Pal_{Bm} protein (panel B). Alkaline-phosphatase-conjugated goat anti-mouse antibodies (light and heavy chains) were used for detection. Serum samples were tested in duplicate on at least 2 separate occasions. The results are expressed as the mean (plus standard error) reciprocal endpoint titers. Naïve serum was used to establish background

reactivity, and the endpoint titers correspond to the highest immune serum dilutions giving ELISA values greater than the mean value of naïve serum plus 3 standard deviations. The labels on the x-axis show the source of immune serum samples (collected from survivors in experiments to determine the LD_{50} of *B. mallei* WT and recombinant strains, see Figs 5 and 6). The asterisks indicate that the increase in serum titers, compared to samples from mice infected with *pal* KO (pBHR1ΔDra) bacteria, is statistically significant. The hashtags indicate that the increase in serum titers, compared to samples from mice infected with WT bacteria, is statistically significant.

Figure 4.8

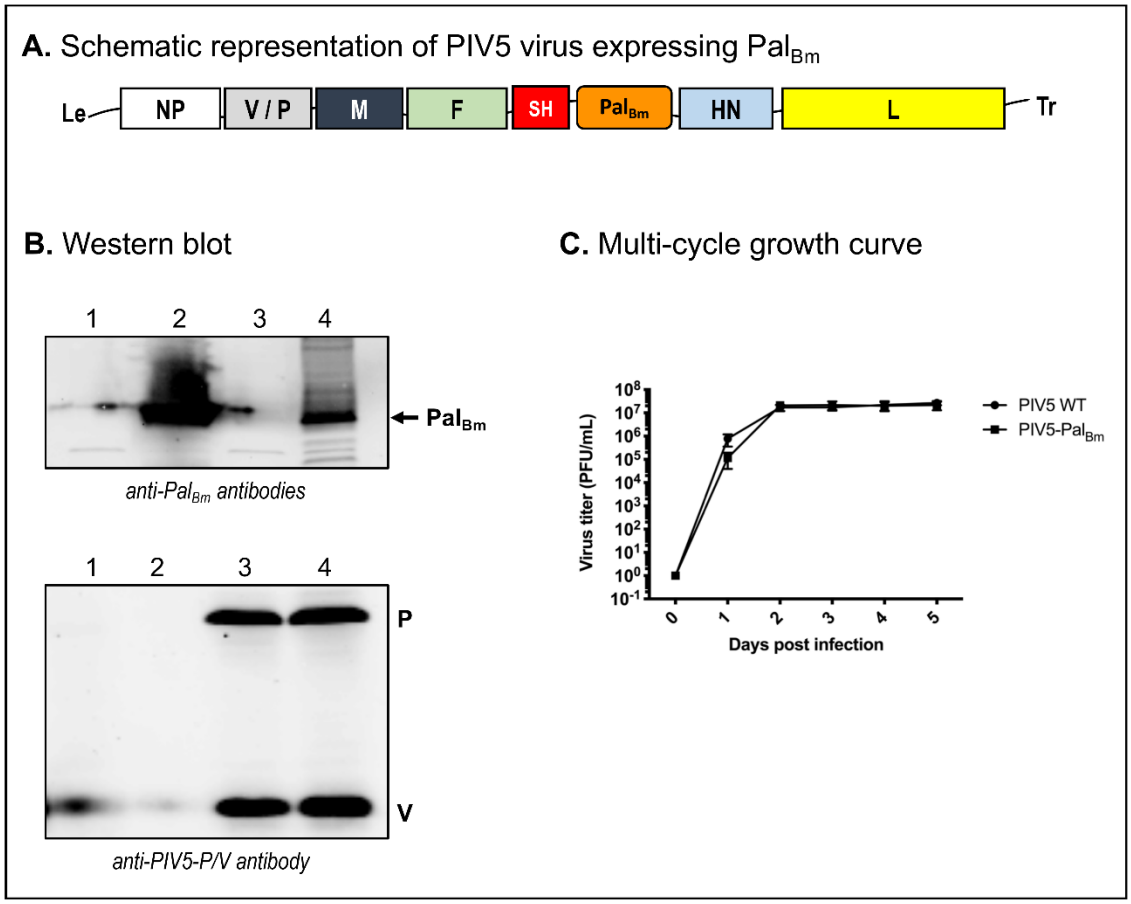

Characterization of recombinant PIV5 virus expressing Pal_{Bm}. (A) Schematic of PIV5-Pal_{Bm} vaccine construct. NP, nucleoprotein; V, V protein; P, phosphoprotein; M, matrix protein; F, fusion protein; SH, small hydrophobic protein; HN, hemagglutinin-neuraminidase protein; L, RNA-dependent RNA polymerase; Pal_{Bm}, *B. mallei* Pal protein residues 22-170. (B) Equivalent protein amounts of lysates from cells infected with PIV5-Pal_{Bm} and PIV5 viruses were analyzed by Western blotting with mouse Pal_{Bm}-specific polyclonal and PIV5-P/V antibodies. Lane 1= mock infected cells; Lane 2=purified His-tagged PalBm; Lane 3=cells infected with WT PIV5 virus; Lane 4=cells infected with PIV5-Pal_{Bm} virus (C) MDBK cells were infected in triplicate with PIV5-Pal_{Bm} and PIV5

viruses at an MOI of 0.01. Aliquots of supernatant from the infected cell cultures were collected at 24-hour intervals for a period of 5 days post-infection and titers were determined by plaque assays using BHK21 cells. The results are expressed as the mean (± standard error of the mean) log10 PFU/mL. There was no statistically significant difference between viruses.

Figure 4.9

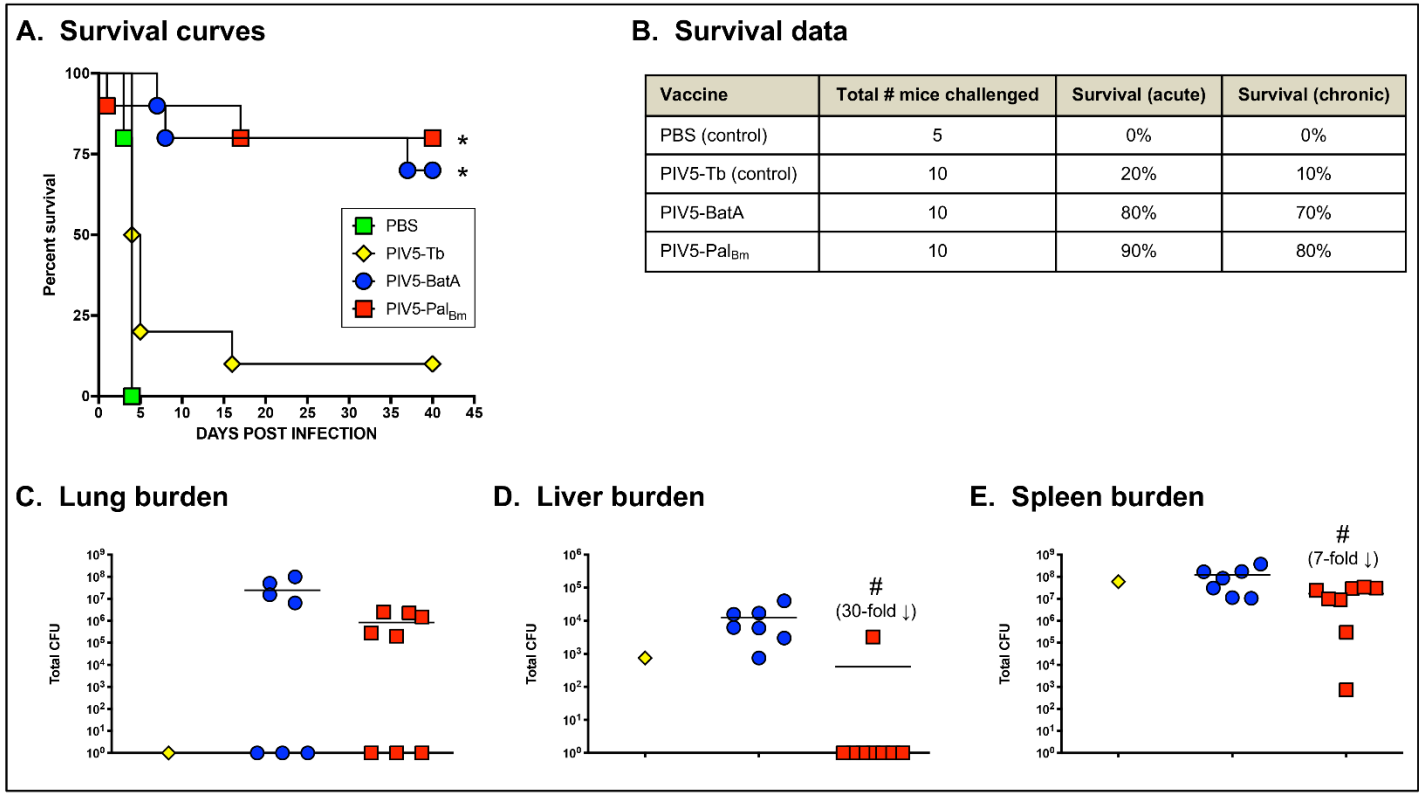

Vaccine	Total # mice challenged	Survival (acute)	Survival (chronic)
PBS (control)	5	0%	0%
PIV5-Tb (control)	10	20%	10%
PIV5-BatA	10	80%	70%
PIV5-Pal_{Bm}	10	90%	80%

Vaccination with PIV5-Pal_{Bm} provides protection against challenge with a lethal dose of WT *B. mallei*. BALB/c mice vaccinated intranasally with PIV5 viruses were challenged with 10 LD_{50} of *B. mallei* ATCC 23344 using a Microsprayer device and monitored daily for clinical signs of illness and morbidity. (A) Kaplan-Meier survival curves. (B) Survival data during the acute (days 1 through

10 post-challenge) and chronic (days 11 through 40 post-challenge) phases of infection. (C, D, E) At study end-points, tissues collected from survivors were homogenized, diluted, and spread on agar plates to determine bacterial loads. Symbols represent individual animals; horizontal lines show the mean total CFU for each group. The asterisks indicate that the survival curves were found to be significantly different from mice vaccinated with PBS and the control vaccine PIV5-Tb. The hashtags indicate that the decrease in bacterial burden, compared to mice vaccinated with PIV5-BatA, is statistically significant. Although a 30-fold decrease in lung bacterial burden was observed between mice vaccinated with PIV5-Pal_{Bm} and PIV5-BatA, this decrease was not statistically significant (panel C).

CHAPTER 5

THE OMPR-LIKE *BURKHOLDERIA MALLEI* DNA BINDING RESPONSE REGULATOR BORP REGULATES BIOFILM FORMATION AND VIRULENCE

Dyke J.S., Holladay N.E., Michel F., Hogan R.J., and Lafontaine E.R.

To be submitted to PLOS One

ABSTRACT

Burkholderia mallei and *Burkholderia pseudomalle* are two closely related Gram-negative bacterial species that cause the fatal diseases glanders and melioidosis respectively. Both organisms contain the *bpaB* gene within their genome. Upstream of this gene in *B. mallei* is the *bma0838* gene. We investigated this gene and discovered that it is an OmpR-like DNA-binding protein. Due to its structural characteristic being similar to the OmpR protein, we named the gene product BorP which was short for ***B****urkholderia* **O**mp**R**-like **P**rotein. A mutant lacking the expression of BorP was highly attenuated in virulence in a BALB/c mouse model. Additionally, when expression of BorP was constitutively expressed in this mutant, we found a corresponding expression of BpaB. Use of Electrophoretic Mobility Shift Assays (EMSAs) demonstrated that the BorP specifically binds a predicted promoter region upstream of the *bpaB* gene. Here, we present data supporting our hypothesis that the BorP DNA-binding protein positively regulates the expression of the BpaB trimeric autotransporter protein directly, rather than indirectly as a global virulence regulator.

INTRODUCTION

Burkholderia mallei and *Burkholderia pseudomallei* are two closely related Gram-negative bacteria that cause the severe respiratory illnesses glanders and melioidosis, respectively (37, 97). *Burkholderia mallei* is endemic to parts of Asia, Africa, the Middle East, and South America (97). *Burkholderia pseudomallei* is endemic to countries bordering the equator, with endemicity being particularly high in Northern Australia and Southeast Asia (37). Comparative sequence analyses indicate that *B. mallei* evolved from the environmental saprophyte *B. pseudomallei* through a large gene deletion event (171,

182, 200). While the genome of *B. mallei* is smaller than *B. pseudomallei* due to this genetic reduction, the respective genomes have >99% similarity where their remains overlap (97, 171, 226, 233). As a consequence of this genetic similarity, there is a high degree of similarity between the diseases caused by both organisms. Both illnesses can present as an acute or chronic infection, and the most common manifestations are severe pneumonia with accompanying bacteremia (85, 97).

Burkholderia mallei and *B. pseudomallei* are highly infectious, difficult to diagnose, and are difficult to treat due to intrinsic resistance to most antibiotics (216). Glanders and melioidosis have high morbidity and mortality rates (85, 97). Further, there is no vaccine to reduce the risk of infection. In addition, there are concerns that *B. mallei* and *B. pseudomallei* could be misused as biological warfare agents. For these reasons, the organisms are classified as Tier 1 Select Agents and the development of efficacious countermeasures is a priority. The high level of genetic relatedness between the organisms, and the striking similarities in the clinical and pathological manifestations of disease they cause, support the feasibility of devising a single vaccine that protects against both *B. mallei* and *B. pseudomallei*.

A major hallmark of *B. mallei* and *B. pseudomallei* virulence, is the ability to persist for long periods of time in a host, surviving and replicating within professional and non-professional phagocytic cells, and evading clearance by the immune system through modulation of the expression of surface antigens (251). A major determinant in the bacterial ability to evade the immune system and persist within the host environment is the presence of surface exposed autotransporter proteins (4, 5, 6). These molecules form one of the largest family of virulence factors in Gram-negative bacteria and contribute to a wide

range of pathogenic phenotypes including the formation of biofilms (3, 296), complement resistance (5), intracellular motility and replication (236, 237, 244), and lipolytic activity (295). The genomes of *B. mallei* and *B. pseudomallei* isolates have in common eight autotransporter gene products. Previous work by the Lafontaine laboratory has functionally characterized four of these in *B. mallei*, namely BoaA (155), BpaC (22), BpaB (296), and BatA (157, 295). One of these autotransporter gene products, BpaB, has previously been shown to be involved in adhesion to human lung cells and the production of a biofilm (296), two vital steps in the pathogenesis of *B. mallei* and *B. pseudomallei*. BpaB, as well as many other virulence factors of *B. mallei* and *B. pseudomallei*, have also been shown to be expressed *in vivo* but not at detectable levels *in vitro* under routine culture conditions (22, 155, 157, 295, 296). The underlying genetic factors controlling this *in vivo* vs *in vitro* expression are not yet understood.

Two-Component Systems (TCS) are the primary method with which bacteria sense and respond to environmental conditions and allow for the tight regulation of gene expression in response to extracellular stresses and conditions (13, 18, 28, 83, 86, 94, 101, 114, 171, 183, 248). The prototypical TCS is the EnvZ/OmpR two-component osmoregulation system. First identified in *E. coli* K-12, it consists of an environment sensing histidine kinase (EnvZ) (235, 273) and a corresponding response regulator (OmpR) (18, 24, 27, 46, 52, 55, 88, 120, 122, 128, 158, 235). The transmembrane EnvZ senses osmotic changes in the environment and in response undergoes autophosphorylation. A phosphate group is transferred from EnvZ to OmpR, resulting in a conformational change (OmpR-P) and a consequential differential change of expression in the *ompF*/*ompC* genes which encode a large and small diameter outer membrane porin channel, respectively. (24,

27, 46, 88, 104, 122, 129, 286, 287). Under low osmotic conditions, *E. coli* will preferentially express the larger OmpF porin, allowing a higher level of passive diffusion (30, 122, 129, 140, 158, 177, 287). When osmotic conditions reach a sufficient threshold, OmpR is subsequently phosphorylated, then binds the promoter regions of *ompF* and *ompC* leading to differential expression where *ompf* is repressed and *ompC* is upregulated (30, 34, 129, 158, 177, 287). Through this mechanism *E. coli* are able to persist in two diametrically opposing environments, one being a low nutrient environment and the other being a high nutrient host setting. TCS have been shown in many bacterial pathogens to be involved in the differential expression of virulence determinants such as biofilms (7, 14, 71, 179, 191, 209, 229, 243, 258, 265, 293), adherence (170, 217, 259, 293), motility (2, 25, 64, 103, 209, 213, 258), antimicrobial efflux pumps (26, 28, 71, 107, 183, 221 278), toxin production (31, 54, 127, 221), serum resistance (143, 207), and environmental stress responses (12, 16, 20, 23, 36, 38, 40, 53, 55, 77, 104, 115, 183, 212, 218, 241,294), at both the local and global level (12, 28, 153, 160, 225).

The use of TCS in *Burkholderia* species to selectively regulate genes is well documented. For example, the BceS/BceR TCS of *B. cenocepacia* has been demonstrated to play a vital role in swimming motility and quorum sensing (179). A *B. pseudomallei* K96243 mutant lacking expression of the BprR/BprS TCS was shown to be attenuated in virulence (2). Additionally, a *B. mallei* ATCC 23344 mutant lacking expression of the VirG portion of the VirAG TCS was avirulent in hamsters (227). A common feature of TCS gene modulation is a selective *in* vivo vs *in vitro* expression of genes, particularly those related to virulence. As this is an observed phenomena in *B. mallei* and *B. pseudomallei*, it is reasonable to assume that TCS may play a role in the selective expression of virulence

determinants during infection with either organism. One virulence determinant that is particularly interesting to the Lafontaine Lab is the autotransporter BpaB. BpaB is a large (>300-kDa) trimeric oligomeric autotransporter that has previously been described by our lab (296). As aforementioned, it was shown to mediate adherence to human lung cells (296) and was the first described biofilm formation factor in *B. mallei* (296). Additionally, it was shown to be a virulence determinant, as a mutant lacking its expression was reduced in virulence (296). While characterizing BpaB, it was observed that immediately upstream of the *bpaB* gene lies *bma0838*, a predicted TCS response regulator. While the mechanisms of TCS in general have been well studied and documented in other bacterial pathogens, there remains a considerable knowledge gap of TCS activity in *B. mallei* and *B. pseudomallei*, particularly with respect to *in vivo* expressed virulence factors not able to be studied *in vitro*. Here, we investigate the involvement if the *bma0838* gene in the *in vivo* expression of BpaB in *B. mallei* ATCC 23344.

RESULTS

Bioinformatics characterization of the *B. mallei bma0838* gene product.

The open reading frame of the *B. mallei* ATCC 23344 *bma0838* gene is found on chromosome 1, 696 nucleotides in length, and predicted to encode a 231 amino acid 26.44 kDa gene product. Analysis by the NCBI Conserved Domain Database (CDD) service indicated that the *bma0838* gene product is a member of the OmpR superfamily (Domain ID: cl34028; E value of $2.59e^{-58}$) of DNA binding response regulators. OmpR-like DNA binding response regulators are comprised of two distinct domains. The N-terminal receiver domain, or REC domain, is the most highly conserved domain of all response regulators and is responsible for the phosphorylation-mediated activation of attached output domains (35, 95). While the function of the output domains attached to REC domains can widely vary within bacteria, most of the > 60 described are involved in regulation (95). The second domain of OmpR-like DNA binding response regulators is the C-terminal winged-helix DNA binding domain. The winged-helix, or winged-helix-turn-helix (wHTH) structure is a variation of the typical helix-turn-helix (HTH) in that in addition to the three helices it also contains dual wing structures (10, 93, 175). The prototypical OmpR-wHTH contains two loops, or wings, three alpha helices, and three beta-sheets. The second helix in the structure, referred to as the recognition helix, binds to DNA in a sequence-specific manner, and makes direct contact with the major groove of DNA (175). The two wing structures also make DNA contact, though in an area separate from the recognition helix, and most often interact with the minor groove (10, 39, 93, 147, 174, 175).

Consistent with the prediction that the *bma0838* gene product was an OmpR-like DNA-binding response regulator, the amino acid sequence of the *bma0838* gene product contained conserved REC and wHTH domains at positions 63-117 and 127-227 respectively. Further, the predicted amino acid sequence of the *bma0838* gene specifies a potential phosphorylation site at position 52, which is highly conserved among OmpR-like response regulators. (24, 47, 88, 123). We compared the amino acid sequence of the DNA-binding region of the *bma0838* gene product to other OmpR-like regulators and found that there was a high degree of similarity (Fig 5.1A). There were several residues that were conserved across Gram-negative, Gram-positive, and *Mycobacterium* species. The crystal structure of BMA0838 has not been determined, but *in silico* analysis using the online tools PSIPRED and Phyre^2 indicates that the OmpR-like DNA binding domain of BMA0838 shares many of the secondary structures of the prototypical *E. coli* K12 OmpR protein, but is not completely identical (Fig 5.1B).

NCBI BLAST Searches identified *bma0838* orthologs in all *B. mallei* (n = 51) and *B. pseudomallei* (n > 1,000) genomes that were available to be searched. Within the available *B. mallei* and *B. pseudomallei* genomes, the *bma0838* gene was identical. A similar gene was not found in the closely related organism *Burkholderia thailandensis*; however, with the most related gene being 40% identical. This further strengthens the argument that the *bma0838* gene product is somehow involved with BpaB, as *B. thailandensis* also lacks the *bpaB* gene (296). Based on the similarity between the *bma0838* gene product and OmpR, we named the protein **B**urkholderia **O**mp**R**-like **P**rotein, or BorP.

Constitutive Expression of the *B. mallei* ATCC 23344 BorP Protein Results in Expression of BpaB

In order to examine the biological role of the BorP protein in *B. mallei*, we first engineered an isogenic mutant strain of *B. mallei* ATCC 23344 that lacked expression of the *borP* gene. We constructed this mutant using genomic homologous recombination of a DNA fragment that contained the *borP* open reading frame that had been disrupted with a zeocin resistance marker. Once the mutant was generated, it was complemented with the plasmids pBHR1ΔDra, an empty control vector, and pBorP, a pBHR1 plasmid that specifies constitutive expression of the *borP* gene. To confirm a lack of BorP expression by the mutant, whole cell lysates from wild-type (WT) and the recombinant strains were generated and analyzed by Western blotting with polyclonal antibodies reactive with BorP. The lack of reactivity between the BorP specific antibodies and the whole cell lysates from the *borP* knockout mutant carrying the control plasmid pBHR1ΔDra confirmed a lack of production of BorP by the recombinant bacteria (Fig 5.2A, lane 2). We also found that the BorP specific antibodies did not react with lysates generated from WT *B. mallei* ATCC 23344 (Fig 5.2A, lane 1) and a *bpaB* isogenic mutant control strain that harbors the plasmid pBpaB and constitutively produces the autotransporter BpaB. (296) (Fig 5.2A, lane 4). As expected, the anti-BorP polyclonal serum reacted with a protein of the appropriate size for BorP in the lysate from the *borP* KO mutant carrying the pBorP plasmid (Fig 5.2, lane 3) as well as 5 μg of purified His-tagged BorP (Fig 5.2, lane 5). To demonstrate that equivalent amounts of lysates were analyzed for each strain, polyclonal antibodies against the *B. mallei* LolC protein were used in western blotting (Fig 5.2B). Based on the equivalent loads of lysates and the lack of reactivity of polyclonal sera with WT *B. mallei* ATCC 23344 we

concluded that BorP is not produced at detectable levels by WT *B. mallei* under standard laboratory culture conditions. We further concluded that the anti-BorP polyclonal serum antibodies were specifically reactive with the BorP protein as they reacted with both the purified protein and the lysate from recombinant *B. mallei* bacteria constitutively producing the *borP* gene product (i.e. *borP* KO mutant carrying plasmid pBorP), but not with the lysates from WT bacteria and negative control (i.e. *borP* KO mutant carrying the vector pBHR1ΔDra).

In order to examine the presence or absence of BpaB production by the strains, and test the hypothesis that BorP positively regulates expression for the autotransporter, lysates were analyzed by Western blotting with the monoclonal antibody BpaB-MAb#4, which has previously been shown to have high reactivity and specificity for the BpaB protein (296). Lack of reactivity between BpaB-MAb#4 and the lysates from the *borP* KO mutant carrying the control plasmid pBHR1ΔDra confirmed a lack of production of BpaB by the mutant (Fig 5.2C, lane 2). The *B. mallei* ATCC 23344 WT strain also did not produce BpaB, demonstrated by a lack of reactivity between the αBpaB monoclonal antibody, which was unsurprising as our lab has previously demonstrated that BpaB is not produced at detectable levels *in vitro* (296). Additionally, there was high reactivity between BpaB-MAb#4 and lysates from the *bpaB* KO mutant carrying the BpaB constitutive expression plasmid pBpaB (Fig 5.2C, lane 4) which was also unsurprising, as this has also already been observed previously (296). However, lysates from the *borP* KO mutant carrying the BorP constitutive expression vector pBorP were reactive with BpaB-MAb#4 (Fig 5.2C, lane 3), demonstrating that constitutive expression of BorP results in production of

detectable amounts of BpaB, which in turn suggests that BorP positively regulates expression of the autotransporter.

Constitutive Expression of BorP Results in a Biofilm Formation Phenotype

One hallmark pathogenicity trait of *B. mallei* is the ability to survive and replicate within professional phagocytic cells (5, 6, 67, 91, 279). Due to the importance of this phenotype, we examined the role of BorP in intracellular fitness using J774 murine macrophage cell cultures. This was accomplished by comparing the replication rate of isogenic mutant strains compared to that of WT *B. mallei* ATCC 23344 bacteria. The results of the assays demonstrated that the BorP mutant carrying the control vector plasmid pBHR1ΔDra had no statistically significant difference in its ability to survive and replicate within professional phagocytic cells compared to WT *B. mallei* bacteria and the *bpaB* KO mutant carrying the pBorP plasmid (Fig 5.3B). Therefore, the *borP* gene does not appear to play a role in the intracellular fitness of *B. mallei*.

A key step in bacterial invasion into a host cell is adherence to the exterior of the cell surface. In order to examine the ability of the *borP* KO mutant to adhere to eukaryotic cells, quantitative adherence assays were performed using A549 human type II alveolar epithelial cells from ATCC. In the course of performing these assays, we found that the BorP mutant carrying the control vector plasmid pBHR1ΔDra had no statistically significant difference in its ability to adhere to A549 lung epithelial cells compared to WT *B. mallei* bacteria and the *bpaB* KO mutant carrying the pBorP plasmid (Fig 5.3C). The

lack of a statistically significant difference between the abilities of the *borP* KO mutant constitutively expressing BorP to adhere to mammalian cells compared to WT *B. mallei* bacteria was interesting. Previously published work by the Lafontaine lab has shown that while an *E. coli* strain carrying the pBpaB constitutive expression plasmid specifying expression of BpaB also has a > 4-fold increase in its ability to adhere to A549 cells, a *B. mallei* mutant carrying the same pBpaB plasmid conferring constitutive expression of BpaB had no difference in its ability to adhere to A549 cells compared to WT *B. mallei* (296). Additionally, the BpaB mutant complemented with pBpaB also had no increased or impaired ability to survive within J774 murine macrophages. The results of our experiments with the *borP* KO mutant recapitulate these findings in the *B. mallei* mutant, as we also failed to find a significant difference in the ability of a mutant expressing BpaB (indirectly as a consequence of BorP constitutive expression) to adhere to or invade mammalian cells at levels increased or impaired when compared to WT *B. mallei*. We then compared the growth rates of WT *B. mallei* ATCC 23344 and mutant strains in liquid broth cultures and found that there was no difference in their replication rates (Fig 5.3A), therefore loss of production of the BorP protein or its subsequent constitutive expression does not appear to result in a generalized growth defect that could explain this finding.

Previous work by the Lafontaine lab also demonstrated that BpaB is a biofilm formation factor for *B. mallei* (296). In order to investigate the role of BorP in BpaB mediated production of biofilm crystal violet staining biofilm assays were performed. We felt that this was an important avenue of investigation due to the discovery that constitutive expression of BorP resulted in a corresponding expression of BpaB. We found that the *bpaB* isogenic mutant control strain carrying the BpaB constitutive expression plasmid

pBpaB produced a biofilm ring at the liquid-air interface, as previously described (296), while WT *B. mallei* bacteria and the *borP* KO mutant carrying the control vector pBHR1ΔDra did not (Fig 5.4A and B). However, there was also a visible biofilm ring found in the wells containing the *borP* KO mutant complemented with the pBorP constitutive expression plasmid (Fig 5.4A and 3B). When the crystal violet stain was extracted and measured as a quantitative measurement of biofilm formation, there was no statistical significance between the broth control, *borP* KO mutant carrying pBHR1ΔDra, or WT *B. mallei* (Fig 5.4C). However, both the *borP* KO and *bpaB* KO mutant strains carrying the pBorP and pBpaB constitutive expression plasmids, respectively, were both significantly higher than the control well values (Fig 5.4C). From this data we can conclude that the expression of BorP positively regulates a biologically active form of BpaB resulting in the production of a biofilm. Another observation from the crystal violet staining biofilm assays was that the *bpaB* KO mutant carrying the pBpaB constitutive expression plasmid produced a larger biofilm when compared to the *borP* KO mutant carrying the pBorP constitutive expression plasmid. The difference in the level of biofilm formation was large enough to be detected both quantitatively and qualitatively (i.e. visually discernable). This difference between the two levels of biofilm production is consistent with the results of the western blot analyses examining the production of BpaB by both the *bpaB* mutant strain complemented with the BpaB constitutive expression plasmid pBpaB (Fig 5.2C, lane 4) and the *borP* mutant strain complemented with the BorP constitutive expression plasmid pBorP (Fig 5.2C lane 3). Both strains produced BpaB, and thus both strains also produced a biofilm. However, the level of reactivity between the BpaB specific monoclonal antibody and the whole cell lysate of the *bpaB* isogenic mutant strain

complemented with pBpaB or and the level of corresponding biofilm production was much higher where BpaB was constitutively expressed directly by plasmid.

We present strong evidence that BorP positively regulates the expression of BpaB. We asserted that this regulation was occurring at the local level rather than the global level, but this could not be conclusively stated based on the results of the data we had generated thus far. We reasoned that while it was possible that BorP could be regulating other genes, it seemed more likely to be a direct regulator of BpaB rather than a global virulence regulator as removal of its expression in *B. mallei* had no effect on the key virulence phenotypes that we examined. While the examined virulence phenotypes were by no means an exhaustive examination of the full pathogenesis process of *B. mallei*, it is unlikely that disrupting the expression of a regulator that is modulating the expression of multiple virulence genes would not have some measurable impact in two of the most significant pathogenesis steps in the establishment of an infection by *B. mallei* (i.e. adherence to and invasion of eukaryotic cells), which were a primary focus of the *in vitro* analyses. Due to these observations, we hypothesized that BorP was regulating the expression of BpaB directly, rather than indirectly as a global virulence regulator.

BorP Directly Regulates *bpaB* Gene Expression

To examine our hypothesis that BorP was regulating the expression of BpaB directly, rather than indirectly, a series of electrophoretic mobility shift assays (EMSAs) were used to determine if BorP was capable of binding to the promoter of *bpaB*. The online prokaryote promoter prediction software, PePPER, indicated the presence of a prokaryotic

promoter sequence 363 nucleotides upstream of the *bpaB* ORF (Fig 5.5A). EMSAs were performed using a commercially available kit, which included components for making positive binding control reactions; namely, Epstein-Barr virus (EBV) Nuclear Antigen 1 (EBNA) and a known segment of biotinylated EBV DNA that can be bound by EBNA which can be detected by a horseradish peroxidase conjugated Streptavidin solution. Control reactions using kit components were run alongside the purified His-BorP protein and biotinylated DNA fragments generated by our lab to ensure that the kit was working appropriately. 500 bp and 250 bp segments that included the predicted *bpaB* promoter were amplified and biotinylated. Additionally, we prepared and used identically sized segments of *rrsB*, the B. mallei 16s ribosomal RNA gene, as a negative binding control.

The EBV control reactions produced the desired results (Fig 5.5 B), indicating that the EMSA kit was functioning appropriately. As anticipated, we found that the BorP protein bound to both the 500 bp (Fig 5.5C) and 250 bp (Fig 5.5 D) DNA segments upstream of the *bpaB* ORF, but did not bind to those upstream of the *rrsB* gene (Fig 5.5 C and D). The reduced biotinylated DNA band (characteristic of a DNA shift) can be seen in the lanes containing *bpaB* upstream sequences mixed with purified BorP, but not the rrsB upstream sequences (Fig 5.5 C and D). The lack of reactivity with *rrsB* fragments indicates the binding of BorP is not promiscuous but rather specific for the DNA sequence upstream of *bpaB*.

To confirm that the band intensity reduction observed was not just an artifact, aliquots of these mixtures were also spiked with 20-fold higher concentrations of unbiotinylated DNA fragments from the aforementioned upstream regions of *bpaB*. Stoichiometrically, BorP is more likely to bind the unbiotinylated segments of DNA rather

than the biotinylated DNA fragments; thus, a partial restoration of the band corresponding with biotinylated DNA would be expected. Figure 5.5 C and D indicate that the addition of unbiotinylated 500 bp and 250 bp fragments partially restores the unbound, biotinylated DNA band, which is consistent with a decreased shift due to BorP binding the unbiotinylated *bpaB* promoter region. Overall, these data support the hypothesis that the BorP protein is directly binding to the upstream promoter region of *bpaB* as a positive regulator.

A Mutant Strain Lacking Expression of *borP* is Reduced in Virulence

Given that a mutation in *bpaB* attenuates the virulence of *B. mallei* ATCC23344 (296) and that our in vitro data suggested BorP was playing a role in the expression BpaB-mediated biofilm formation, we hypothesized that a mutant lacking expression of the *borP* gene would be reduced in virulence. To test this, we used an aerosol mouse model (156) to determine the median lethal dose (LD_{50}) of the isogenic *borP* mutant strains complemented with pBHR1ΔDra (empty vector control) or pBorP (constitutively expresses BorP) and compared them to that of WT *B. mallei* bacteria. Survivors were humanely euthanized at the study endpoints, and the hallmark target organs of *B. mallei* (spleen, liver, and lung) were collected to determine their bacterial burdens. Compared to wild-type, the LD_{50} of the isogenic *borP* mutant was approximately 30-fold higher than that of WT *B. mallei* and the complemented mutant expressing BorP had an even greater reduction in virulence (Fig. 5.6A and 5.7A), both of which are consistent with what has been described previously (296). Despite being attenuated in virulence, both the isogenic *borP* mutant and complemented mutant were able to colonize the mouse lung, liver, and spleen (Fig 5.6 and

5.7 BCD), yet another finding consistent with the previous characterization of the BpaB in mice (296). Taken together, these *in vivo* results complement the *in silico* and *in vitro* data presented by us and support our assertion that BorP is an important contributor to the pathogencity of *B. mallei* as a transcriptional regulator of BpaB and thus biofilm formation. This ability to colonize and persist within the host is a hallmark virulence determinant of *B. mallei*, and represents the largest hurdle currently faced in the field of medical countermeasure development.

DISCUSSION

Burkholderia mallei and *B. pseudomallei*, the two closely related bacterial species that cause the diseases glanders and melioidosis respectively, are difficult to diagnose and treat, lack effective diagnostic tools, and have no commercially available vaccine. Further, there is legitimate concern that they could be misused as biological terrorism agents. For these reasons they are classified as Tier 1 Select Agents. Both diseases have distinct acute and chronic phases. While a significant amount of progress has been made in the laboratory setting protecting model animals from acute lethal infection, there remains a considerable gap of progress to be made with the chronic phase of infection. One confounding issue is a lack of *in vitro* expression of major virulence determinants. A well-documented phenomena is the ability of bacterial pathogens to readily alter their expression profile based on situational cues such as temperature (54), pH (16, 23, 53, 55, 104, 139, 212), nutrient availability (9), antibiotic stress (9, 183), and the presence or absence of other cells, including eukaryotic vs prokaryotic or, members of their same species vs non-member species (127, 173). This differential expression of potential high value antigens has stymied the discovery of novel antigens. While the discovery of novel antigens is an important endeavor, understanding the mechanisms underlying this differential expression can be equally important.

Bacteria have numerous methods of regulating DNA expression at their disposal, but two-component regulatory systems (TCS) are the most widely used, and allow for the modulation of bacterial gene expression as a direct result of environmental stimuli. TCS have been demonstrated to be a major component of bacterial pathogenesis, the most common of which in prokaryotes is the OmpR-like TCS. OmpR orthologs have been

demonstrated to modulate expression of numerous virulence pathways in prokaryotes, including the ToxR/TcpP/ToxT virulence cascade in *Vibrio cholerae* (221), the SsrA-SsrB regulatory system of *Salmonella enterica* serovar Typhimurium (23), and the FlhDC master flagellar activator in *Yersinia enterocolitica* O:9 (40, 213). While they have been demonstrated to be involved in many stages of bacterial pathogenesis, one mechanism that OmpR orthologs have been shown to be highly involved in during the pathogenesis process is the situational expression of biofilms. One example of TCS regulation of biofilms is the BfmR OmpR-like regulatory protein of *Acinetobacter baumannii* (258).

One class of virulence factors that is an area of focus of our laboratory is the autotransporter family of proteins. Previous work done by our laboratory to characterize autotransporters has shown them to be a key component of the *B. mallei* pathogenesis process. In the course of these works it was demonstrated that many of these autotransporters were produced *in vivo*, but not at detectable levels under routine culture conditions in the lab (i.e. *in vitro*.) (22, 155,295, 296). As these proteins have been shown to be major virulence determinants, it was important to understand the mechanisms behind their selective *in vivo* versus *in vitro* expression. While examining the biological role of one of these proteins, BpaB, it was determined to be the first biofilm formation factor described in *B. mallei* (296). During the course of characterizing the role of BpaB in the pathogenesis of *B. mallei*, it was noted that upstream of the *bpaB* ORF was the *borP* gene, which *in silico* analysis suggested was an OmpR-like DNA binding response regulator. Due to the proximity of the two genes, the involvement of BpaB in the production of biofilms (296), and the predicted DNA-binding response regulator function of BorP, we

hypothesized that BorP was regulating the expression of BpaB either directly as a regulator, or indirectly as a global virulence regulator.

We found that constitutive expression of BorP by an isogenic mutant complemented with a constitutive expression vector specifying the expression of *borP* led to the corresponding expression of BpaB (Fig 5.2 C). This was an interesting finding, as prior to this observation BpaB had not been demonstrated to be expressed *in vitro* without the use of constitutive expression vectors specifically expressing BpaB (296). Additionally, the expression of BpaB found in the mutant carrying the BorP constitutive expression vector also resulted in the corresponding biofilm formation phenotype, as demonstrated by the presence of a biofilm ring at the air-liquid interface in crystal violet staining assays (Fig 5.4). It is important to note that the expression of BpaB was only detected in the *borP* mutant that was carrying the pBorP constitutive expression vector, and not in the mutant carrying the pBHR1ΔDra plasmid or WT *B. mallei* bacteria. These data suggest that the observed expression of BpaB is due to the presence of BorP, rather than to something inherent to the pBHR1 plasmid or some other endogenous factor shared by the mutants and the WT *B. mallei* backbone. This finding was encouraging, as it demonstrated that not only does BorP expression result in a corresponding expression of BpaB, but it leads to the production of a biologically active form of BpaB. Additionally, it indicates the deletion of BorP did not cause a polar mutation of the downstream BpaB gene, so we can conclude that BorP is positively regulating the expression of BpaB.

Along with the observed expression of BpaB by the complemented BorP mutant, the results of the *in vitro* experiments closely resembled those found during the characterization of BpaB (296). In both sets of experiments, the constitutive expression of

the respective genes of interest resulted in similar levels of biofilm formation with respect to the quantitative results (Fig 5.4 C) (296). Removal of the expression of the *borP* and *bpaB* genes also failed to produce a biofilm formation phenotype (296). One observation to note is that while the overall production of biofilm was similar, the level of biofilm production by the *borP* mutant constitutively expressing BorP is slightly lower than that of the *bpaB* mutant constitutively expressing BpaB. One reason for this could be that the constitutive expression BorP is indirectly resulting in less production of BpaB and thus biofilm formation while the direct constitutive expression of BpaB produces more and thus more biofilm formation.

We hypothesized that the predicted DNA-binding characteristics of the *borP* gene product meant that the regulation of BpaB by the BorP protein was done at the transcriptional level rather than the translational level, but we had not addressed whether or not this regulation of BpaB expression was done directly or indirectly as a global virulence regulator. Based on the results of the assays performed up to that point, we hypothesized that BorP was most likely regulating the expression of BpaB locally, rather than as a global virulence regulator. To address this hypothesis, **E**lectrophoretic **M**obility **S**hift **A**ssays (EMSAs) were performed using both 500 bp (Fig 5.4B) and 250 bp (Fig 5.4C) regions of the DNA upstream of the *bpaB* and *rrsB* ORFs. The *rrsB* gene is the 16s ribosomal RNA gene, and it was used as a negative binding control to examine the possibility of non-specific binding of DNA by the His-BorP protein. To perform the EMSA experiments, we used a commercially available EMSA kit manufactured by ThermoFisher which supplied us with established protocols and quality controlled binding mixture components. This decision was made for ease of use, as protocols available in the broad

scope of the literature can vary widely, and attempts to utilize some published methodologies failed to perform consistently. By using the reaction mixture components and protocols available from ThermoFisher, we demonstrated that BorP was directly and specifically binding the upstream region of the *bpaB* gene. While this finding supported our hypothesis that BorP is binding upstream of the *bpaB* ORF and regulating its expression directly, it cannot be conclusively stated that this is the sole region of DNA bound by this protein. It has been well documented in other publications that OmpR-like DNA binding response regulators can bind multiple promoters. For example, the prototypical OmpR DNA binding response regulator of *E. coli* binds to the promoter regions of both the *ompF* and *ompC* genes (296).

Since *borP* is involved in the expression of at least one virulence factor, we hypothesized that the inability to express the *borP* gene would reduce the virulence of *B. mallei* in our aerosol mouse model of infection. Because we could not conclusively state that BorP is solely binding the upstream region of *bpaB*, not acting as a global regulator of virulence, we felt it was important to examine how a lack of *borP* expression would affect the overall virulence of the organism. If we disrupted the *borP* gene and found that the organism had a higher level of attenuation than that found while characterizing the *bpaB* mutant of *B. mallei*, it would suggest that BorP is acting on other genes in addition to BpaB. We found that when we disrupted the *borP* gene and used that mutant in aerosol infection experiments, there was a reduction in virulence compared to WT *B. mallei*, but not complete attenuation. Additionally, constitutive expression of the BorP protein led to an even greater of virulence (Figs 5.6 and 5.7). This finding was consistent with the published *in vivo* infection experiment results of the *bpaB* gene deletion mutant. In both data sets, the

deletion of the genes of interest resulted in a greater than 10-fold reduction in virulence (296), with constitutive expression resulting in an approximately 60-fold reduction in virulence (296). The roughly equivalent reductions in virulence support the hypothesis that BorP is directly regulating the *bpaB* gene, and is not acting on other key virulence genes.

Based on the results of this study, we suspect that BorP is directly regulating the expression of the *bpaB* ORF, and is less likely to be a global virulence regulator. In support of this argument, we have clearly demonstrated that expression of BpaB is positively regulated by BorP and promotes biofilm formation. Further, we have shown that BorP is binding to the promoter region of *bpaB*, which is suggestive of direct and possibly singularly focused regulation. However, there are a few missing pieces of the picture that need to be resolved before drawing such conclusions. Future directions for examining the BorP transcriptional regulator should include RT-PCR and RNA-Seq. Qualitative RT-PCR would allow us to conclusively demonstrate that when we constitutively express BorP, we see the transcription of the *bpaB* gene compared to a lack of transcription by WT *B. mallei* and the *bpaB*, and *borP* mutants. Quantitative (qRT-PCR) would allow for quantification of these expression levels, which may be needed in the event basal levels of *bpaB* transcripts are made by WT *B. mallei* but regulated further downstream. While this RT-PCR data would further support our claim, the evaluation of the full transcriptome of the *borP* KO mutant compared to WT *B. mallei* and the *borP* KO mutant complemented with pBorP is required to determine whether BorP is a global virulence regulator or not. Should other potential changes in gene expression be found by RNA-seq, those findings would have to be confirmed with a traditional reverse genetic approach.

Future work should also focus on identifying and characterizing the proteins that interact with and modulate the activity of BorP. A major component of OmpR-like TCS DNA-binding response regulators is a corresponding environmental sensor. Presently, we do not have any data to suggest a potential environmental sensing binding partner for BorP may be. Understanding the environmental signals cues and signaling that lead to the expression of BorP could have major implications in the understanding of the ability of *B. mallei* to produce a biofilm, which our lab has shown to be a major virulence determinant of the organism. Typically, though not universally, the gene encoding the corresponding environmental sensor of an OmpR-like DNA binding response regulator is located nearby in the genome. However, sequence analysis of the *B. mallei* genome fails to identify any such predicted protein in the adjacent upstream or downstream regions of the *B. mallei* chromosomal DNA. Instead, we found that there are numerous other predicted TCS DNA-binding response regulators such as BMA0833, which is predicted to be another OmpR-like DNA binding response regulator, or BMA0832 which is a predicted LysR family transcriptional regulator. It's possible that these genes form a regulon, which is regulated by some global regulator that is itself stimulated by an extracellular signal. One such regulator could be fumarate-nitrate reductase (FNR), an oxygen sensing response regulator that has been shown to be involved in biofilm expression of other organisms (20), including *B. pseudomallei* (189).

MATERIALS AND METHODS

Bioinformatics

Bioinformatics analyses were performed using tools available online from ExPASy. Their tools are available using an online portal at https://www.expasy.org. The identification of conserved domains was performed by analyzing sequences using the NCBI Conserved Domain Database (CCD) which is freely available online at https://www.ncbi.nlm.nih.gov/cdd/. The identification of *borP* orthologs in *B. mallei*, *B. pseudomallei*, and *B. thailandensis* genomes was performed using NCBI BLAST, which is available online at http://blast.ncbi.nlm.nih.gov/Blast.cgi. The secondary and tertiary of structures of the BorP protein were examined using PSIPRED and Phyre^2 which are available online at http://bioinf.cs.ucl.ac.uk/psipred/ and http://www.sbg.bio.ic.ac.uk/~phyre2/html/page.cgi?id=index respectively. Prokaryotic promoter sequence prediction was performed using PePPER, available freely online at http://genome2d.molgenrug.nl/g2d_pepper_promoters.php

Bacterial strains, plasmids, and culture conditions

All strains and plasmids that are discussed in this manuscript are listed in Table 5.1. *B. mallei* was grown at 37 ^{o}C using Brucella medium (manufactured by BD Biosciences). Brucella medium used to grow *B. mallei* was supplemented with 50% glycerol to a final concentration of 5% glycerol (vol/vol). In growth conditions that required the use of selective pressure (i.e. mutagenesis, complementation, etc.) the growth medium was supplemented with 5 ug/mL polymyxin B, 5 ug/mL kanamycin, and/or 7.5 ug/mL zeocin.

In order to perform the *in vivo* and *in vitro* infection experiments, *B. mallei* was grown on plates for 40 hours at 37ºC. During experiments, cells were suspended in 1x phosphate-buffered saline (PBS) at a concentration of $1.0x10^9$CFU per mL. In order to prepare inoculations or working suspensions of bacterial strains for *in vitro* and *in vivo* experiments, plate grown bacteria were suspended in 1x PBS to a desired optical density (OD_{600}), the total CFU of which was confirmed by spotting 100 uL of serially diluted suspensions on the appropriate growth medium and grown for 40 hours at 37 ºC then counting the obtained CFU. In methods requiring the use of *E. coli* strains, they were grown on low-salt LB medium at 37 ºC. Any experiment requiring selective pressure of *E. coli* strains used bacteria grown in liquid media or on agar media supplemented with 15 ug/mL chloramphenicol, 50 ug/mL kanamycin, 50 ug/mL zeocin, and/or 15 ug/mL tetracycline.

Recombinant DNA

Genomic DNA was purified from *B. mallei*, *B. pseudomallei*, *B. thailandensis*, or *E. coli* using the ThermoFisher Scientific Easy-DNA gDNA purification kit. When used, this kit was used protocol supplied with the kit materials. Where applicable, plasmid DNA was purified by using the Qiagen QIAprep Spin Miniprep kit. When used, the kit was used according to the manufacturer's instructions. Polymerase Chain Reaction (PCR) was performed using the Epicenter/Lucigen FailSafe PCR and/or the Platinum Pfx PCR kit manufactured by ThermoFisher/Invitrogen. Where applicable, recombinant plasmid and cloning was achieved using restriction endonucleases and T4 DNA ligase available from New England Biolabs Inc. Plasmids were propagated by electroporation and summary culturing of EPI300 and EC100D pir^+ electrocompetent *E. coli.*

A 1049 nucleotide DNA fragment which contained the *B. mallei* ATCC 23344 *borP* gene as well as flaking upstream and downstream sequences of DNA was created using primers CCGAGTCCTTCGGATTCCTGGCTGTTCA and CATGCCATGGCATGGCGGATTTGATTTCGG. These primers included unique 5'-DraI and 3'-NcoI restriction sites, which allowed for directional cloning. Once generated, this fragment was inserted between the DraI and NcoI sites of the pBHR1 vector. In parallel, a second plasmid had the DraI-NcoI segment of the plasmid excised and religated. The vector that received the *borP* fragment of DNA was termed pBorP, while the vector that was given no insert was termed pBHR1ΔDra. The production of a mutation-free vector was confirmed through Sanger sequencing done by the Georgia Genomics and Bioinformatics Core (GGBC) of the University of Georgia, and the confirmed vector was propagated in EPI300 *E. coli*. The mutation-free pBorP vector had its *borP* open reading frame disrupted through the insertion of a 0.6 kb zeocin resistance marker which was obtained from the pEM7Zeo vector. The Zeocin resistance marker was inserted into the pBorP vector at a unique EcoRI site located near the center of the ORF. Once disrupted, the yielded plasmid was termed pBorPZeo, and it was also propagated in *E. coli* EPI300. Purified pBorPZeo plasmids were used as templates to obtain DNA fragments containing the *borP* ORF disrupted with the zeocin resistance cassette, which was gel-purified with the Roche Life Sciences High Pure PCR product purification kit and inserted into the EcoRV site of the gene replacement vector pKAS46, yielding pKASBorPZeo. The pKASBorPZeo plasmid was inserted into E. coli pir+ to obtain large quantities of pKASBorPZeo. Plasmid pKASBorPZeo obtained from E. coli pir+ was inserted into E. coli S17. The pKASBorPZeo was confirmed to be mutation-free through Sanger

sequencing as described before. A DNA fragment containing the full ORF of the borP gene flanked by NheI and PacI on the 5' and 3' ends respectively inserted into pUC57 was synthesized by Genscript. The borP ORF was excised by digestion with NheI and PacI, gel-purified with the High Pure PCR product purification kit (Roche Life Sciences), and ligated into the corresponding sites of vector pETcoco-1. The resulting construct was labeled pET-HisBorP, which carries the borP gene product fused to an N-terminal His-tag. All plasmids were introduced into E. coli strains by electroporation using a BTX Transporator Plus apparatus and plasmids pBHR1ΔDra, pBorP, and pKASBorPZeo were transferred from *E. coli* S17 to *B. mallei* by conjugation as previously outlined (295, 296).

Construction of *borP* isogenic mutant strains of *B. mallei* ATCC 23344

After pKas46BorPZeo was inserted into *B. mallei* ATCC 23344 via conjugative transfer, colonies were screened on agar media. Colonies were selected based on their resistance polymyxin B (exclusive of *E. coli*) and zeocin (selective for possession of *borP* gene disrupted by zeocin) and a sensitivity to kanamycin (exclusive of bacteria that have incorporated the plasmid vector into their genome). Colonies were analyzed by PCR with primers CCGAGTCCTTCGGATTCCTGGCTGTTCA and CATGCCATGGCATGGCGGATTTGATTTCGG, which produced an amplicon of approximately 1 kb in WT *B. mallei* ATCC 23344 and a larger DNA fragment of 1.6 kb in the *B. mallei* BorP mutant containing a zeocin disrupted *borP* mutant. After conjugation to introduce plasmids pBHR1ΔDra and pBorP into the *B. mallei borP* mutant strain, polymyxin B resistant colonies were selected for resistance to both zeocin and kanamycin to identify colonies that maintained the inactivated copy of borP in their genomes and also

contained copies of pBHR1ΔDra and pBorP. The difference in size as well as the resistance to zeocin was used as confirmation of successful insertion of the zeocin cassette into the borP ORF. Plasmid DNA was then isolated from selected and stocked strains and analyzed with restriction endonucleases to verify constructs.

Animal infection experiments

In all animal experiments, female BALB/c mice between the ages of 6-8 weeks were used. Infection experiments were performed using a microsprayer as previously described (156, 157, 295, 296). Infected animals were monitored daily, and humane terminal endpoints were observed. Where applicable, terminal mice were euthanized in accordance with the AVMA Guidelines for the Euthanasia of Animals. At study endpoints, mice were euthanized and target tissues were harvested, specifically the spleens, livers, and lungs. These tissues were homogenized using disposable tissue homogenizers, serially diluted 10-fold in 1 mL volumes, and plated in 100 uL volumes on the appropriate agar media plates.

Antigen preparation

Whole cell lysates were generated by suspending plate-grown bacteria in 1x PBS to a desired concentration. These suspensions were pelleted, and the pellets were washed with 1x PBS. Pellets were resuspended in 500 uL of BugBuster HT Protein Extraction Reaction (Millipore Sigma) supplemented with 1uL/mL rLysozyme. Lysed pellets were incubated for 30 minutes at 65 ^{o}C. Western blot analyses were performed as previously

described (295, 296). Recombinant proteins were generated by inducing plasmids pET-HisBorP and pET-HisLolC using isopropyl-β-D-thiogalactopyranoside (IPTG, final concentration of 1 mM) in TUNER *E. coli* strains grown in liquid broth for 5 hours at 37 ^{o}C on 200 RPM mix. Bacteria were pelleted, washed, and treated with Bugbuster HT Protein Extraction Reagent supplemented with rLysozyme Solution as previously described. His-Tagged LolC and BorP proteins were purified from the soluble and insoluble fractions of cell lysates, respectively, using a His-Bind Purification kit manufactured by Millipore Sigma according to the manufacturer's instructions. Once proteins were purified, they were dialyzed with 1x PBS. The concentration of purified proteins was determined using a bicinchoninic acid (BCA) protein quantification assay. Where applicable, ELISAs were performed as previously described (295, 296). Briefly, wells of an Immulon 2HB plate were coated with purified antigens, or paraformaldehyde-fixed bacteria, which was then used as a substrate to determine antibody reactivity.

Antibodies

BALB/c mice were immunized with 25 ug of purified His-Tagged BorP and LolC mixed at a ratio of 1:1 with Freund's Adjuvant. Mice were administered three separate doses of the purified protein and adjuvant mixture over 42 days (14 days between doses), which were delivered subcutaneously. Initial vaccination was performed using Freund's Complete Adjuvant, while subsequent vaccinations were performed using Freund's Incomplete Adjuvant. After the third dose, Immune serum was collected by tail bleed. Collected serum was pooled, and used as polyclonal antibody stocks to be used in Western blot analyses.

Macrophage killing assays

J774.A1 murine macrophage cells (ATCC TIB-67) were cultured as previously described (295, 296). For macrophage killing assays, plate grown *B. mallei* was used for all inoculations. Macrophage monolayers in 24-well tissue culture plates were inoculated with *B. mallei* as previously described (295, 296). In all assays, the use of 50 ug/mL of streptomycin was used to kill any extracellular bacteria.

Human lung epithelial cell adherence assays

A549 human lung epithelial cells (ATCC CRM-CCL-185) were cultured as previously described (295, 296). Monolayers of A549 cells were inoculated with plate-grown *B. mallei* organisms as previously described (295, 296). For all adherence assays, cells were seeded in 24-well tissue culture plates as previously described (295,296).

Electrophoretic mobility shift assays

500 and 250 bp DNA fragments of the *bpaB*, and *rrsB* genes of *B. mallei* ATCC 23344 were generated using the primers listed in table 5.2. 500 and 250 bp DNA fragments were biotinylated using the Pierce™ Biotin 3' End DNA Labeling Kit according to the manufacturer's instructions. Electrophoretic mobility shift assays (EMSA) was performed using the ThermoFisher LightShift™ Chemiluminescent EMSA Kit according to the manufacturer's instructions using pre-cast 6% DNA Retardation gels. Briefly,

approximately 70 fmol of biotinylated 500 or 250 bp DNA fragments were incubated with pre-determined volumes of sterile ultrapure water, 10x binding buffer, 1ug/ul Poly (dI◦dC), 50% glycerol, 1% NP-40, 1M KCl, 100mM $MgCl_2$, and 200 mM EDTA as directed by the manufacturer's directions. EMSA mixtures were $^{+}/_{-}$ supplemented with 10mM His-BorP to a final concentration of 6.5 mM and/or approximately 1400 pmol of corresponding unbiotinylated DNA fragments, then incubated statically at room temperature for 20 minutes.Final reaction mixtures were 20 uL, and after 20 minutes 5 uL of 5x loading buffer was added to each mix. Reactions were loaded into the wells of 6% DNA Retardation gels that had undergone pre-electrophoresis for 30 minutes. Mixtures underwent electrophoresis at 100V for 60 minutes, whereupon the DNA was transferred from the gel to Biodyne-B vinyl membrane at 380 mA for 30 minutes in x TBE that had been cooled to 4°C. After transfer to Biodyne-B vinyl membranes, DNA was crosslinked by placing transfer-side down onto a 312 nm UV light source for 15 minutes. After crosslinking, blots were processed using the DNA detection module portion of the ThermoLightshift EMSA kit according to the manufacturer's instructions.

Crystal violet biofilm assays

Crystal violet biofilm assays were performed as previously described (296). For all crystal violet assays, suspensions of plate-grown *B. mallei* were seeded into wells of round bottom polyvinyl chloride (PVC) 96 well plates. Plates were incubated at 37°C for 48 hours. After 48 hours, wells were stained with a 0.035% (wt/vol) crystal violet solution in Hams F12 medium. After staining, wells were washed with dH_2O, and plates were allowed to dry completely. Dry plates were imaged using a digital camera, then the crystal violet

was extracted from the stained biofilm rings using methanol. Destained well contents were collected, then quantified using a spectrophotometer at a wavelength of 570 nm.

Data Analysis

Mouse survival curve data was analyzed using the Kaplan Meier method. ELISA, bacterial burden data, and cell culture results were compared using Student's *t* and Mann-Whitney tests. Macrophage killing assay results were compared using the Menjamini, Krieger, and Yekutieli method. LD_{50} values were determined using the Reed and Meunch method (215). All analyses were performed using GraphPad Prism software. Where applicable, *P* values of < 0.05 are reported as statistically significant.

Compliance and Ethics

All experiments in this study were approved by The University of Georgia's Institutional Biosafety Committee. All experiments using live select agents were performed within a Class II biosafety cabinet, which was itself within a biosafety level 3 laboratory space that is maintained in compliance with the regulations of the U.S. Federal Select Agent Program. Animals using in *in vivo* experiments were housed in an Innorack IVC dual-HEPA-filtered ventilated system, which was itself located within an Animal BSL3 laboratory space that is maintained in compliance with the regulations of the U.S. Federal Select Agent Program. All *in vivo* experiments were approved by The University of Georgia's Institutional Animal Care and Use Committee. All *in vivo* experiments were performed according to the guidelines found in the Guide for the Care and Use of

Laboratory Animals. For all *in vivo* experiments, human terminal endpoints were strictly observed to minimize animal suffering.

TABLES AND FIGURES

Table 5.1

Strain or plasmid	Description	Source or reference
B. mallei		
ATCC 23344	Wild-type strain; polymyxin B resistant, kanamycin and zeocin sensitive	(194)
BorPKO	Isogenic *borP* mutant strain of ATCC 23344; resistant to polymyxin B and zeocin, sensitive to kanamycin	This study
BorPKO pBorP	Isogenic *borP* mutant strain of ATCC 23344 harboring a pBHR1 plasmid containing the entire open reading frame of BorP (pBorP); resistant to polymyxin B, zeocin, and kanamycin	This study
BpaBKO pBpaB	Isogenic *bpaB* mutant strain of ATCC 23344 harboring a pBHR1 plasmid containing the *bpaB* gene; resistant to polymyxin B, zeocin, and kanamycin	(296)
E. coli		
EPI300	Strain used for general recombinant DNA manipulations; sensitive to kanamycin, zeocin, tetracycline, and chloramphenicol	epicenter/Lucigen
EC100D *pir*$^{+}$	Strain used for recombinant DNA manipulations of plasmid pKAS46 and derivatives; sensitive to kanamycin and zeocin	epicenter/Lucigen
S17	Strain used for conjugational transfer of plasmids to *B. mallei*; sensitive to kanamycin, zeocin, and polymyxin B	(234)
TUNER	Protein expression strain used to purify His-tagged Pal_{Bm} and $LolC_{Bm}$ proteins; chloramphenicol sensitive	Millipore Sigma
Plasmids		
pBHR1	Cloning vector; confers resistance to chloramphenicol and kanamycin	MoBiTec
pBHR1Δ Dra	pBHR1 containing a 339 bp deletion in the chloramphenicol	(296)

	resistance marker; confers resistance to kanamycin but not chloramphenicol	
pBorP	pBHR1 in which the *borP* gene of *B. mallei* ATCC 23344 was inserted; confers resistance to kanamycin but not chloramphenicol	This study
pBpaB	pBHR1 in which the *bpaB* gene of *B. mallei* ATCC 23344 was inserted; confers resistance to kanamycin but not chloramphenicol.	(296)
pEM7/ZEO	Source of the zeocin resistance cassette; confers resistance to zeocin	ThermoFisher Scientific
pKAS46	Gene replacement vector; confers resistance to kanamycin	(238)
pKASBorPZeo	pKAS46 containing the *borP* gene interrupted with a zeocin resistance cassette; confers resistance to kanamycin and zeocin	This study
pETcoco-1	His-tagged protein expression vector; confers resistance to chloramphenicol	Millipore Sigma
pET-HisBorP	pETcoco-1 in which the *borP* gene of ATCC 23344 had been inserted; confers resistance to chloramphenicol	This study
pHisLolC	pETcoco-1 in which a gene fragment encoding amino acids 47 to 243 of *B. mallei* ATCC 23344 LolC was inserted; confers resistance to chloramphenicol	This study

Table 5.2

Gene	Size	Orientation and Sequence
borP	500 nt	5’ – AAATCGTCGGGGATGCGCATGGCGTTT 3’ – TTTTTGTCTCGACAACCAGCGACCAC
borP	250 nt	5’ – AAATCGTCGGGGATGCGCATGGCGTTT 3’ – ACCAGGCCACTGACCGCCGATCCGTAG
bpaB	500 nt	5’ – CCCGTTCGCTCGATACTCACATCTACC 3’ – TTCATCCTCACGCAAATAAGCTTCGAA
bpaB	250 nt	5’ – CCCGTTCGCTCGATACTCACATCTACC 3’ – CGCCGCGCATGCCCGCTCGTGCCGCGC
rrsB	500 nt	5’ – GGCGCACAGGTGCTGCATGGCTGTC 3’ - AGAAAGGAGGTGATCCAGCCGCACC
rrsB	250 nt	5’ – CCCAGAAAACCGATCGTAGTCCGGA 3’ – TCCGGACTACGATCGGTTTTCTGGG

Figure 5.1

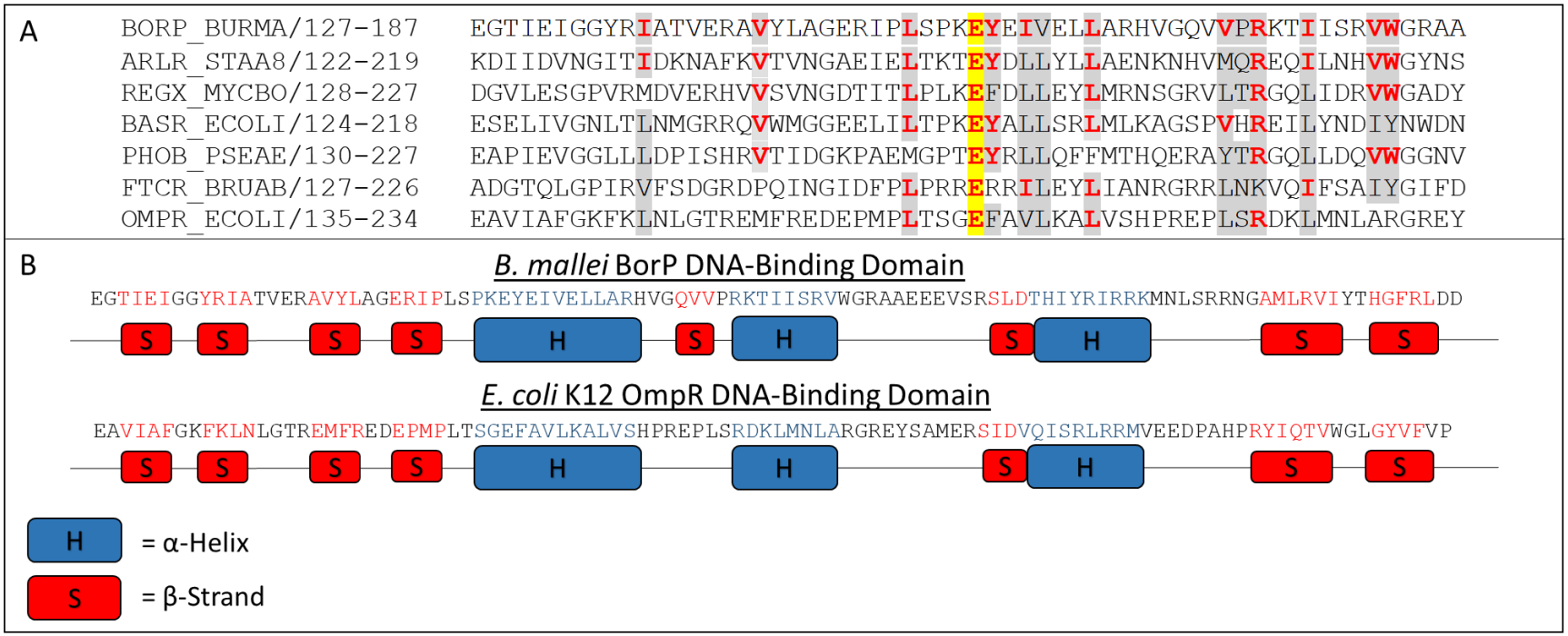

The amino acid sequence of the DNA-binding domain of BorP was compared with those of several other OmpR-like DNA-binding response regulators (Panel A). In order, the sequences belong to: BorP of *B. mallei*, ArlR of *Staphylococcus aureus*, RegX3 of *Mycobacterium tuberculosis*, BasR of *E. coli*, PhoB of *Pseudomonas aeruginosa*, FtcR of *Brucella abortis*, and OmpR of *E. coli*. Identical amino acids are shown in red. Similar amino acids (i.e. a non-polar amino acid substituted for a different non-polar amino

acid) are highlighted in grey. Highlighted in yellow is a single residue in the first helix that was conserved amongst all of the OmpR-like protein sequences. This alignment shows several residues from the DNA-binding domain of BorP that were conserved amongst not only Gram-negative and Gram-positive bacteria but also Mycobacteria. The secondary structure of the BorP DNA-binding domain strongly resembles that of the prototypical *E. coli* K12 OmpR protein, except for the inclusion of a single β-strand structure in the BorP domain at positions 170-172 (Panel B).

Figure 5.2

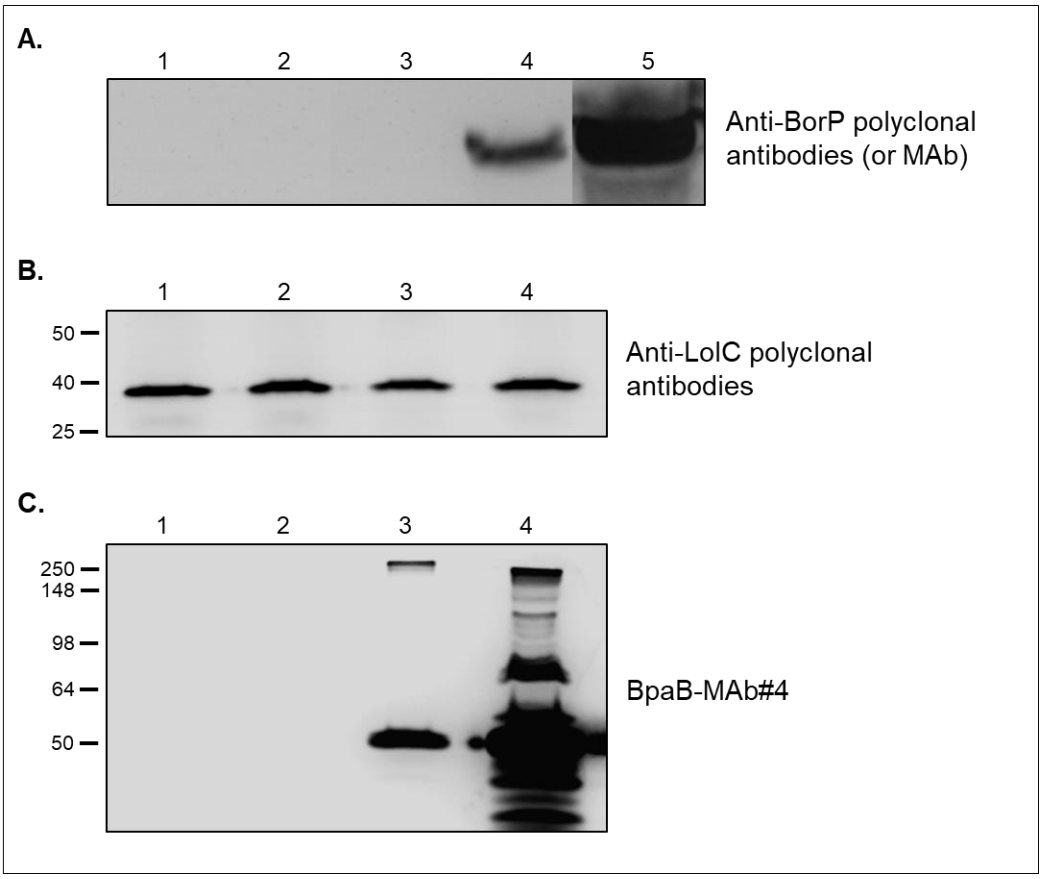

Western blot analysis of *B. mallei* WT and recombinant strains. Whole cell lysates were prepared from WT *B. mallei* ATCC 23344 bacteria (lane 1), the *borP* KO mutant strain carrying the plasmids pBHR1ΔDra (lane 2) and pBorP (lane 3), and the *bpaB* KO mutant strain carrying plasmid pBpaB (lane 4), and analyzed by Western blotting with the BorP polyclonal antibodies (panel A), polyclonal antibodies against the LolC protein (panel B, used as loading control to demonstrate that equivalent amounts of proteins were analyzed), and the monoclonal antibody BpaB-MAb#4 (panel C). Molecular mass markers are shown to the left in kilodaltons. Lane 5 in panel A corresponds to 5 ug of purified of His-tagged BorP protein (used as positive control to demonstrate reactivity and specificity of anti-BorP polyclonal antibodies).

Figure 5.3

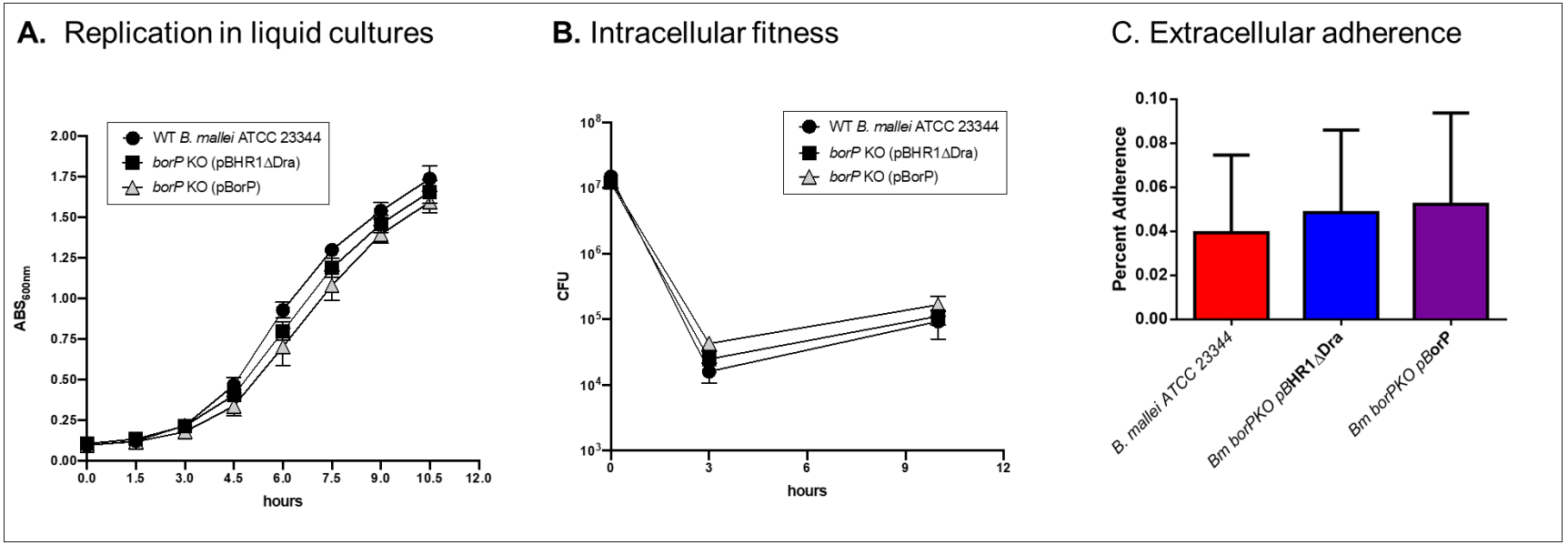

In vitro replication rate in liquid cultures, intracellular fitness, and adherence to lung epithelial cells of *B. mallei* WT and recombinant strains. (A) Plate-grown bacteria were suspended in broth to an optical density at wavelength 600 nm (ABS_{600nm}) of 0.1. Following this, suspended bacteria were incubated at 37◦C with shaking (200-rpm) and the optical density of cultures was measured at the indicated time intervals. Strains were tested on at least 3 separate occasions. The graph shows cumulative results. The error bars correspond to standard errors of the mean. (B) Plate-grown bacteria were suspended in 1x PBS and used to infect 3 wells of duplicate tissue culture plates seeded with murine J774 macrophages (multiplicity of infection of 10:1). The infected cells were incubated for 1 hour at 37◦C to allow phagocytosis of the bacteria, washed, and treated with antibiotic

for 2 hours to kill extracellular bacteria. Cells from one tissue culture plate were lysed, diluted, and plated onto agar medium to determine the number of bacteria phagocytized. The other tissue culture plate was incubated for an additional 7 hours, after which the cells were washed, lysed, diluted, and spread onto agar plates to calculate the number of intracellular organisms. The results are expressed as the mean CFU per well. The assays were performed on 3 separate occasions. The graphs shows cumulative results. The error bars correspond to standard errors of the mean. (C) Plate-grown bacteria were suspended in 1x PBS and used to infect 3 wells tissue culture plates seeded with A549 human lung epithelial cells (multiplicity of infection 100:1). The infected cells were incubated for 1 hour at 37◦C for 1 hour to allow the bacteria to adhere to the exterior of the cell, then washed. Well contents were collected, cells were lysed, diluted, and plated onto agar medium to determine the number of bacteria that were adhered to the exterior of the A549 cells. The results are expressed as the mean CFU per well. The assays were performed on 3 separate occasions. The graph shows cumulative results. The error bars correspond to standard errors of the mean.

Figure 5.4

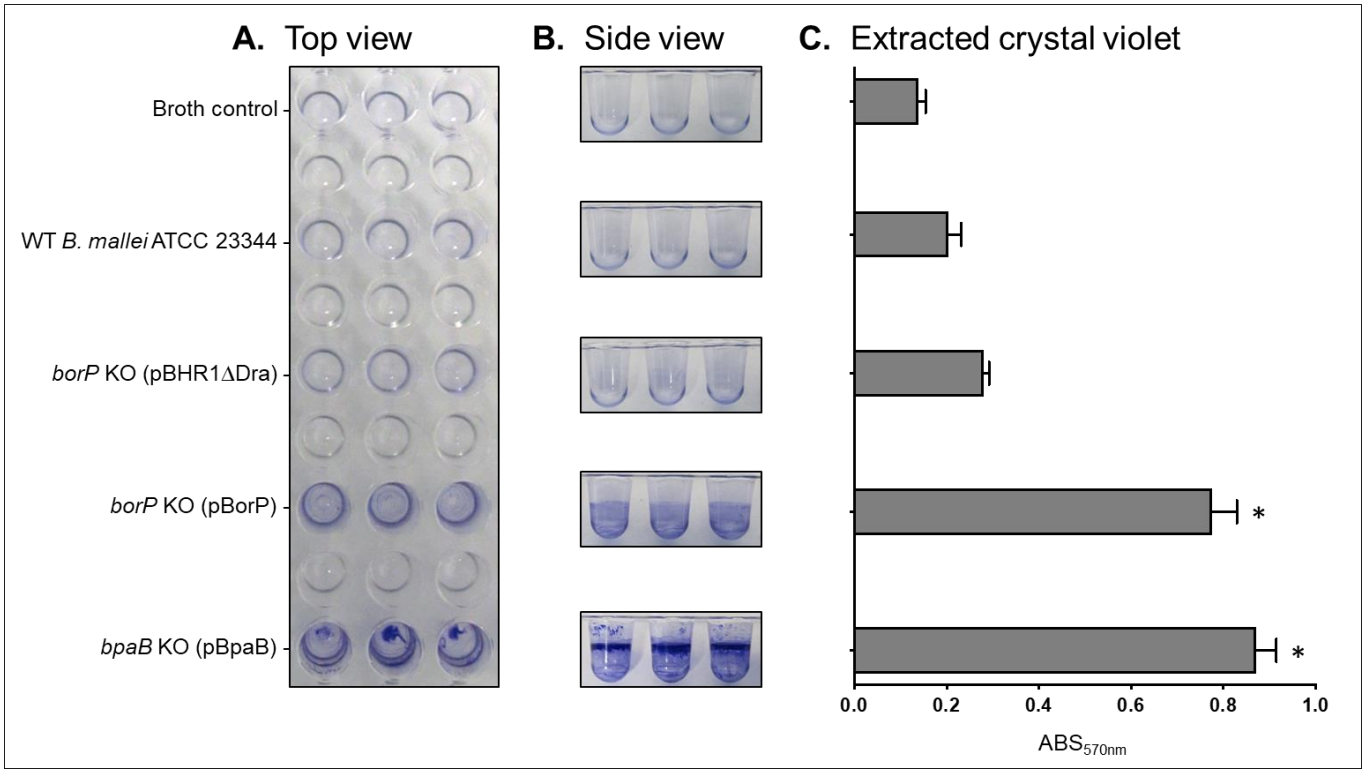

Biofilm assay with *B. mallei* WT and recombinant strains. *B. mallei* strains were cultured in the wells of PVC microplates, stained with crystal violet, washed with deionized water, and the wells were photographed (panels A and B). Biofilm formation (*i.e.* formation of pellicle/ring) was quantitated by extracting crystal violet with methanol and measuring absorbance at a wavelength of 570 nm (panel C). The results are expressed as the mean (± standard error) absorbance. The asterisks indicate that the increase in ABS_{570nm} (and therefore biofilm formation), compared to broth

control, WT *B. mallei* and the *borP* KO mutant carrying plasmid pBHR1ΔDra, is statistically significant. Biofilm assays were performed in triplicate on at least 3 separate occasions. The pictures in panels A and B show one representative assay. The graph in panel C show cumulative results (*n*=3 independent experiments).

Figure 5.5

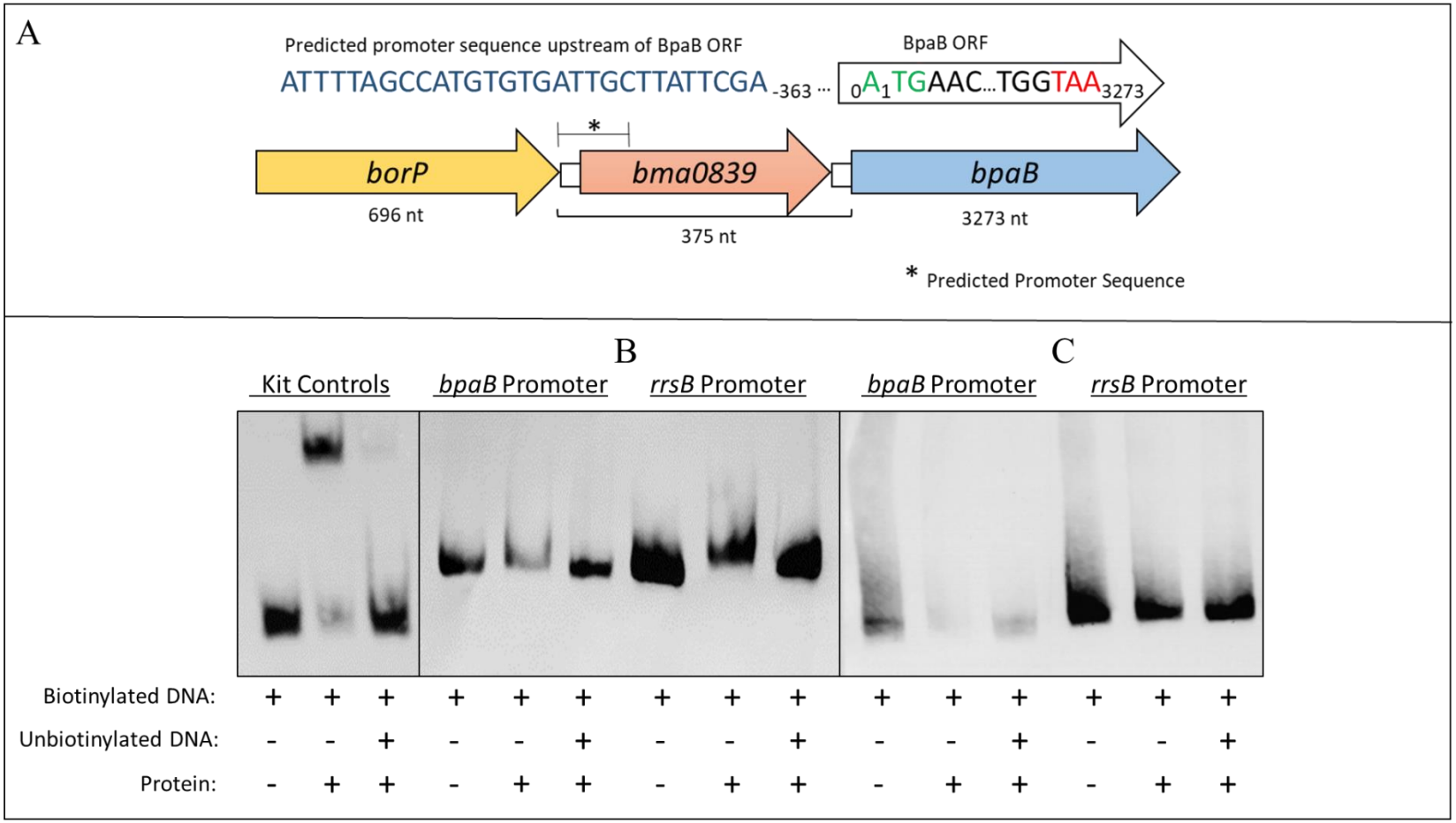
A
Predicted promoter sequence upstream of BpaB ORF
ATTTTAGCCATGTGTGATTGCTTATTCGA -363 ...
BpaB ORF
0A1TGAAC...TGGTAA3273
*
borP
bma0839
bpaB
696 nt
375 nt
3273 nt
* Predicted Promoter Sequence
B
C
Kit Controls
bpaB Promoter
rrsB Promoter
bpaB Promoter
rrsB Promoter
Biotinylated DNA: + + + + + + + + + + + + + + +
Unbiotinylated DNA: - - + - - + - - + - - + - - +
Protein: - + + - + + - + + - + + - + +

Panel A depicts a possible promoter sequence (blue text) 363 bp upstream of the *bpaB* open reading frame (ORF) that was identified by PePPER, an online prokaryotic promoter prediction algorithm. The genome schematic shows the location of the predicted promoter region (*) upstream and within the *bma0839* ORF. In panel B, Electrophoretic Mobility Shift Assays (EMSAs) were used to demonstrate the ability of purified His-tagged BorP to bind to the upstream regions of either *bpaB* or *rrsB*. A commercially available EMSA kit was used, which included control mixtures that were used to ensure that the components of the kit were viable. The kit control mixtures included a biotinylated fragment of a known palindromic binding site present in the Epstein-Barr virus genome that has been shown to be bound by the Epstein-Barr Nuclear Antigen (EBNA). Kit control mixtures (Panel B) include biotinylated control DNA only, biotinylated control DNA mixed with purified EBNA protein, and biotinylated control DNA mixed with purified EBNA protein and unbiotinylated control DNA. Both 500 bp (panel C) and 250 bp (panel D) segments of biotinylated DNA fragments containing the DNA upstream of either the *bpaB* or *rrsB* genes were used. Each respective DNA segment was tested without His-BorP, with His-BorP only, and with a combination of His-BorP and excess unbiotinylated DNA. The decrease in the intensity of the bands in the lanes containing the *bpaB* upstream region DNA combined with His-BorP indicate that His-BorP binds to the *bpaB* promoter, but not the *rrsB* promoter. Further, when spiked with excess unbiotinylated DNA, there was a visible restoration of the biotinylated DNA bands that indicates His-BorP is specifically binding to the unbiotinylated *bpaB* promoter.

Figure 5.6

A. Survival data and LD_{50} values

Strain	Inoculum (CFU)	% survival	LD50 (CFU)
WT	340,000	0	144
	34,000	0	
	3,400	20	
	340	40	
	34	100	
borP KO (pBHR1ΔDra)	260,000	0	6,095
	26,000	0	
	2,600	80	
	260	100	
	26	100	
borP KO (pBorP)	260,000	0	8,221
	26,000	20	
	2,600	100	
	260	80	
	26	100	

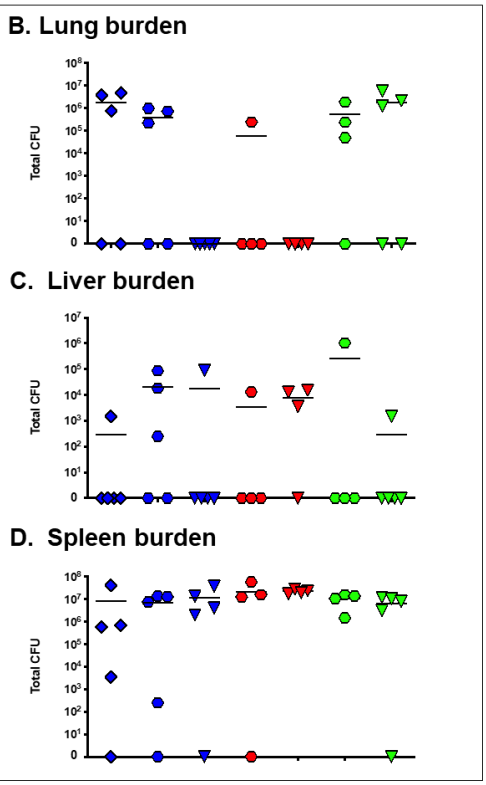

Median lethal dose comparison for *B. mallei* WT and recombinant strains. BALB/c mice were inoculated with a Microsprayer device to aerosolize the indicated numbers of bacterial CFU directly into the lungs (*n*=5 mice/dose). The animals were then monitored daily for clinical signs of illness and morbidity. (A) Survival data and calculated LD_{50} values. (B, C, and D) Tissues were collected from mice that survived challenge (day 26), homogenized, diluted, and spread on agar plates to determine bacterial loads. The symbols represent data from individual animals; horizontal lines represent the mean total number of CFU for each group.

Figure 5.7

A. Survival data and LD_{50} values

Strain	Inoculum (CFU)	% survival	LD50 (CFU)
WT	170,000	0	251
	17,000	0	
	1,700	0	
	170 ◆	60	
	17 ◆	100	
borP KO (pBHR1ΔDra)	220,000	0	3,254
	22,000	0	
	2,200 ●	60	
	220 ●	100	
	22 ●	100	
borP KO (pBorP)	190,000	0	4,506
	19,000	0	
	1,900 ▼	80	
	190 ▼	60	
	19 ▼	100	

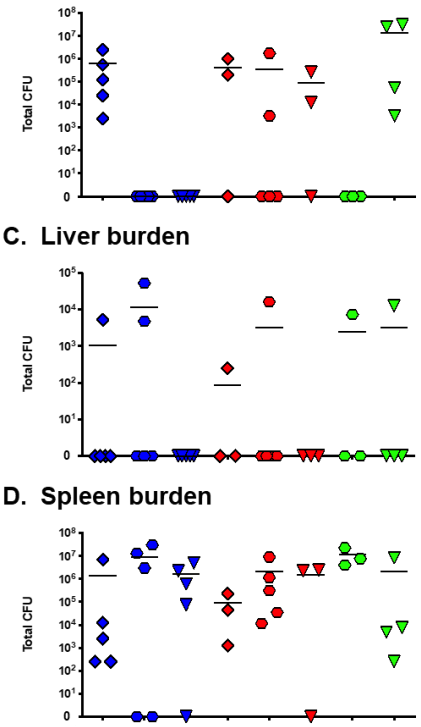

Median lethal dose comparison for *B. mallei* WT and recombinant strains. BALB/c mice were inoculated with a Microsprayer device to aerosolize the indicated numbers of bacterial CFU directly into the lungs (*n*=5 mice/dose). The animals were then monitored daily for clinical signs of illness and morbidity. (A) Survival data and calculated LD_{50} values. (B, C, and D) Tissues were collected from mice that survived challenge (day 22), homogenized, diluted, and spread on agar plates to determine bacterial loads. The symbols represent data from individual animals; horizontal lines represent the mean total number of CFU for each group.

CHAPTER 6

CONCLUSIONS

Burkholderia mallei and *Burkholderia pseudomallei* are two closely-related Gram-negative bacteria that cause the severe respiratory illnesses glanders and melioidosis, respectively (37, 97). *Burkholderia mallei* is endemic to parts of Asia, Africa, the Middle East, and South America (97). *Burkholderia pseudomallei* is endemic to countries bordering the equator, with levels of endemicity especially high in Northern Australia and Southeast Asia (37). Both illnesses can present as an acute or chronic infection, and the most common manifestations are severe pneumonia with accompanying bacteremia (37, 97). *Burkholderia mallei* and *B. pseudomallei* are highly infectious, difficult to diagnose, and are difficult to treat due to intrinsic resistance to most antibiotics (216). Both organisms cause high morbidity and mortality rates and there is no vaccine to reduce the risk of infection. In addition, there are concerns that *B. mallei* and *B. pseudomallei* could be misused as biological terrorism agents. For these reasons, the organisms are classified as Tier 1 Select Agents, placing them in the highest biothreat category level, and the development of efficacious countermeasures is a priority. The high level of genetic relatedness between the organisms, and the striking similarities in the clinical and pathological manifestations of disease they cause, support the feasibility of devising a single vaccine that protects against both *B. mallei* and *B. pseudomallei*.

Thus far, there have been a number of promising vaccine candidates identified and characterized, such as capsular polysaccharide (CPS) (15,193, 230), the oligosaccharide chain of LPS (OPS) (193, 275), and the Type 6 Secretion System protein Hcp1 (62, 149), just to name a few (203). While these, and others, have been capable of establishing high levels of protection against acute lethal infection with *B. mallei* and/or *B. pseudomallei*, there remains a significant level of chronic infection. One confounding issue in this area is a lack of *in vitro* expression of major virulence determinants. Because of this, there is a large body of work examining constitutively (i.e. *in vitro*) expressed antigens, with little to show for it to address chronic infection. Because of this lack of progress, the field as a whole is still in the antigen discovery phase.

One major component of the *B. mallei* pathogenesis process that is of particular interest to our lab is the autotransporter family of proteins. These molecules form one of the largest families of virulence factors in Gram-negative bacteria and contribute to a wide range of pathogenic phenotypes including the formation of biofilms (3, 296), complement resistance (5), intracellular motility (236) and replication (252), and lipolytic activity (295). Autotransporters are also expressed on the bacterial surface, which puts them at a prime location at the host-pathogen interface and readily accessible to the immune system. ATs represent excellent targets for developing countermeasures that would interfere with the ability of pathogenic organisms to establish themselves in a host, persist, and cause disease. There is also precedent to study autotransporter proteins as they have been shown to be high value targets in the study of other bacterial pathogens. For example, the inclusion of the ATs Pertactin and NadA in licensed vaccines for *Bordetella pertussis* (131) and *Neisseria meningitidis* (134), respectively. Further, autotransporter proteins are also shared

between *B. mallei* and *B. pseudomallei*. The genomes of *B. mallei* and *B. pseudomallei* isolates have in common eight autotransporter gene products. Previous work by the Lafontaine laboratory has functionally characterized four of these in *B. mallei*, namely BoaA (155), BpaC (22), BpaB (296), and BatA (295). One finding that was made while examining the four aforementioned autotransporter proteins was that they were not produced at detectable levels by wild-type bacteria under routine culture conditions. However, they were unequivocally expressed *in vivo* evidenced by the production of antibodies against them during the course of *B. mallei* infection in mice (BoaA, BpaC, BpaB, and BatA), horses (BoaA, BpaC, BpaB, BatA), and humans (BoaA, BpaB). One of these proteins, the BpaB autotransporter, is one that is of particular interest to the Lafontaine lab, and will be discussed further later in this chapter.

During the characterization of the BatA autotransporer protein, we discovered that a mutant lacking expression of the *batA* gene was largely attenuated in virulence, as BALB/c mice that were infected with the equivalent of 80 LD_{50} were able to completely clear the organism (295). The discovery that mice were able to fully clear the mutant led us to test the hypothesis that the *batA* mutant strain could be used as a vaccine strain that elicits protective immunity against subsequent challenge with wild-type *B. mallei*. While examining this hypothesis, we found that vaccination with the *batA* mutant provided a high level of protection against back-challenge with *B. mallei*. Further, we found that there was a high degree of cross-protection against *B. pseudomallei* as well. While further examining the immune response to understand our findings, it was determined that passive transfer experiments using serum depleted of its reactivity with constitutively expressed (i.e. *in vitro*) antigens was also capable of conferring protection against both *B. mallei* and *B.*

pseudomallei. This finding demonstrated that cross-protective immunity is predominantly afforded by antibodies recognizing antigens expressed exclusively *in vivo* (295). Due to this level of cross-protection, as well as the already demonstrated selective *in vitro* vs *in vivo* expression dynamic of known virulence factors, we hypothesized that there are antigens expressed exclusively *in vivo* that are spurring the production of these antibodies and that these antigens represent high value immunoprotective targets for developing countermeasures.

Because these antigens are expressed exclusively *in vivo*, and are thus not detectable under routine growth conditions *in vitro*, there is a high degree of difficulty in discovering and characterizing them. This hurdle is a major contributing issue in the lack of meaningful progress on the development of vaccines and medical counter measures for both organisms. Often, research on vaccine and countermeasure development is linear moving from *in silico* analysis to *in vitro* characterization to *in vivo* analysis. This is an exceedingly effective method for the discovery and characterization of novel antigens, but it is dependent on the ability to identify an antigen prior to beginning *in vitro* and *in vivo* examination. By focusing on the end product, in our case immune serum antibodies, we aimed to go from *in vivo* product to *in vitro* analysis, to *in silico* characterization, resulting in an *in vivo* end product. Our rationale was that an antibody was generated against an antigenic epitope *in vivo*, and if an artificial epitope could be captured by this highly valuable antibody, vaccination with that epitope could lead to the production of a similarly valuable antibody. In this method, artificial epitopes could be used as a mimetic vaccine, referred to as a mimotope vaccine in other publications (66, 70, 87, 90, 119, 141, 163, 165, 220, 247, 268, 289).

The use of mimotopes as vaccines, or as the driving force behind novel antigen discovery, is dependent upon the ability to capture epitopes that are bound to a recoverable surface, and manipulate them in a manner conducive to amplification and subsequent downstream uses. The method that we used was a viral expression platform that was commercially available. Specifically, the platform that was used to discover novel antigenic epitopes was the New England Biolabs PhD-12 phage display library. This phage display system uses linear 12-mer randomly generated amino acid sequences which are expressed in 5 identical copies on the minor coat protein of the M13 bacteriophage virion. This system was advantageous as it allowed us to rapidly screen high numbers of individual epitopes by incubating the stock library with high value antibodies that were conjugated to recoverable magnetic beads. Additionally, the library was able to be pre-cleared of irrelevant epitopes through incubation with beads that were saturated with antibodies from naïve mouse serum. Further, by nature of being an M13 bacteriophage, selected phages could be readily amplified to obtain large quantities of epitopes for downstream applications.

Before we could start the process of probing the library, we first had to address our starting material. While examining the antibody reactivity profile, we discovered that immune serum that was allegedly free of reactivity with constitutively expressed antigens was reactive with whole cell lysates of plate grown *B. mallei*. We reasoned that this was residual reactivity due to a lack of clearance of antibodies reactive to epitopes within the bacterial cell that were not exposed during the adsorption process using whole cell live bacteria, but would be exposed by an antigen presenting cell during an endogenous immune response. To address this, the serum was further cleared with whole cell lysates, rather than

whole cell bacteria, and upon testing we found it was now free of reactivity with whole cell lysates. However, it retained a high degree of reactivity with tissue lysates from mice that had been infected with *B. mallei*. Due to the lack of reactivity with the plate grown bacterial whole cell lysates, we reasoned that this observed reactivity must be to antigens that were expressed by the bacteria during the course of infection that were not present in the plate grown bacteria to clear reactivity.

In order to probe the library, we needed antibodies that were affixed to a surface that could be manipulated and recovered in order to retrieve the bound epitopes. Antibodies can be affixed to many objects, ranging from metallic nanoparticles to 96 well plates. For our purposes we chose protein G beads manufactured by MiltenyiBiotec. The reason for this was that the beads bind the Fc region of antibodies leaving the antigen recognition (Fab) portion projected outward to readily bind available antigens. In addition to binding the antibodies in a preferred way, the beads were also small in nature, and were magnetic, both of which made the recovery of beads easily accomplished. Through the use of magnetic separation columns, also manufactured by MiltenyiBiotec, we were able to incubate beads that were conjugated to a surface that was easily recovered and manipulated, and also wash away unbound portions of the binding mixtures. The only major hurdle from a technical standpoint was ensuring that the coating surfaces of the beads were fully saturated with immune serum IgG antibodies. It was important that no protein G binding surface was available, as we were not sure if the M13 bacteriophages would be non-specifically bound by the surface or not. M13 phages are often referred to as “sticky” and will non-specifically adhere to many surfaces, which is a major cause of phage contamination of workspaces in laboratories. They are also quite durable, able to withstand

a broad range of temperatures, UV exposure, and pH conditions, further complicating any work done with them. To avoid an issue, we wanted to be proactive and eliminate as many potential confounding issues as possible, and take protein G binding surface out of the equation. To ensure that the beads were saturated, we incubated the beads with a FITC-conjugated IgG2a mouse monoclonal antibody. We used an IgG2a antibody as the included literature with the beads indicated that the mouse IgG2a antibody was bound with the highest affinity to the protein G beads, thus any available binding surface, or any surface loosely bound with immune serum IgG antibodies, would likely be bound or displaced by the FITC-tagged monoclonal antibody. The FITC-conjugation on each antibody allowed us to run a portion of our beads through a flow cytometer. By doing this, we could look for a characteristic presence of fluorescence indicating that the beads were not fully saturated and bound the FITC-tagged antibodies. Once beads were confirmed to be saturated, they were deemed fit to be used in the downstream panning processes.

By nature of containing randomly generated antigens, on the order of approximately $1.0x10^9$ unique epitopes, the NEB PhD-12 kit that was to be used as a binding substrate would necessarily contain many antigens that were either broadly reactive with both immune and naïve serum, or antigens that were solely reactive with naïve serum. Regardless of which category an antigen may fit into, their presence served as interference in the ability of the high value immune serum that was conjugated to the beads to bind antigens they were able to recognize. In order to give the mimotopes the best opportunity to be recognized and bound by our high value serum, we devised a method to cut through the noise and reduce our total population of phages. Beads were saturated with IgG from naïve mouse serum, and the stock PhD-12 kit was incubated with these beads.

We reasoned that this would allow any mimotope that is recognized by naïve serum would either be broadly reactive, or would be a mimotope of a constitutively expressed antigen, neither of which we were looking for.

Once the PhD-12 library was pre-cleared of irrelevant epitopes, we were able to proceed with our search for mimotopes reactive with our immune serum. The pre-cleared library was incubated with the immune serum coated beads, and after a period of time nonreactive epitopes were washed away. At the end of our process, we were left with what we believed with potentially high value mimotopes. These mimotopes were scaled up, and screened with reactivity through a modification of the titering protocol included with the PhD-12 kit. In short, *E. coli* cultures were infected with aliquots of the obtained phage mimotopes and allowed to form plaques. These plaque filled lawns of bacterial growth were then incubated with PVDF circles overlain on top of them, which allowed for phage plaque rings to embed within a surface that could be further probed using a protocol reminiscent of a Western blot. Through this method, we were able to rapidly screen phages and pinpoint specific phage plaques that met specific conditions such as reactivity with immune serum or a lack of reactivity with naïve serum. The ability to identify specific phage plaques, as well as the nature of each phage only containing one specific mimotope, allowed us to screen, identify, collect, and amplify, specific mimotopes that were reactive with our immune serum. In-so-doing, we were able to fulfil the first portion of our desired workflow, going from *in vivo* end product (antibodies) to *in vitro* analysis (selection of phages of interest), and now needed to focus on *in silico* characterization.

While manufacturing the PhD-12 library, NEB inserted a specific sequence immediately upstream of the mimotope sequence portion of the DNA. The company also

provided sequencing primers to a location slightly further upstream of the mimotope sequence, which allowed us to sequence our obtained phages and determine the DNA sequence of the mimotopes of interest. Once we had the DNA sequence we were able to translate it into the corresponding amino acid sequence and further analyze each mimotope. Because the mimotopes were both obtained and screened by reactivity with antibodies, and because of our data finding that antibodies are a major contributor to immunity against infection with *B. mallei* and *B. pseudomallei*, we focused on the role of mimotopes in the production of antibodies. To examine this, we used an online B-cell epitope identification algorithm available from the Immune Epitope Database and Analysis Resource, a freely available online service funded by NIAID. Each sequenced mimotope was analysed using this resource. In parallel, we also performed a pBLAST search of the entire proteome of *B. mallei* and *B. pseudomallei* using the obtained sequences. Based on the results of the serum screening, the B-cell epitope analysis, and the corresponding pBLAST search results, we subjectively ranked the mimotopes from most valuable to least. This concluded our *in silico* analysis, and from there we moved on to examining the ability of these mimotopes to be used as vaccine targets. While the work that had been performed up to this point was interesting in its own right, there remained the need for an end product as the purpose of this work is ultimately to address the lack of available epitopes through the discovery of novel *in vivo* expressed antigens.

The ability of the mimotopes to produce a meaningful immune response was examined numerous times and under multiple conditions. Different avenues of investigation included the use of the phages themselves expressing the mimotopes, conjugations of synthesized mimotopes to various immunogenic carriers, and the

production of fully mature proteins identified based on the results of the pBLAST analyses. For each trial, mimotopes were given over multiple doses using Freund's Complete and Incomplete adjuvants. These adjuvants were used as they lead to high antibody production, and we wanted to maximize antibodies due to their role in protective immunity. In the end, we were not able to produce a meaningful level of production using any of the methods we employed to examine the mimotopes and their feasibility for use as vaccine candidates. This was an unfortunate result, as up to this point results were promising. The phages were highly reactive with immune serum, lacked reactivity with naïve serum, and pBLAST searches showed large areas of overlap with the 12-mer amino acid sequences and endogenous proteins that were likely involved in pathogenesis.

One reason for this lack of protection may be either a lack of production of antibodies against multiple portions of the same antigen, or a lack of antibodies against epitopes important for the clearance of the organism at that particular time, resulting in an underwhelming reaction to an antigen of interest. A single antibody recognition site can bind to an amino acid sequence as large as 10 amino acids, which is essentially the entirety of our 12-mer amino acid sequences. While it seems like a large fraction of an antigen compared to our mimotopes, when compared to an endogenous protein, it is only a fraction of the possible size. During the course of an *in vivo* infection with *B. mallei* or *B. pseudomallei*, numerous regions within the same antigen are likely going to be recognized and have a specific immune response against them. There will also be a wide array of antigens that are recognized, that may or may not be represented by our lead 12-mer mimotopes. Some of this antibody binding will be done at high affinity levels, while others will be transiently bound. Finding the epitope that lends itself toward high affinity binding

by antibodies is going to lead to increased recognition by the immune system against antigens expressed *in vivo* that could provide a much more meaningful response. It's possible that while we are finding a portion of amino acids that high value antibodies are targeting, and even producing antibodies *in vivo* that can also target those same sequences, we aren't producing enough antibodies targeting either the correct antigens/portion of antigens in question to cause the desired immune response, or a broad enough number of antibodies to target the bacteria cell to see a meaningful humoral immune response.

An additional benefit of using this linear 12-mer system is that the amino acid sequences of the epitopes that are captured by the antibodies can be used to probe the endogenous proteome of *B. mallei* and *B. pseudomallei*. This yielded several proteins that had either an entire 12 amino acid sequence or a large portion of one, shared between the mimotope and the endogenous antigen. Based on these results, we selected a suite of proteins that shared sequence overlap and were relevant to the *in vivo* pathogenesis setting, and had an NIH collaborative protein synthesis service produce the full mature proteins used in the previously mentioned vaccine tests. The process was not a waste, despite failing to provide a meaningful level of protection, as proteins were discovered that were linked by shared reactivity to antibodies that were only reactive with exclusively *in vivo* expressed antigens. These proteins could retain a high degree of value as gene knockout models for use as live attenuated strain vaccines. Further, they could provide insight into potential therapeutics as drugs that target the mechanism of action these proteins are responsible for could potentially disrupt their ability to work and thus disrupt the *in vivo* disease process.

The proteins that were synthesized and used in vaccination tests were only done so as they were the proteins that were readily available from the protein manufacturing service

that was used. In reality, each protein was just the best available protein from a list of potential hits. A non-comprehensive list of various endogenous proteins that were identified based on shared sequence homology between the epitopes and the proteins include outer membrane porin proteins, Type III secretion system proteins, and Type VI secretion system proteins, all of which likely play a role in the virulence in *B. mallei* and *B. pseudomallei*. An argument can be made that the process of using antibodies to obtain synthetic mimotopes capable of conferring protection against *B. mallei* and *B. pseudomallei* was a failure. However, it provided direct evidence tying specific gene products of *B. mallei* to antibodies that are capable of conferring protection, which underscores their importance as antigens of interest. In a field that is still in the antigen discovery phase despite decades of research, this is a meaningful and fruitful result that broadens the field as a whole. Additionally, these phages represent the culmination of 10 selected mimotopes that were themselves selected from a sea of approximately $1.0x10^9$ epitopes. It is highly unlikely that if this process were repeated from the first step, the same phages would be the end product. It is not only possible, but probable, that there are other antigens of interest that are equally as valuable as the antigens described herein that remain undiscovered within the library of mimotopes.

It is also important to note that the aforementioned use of the phage display library and the obtained results only describe the use of one epitope library, made by a single manufacturer. It does not discuss the use of other libraries made by NEB, such as the PhD-C7C library which uses amino acids arranged in a constrained loop, rather that linear chains, to present epitopes. This work also does not describe the use of libraries available from other manufacturers, nor does it describe the use of custom made >20 amino acid

libraries which are widely used in the literature. However, the streamlined methodology presented which could be used to screen virtually any viral vector based epitope library, which would allow for a rapid turn-around time should the lab desire to return to the use of mimotope vaccine library screening at a future date.

Mimotope libraries represent just a single method for the discovery of novel antigens, however, immunoproteomic analyses of many types have been employed to examine *in vivo* expressed antigens. One antigen that has been previously discovered and described in *B. pseudomallei* through the use of other means is the BPSL2765 antigen (84,109). Previous work in the field has shown that the antigen BPSL2765 was capable of inducing an immune response that was consistent with a lower incidence of chronic melioidosis (109). In a laboratory setting, BPSL2765 was also capable of inducing an immune response in mice that provided partial protection against intraperitoneal challenge of *B. pseudomallei* (109). Further work in the field has shown through comparative sequence analysis as well as the determination of the proteins crystal structure that BPSL2765 is an orthlog of the Peptidoglycan-associated lipoprotein. The Peptidoglycan-Associated lipoprotein, or Pal, of Gram-negative bacteria, is a component of the Tol-Pal system. The Tol-Pal system, which is a complex of 5 core proteins (TolQ, TolR, TolA, TolB, Pal) that spans the inner and outer membranes, is required for maintaining the bacterial cell wall (105), invagination during cellular division (105), and has been shown to be important for the uptake of bacteriophages (105, 166), colicin (166), and other small molecule effectors (166).

Despite being a well characterized antigen in other organisms, we are the first to characterize it in *B. mallei*. While examining its role in the pathogenesis of *B. mallei*, we

discovered that it was not produced *in vitro* at detectable levels by *B. mallei*. We removed the expression of Pal from *B. mallei* ATCC 23344 through the creation of an isogenic mutant strain. While trying to construct the mutant we noted that it was highly sensitive to polymyxin B, which was unusual as most *Burkholderia* species are largely unaffected by high concentrations of polymyxin B. This reduced fitness was consistent across many other common *in vitro* analyses performed by our lab. The mutant failed to survive within J774 murine macrophages and in the presence of serum components, both of which are hallmark virulence traits of *B. mallei*. Additionally, the mutant displayed a reduced ability to survive under osmotic stress when grown on plates supplemented with KCl, and under osmotic stress in the presence of polymyxin B supplemented plates. When the isogenic mutant was complemented with a plasmid that conferred constitutive expression of the *pal* gene the mutant, all of the deficiencies were returned fully, or mostly, in the case of serum resistance, to the same level as the wild-type backbone strain. To ensure that the difference in fitness between the mutant and the wild-type was not due to a general growth defect, we compared their replication rates in liquid broth and found that they were identical, meaning this difference could not be attributed to an inability to grow at the same rate. To examine what role Pal had in the pathogenesis of *B. mallei*, we determined the LD_{50} of the isogenic mutant strain compared to wild-type using our aerosol model of infection in mice (156). While characterizing the *in vivo* virulence, we discovered that a lack of expression of the *pal* gene resulted in complete attenuation of the organism, with mice inoculated with the equivalent of 2,500 LD_{50} not only surviving but also achieving full clearance. When examined as a whole, our data suggested that Pal is an important virulence factor of *B. mallei*, and plays a major role in the stability of the cell wall. Its importance to the cell wall

of *B. mallei* appears to be so vital, in fact, that while we can rule out the observed fitness deficiencies being due to a generalized growth defect, it is very likely that they are due to a greatly reduced cell wall stability. At this time, we have no data to show this conclusively, but it follows logically, and would mirror the results of *pal* mutants in other organisms.

In addition to playing a major role in the structural stability of many organisms, the Pal proteins of many Gram-negative bacteria have also shown to be highly immunogenic, including the Pal proteins of *H. influenzae* (110, 111) and *K. pneumoniae* (138) to name a few. Also, as mentioned previously, the *B. pseudomallei* Pal ortholog BPSL2765 was shown to provide partial protection of mice against challenge with wild-type *B. pseudomallei*. To examine what potential the Pal protein of *B. mallei* may have as a vaccine antigen, we constructed a PIV5 vectored Pal vaccine. A PIV5 vectored vaccine was chosen as our lab has previously worked with a PIV5 vector that was expressing the BatA autotransporter protein and found that it provided a robust immune response with a high level of protection. Mice were provided a single intranasal dose of the PIV5-Pal construct, equivalent to a dose of $1.0x10^7$ PFU of PIV5, then challenged 6 weeks later with 10 LD_{50} of wild-type *B. mallei*. Our experiments showed that the PIV5-Pal vaccine protected 90% of back-challenged mice through acute infection, and 80% of mice through the chronic phase to the end of the experiment. However, all of the mice were colonized by the wild-type organism, meaning that complete clearance was not accomplished, though a total of 3 mice that has been vaccinated with the PIV5-Pal vaccine had no bacteria in their lungs.

This work represents the first characterization of the *B. mallei* Pal protein both as a potential vaccine target as well as at the host-pathogen interaction level. Our findings are consistent with the results of other labs that have studied Pal in other organisms.

Additionally, we have demonstrated that the Pal protein is highly immunogenic, and under the correct circumstances could potentially be a major vaccinogenic target in the field that is currently in great need of new antigens. While we did not examine the specific mechanism of protection of the PIV5-Pal vector, we did demonstrate a significantly high level of protection with a single dose of vaccine. Future work on the Pal protein should focus on what effect a prime-boost effect might have on the level of protection obtained. It is not impossible that a prime-boost approach would not have an effect on the level of protection, but it is unlikely, and it could potentially be a major change to a field that is currently highly dependent upon the use of live attenuated strain vaccines, which are unlikely to ever be licensed due to risks of reversion of a pathogen that has been eradicated from the United States, Canada, and Western Europe.

When taken together, the results of the Pal data as well as the mimotope data emphasize how important the discovery of novel *in vivo* expressed antigens is to the field of vaccinology. While the discovery of novel *in vivo* antigens is important, understanding the differential expression leading to their expression can be equally important. Differential expression of antigens of interest is a well-documented phenomena in the study of bacteria. As bacteria traverse numerous environmental and temporal settings, they require tight modulation of their proteome. Sensing environmental cues and enacting a corresponding change of gene expression is a particularly important component of the bacterial ability to persist in a wide range of environments.

There are numerous methods at the disposal of bacteria in regulating their DNA expression, but the two-component regulatory system is the most widely used system and enables the change in bacterial expression as a direct response to environmental stimuli.

Two-component regulatory systems, or TCS, have also been demonstrated to be major components of bacterial pathogenesis, the most common of which is the OmpR-like TCS. OmpR orthologs have been demonstrated to modulate the expression of many virulence pathways in bacteria, such as the expression of the ToxR/TcpP/ToxT virulence cascade in *Vibrio cholera* (221), the SsrA/SsrB regulatory system of *salmonella enterica* serovar Typhimurium (33), and the FlhDC master flagellar activator of *Yersinia enterocolitica* O:9 (98, 162, 213, 214). While they have been shown to be involved in many stages of the bacterial pathogenesis process, one area that they have proven to be widely involved in is the situational expression of biofilms, one example of which is the BfmR OmpR-like TCS of *Acinetobacter baumannii* (258). As was previously discussed, one class of virulence factors that the Lafontaine lab has contributed a significant amount of work toward is the characterization of autotransporter family proteins. As was also previously discussed, while characterizing them, we found that they are not produced at detectable levels under routing culture conditions, but are demonstrably expressed *in vivo* (3, 4, 155, 157, 295, 296). While characterizing BpaB autotransporter protein, it was shown to be the first biofilm formation factor yet described in *B. mallei*. During the course of characterizing the protein, it was noted that upstream of the *bpaB* open reading frame (ORF) sat BorP (296). Due to the proximity of the two genes, the involvement of BpaB in the production of biofilms, the precedent that TCS are often involved in biofilm formation, and the predicted DNA-binding response regulator function of BorP, we hypothesized that BorP was regulating the expression of BpaB either directly as a regulator, or indirectly as a global virulence regulator.

Over the course of our examination of BorP, we found that constitutive expression of BorP by an isogenic mutant we created lacking the expression of *borP* that we complemented with a constitutive expression vector specifying the expression of *borP* led to a corresponding expression of BpaB. This was an encouraging finding, as up to this point in the literature, BpaB has not been demonstrated to be expressed *in vitro* without the use of constitutive expression vectors specifically expressing BpaB (296). In addition to demonstrating expression of BpaB, we also recapitulated the described biofilm phenotype of the published BpaB constitutive expression mutant (296) by noting the presence of a biofilm ring during crystal violet biofilm staining assays. Further, this phenotype was not present in the *borP* isogenic mutant strain that lacked the BorP constitutive expression vector. This was a beneficial finding as it indicated that not only were we demonstrating a production of BpaB are a result of the expression of BorP, but the end result was a biologically active form of BpaB. This meant that the deletion of BorP did not cause a polar mutation of the downstream BpaB gene, and also that we could conclusively say that BorP was regulating the expression of BpaB at either the transcriptional or translational level. We hypothesized that the DNA-binding characteristics of the BorP protein necessarily meant that it could not be regulating it at the translational level, but we still had not yet addressed whether or not BorP was binding the upstream region of the *bpaB* ORF and regulating it directly, or if it was regulating it indirectly as a global virulence regulator.

To address this gap of knowledge, we performed **E**lectrophoretic **M**obility **S**hift **A**ssays (EMSAs). For our EMSA reactions, we used both 500 and 250 nucleotide regions of the upstream DNA regions of the *bpaB* gene and the *rrsB* gene, the ribosomal 16s RNA gene, that had been biotinylated using a commercially available kit. The *rrsB* gene was

used as a negative binding control, to ensure that our purified His-BorP was not just a "sticky" protein that bound promoter sequences non-specifically. Using reaction mixture components and a protocol available from ThermoFisher, we demonstrated that BorP was binding the upstream region of the *bpaB* gene, and that this binding was not done in a non-specific manner. This was shown as a characteristic shift in where the band of the biotinylated DNA can be seen on the gel, as DNA bound by a protein will migrate at a much slower rate than DNA free from any inhibiting influence. To further show specificity for the upstream region, chase reactions were performed for each mixture in which approximately 100-fold increased concentrations of unbiotinylated DNA was included in each mixture. This inclusion of unbiotinylated DNA was done so that the unlabeled DNA would be bound at higher levels than the labeled DNA, due solely to increased numbers of DNA segments, and a restoration of the shifted DNA would be visible. Through these experiments, we showed that the shift of DNA for the upstream region of *bpaB* was reduced, and that none of the conditions had any binding effect on the upstream region of *rrsB*.

Since *borP* is involved in the expression of at least one virulence factor, we hypothesized that the inability to express the *borP* gene would reduce the virulence of *B. mallei* in our aerosol mouse model of infection. Because we could not conclusively state that BorP is solely binding the upstream region of *bpaB*, not acting as a global regulator of virulence, we felt it was important to examine how a lack of *borP* expression would affect the overall virulence of the organism. If we disrupted the *borP* gene and found that the organism was no longer virulent, or had a much higher level of attenuation, it would suggest that BorP is acting on other genes in addition to BpaB. What we found with these

in vivo experiments was that indeed the isogenic mutant strain that lacked expression of *borP* had a reduction in virulence comparable to that of the previously described BpaB mutant (296). Further, we found that the constitutive expression of the *borP* ORF by the mutant strain that had been complemented with a constitutive expression plasmid conferring expression of BorP had been further attenuated, and at levels similar to that of the previously described BpaB mutant (296). From this we concluded that BorP is solely regulating the expression of BpaB, and is not a global virulence regulator.

We felt that we had sufficient data to accept our hypothesis that BorP is directly regulating the expression of *bpaB* at the transcriptional level, and is not a global virulence regulator, but we did not show this conclusively. Future work on this project should include RT-PCR, and perhaps RNA-Seq. RT-PCR would allow us to conclusively demonstrate that when we express BorP, we see a corresponding transcription of the *bpaB* gene, but in wild-type, *bpaB,* and *borP* mutants we do not see transcription of the *bpaB* gene. If we found transcripts of the *bpaB* gene in the mutants or wild-type we would have to reject our hypothesis that BorP regulates BpaB at the transcriptional level. RNA-Seq would allow us to address the second part of the hypothesis by examining the total transcriptome of *B. mallei.* If RNA-Seq data showed that when we express BorP we only see a statistically significant increase in *bpaB* transcripts, but not other genes, we could accept our hypothesis that BorP is not a global virulence regulator. If RNA-Seq data instead found that a wide array of genes was up-regulated it would be a welcome and interesting finding, but would force us to reject the hypothesis that BorP is directly regulating BpaB.

Additional future work should also focus on understanding what a corresponding partner protein of BorP might be. A major component of OmpR-like TCS DNA-binding

response regulators is a conserved phosphorylation receiver domain. This domain is often phosphorylated by a corresponding environmental regulator. Presently, we do not have any data to indicate what a potential environmental sensing binding partner for BorP may be, if it even has one. Understanding what could be leading to the expression of BorP as a response to the environment could have major implications in the understanding of the ability of *B. mallei* to produce a biofilm, which our lab has shown to be a major virulence determinant of the organism. Typically, though not universally, the gene encoding the corresponding environmental sensor of an OmpR-like DNA binding response regulator is located nearby in the genome. Sequence analysis of the *B. mallei* genome indicates that no such predicted protein exists in the immediate vicinity. However, there are numerous other predicted TCS DNA-binding response regulators such as BMA0833, which is predicted to be another OmpR-like DNA binding response regulator, or BMA0832 which is a predicted LysR family transcriptional regulator. It's possible that the proximity of these DNA-binding response regulators is not a coincidence and they are all regulated together by some global regulator such as fumarate-nitrate reductase (FNR), an oxygen sensing response regulator that has been shown to be involved in biofilm expression of other organisms (20, 65), including *B. pseudomallei* (189).

The two hypotheses that informed this body of work were that a) there are high value target antigens that are expressed by *B. mallei* exclusively *in vivo* that are capable of producing protective immunity, and that b) the selective *in vivo* expression of these antigens is modulated by global virulence regulators. Chapters 3 and 4 of this dissertation address the first of the two hypotheses directly. Through this work it was shown that immune serum antibodies can be used to rapidly identify antigens that are expressed solely

in vivo. While we were not able to use those same antigens to produce a meaningful immune response, there remains a broad body of work to be done with those targets, and it is likely that removal of their expression will lead to a mutants that have greatly reduced virulence *in vivo*. However, the Pal project more conclusively showed that there are in fact high value antigens selectively expressed *in vivo*, and use of the Pal protein as a vaccine further showed that the use of these antigens is capable of conferring a high level of protection. While the use of the known phage-originated targets may seem more abstract, due to the unlikely nature of a licensed *B. mallei* live attenuated vaccine, the Pal work directly provides the field with an antigen that is suitable for use as part of a subunit vaccine. The BorP portion of this work addressed the second hypothesis, and showed that the expression of at least one known virulence factor is selectively expressed *in vivo* through the modulatory effects of a regulator. While it is unlikely that BorP is itself a global regulator, it's very likely that BorP itself is modulated by one.

There remains a substantial amount of work to be done in the field as a whole in the discovery of novel antigens, as there still remains the problem of surviving the chronic infection of *B. mallei*. It's possible that this hurdle may never be overcome, and the clearance of *B. mallei* may depend on some synergistic treatment such as a vaccine with antibody therapy similar to the treatment of rabies, or the use of antibody therapy mixed with antibiotics similar to the treatment for some ESKAPE pathogens (19, 76, 102, 144, 184, 285) and Tuberculosis (116). However, with the increasing level of antimicrobial resistance worldwide, a single-source treatment for infection with *B. mallei* and *B. pseudomallei* would be the most optimal path forward.

REFERENCES

1. Abe, Y., et al., Lymphocyte proliferative response to P6 of Haemophilus influenzae is associated with relative protection from exacerbations of chronic obstructive pulmonary disease. American Journal of Respiratory and Critical Care Medicine, 2002. 165(7): p. 967-971.

2. Adler, N.R.L., et al., Perturbation of the two-component signal transduction system, BprRS, results in attenuated virulence and motility defects in Burkholderia pseudomallei. Bmc Genomics, 2016. 17.

3. Adler, N.R.L., et al., Identification of a Predicted Trimeric Autotransporter Adhesin Required for Biofilm Formation of Burkholderia pseudomallei. Plos One, 2013. 8(11).

4. Adler, N.R.L., et al., Autotransporters and their role in the virulence of Burkholderia pseudomallei and Burkholderia mallei. Frontiers in Microbiology, 2011. 2.

5. Adler, N.R.L., et al., Systematic Mutagenesis of Genes Encoding Predicted Autotransported Proteins of Burkholderia pseudomallei Identifies Factors Mediating Virulence in Mice, Net Intracellular Replication and a Novel Protein Conferring Serum Resistance. Plos One, 2015. 10(4).

6. Allwood, E.M., et al., Strategies for intracellular survival of Burkholderia pseudomallei. Frontiers in Microbiology, 2011. 2.

7. Alwis, P.A., et al., Disruption of the Burkholderia pseudomallei two-component signal transduction system BbeR-BbeS leads to increased extracellular DNA secretion and altered biofilm formation. Veterinary Microbiology, 2020. 242.

8. Amemiya, K., et al., Comparison of the early host immune response to two widely diverse virulent strains of Burkholderia pseudomallei that cause acute or chronic infections in BALB/c mice. Microbial Pathogenesis, 2015. 86: p. 53-63.

9. Anutrakunchai, C., et al., Role of RelA and SpoT in Burkholderia pseudomallei survival, biofilm formation and ceftazidime tolerance during nutritional stress. Tropical Biomedicine, 2016. 33(4): p. 786-798.

10. Aravind, L., et al., The many faces of the helix-turn-helix domain: Transcription regulation and beyond. Fems Microbiology Reviews, 2005. 29(2): p. 231-262.

11. Aschenbroich, S.A., E.R. Lafontaine, and R.J. Hogan, Melioidosis and glanders modulation of the innate immune system: barriers to current and future vaccine approaches. Expert Review of Vaccines, 2016. 15(9): p. 1163-1181.

12. Ashby, M.K., Survey of the number of two-component response regulator genes in the complete and annotated genome sequences of prokaryotes. Fems Microbiology Letters, 2004. 231(2): p. 277-281.

13. Asmar, A.T., et al., Communication across the bacterial cell envelope depends on the size of the periplasm. Plos Biology, 2017. 15(12).

14. Aubert, D.F., R.S. Flannagan, and M.A. Valvano, A novel sensor kinase-response regulator hybrid controls biofilm formation and type VI secretion system activity in Burkholderia cenocepacia. Infection and Immunity, 2008. 76(5): p. 1979-1991.

15. AuCoin, D.P., et al., Polysaccharide Specific Monoclonal Antibodies Provide Passive Protection against Intranasal Challenge with Burkholderia pseudomallei. Plos One, 2012. 7(4).

16. Audia, J.P., C.C. Webb, and J.W. Foster, Breaking through the acid barrier: An orchestrated response to proton stress by enteric bacteria. International Journal of Medical Microbiology, 2001. 291(2): p. 97-106.

17. Austin, C.R., et al., A Burkholderia pseudomallei Colony Variant Necessary for Gastric Colonization. Mbio, 2015. 6(1).

18. Bachhawat, P., et al., Mechanism of activation for transcription factor PhoB suggested by different modes of dimerization in the inactive and active states. Structure, 2005. 13(9): p. 1353-1363.

19. Bagnoli, F., Staphylococcus aureus toxin antibodies: Good companions of antibiotics and vaccines. Virulence, 2017. 8(7): p. 1037-1042.

20. Baikalov, I., et al., Structure of the Escherichia coli response regulator NarL. Biochemistry, 1996. 35(34): p. 11053-11061.

21. Baker, S.M., et al., A Burkholderia pseudomallei Outer Membrane Vesicle Vaccine Provides Cross Protection against Inhalational Glanders in Mice and Non-Human Primates. Vaccines, 2017. 5(4).

22. Balder, R., et al., Identification of Burkholderia mallei and Burkholderia pseudomallei adhesins for human respiratory epithelial cells. Bmc Microbiology, 2010. 10.

23. Bang, I.S., et al., Autoinduction of the ompR response regulator by acid shock and control of the Salmonella enterica acid tolerance response. Molecular Microbiology, 2002. 44(5): p. 1235-1250.

24. Barbieri, C.M., T. Wu, and A.M. Stock, Comprehensive Analysis of OmpR Phosphorylation, Dimerization, and DNA Binding Supports a Canonical Model for Activation. Journal of Molecular Biology, 2013. 425(10): p. 1612-1626.

25. Barker, C.S., B.M. Pruss, and P. Matsumura, Increased motility of Escherichia coli by insertion sequence element integration into the regulatory region of the flhD operon. Journal of Bacteriology, 2004. 186(22): p. 7529-7537.

26. Barrett, J.F. and J.A. Hoch, Two-component signal transduction as a target for microbial anti-infective therapy. Antimicrobial Agents and Chemotherapy, 1998. 42(7): p. 1529-1536.

27. Batchelor, E. and M. Goulian, Imaging OmpR localization in Escherichia coli. Molecular Microbiology, 2006. 59(6): p. 1767-1778.

28. Beier, D. and R. Gross, Regulation of bacterial virulence by two-component systems. Current Opinion in Microbiology, 2006. 9(2): p. 143-152.

29. Benanti, E.L., C.M. Nguyen, and M.D. Welch, Virulent Burkholderia Species Mimic Host Actin Polymerases to Drive Actin-Based Motility. Cell, 2015. 161(2): p. 348-360.

30. Bergstrom, L.C., et al., Hierarchical and co-operative binding of OmpR to a fusion construct containing the ompC and ompF upstream regulatory sequences of Escherichia coli. Genes to Cells, 1998. 3(12): p. 777-788.

31. Bernardini, M.L., A. Fontaine, and P.J. Sansonetti, THE 2-COMPONENT REGULATORY SYSTEM OMPR-ENVZ CONTROLS THE VIRULENCE OF SHIGELLA-FLEXNERI. Journal of Bacteriology, 1990. 172(11): p. 6274-6281.

32. Bernhards, R.C., et al., Characterization of in vitro phenotypes of Burkholderia pseudomallei and Burkholderia mallei strains potentially associated with persistent infection in mice. Archives of Microbiology, 2017. 199(2): p. 277-301.

33. Bhagwat, A.A., et al., Osmoregulated periplasmic glucans of Salmonella enterica serovar Typhimurium are required for optimal virulence in mice. Microbiology-Sgm, 2009. 155: p. 229-237.

34. Bhate, M.P., et al., Signal Transduction in Histidine Kinases: Insights from New Structures. Structure, 2015. 23(6): p. 981-994.

35. Birck, C., et al., Conformational changes induced by phosphorylation of the FixJ receiver domain. Structure, 1999. 7(12): p. 1505-1515.

36. Bohin, J.P. and J.M. Lacroix, OSMOREGULATION IN THE PERIPLASM. Periplasm, ed. M. Ehrmann. 2007. 325-341.

37. Bondareva, O.S., et al., Burkholderia mallei genotyping based on different region analysis. Molecular Genetics Microbiology and Virology, 2016. 31(1): p. 40-44.

38. Bontemps-Gallo, S. and J.M. Lacroix, New insights into the biological role of the osmoregulated periplasmic glucans in pathogenic and symbiotic bacteria. Environmental Microbiology Reports, 2015. 7(5): p. 690-697.

39. Brennan, R.G. and B.W. Matthews, THE HELIX-TURN-HELIX DNA-BINDING MOTIF. Journal of Biological Chemistry, 1989. 264(4): p. 1903-1906.

40. Brzostek, K., A. Raczkowska, and A. Zasada, The osmotic regulator OmpR is involved in the response of Yersinia enterocolitica O : 9 to environmental stresses and survival within macrophages. Fems Microbiology Letters, 2003. 228(2): p. 265-271.

41. Buddhisa, S., et al., Programmed Death Ligand 1 on Burkholderia pseudomallei-Infected Human Polymorphonuclear Neutrophils Impairs T Cell Functions. Journal of Immunology, 2015. 194(9): p. 4413-4421.

42. Bullard, B., S.L. Lipski, and E.R. Lafontaine, Hag directly mediates the adherence of Moraxella catarrhalis to human middle ear cells. Infection and Immunity, 2005. 73(8): p. 5127-5136.

43. Burtnick, M.N., et al., Identification of the acid phosphatase (acpA) gene homologues in pathogenic and nonpathogenic Burkholderia spp. facilitates TnphoA mutagenesis. Microbiology-Uk, 2001. 147: p. 111-120.

44. Burtnick, M.N., et al., The Cluster 1 Type VI Secretion System Is a Major Virulence Determinant in Burkholderia pseudomallei. Infection and Immunity, 2011. 79(4): p. 1512-1525.

45. Burtnick, M.N., P.J. Brett, and D.E. Woods, Molecular and physical characterization of Burkholderia mallei O antigens. Journal of Bacteriology, 2002. 184(3): p. 849-852.

46. Cai, S.J. and M. Inouye, EnvZ-OmpR interaction and osmoregulation in Escherichia coli. Journal of Biological Chemistry, 2002. 277(27): p. 24155-24161.

47. Cameron, A.D.S. and C.J. Dorman, A Fundamental Regulatory Mechanism Operating through OmpR and DNA Topology Controls Expression of Salmonella Pathogenicity Islands SPI-1 and SPI-2. Plos Genetics, 2012. 8(3).

48. Campos, C.G., M.S. Byrd, and P.A. Cotter, Functional Characterization of Burkholderia pseudomallei Trimeric Autotransporters. Infection and Immunity, 2013. 81(8): p. 2788-2799.

49. Cao, L., et al., Vulnerabilities in Yersinia pestis caf Operon Are Unveiled by a Salmonella Vector. Plos One, 2012. 7(4).

50. Carr-Gregory B, W.D., Medical Aspects of Biological Warfare. Borden Institute, Office of the Surgeon General, AMEDD Center and School, 2007: p. 121-146.

51. Casadevall, A. and L.A. Pirofski, New concepts in antibody-mediated immunity. Infection and Immunity, 2004. 72(11): p. 6191-6196.

52. Castillo-Keller, M., P. Vuong, and R. Misra, Novel mechanism of Escherichia coli porin regulation. Journal of Bacteriology, 2006. 188(2): p. 576-586.

53. Chakraborty, S. and L.J. Kenney, A New Role of OmpR in Acid and Osmotic Stress in Salmonella and E-coli. Frontiers in Microbiology, 2018. 9.

54. Chakraborty, S., et al., Temperature and Mg2+ Sensing by a Novel PhoP-PhoQ Two-component System for Regulation of Virulence in Edwardsiella tarda. Journal of Biological Chemistry, 2010. 285(50): p. 38876-38888.

55. Chakraborty, S., et al., Non-canonical activation of OmpR drives acid and osmotic stress responses in single bacterial cells. Nature Communications, 2017. 8.

56. Champion, O.L., et al., Immunisation with proteins expressed during chronic murine melioidosis provides enhanced protection against disease. Vaccine, 2016. 34(14): p. 1665-1671.

57. Charkowski, A., et al., The Role of Secretion Systems and Small Molecules in Soft-Rot Enterobacteriaceae Pathogenicity, in Annual Review of Phytopathology, Vol 50, N.K. VanAlfen, J.E. Leach, and S. Lindow, Editors. 2012. p. 425-449.

58. Chen, J., Y. Zhao, and W. Feng, Selection, preparation and characterization of scFv against human lipocalin 6 by phage display technology. Protein Expression and Purification, 2020. 171.

59. Chen, Y.H., et al., Regulation of Type VI Secretion System during Burkholderia pseudomallei Infection. Infection and Immunity, 2011. 79(8): p. 3064-3073.

60. Chen, Z., Parainfluenza virus 5-vectored vaccines against human and animal infectious diseases. Reviews in Medical Virology, 2018. 28(2).

61. Chen, Z., et al., Efficacy of parainfluenza virus 5 (PIV5)-based tuberculosis vaccines in mice. Vaccine, 2015. 33(51): p. 7217-7224.

62. Chieng, S., R. Mohamed, and S. Nathan, Transcriptome analysis of Burkholderia pseudomallei T6SS identifies Hcp1 as a potential serodiagnostic marker. Microbial Pathogenesis, 2015. 79: p. 47-56.

63. Chikaev, A.N., et al., Selection of Peptide Mimics of HIV-1 Epitope Recognized by Neutralizing Antibody VRC01. Plos One, 2015. 10(3).

64. Clemmer, K.M. and P.N. Rather, Regulation of flhDC expression in Proteus mirabilis. Research in Microbiology, 2007. 158(3): p. 295-302.

65. Conway, B.A.D., V. Venu, and D.P. Speert, Biofilm formation and acyl homoserine lactone production in the Burkholderia cepacia complex. Journal of Bacteriology, 2002. 184(20): p. 5678-5685.

66. Costa, L.E., et al., Mimotope-Based Vaccines of Leishmania infantum Antigens and Their Protective Efficacy against Visceral Leishmaniasis. Plos One, 2014. 9(10).

67. Cullinane, M., et al., Stimulation of autophagy suppresses the intracellular survival of Burkholderia pseudomallei in mammalian cell lines. Autophagy, 2008. 4(6): p. 744-753.

68. David, J., R.E. Bell, and G.C. Clark, Mechanisms of Disease: Host-Pathogen Interactions between Burkholderia Species and Lung Epithelial Cells. Frontiers in Cellular and Infection Microbiology, 2015. 5.

69. Day, W.A. and A.T. Maurelli, BLACK HOLES AND ANTIVIRULENCE GENES: SELECTION FOR GENE LOSS AS PART OF THE EVOLUTION OF BACTERIAL PATHOGENS. Evolution of Microbial Pathogens, 2006: p. 109-122.

70. De Plano, L.M., et al., Innovative IgG Biomarkers Based on Phage Display Microbial Amyloid Mimotope for State and Stage Diagnosis in Alzheimer's Disease. Acs Chemical Neuroscience, 2020. 11(7): p. 1013-1026.

71. Dean, S.N., et al., Francisella novicida Two-Component System Response Regulator BfpR Modulates iglC Gene Expression, Antimicrobial Peptide Resistance, and Biofilm Production. Frontiers in Cellular and Infection Microbiology, 2020. 10.

72. Deitchman, S. and R. Sokas, Glanders in a military research microbiologist. New England Journal of Medicine, 2001. 345(22): p. 1644-1644.

73. DeMaria, T.F., D.M. Murwin, and E.R. Leake, Immunization with outer membrane protein P6 from nontypeable Haemophilus influenzae induces bactericidal antibody and affords protection in the chinchilla model of otitis media. Infection and Immunity, 1996. 64(12): p. 5187-5192.

74. Dennehy, R., et al., The Burkholderia cenocepacia peptidoglycan-associated lipoprotein is involved in epithelial cell attachment and elicitation of inflammation. Cellular Microbiology, 2017. 19(5).

75. DiGiandomenico, A. and B.R. Sellman, Antibacterial monoclonal antibodies: the next generation? Current Opinion in Microbiology, 2015. 27: p. 78-85.

76. Domenech, M., et al., Combination of Antibodies and Antibiotics as a Promising Strategy Against Multidrug-Resistant Pathogens of the Respiratory Tract. Frontiers in Immunology, 2018. 9.

77. Dorrell, N., et al., Construction and characterisation of a Yersinia enterocolitica O : 8 ompR mutant. Fems Microbiology Letters, 1998. 165(1): p. 145-151.

78. Dubuisson, J.F., et al., Tol-Pal proteins are critical cell envelope components of Erwinia chrysanthemi affecting cell morphology and virulence. Microbiology-Sgm, 2005. 151: p. 3337-3347.

79. Duche, D. and L. Houot, Similarities and Differences between Colicin and Filamentous Phage Uptake by Bacterial Cells. EcoSal Plus, 2019. 8(2).

80. Easton, A., et al., Combining Vaccination and Postexposure CpG Therapy Provides Optimal Protection Against Lethal Sepsis in a Biodefense Model of Human Melioidosis. Journal of Infectious Diseases, 2011. 204(4): p. 636-644.

81. Elschner, M.C. and C. Hansel, Glanders - the longest known horse disease. Tieraerztliche Umschau, 2016. 71(3): p. 58-64.

82. Espinosa, D., et al., Passive Transfer of Immune Sera Induced by a Zika Virus-Like Particle Vaccine Protects AG129 Mice Against Lethal Zika Virus Challenge. Ebiomedicine, 2018. 27: p. 61-70.

83. Fabret, C., V.A. Feher, and J.A. Hoch, Two-component signal transduction in Bacillus subtilis: How one organism sees its world. Journal of Bacteriology, 1999. 181(7): p. 1975-1983.

84. Felgner, P.L., et al., A Burkholderia pseudomallei protein microarray reveals serodiagnostic and cross-reactive antigens. Proceedings of the National Academy of Sciences of the United States of America, 2009. 106(32): p. 13499-13504.

85. Ferster, L.N. and V.Y. Kurilov, FEATURES OF THE INFECTIOUS PROCESS IN ANIMALS SUSCEPTIBLE OR RESISTANT TO GLANDERS. Arkhiv Patologii, 1982. 44(11): p. 24-30.

86. Flamez, C., et al., Phenotypic analysis of Yersinia pseudotuberculosis 32777 response regulator mutants: New insights into two-component system regulon plasticity in bacteria. International Journal of Medical Microbiology, 2008. 298(3-4): p. 193-207.

87. Fleuridor, R., A. Lees, and L.A. Pirofski, A cryptococcal capsular polysaccharide mimotope prolongs the survival of mice with Cryptococcus neoformans infection. Journal of Immunology, 2001. 166(2): p. 1087-1096.

88. Forst, S.A. and D.L. Roberts, SIGNAL-TRANSDUCTION BY THE ENVZ-OMPR PHOSPHOTRANSFER SYSTEM IN BACTERIA. Research in Microbiology, 1994. 145(5-6): p. 363-373.

89. Fortney, K.R., et al., Expression of peptidoglycan-associated lipoprotein is required for virulence in the human model of Haemophilus ducreyi infection. Infection and Immunity, 2000. 68(11): p. 6441-6448.

90. Foster-Waldl, E., et al., Isolation and structural analysis of peptide mimotopes for the disialoganglioside GD2, a neuroblastoma tumor antigen. Molecular Immunology, 2005. 42(3): p. 319-325.

91. French, C.T., et al., Dissection of the Burkholderia intracellular life cycle using a photothermal nanoblade. Proceedings of the National Academy of Sciences of the United States of America, 2011. 108(29): p. 12095-12100.

92. Fushan, A., et al., Genome-wide identification and mapping of variable sequences in the genomes of Burkholderia mallei and Burkholderia pseudomallei. Research in Microbiology, 2005. 156(2): p. 278-288.

93. Gajiwala, K.S. and S.K. Burley, Winged helix proteins. Current Opinion in Structural Biology, 2000. 10(1): p. 110-116.

94. Galperin, M.Y., Bacterial signal transduction network in a genomic perspective. Environmental Microbiology, 2004. 6(6): p. 552-567.

95. Galperin, M.Y., Structural classification of bacterial response regulators: Diversity of output domains and domain combinations. Journal of Bacteriology, 2006. 188(12): p. 4169-4182.

96. Galperin, M.Y. and M.J. Jedrzejas, Conserved core structure and active site residues in alkaline phosphatase superfamily enzymes. Proteins-Structure Function and Bioinformatics, 2001. 45(4): p. 318-324.

97. Galyov, E.E., P.J. Brett, and D. DeShazer, Molecular Insights into Burkholderia pseudomallei and Burkholderia mallei Pathogenesis, in Annual Review of Microbiology, Vol 64, 2010, S. Gottesman and C.S. Harwood, Editors. 2010. p. 495-517.

98. Gao, H., et al., Phenotypic and transcriptional analysis of the osmotic regulator OmpR in Yersinia pestis. Bmc Microbiology, 2011. 11.

99. Garcia-Garcia, A., et al., A novel approach to produce phage single domain antibody fragments for the detection of gluten in foods. Food Chemistry, 2020. 321.

100. Garcia-Quintanilla, F., et al., Production of a recombinant vaccine candidate against Burkholderia pseudomallei exploiting the bacterial N-glycosylation machinery. Frontiers in Microbiology, 2014. 5.

101. Gerken, H., et al., MzrA: a novel modulator of the EnvZ/OmpR two-component regulon. Molecular Microbiology, 2009. 72(6): p. 1408-1422.

102. Ginsburg, A.S. and K.P. Klugman, Vaccination to reduce antimicrobial resistance. Lancet Global Health, 2017. 5(12): p. E1176-E1177.

103. Girgis, H.S., et al., A comprehensive genetic characterization of bacterial motility. Plos Genetics, 2007. 3(9): p. 1644-1660.

104. Glaesmann, M., et al., Molecular quantification of the stress response protein OmpR under osmotic and acidic stress in E. coli. European Biophysics Journal with Biophysics Letters, 2019. 48: p. S204-S204.

105. Godlewska, R., et al., Peptidoglycan-associated lipoprotein (Pal) of Gram-negative bacteria: function, structure, role in pathogenesis and potential application in immunoprophylaxis. Fems Microbiology Letters, 2009. 298(1): p. 1-11.

106. Gong, L., et al., The Burkholderia pseudomallei Type III Secretion System and BopA Are Required for Evasion of LC3-Associated Phagocytosis. Plos One, 2011. 6(3).

107. Gooderham, W.J. and R.E.W. Hancock, Regulation of virulence and antibiotic resistance by two-component regulatory systems in Pseudomonas aeruginosa. Fems Microbiology Reviews, 2009. 33(2): p. 279-294.

108. Goracci, M., Y. Pignochino, and S. Marchio, Phage Display-Based Nanotechnology Applications in Cancer Immunotherapy. Molecules, 2020. 25(4).

109. Gourlay, L.J., et al., Exploiting the Burkholderia pseudomallei Acute Phase Antigen BPSL2765 for Structure-Based Epitope Discovery/Design in Structural Vaccinology. Chemistry & Biology, 2013. 20(9): p. 1147-1156.

110. Green, B.A., T. Quinndey, and G.W. Zlotnick, BIOLOGIC ACTIVITIES OF ANTIBODY TO A PEPTIDOGLYCAN-ASSOCIATED LIPOPROTEIN OF HAEMOPHILUS-INFLUENZAE AGAINST MULTIPLE CLINICAL ISOLATES OF HAEMOPHILUS-INFLUENZAE TYPE-B. Infection and Immunity, 1987. 55(12): p. 2878-2883.

111. Green, B.A., et al., EVALUATION OF MIXTURES OF PURIFIED HAEMOPHILUS-INFLUENZAE OUTER-MEMBRANE PROTEINS IN PROTECTION AGAINST CHALLENGE WITH NONTYPABLE HAEMOPHILUS-INFLUENZAE IN THE CHINCHILLA OTITIS-MEDIA MODEL. Infection and Immunity, 1993. 61(5): p. 1950-1957.

112. Gregory, A.E., et al., A gold nanoparticle-linked glycoconjugate vaccine against Burkholderia mallei. Nanomedicine-Nanotechnology Biology and Medicine, 2015. 11(2): p. 447-456.

113. Grijpstra, J., et al., Autotransporter secretion: varying on a theme. Research in Microbiology, 2013. 164(6): p. 562-582.

114. Groisman, E.A., Feedback Control of Two-Component Regulatory Systems, in Annual Review of Microbiology, Vol 70, S. Gottesman, Editor. 2016. p. 103-124.

115. Gueguen, E., et al., Expression of a Yersinia pseudotuberculosis Type VI Secretion System Is Responsive to Envelope Stresses through the OmpR Transcriptional Activator. Plos One, 2013. 8(6).

116. Guirado, E., et al., Passive serum therapy with polyclonal antibodies against Mycobacterium tuberculosis protects against post-chemotherapy relapse of tuberculosis infection in SCID mice. Microbes and Infection, 2006. 8(5): p. 1252-1259.

117. Gurung, S., et al., Phage display-identified PD-L1-binding peptides reinvigorate T-cell activity and inhibit tumor progression. Biomaterials, 2020. 247.

118. Gutierrez, M.G., T.L. Pfeffer, and J.M. Warawa, Type 3 Secretion System Cluster 3 Is a Critical Virulence Determinant for Lung-Specific Melioidosis. Plos Neglected Tropical Diseases, 2015. 9(1).

119. Hafner, C., et al., A mimotope-based anti-cancer vaccine against malignant melanoma. Journal of Investigative Dermatology, 2006. 126: p. 145-145.

120. Hall, M.N. and T.J. Silhavy, GENETIC-ANALYSIS OF THE OMPB LOCUS IN ESCHERICHIA-COLI K-12. Journal of Molecular Biology, 1981. 151(1): p. 1-15.

121. Hara, Y., R. Mohamed, and S. Nathan, Immunogenic Burkholderia pseudomallei Outer Membrane Proteins as Potential Candidate Vaccine Targets. Plos One, 2009. 4(8).

122. Harlocker, S.L., L. Bergstrom, and M. Inouye, TANDEM BINDING OF 6 OMPR PROTEINS TO THE OMPF UPSTREAM REGULATORY SEQUENCE OF ESCHERICHIA-COLI. Journal of Biological Chemistry, 1995. 270(45): p. 26849-26856.

123. Harrison-McMonagle, P., et al., Orientation of OmpR monomers within an OmpR : DNA complex determined by DNA affinity cleaving. Journal of Molecular Biology, 1999. 285(2): p. 555-566.

124. Hatcher, C.L., et al., Burkholderia mallei CLH001 Attenuated Vaccine Strain Is Immunogenic and Protects against Acute Respiratory Glanders. Infection and Immunity, 2016. 84(8): p. 2345-2354.

125. Hatcher, C.L., L.A. Muruato, and A.G. Torres, Recent Advances in Burkholderia mallei and B. pseudomallei Research. Current tropical medicine reports, 2015. 2(2): p. 62-69.

126. He, B., et al., Recovery of infectious SV5 from cloned DNA and expression of a foreign gene. Virology, 1997. 237(2): p. 249-260.

127. He, Y.W., et al., Co-regulation of Xanthomonas campestris virulence by quorum sensing and a novel two-component regulatory system RavS/RavR. Molecular Microbiology, 2009. 71(6): p. 1464-1476.

128. Whitmore A, Krishnaswami CS. An account of the discovery of a hitherto undescribed infective disease occurring among the population of Rangoon. Indian Meg. Gaz. 1912;47:262-267

129. Head, C.G., A. Tardy, and L.J. Kenney, Relative binding affinities of OmpR and OmpR-phosphate at the ompF and ompC regulatory sites. Journal of Molecular Biology, 1998. 281(5): p. 857-870.

130. Healey, G.D., et al., Humoral and cell-mediated adaptive immune responses are required for protection against Burkholderia pseudomallei challenge and bacterial clearance postinfection. Infection and Immunity, 2005. 73(9): p. 5945-5951.

131. Henderson, I.R. and M. Desvaux, The type V secretion pathway: a premium source of virulence factors? Drug Discovery Today, 2004. 9(5): p. 241-241.

132. Henderson, I.R., et al., Type V protein secretion pathway: the autotransporter story. Microbiology and Molecular Biology Reviews, 2004. 68(4): p. 692-+.

133. Holden, M.T.G., et al., Genornic plasticity of the causative agent of melioidosis, Burkholderia pseudomallei. Proceedings of the National Academy of Sciences of the United States of America, 2004. 101(39): p. 14240-14245.

134. Holst, J., et al., Properties and clinical performance of vaccines containing outer membrane vesicles from Neisseria meningitidis. Vaccine, 2009. 27: p. B3-B12.

135. Holst, J., et al., Vaccines against meningococcal serogroup B disease containing outer membrane vesicles (OMV) Lessons from past programs and implications for the future. Human Vaccines & Immunotherapeutics, 2013. 9(6): p. 1241-1253.

136. Hopf, V., et al., BPSS1504, a Cluster 1 Type VI Secretion Gene, Is Involved in Intracellular Survival and Virulence of Burkholderia pseudomallei. Infection and Immunity, 2014. 82(5): p. 2006-2015.

137. Hotomi, M., et al., Antibody responses to the outer membrane protein P6 of non-typeable Haemophilus influenzae and pneumococcal capsular polysaccharides in otitis-prone children. Acta Oto-Laryngologica, 1999. 119(6): p. 703-707.

138. Hsieh, P.-F., et al., Klebsiella pneumoniae Peptidoglycan-Associated Lipoprotein and Murein Lipoprotein Contribute to Serum Resistance, Antiphagocytosis, and Proinflammatory Cytokine Stimulation. Journal of Infectious Diseases, 2013. 208(10): p. 1580-1589.

139. Hu, Y.B., et al., OmpR positively regulates urease expression to enhance acid survival of Yersinia pseudotuberculosis. Microbiology-Sgm, 2009. 155: p. 2522-2531.

140. Huang, K.J. and M.M. Igo, Identification of the bases in the ompF regulatory region, which interact with the transcription factor OmpR. Journal of Molecular Biology, 1996. 262(5): p. 615-628.

141. Istvan, H., et al., Monoclonal antibody proteomics: Use of antibody mimotope displaying phages and the relevant synthetic peptides for mAb scouting. Immunology Letters, 2014. 160(2): p. 172-177.

142. Jelesijevic, T., et al., Use of the Common Marmoset to Study Burkholderia mallei Infection. Plos One, 2015. 10(4).

143. Jiang, S.M., et al., Regulation of virulence by a two-component system in group B Streptococcus. Journal of Bacteriology, 2005. 187(3): p. 1105-1113.

144. Joao, C., et al., Passive Serum Therapy to Immunomodulation by IVIG: A Fascinating Journey of Antibodies. Journal of Immunology, 2018. 200(6): p. 1957-1963.

145. Kager, L.M., et al., Deficiency of protease-activated receptor-1 limits bacterial dissemination during severe Gram-negative sepsis (melioidosis). Microbes and Infection, 2014. 16(2): p. 171-174.

146. Kang, W.T., et al., Functional Characterizations of Effector Protein BipC, a Type III Secretion System Protein, in Burkholderia pseudomallei Pathogenesis. Journal of Infectious Diseases, 2015. 211(5): p. 827-834.

147. Kenney, L.J., Structure/function relationships in OmpR and other winged-helix transcription factors. Current Opinion in Microbiology, 2002. 5(2): p. 135-141.

148. Kettle, A.N.B. and U. Wernery, Glanders and the risk for its introduction through the international movement of horses. Equine Veterinary Journal, 2016. 48(5): p. 654-658.

149. Khakhum, N., et al., Burkholderia pseudomallei Delta tonB Delta hcp1 Live Attenuated Vaccine Strain Elicits Full Protective Immunity against Aerosolized Melioidosis Infection. Msphere, 2019. 4(1).

150. Khakhum, N., et al., Evaluation of Burkholderia mallei Delta tonB Delta hcp1 (CLH001) as a live attenuated vaccine in murine models of glanders and melioidosis. Plos Neglected Tropical Diseases, 2019. 13(7).

151. Khan, I., et al., Glanders in Animals: A Review on Epidemiology, Clinical Presentation, Diagnosis and Countermeasures. Transboundary and Emerging Diseases, 2013. 60(3): p. 204-221.

152. Kodama, H., et al., Cellular immune response of adenoidal and tonsillar lymphocytes to the P6 outer membrane protein of non-typeable Haemophilus influenzae and its relation to otitis media. Acta Oto-Laryngologica, 1999. 119(3): p. 377-383.

153. Koretke, K.K., et al., Evolution of two-component signal transduction. Molecular Biology and Evolution, 2000. 17(12): p. 1956-1970.

154. Kyd, J.M., M.L. Dunkley, and A.W. Cripps, ENHANCED RESPIRATORY CLEARANCE OF NONTYPABLE HAEMOPHILUS-INFLUENZAE FOLLOWING MUCOSAL IMMUNIZATION WITH P6 IN A RAT MODEL. Infection and Immunity, 1995. 63(8): p. 2931-2940.

155. Lafontaine, E.R., et al., Characterization of an autotransporter adhesin protein shared by Burkholderia mallei and Burkholderia pseudomallei. Bmc Microbiology, 2014. 14.

156. Lafontaine, E.R., et al., Use of a Safe, Reproducible, and Rapid Aerosol Delivery Method to Study Infection by Burkholderia pseudomallei and Burkholderia mallei in Mice. Plos One, 2013. 8(10).

157. Lafontaine ER, C.Z., Huertas-Diaz MC, Dyke JS, Jelesijevic T, Michel F, et al., The autotransporter protein BatA is a protective antigen against lethal aerosol infection with Burkholderia mallei and Burkholderia pseudomallei. Vaccine: X, 2019.

158. Lan, C.Y. and M.M. Igo, Differential expression of the OmpF and OmpC porin proteins in Escherichia coli K-12 depends upon the level of active OmpR. Journal of Bacteriology, 1998. 180(1): p. 171-174.

159. Larsen, J.C. and N.H. Johnson, Pathogenesis of Burkholderia pseudomallei and Burkholderia mallei. Military Medicine, 2009. 174(6): p. 647-651.

160. Laub, M.T. and M. Goulian, Specificity in two-component signal transduction pathways. Annual Review of Genetics, 2007. 41: p. 121-145.

161. Laws, T.R., G.C. Clark, and R.V. D'Elia, Immune profiling of the progression of a BALB/c mouse aerosol infection by Burkholderia pseudomallei and the therapeutic implications of targeting HMGB1. International Journal of Infectious Diseases, 2015. 40: p. 1-8.

162. Lee, C. and C. Park, Mutations upregulating the flhDC operon of Escherichia coli K-12. Journal of Microbiology, 2013. 51(1): p. 140-144.

163. Legutki, J.B., et al., Analysis of peptide mimotopes of Burkholderia pseudomallei exopolysaccharide. Vaccine, 2007. 25(45): p. 7796-7805.

164. Lei, L., et al., DNA vaccine encoding OmpA and Pal from Acinetobacter baumannii efficiently protects mice against pulmonary infection. Molecular Biology Reports, 2019. 46(5): p. 5397-5408.

165. Li, M., et al., Development of a mimotope-based vaccine against CD20 antigen. Protein and Peptide Letters, 2007. 14(6): p. 610-614.

166. Lim, A., et al., Molecular and immunological characterization of OprL, the 18 kDa outer-membrane peptidoglycan-associated lipoprotein (PAL) of Pseudomonas aeruginosa. Microbiology-Sgm, 1997. 143: p. 1709-1716.

167. Lim, Y.T., et al., Extended Loop Region of Hcp1 is Critical for the Assembly and Function of Type VI Secretion System in Burkholderia pseudomallei. Scientific Reports, 2015. 5.

168. Limmathurotsakul, D., et al., Predicted global distribution of Burkholderia pseudomallei and burden of melioidosis. Nature Microbiology, 2016. 1(1).

169. Lipsitz, R., et al., Workshop on treatment of and postexposure prophylaxis for Burkholderia pseudomallei and B. mallei Infection, 2010. Emerging infectious diseases, 2012. 18(12): p. e2-e2.

170. Lopez-Goni, I., et al., Regulation of Brucella virulence by the two-component system BvrR/BvrS. Veterinary Microbiology, 2002. 90(1-4): p. 329-339.

171. Losada, L., et al., Continuing Evolution of Burkholderia mallei Through Genome Reduction and Large-Scale Rearrangements. Genome Biology and Evolution, 2010. 2: p. 102-116.

172. Ma, C.X., et al., Screening of a specific peptide binding to esophageal squamous carcinoma cells from phage displayed peptide library. Molecular and Cellular Probes, 2015. 29(3): p. 182-189.

173. Majerczyk, C., et al., Virulence of Burkholderia mallei Quorum-Sensing Mutants. Infection and Immunity, 2013. 81(5): p. 1471-1478.

174. MartinezHackert, E. and A.M. Stock, Structural relationships in the OmpR family of winged-helix transcription factors. Journal of Molecular Biology, 1997. 269(3): p. 301-312.

175. MartinezHackert, E. and A.M. Stock, The DNA-binding domain of OmpR: Crystal structure of a winged helix transcription factor. Structure, 1997. 5(1): p. 109-124.

176. Massey, S., et al., Comparative Burkholderia pseudomallei natural history virulence studies using an aerosol murine model of infection. Scientific Reports, 2014. 4.

177. Mattison, K., et al., A phosphorylation site mutant of OmpR reveals different binding conformations at ompF and ompC. Journal of Molecular Biology, 2002. 315(4): p. 497-511.

178. Maurelli, A.T., Black holes, antivirulence genes, and gene inactivation in the evolution of bacterial pathogens. Fems Microbiology Letters, 2007. 267(1): p. 1-8.

179. Merry, C.R., et al., Characterization of a Novel Two-Component System in Burkholderia cenocepacia. Current Microbiology, 2015. 70(4): p. 556-561.

180. Michel, L.V., et al., Dual orientation of the Outer membrane lipoprotein Pal in Escherichia coli. Microbiology-Sgm, 2015. 161: p. 1251-1259.

181. Mobarez, A.M., et al., Induction of protective immunity by recombinant peptidoglycan associated lipoprotein (rPAL) protein of Legionella pneumophila in a BALB/c mouse model. Microbial Pathogenesis, 2019. 128: p. 100-105.

182. Monastyrskaya, G., et al., Genome-wide comparison reveals great inter- and intraspecies variability in B pseudomallei and B mallei pathogens. Research in Microbiology, 2004. 155(9): p. 781-793.

183. Morel-Deville, F., F. Fauvel, and P. Morel, Two-component signal-transducing systems involved in stress responses and vancomycin susceptibility in Lactobacillus sakei. Microbiology-Sgm, 1998. 144: p. 2873-2883.

184. Motley, M.P. and B.C. Fries, A New Take on an Old Remedy: Generating Antibodies against Multidrug-Resistant Gram-Negative Bacteria in a Postantibiotic World. Msphere, 2017. 2(5).

185. Mott, T.M., et al., Characterization of the Burkholderia mallei tonB Mutant and Its Potential as a Backbone Strain for Vaccine Development. Plos Neglected Tropical Diseases, 2015. 9(6).

186. Moustafa, D.A., et al., Recombinant Salmonella Expressing Burkholderia mallei LPS O Antigen Provides Protection in a Murine Model of Melioidosis and Glanders. Plos One, 2015. 10(7).

187. Muangsombut, V., et al., Inactivation of Burkholderia pseudomallei bsaQ results in decreased invasion efficiency and delayed escape of bacteria from endocytic vesicles. Archives of Microbiology, 2008. 190(6): p. 623-631.

188. Muller, C.M., et al., Role of RelA and SpoT in Burkholderia pseudomallei Virulence and Immunity. Infection and Immunity, 2012. 80(9): p. 3247-3255.

189. Mangalea, M.R., B.A. Plumley, and B.R. Borlee, Nitrate Sensing and Metabolism Inhibit Biofilm Formation in the Opportunistic Pathogen Burkholderia pseudomallei by Reducing the Intracellular Concentration of c-di-GMP. Frontiers in Microbiology, 2017. 8.

190. Murphy, T.F., C. Kirkham, and A.J. Lesse, Construction of a mutant and characterization of the role of the vaccine antigen P6 in outer membrane integrity of nontypeable Haemophilus influenzae. Infection and Immunity, 2006. 74(9): p. 5169-5176.

191. Mussi, M.A., et al., The Opportunistic Human Pathogen Acinetobacter baumannii Senses and Responds to Light. Journal of Bacteriology, 2010. 192(24): p. 6336-6345.

192. Nelson, M., et al., Characterization of lesion formation in marmosets following inhalational challenge with different strains of Burkholderia pseudomallei. International Journal of Experimental Pathology, 2015. 96(6): p. 414-426.

193. Nelson, M., et al., Evaluation of lipopolysaccharide and capsular polysaccharide as subunit vaccines against experimental melioidosis. Journal of Medical Microbiology, 2004. 53(12): p. 1177-1182.

194. Nierman, W.C., et al., Structural flexibility in the Burkholderia mallei genome. Proceedings of the National Academy of Sciences of the United States of America, 2004. 101(39): p. 14246-14251.

195. Nieves, W., et al., A naturally derived outer-membrane vesicle vaccine protects against lethal pulmonary Burkholderia pseudomallei infection. Vaccine, 2011. 29(46): p. 8381-8389.

196. Nieves, W., et al., A Burkholderia pseudomallei Outer Membrane Vesicle Vaccine Provides Protection against Lethal Sepsis. Clinical and Vaccine Immunology, 2014. 21(5): p. 747-754.

197. Norris, M.H., et al., Outer Membrane Vesicle Vaccines from Biosafe Surrogates Prevent Acute Lethal Glanders in Mice. Vaccines, 2018. 6(1).

198. Norris, M.H., et al., An avirulent Burkholderia pseudomallei Delta purM strain with atypical type B LPS: expansion of the toolkit for biosafe studies of melioidosis. Bmc Microbiology, 2017. 17: p. 1-14.

199. Norris, M.H., et al., The Burkholderia pseudomallei Delta asd Mutant Exhibits Attenuated Intracellular Infectivity and Imparts Protection against Acute Inhalation Melioidosis in Mice. Infection and Immunity, 2011. 79(10): p. 4010-4018.

200. Ooi, W.F., et al., The Condition-Dependent Transcriptional Landscape of Burkholderia pseudomallei. Plos Genetics, 2013. 9(9).

201. Pasqualini, R. and E. Ruoslahti, Organ targeting in vivo using phage display peptide libraries. Nature, 1996. 380(6572): p. 364-366.

202. Patel, N., et al., Development of vaccines against Burkholderia pseudomallei. Frontiers in Microbiology, 2011. 2.

203. Pilatz, S., et al., Identification of Burkholderia pseudomallei genes required for the intracellular life cycle and in vivo virulence. Infection and Immunity, 2006. 74(6): p. 3576-3586.

204. Ploss, M., et al., Selection of peptides binding to metallic borides by screening M13 phage display libraries. Bmc Biotechnology, 2014. 14.

205. Poirel, L., A. Jayol, and P. Nordmann, Polymyxins: Antibacterial Activity, Susceptibility Testing, and Resistance Mechanisms Encoded by Plasmids or Chromosomes. Clinical Microbiology Reviews, 2017. 30(2): p. 557-596.

206. Pradenas, G.A., B.N. Ross, and A.G. Torres, Burkholderia cepacia Complex Vaccines: Where Do We Go from here? Vaccines, 2016. 4(2).

207. Pragman, A.A., et al., Characterization of virulence factor regulation by SrrAB, a two-component system in Staphylococcus aureus. Journal of Bacteriology, 2004. 186(8): p. 2430-2438.

208. Propst, K.L., et al., A Burkholderia pseudomallei Delta purM Mutant Is Avirulent in Immunocompetent and Immunodeficient Animals: Candidate Strain for Exclusion from Select-Agent Lists. Infection and Immunity, 2010. 78(7): p. 3136-3143.

209. Pruss, B.M., Involvement of Two-Component Signaling on Bacterial Motility and Biofilm Development. Journal of Bacteriology, 2017. 199(18).

210. Pumirat, P., et al., Analysis of the Prevalence, Secretion and Function of a Cell Cycle-Inhibiting Factor in the Melioidosis Pathogen Burkholderia pseudomallei. Plos One, 2014. 9(5).

211. Pumirat, P., et al., Global transcriptional profiling of Burkholderia pseudomallei under salt stress reveals differential effects on the Bsa type III secretion system. Bmc Microbiology, 2010. 10.

212. Quinn, H.J., A.D.S. Cameron, and C.J. Dorman, Bacterial Regulon Evolution: Distinct Responses and Roles for the Identical OmpR Proteins of Salmonella Typhimurium and Escherichia coli in the Acid Stress Response. Plos Genetics, 2014. 10(3).

213. Raczkowska, A., et al., OmpR controls Yersinia enterocolitica motility by positive regulation of flhDC expression. Antonie Van Leeuwenhoek International Journal of General and Molecular Microbiology, 2011. 99(2): p. 381-394.

214. Reboul, A., et al., Yersinia pestis Requires the 2-Component Regulatory System OmpR-EnvZ to Resist Innate Immunity During the Early and Late Stages of Plague. Journal of Infectious Diseases, 2014. 210(9): p. 1367-1375.

215. Reed, L.J. and H. Muench, A simple method of estimating fifty per cent endpoints. Amer Jour Hyg, 1938. 27((3)): p. 493-497.

216. Rhodes, K.A. and H.P. Schweizer, Antibiotic resistance in Burkholderia species. Drug Resistance Updates, 2016. 28: p. 82-90.

217. Rolhion, N., F.A. Carvalho, and A. Darfeuille-Michaud, OmpC and the sigma(E) regulatory pathway are involved in adhesion and invasion of the Crohn's disease-associated Escherichia coli strain LF82. Molecular Microbiology, 2007. 63(6): p. 1684-1700.

218. Rychlik, I. and P.A. Barrow, Salmonella stress management and its relevance to behaviour during intestinal colonisation and infection. Fems Microbiology Reviews, 2005. 29(5): p. 1021-1040.

219. Sabirov, A., et al., Intranasal immunization enhances clearance of nontypeable Haemophilus influenzae and reduces stimulation of tumor necrosis factor alpha production in the murine model of otitis media. Infection and Immunity, 2001. 69(5): p. 2964-2971.

220. Saito, M., et al., Identification of anti-CD98 antibody mimotopes for inducing antibodies with antitumor activity by mimotope immunization. Cancer Science, 2014. 105(4): p. 396-401.

221. Samanta, P., et al., A Point Mutation in carR Is Involved in the Emergence of Polymyxin B-Sensitive Vibrio cholerae O1 El Tor Biotype by Influencing Gene Transcription. Infection and Immunity, 2020. 88(5).

222. Sambrook, J., et al., Molecular cloning: A laboratory manual. Molecular cloning: A laboratory manual. 2001.

223. Samy, R.P., et al., Melioidosis: Clinical impact and public health threat in the tropics. Plos Neglected Tropical Diseases, 2017. 11(5).

224. Sarovich, D.S., et al., Variable Virulence Factors in Burkholderia pseudomallei (Melioidosis) Associated with Human Disease. Plos One, 2014. 9(3).

225. Schaefers, M.M., Regulation of Virulence by Two-component Systems in Pathogenic *Burkholderia*. Infection and Immunity, 2020: p. IAI.00927-19.

226. Schell, M.A., L. Lipscomb, and D. DeShazer, Comparative genomics and an insect model rapidly identify novel virulence genes of Burkholderia mallei. Journal of Bacteriology, 2008. 190(7): p. 2306-2313.

227. Schell, M.A., et al., Type VI secretion is a major virulence determinant in Burkholderia mallei. Molecular Microbiology, 2007. 64(6): p. 1466-1485.

228. Schell, M.A., P. Zhao, and L. Wells, Outer Membrane Proteome of Burkholderia pseudomallei and Burkholderia mallei From Diverse Growth Conditions. Journal of Proteome Research, 2011. 10(5): p. 2417-2424.

229. Schwan, W.R., Survival of uropathogenic Escherichia coli in the murine urinary tract is dependent on OmpR. Microbiology-Sgm, 2009. 155: p. 1832-1839.

230. Scott, A.E., et al., Burkholderia pseudomallei Capsular Polysaccharide Conjugates Provide Protection against Acute Melioidosis. Infection and Immunity, 2014. 82(8): p. 3206-3213.

231. Sharrer, G.T., THE GREAT GLANDERS EPIZOOTIC, 1861-1866 - A CIVIL-WAR LEGACY. Agricultural History, 1995. 69(1): p. 79-101.

232. Silva, E.B., et al., Correlates of Immune Protection following Cutaneous Immunization with an Attenuated Burkholderia pseudomallei Vaccine. Infection and Immunity, 2013. 81(12): p. 4626-4634.

233. Sim, S.H., et al., The Core and Accessory Genomes of Burkholderia pseudomallei: Implications for Human Melioidosis. Plos Pathogens, 2008. 4(10).

234. Simon, R., U. Priefer, and A. Puhler, A BROAD HOST RANGE MOBILIZATION SYSTEM FOR INVIVO GENETIC-ENGINEERING - TRANSPOSON MUTAGENESIS IN GRAM-NEGATIVE BACTERIA. Bio-Technology, 1983. 1(9): p. 784-791.

235. Siryaporn, A. and M. Goulian, Cross-talk suppression between the CpxA-CpxR and EnvZ-OmpR two-component systems in E-coli. Molecular Microbiology, 2008. 70(2): p. 494-506.

236. Sitthidet, C., et al., Identification of Motifs of Burkholderia pseudomallei BimA Required for Intracellular Motility, Actin Binding, and Actin Polymerization. Journal of Bacteriology, 2011. 193(8): p. 1901-1910.

237. Sitthidet, C., et al., Actin-Based Motility of Burkholderia thailandensis Requires a Central Acidic Domain of BimA That Recruits and Activates the Cellular Arp2/3 Complex. Journal of Bacteriology, 2010. 192(19): p. 5249-5252.

238. Skorupski, K. and R.K. Taylor, Positive selection vectors for allelic exchange. Gene, 1996. 169(1): p. 47-52.

239. Smith, G.P. and V.A. Petrenko, Phage display. Chemical Reviews, 1997. 97(2): p. 391-410.

240. Song, H., et al., The Early Stage of Bacterial Genome-Reductive Evolution in the Host. Plos Pathogens, 2010. 6(5).

241. Spector, M.P. and W.J. Kenyon, Resistance and survival strategies of Salmonella enterica to environmental stresses. Food Research International, 2012. 45(2): p. 455-481.

242. Srilunchang, T., et al., CONSTRUCTION AND CHARACTERIZATION OF AN UNMARKED AROC DELETION MUTANT OF BURKHOLDERIA PSEUDOMALLEI STRAIN A2. Southeast Asian Journal of Tropical Medicine and Public Health, 2009. 40(1): p. 123-130.

243. Steenackers, H., et al., Salmonella biofilms: An overview on occurrence, structure, regulation and eradication. Food Research International, 2012. 45(2): p. 502-531.

244. Stevens, J.M., et al., Actin-binding proteins from Burkholderia mallei and Burkholderia thailandensis can functionally compensate for the actin-based motility defect of a Burkholderia pseudomallei bimA mutant. Journal of Bacteriology, 2005. 187(22): p. 7857-7862.

245. Stevens, M.P., et al., A Burkholderia pseudomallei type III secreted protein, BopE, facilitates bacterial invasion of epithelial cells and exhibits guanine nucleotide exchange factor activity. Journal of Bacteriology, 2003. 185(16): p. 4992-4996.

246. Stevens, M.P., et al., Identification of a bacterial factor required for actin-based motility of Burkholderia pseudomallei. Molecular Microbiology, 2005. 56(1): p. 40-53.

247. Steward, M.W., The development of a mimotope-based synthetic peptide vaccine against respiratory syncytial virus. Biologicals, 2001. 29(3-4): p. 215-219.

248. Stock, A.M., V.L. Robinson, and P.N. Goudreau, Two-component signal transduction. Annual Review of Biochemistry, 2000. 69: p. 183-215.

249. Stone, J.K., et al., Melioidosis: molecular aspects of pathogenesis. Expert Review of Anti-Infective Therapy, 2014. 12(12): p. 1487-1499.

250. Stoyanova, M., et al., Biodiversity and incidence of Burkholderia species. Biotechnology & Biotechnological Equipment, 2007. 21(3): p. 306-310.

251. Su, Y.-C., et al., A genome level survey of Burkholderia pseudomallei immunome expressed during human infection. Microbes and Infection, 2008. 10(12-13): p. 1335-1345.

252. Sun, Y. and M.X.D. O'Riordan, Branched-Chain Fatty Acids Promote Listeria monocytogenes Intracellular Infection and Virulence. Infection and Immunity, 2010. 78(11): p. 4667-4673.

253. Suparak, S., et al., Multinucleated giants cell formation and apoptosis in infected host cells is mediated by Burkholderia pseudomallei type III secretion protein BipB. Journal of Bacteriology, 2005. 187(18): p. 6556-6560.

254. Sutthirattana, S., et al., INCIDENCE AND CASE FATALITY RATES OF BURKHOLDERIA PSEUDOMALLEI BACTEREMIA IN EASTERN AND NORTHEASTERN THAILAND. American Journal of Tropical Medicine and Hygiene, 2008. 79(6): p. 124-124.

255. Suwannasaen, D., et al., Human Immune Responses to Burkholderia pseudomallei Characterized by Protein Microarray Analysis. Journal of Infectious Diseases, 2011. 203(7): p. 1002-1011.

256. Sverzhinsky, A., et al., Membrane Protein Complex ExbB(4)-ExbD(1)-TonB(1) from Escherichia coli Demonstrates Conformational Plasticity. Journal of Bacteriology, 2015. 197(11): p. 1873-1885.

257. Teh, B.E., et al., Type three secretion system-mediated escape of Burkholderia pseudomallei into the host cytosol is critical for the activation of NF kappa B. Bmc Microbiology, 2014. 14.

258. Tipton, K.A. and P.N. Rather, An ompR-envZ Two-Component System Ortholog Regulates Phase Variation, Osmotic Tolerance, Motility, and Virulence in Acinetobacter baumannii Strain AB5075. Journal of Bacteriology, 2017. 199(3).

259. Toesca, I.J., C.T. French, and J.F. Miller, The Type VI Secretion System Spike Protein VgrG5 Mediates Membrane Fusion during Intercellular Spread by Pseudomallei Group Burkholderia Species. Infection and Immunity, 2014. 82(4): p. 1436-1444.

260. Torres, A.G., et al., Protection of non-human primates against glanders with a gold nanoparticle glycoconjugate vaccine. Vaccine, 2015. 33(5): p. 686-692.

261. Urich, R.L. and D. DeShazer, Type III secretion: a virulence factor delivery system essential for the pathogenicity of Burkholderia mallei. Infection and Immunity, 2004. 72(2): p. 1150-1154.

262. Van Zandt, K.E., M.T. Greer, and H.C. Gelhaus, Glanders: an overview of infection in humans. Orphanet Journal of Rare Diseases, 2013. 8.

263. Vander Broek, C.W., et al., Quantitative Proteomic Analysis of Burkholderia pseudomallei Bsa Type III Secretion System Effectors Using Hypersecreting Mutants. Molecular & Cellular Proteomics, 2015. 14(4): p. 905-916.

264. Varga, J.J., et al., Distinct human antibody response to the biological warfare agent Burkholderia mallei. Virulence, 2012. 3(6): p. 510-514.

265. Vidal, O., et al., Isolation of an Escherichia coli K-12 mutant strain able to form biofilms on inert surfaces: Involvement of a new ompR allele that increases curli expression. Journal of Bacteriology, 1998. 180(9): p. 2442-2449.

266. Vipond, C., et al., Proteomic analysis of a meningococcal outer membrane vesicle vaccine prepared from the group B strain NZ98/254. Proteomics, 2006. 6(11): p. 3400-3413.

267. Wang, H., et al., Characterization and utility of phages bearing peptides with affinity to porcine reproductive and respiratory syndrome virus nsp7 protein. Journal of Virological Methods, 2015. 222: p. 231-241.

268. Wang, H.J., et al., Identification and immunogenicity of an immunodominant mimotope of Avibacterium paragallinarum from a phage display peptide library. Veterinary Microbiology, 2007. 119(2-4): p. 231-239.

269. Wang, L.F. and M. Yu, Epitope identification and discovery using phage display libraries: Applications in vaccine development and diagnostics. Current Drug Targets, 2004. 5(1): p. 1-15.

270. Warawa, J. and D.E. Woods, Type III secretion system cluster 3 is required for maximal virulence of Burkholderia pseudomallei in a hamster infection model. Fems Microbiology Letters, 2005. 242(1): p. 101-108.

271. Warawa, J.M. and F.C. Gherardini, Modeling of Acute Respiratory Melioidosis and Glanders. National Institute of Allergy and Infectious Diseases, Nih, Vol 3: Intramural Research, ed. V. St Georgiev and K.C. Zoon. 2010. 117-120.

272. Welkos, S.L., et al., Characterization of Burkholderia pseudomallei Strains Using a Murine Intraperitoneal Infection Model and In Vitro Macrophage Assays. Plos One, 2015. 10(4).

273. West, A.H. and A.M. Stock, Histidine kinases and response regulator proteins in two-component signaling systems. Trends in Biochemical Sciences, 2001. 26(6): p. 369-376.

274. Wheelis, M., First shots fired in biological warfare. Nature, 1998. 395(6699): p. 213-213.

275. Whitlock, G.C., et al., Protective response to subunit vaccination against intranasal Burkholderia mallei and B. pseudomallei challenge, in 3rd Vaccine Global Congress, Singapore 2009, R. Spier, Editor. 2010. p. 73-77.

276. Wiersinga, W.J., et al., Melioidosis: insights into the pathogenicity of Burkholderia pseudomallei. Nature Reviews Microbiology, 2006. 4(4): p. 272-282.

277. Wiersinga, W.J., et al., Melioidosis. Nature Reviews Disease Primers, 2018. 4.

278. Wietzorrek, A. and M. Bibb, A novel family of proteins that regulates antibiotic production in streptomycetes appears to contain an OmpR-like DNA-binding fold. Molecular Microbiology, 1997. 25(6): p. 1181-1184.

279. Willcocks, S.J., et al., Intracellular replication of the well-armed pathogen Burkholderia pseudomallei. Current Opinion in Microbiology, 2016. 29: p. 94-103.

280. Wu, R.P., et al., A novel neutralizing antibody against diverse clades of H5N1 influenza virus and its mutants capable of airborne transmission. Antiviral Research, 2014. 106: p. 13-23.

281. Yamanaka, N. and H. Faden, ANTIBODY-RESPONSE TO OUTER-MEMBRANE PROTEIN OF NONTYPABLE HAEMOPHILUS-INFLUENZAE IN OTITIS-PRONE CHILDREN. Journal of Pediatrics, 1993. 122(2): p. 212-218.

282. Yang, H., et al., Detection of Mycobacterium tuberculosis based on H37Rv binding peptides using surface functionalized magnetic microspheres coupled with quantum dots - a nano detection method for Mycobacterium tuberculosis. International Journal of Nanomedicine, 2015. 10: p. 77-88.

283. Yang, X., et al., Flagella Overexpression Attenuates Salmonella Pathogenesis. Plos One, 2012. 7(10).

284. Yang, Y.P., et al., Effect of lipid modification on the physicochemical, structural, antigenic and immunoprotective properties of Haemophilus influenzae outer membrane protein P6. Vaccine, 1997. 15(9): p. 976-987.

285. Yokota, P.K.O., et al., Impact of Appropriate Antimicrobial Therapy for Patients with Severe Sepsis and Septic Shock - A Quality Improvement Study. Plos One, 2014. 9(11).

286. Yoshida, T., S.J. Cai, and M. Inouye, Interaction of EnvZ, a sensory histidine kinase, with phosphorylated OmpR, the cognate response regulator. Molecular Microbiology, 2002. 46(5): p. 1283-1294.

287. Yoshida, T., et al., Transcription regulation of ompF and ompC by a single transcription factor, OmpR. Journal of Biological Chemistry, 2006. 281(25): p. 17114-17123.

288. Yu, P.X., et al., Phage-Displayed Peptide of Keratinocyte Growth Factor and Its Biological Effects on Epidermal Cells. International Journal of Peptide Research and Therapeutics, 2020. 26(2): p. 661-666.

289. Yuan, Q.P., et al., Identification of mimotope peptides which bind to the mycotoxin deoxynivalenol-specific monoclonal antibody. Applied and Environmental Microbiology, 1999. 65(8): p. 3279-3286.

290. Zauner, S., Equine epidemics of the horses of the bavarian army between 1880 and 1920 based on files of the Munich War Archive. Pferdeheilkunde, 2010. 26(5): p. 712-720.

291. Zhang, H.L., Z.J. Zhong, and L.A. Pirofski, Peptide epitopes recognized by a human anti-cryptococcal glucuronoxylomannan antibody. Infection and Immunity, 1997. 65(4): p. 1158-1164.

292. Zhang, L.M., et al., Production of mouse monoclonal antibody against Streptococcus dysgalactiae GapC protein and mapping its conserved B-cell epitope. Research in Veterinary Science, 2015. 98: p. 39-41.

293. Zhang, M.M., et al., Comparative transcriptome and phenotype analysis revealed the role and mechanism of ompR in the virulence of fish pathogenic Aeromonas hydrophila. Microbiologyopen.

294. Zhao, Z.P., et al., A response regulator of the OmpR family is part of the regulatory network controlling the oxidative stress response of Rhodobacter sphaeroides. Environmental Microbiology Reports, 2019. 11(2): p. 118-128.

295. Zimmerman, S.M., et al., Antibodies against In Vivo-Expressed Antigens Are Sufficient To Protect against Lethal Aerosol Infection with Burkholderia mallei and Burkholderia pseudomallei. Infection and Immunity, 2017. 85(8).

296. Zimmerman, S.M., et al., The Autotransporter BpaB Contributes to the Virulence of Burkholderia mallei in an Aerosol Model of Infection. Plos One, 2015. 10(5).

297. Zoued, A., et al., Architecture and assembly of the Type VI secretion system. Biochimica Et Biophysica Acta-Molecular Cell Research, 2014. 1843(8): p. 1664-1673.